The Role of the Paraventricular Nucleus of the Hypothalamus in the Central Control of the Autonomic Nervous System

Thesis submitted in accordance with the requirements of the University of Liverpool for the degree of Doctor of Philosophy

By

Claire H. Feetham

September 2014

Abstract

The paraventricular nucleus (PVN) is a region of the hypothalamus considered the "master controller" of the autonomic nervous system. A subregion of the PVN, the parvocellular subnucleus, is believed to be involved in autonomic control, but its physiological importance is not fully understood. This thesis aimed to investigate the role of the parvocellular PVN in autonomic control and the underlying mechanisms responsible.

In slice cell-attached patch action current recordings showed that putative parvocellular neurones are sensitive to osmolality and that a member of the mechanosensitive transient receptor potential ion channel (TRP) family TRPV4 plays a role in this osmosensing. TRPV4 agonists gave a similar reduction in action current frequency (ACf) to hypotonic challenge, which was reversed by selective TRPV4 inhibitors. Single-channel recordings identified a TRP-like channel on parvocellular neurones, and the activity of this channel was increased by the TRPV4 agonist 4αPDD. Intracellular calcium recordings showed increases in Ca^{2+} in response to either hypotonic challenge or 4αPDD. Furthermore, a role for TRPV4 was verified in central osmosensing at the whole animal level; central injections of hypotonic solution decreased blood pressure; an effect ablated by a TRPV4 inhibitor.

Functional coupling between TRPV4 channels and Ca^{2+}-activated K^+ (K_{Ca}) channels was also explored. The effect of hypotonic challenge was reversed by inhibition of the small-conductance K_{Ca} (SK) channel. Since the effects of TRPV4 could also be blocked by an SK inhibitor, it is proposed that TRPV4 is coupled to SK to modulate neuronal activity. During calcium recordings Aaplication of a TRPV4 agonist in the presence of an SK inhibitor showed a reduced, but sustained Ca^{2+} rise compared to TRPV4 agonist application alone, suggesting feedback mechanisms are also in play. These mechanisms were also verified, quantitatively, with a mathematical model written in the NEURON simulation environment and incorporating experimentally derived parameters.

A role for this area of the PVN in temperature sensing was also discovered, with ACf decreasing with an increase in temperature from 25^{o}C to 37^{o}C. Pharmacological investigation identified another TRP channel, TRPM2, to be central for the PVN response to temperature.

ECG recordings from rats implanted with telemeters confirmed roles for neurokinin 1 receptor (NK1) expressing neurones in the PVN in the cardiovascular response to psychological stress and in the setting of circadian heart rate. Heart rate variability analysis showed that increases in the sympathetic activity indicator, "LF/HF", in response to handling stress were ablated by specific lesioning of the NK1 neurones in the PVN. In addition these animals had a significant shift in the daily variation of their average day/night heart rate.

In conclusion this thesis identifies the mechanisms underlying several different functional roles for parvocellular PVN neurones and indicates the PVN may be a multifunctional homeostatic "detector".

Acknowledgements

Firstly, I would like to thank my supervisors Dr Richard Barrett-Jolley and Dr Caroline Dart, who conceived this project. I thank them for their continued guidance and support, and for teaching me to “be more dog”.

I would also like to thank the Biotechnology and Biological Sciences Research Council; these studies would never have taken place without the funding provided.

Thank you to Becky Lewis, for teaching me electrophysiology (amongst other things), for her invaluable guidance and for keeping me well caffeinated throughout these 4 years. Thanks to Nic Nunn for teaching me surgery techniques and for always being helpful, and thanks to Iain Young for his guidance and support. I would also like to thank Caroline Staunton, who has helped to keep me sane with her joyful singing.

I also need to thank my family, Mum and Dad I thank for their constant support and for checking up on me, Richard, thanks for making me laugh and Louise for being a source of encouragement throughout whatever I wanted to do (and Marlowe for his cheeky smile).

Finally, a word of thanks to my friends, particularly to Rose and Beth, as without them, I never would have succeeded. Thank you for always listening and keeping me afloat.

Contents

List of Figures

List of Tables

Abbreviations

This section lists the abbreviations used in this thesis. SI units and chemical element symbols are omitted from this list.

4αPDD	4 alpha-Phorbol 12,13-Didecanoate
ACf	action current frequency
ACSF	artificial cerebrospinal fluid
ACTH	adrenocorticotropic hormone
AHP	after-hyperpolarisation
Ang II	angiotensin II
ASIC	acid-sensing ion channel
AT	angiotensin receptor
ATP	adenosine triphosphate
BAT	brown adipose tissue
BK	large conductance Ca^{2+} activated K^{+} channel
CRF	corticrotrophin releasing factor
CRF_x	corticrotrophin releasing factor receptor
D1/2	dopamine receptors
DEM	data exchange matrix

DMH	dorsomedial hypothalamus
DMSO	dimethyl sulfoxide
ECG	electrocardiogram
EGTA	ethylene glycol tetraacetic acid
ENaC	epithelial sodium channel
FCS	fetal calf serum
FFT	Fast Fourier transform
GABA	γ-aminobutyric acid
GIRK	G protein-coupled inwardly-rectifying K^+ channel
HCN	hyperpolarisation-activated cyclic nucleotide-gated channel
HF	high frequency
HRV	heart rate variability
ICV	intracerebroventricular
IK	intermediate conductance Ca^{2+} activated K^+ channel
IML	intermediolateralis
IP	intraperitoneal
K_{ATP}	ATP-sensitive K^+ channel
K_{Ca}	Ca^{2+} activated K^+ channel

KO	knock out
K_V	voltage-gated K^+ channel
LF	low frequency
Na_V	voltage-gated Na^+ channel
NK	neurokinin receptor
nNOS	neuronal nitric oxide synthase
NMDA	N-methyl-D-aspartate receptor
NO	nitric oxide
NOS	nitric oxide synthase
NTS	nucleus tractus solitaries
MPo	medial preoptic area
OT-R	oxytocin receptor
P1/2	purinergic receptors
PBS	phosphate-buffered saline
PFA	paraformaldehyde
PNS	parasympathetic nervous system
PVN	paraventricular nucleus
RMP	resting membrane potential

RSNA	renal sympathetic nervous activity
RT-PCR	reverse-transcription polymerase chain reaction
RVLM	rostral ventrolateral medulla
SCN	suprachiastmatic nucleus
SFO	subfornical organ
SK	small conductance Ca^{2+} activated K^{+} channel
SNA	sympathetic nervous activity
SNS	sympathetic nervous system
SP	substance P
SSP-SAP	substance P saporin
TRP	transient receptor potential
TRPA	transient receptor potential ankyrin
TRPC	transient receptor potential canonical
TRPM	transient receptor potential melastatin
TRPML	transient receptor potential mucolipin
TRPP	transient receptor potential polycystin
TRPV	transient receptor potential vanilloid
V1a-R	vasopressin 1a-receptor

V_j	junction potential
VMH	ventromedial hypothalamus

1 Introduction

The paraventricular nucleus (PVN) is a region of the hypothalamus, located adjacent to the third ventricle. Composed of several functionally distinct subnuclei, the PVN has a fundamental role in both the endocrine and autonomic systems, even being described as the "master controller" of the autonomic system (Liposits *et al.*, 1986). The cytoarchitecture and projections of the PVN have been extensively studied, providing abundant support for this role (Sawchenko and Swanson, 1982; Swanson and Sawchenko, 1983; Swanson and Kuypers, 1980). The PVN is able to exert influence over the autonomic nervous system via its projections to other sites of autonomic influence, such as the rostral ventrolateral medulla (RVLM) and the spinal cord (Sawchenko and Swanson, 1982). Due to its vast number of projections the PVN is considered an important integrative centre involved in autonomic regulation, particularly during times of disturbed homeostasis (Cham and Badoer, 2008; Lovick *et al*., 1993; Stocker *et al*., 2004). In addition, the neurotransmitters produced by and acting on the neurones within the PVN have been extensively studied (Bains and Ferguson, 1995; Conn and Pin, 1997; Park and Stern., 2005; Sawchenko and Swanson, 1982; Zhang *et al*., 2001; (see reviews by Nunn *et al.*, 2011; Pyner, 2009)). However, despite this combined knowledge the autonomic role of the PVN in a resting situation is currently disputed and the ionic mechanisms responsible for modulating neuronal activity remain unclear. This is of particular importance as evidence suggests that a disruption in sympathetic nervous activity (SNA) is associated with cardiovascular complications such as heart failure (Floras, 2009; Grassi *et al.*, 2003). This thesis aims to address some of the questions

regarding the mechanisms involved in the autonomic influence and normal functional role of this nucleus.

1.1 Cytoarchitecture of the PVN

The cytoarchitecture of the PVN has been studied extensively in several early immunohistochemical studies on rats, with two main divisions being identified; the magnocellular and parvocellular regions (Figure 1.1) (Swanson and Kuypers, 1980; Swanson and Sawchenko, 1980; Kiss et al., 1991).

The magnocellular area contains neurosecretory neurones, known to secrete the neurotransmitters vasopressin and oxytocin. Three magnocellular subdivisions have been identified: 1. anterior, 2. posterior and 3. medial (Figure 1.1). These neurones project to the neurohypophysis to stimulate production of pituitary hormones and have been investigated more extensively than the parvocellular area.

The parvocellular PVN contains neurosecretory neurones projecting to other areas in the hypothalamic-pituitary adrenal axis (HPA axis) and preautonomic neurones known to activate the sympathetic nervous system (SNS) (Koutcherov *et al.*, 2000b; Loewy, 1991; Swanson and Kuypers, 1980). In fact, approximately 2000 neurones from the PVN project directly to the intermediolateralis (IML) of the spinal cord (Lovick et al., 1993; Pyner and Coote, 2000; Shafton et al., 1998; Yamashita et al., 1984). Neurones within the parvocellular area are compartmentalised into subdivisions; dorsal and lateral, where the preautonomic neurones are concentrated, and the medial, periventricular and anterior parvocellular subnuclei where neurosecretory neurones can be found (Figure 1.1) (Armstrong *et al*., 1980).

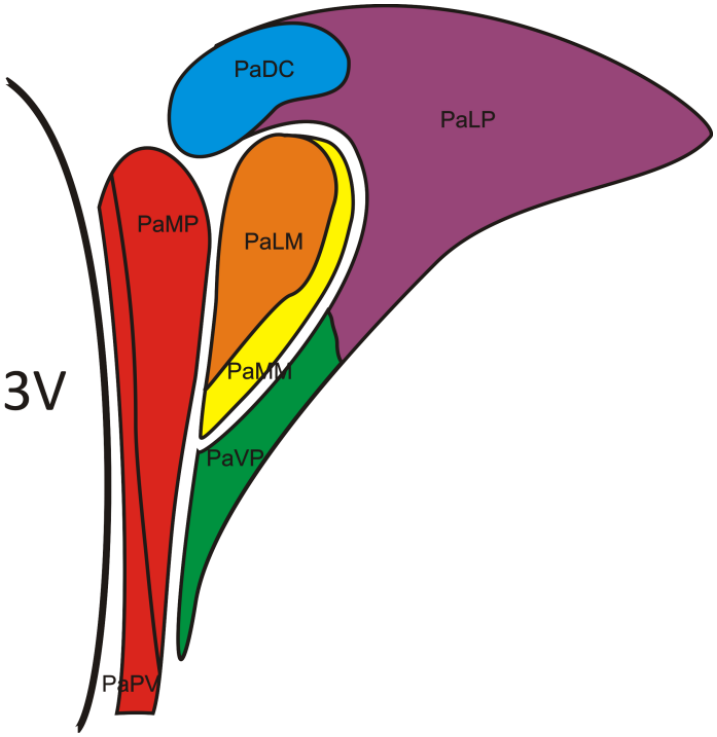

Figure 1.1 Diagram of the subdivisions of the paraventricular nucleus.
The subdivisions of the PVN are adjacent to the third ventricle (3V). PaLM – lateral magnocellular part, PaMM – medial magnocellular part, PaMP – medial parvocellular part, PaLP – lateral parvocellular part, PaPV – periventricular subnucleus, PaVP – medial ventral parvocellular part and PaDC – dorsal cap.

Neurogenic control of the autonomic nervous system is well established, with several main areas of the brain regulating sympathetic outflow; including the raphe pallidus (RPa), rostral ventrolateral medulla (RVLM), ventromedial medulla, A5 cell group and the PVN (Strack *et al*., 1989a, refer to review by Dampney *et al.*, 2005). However, despite the important role of the PVN in autonomic function, the parvocellular region of the PVN has been much less studied than its magnocellular counterpart.

1.2 Projections of the parvocellular PVN

A great level of attention has been paid to the efferent and afferent connections of the paraventricular nucleus in recent years. This is due to a combination of factors; not only is it considered an important integratory area of the brain, but it also projects to the posterior lobe of the pituitary and other areas of autonomic influence. Of particular interest is evidence suggesting that abnormal elevated sympathetic activation, potentially driven by the parvocellular PVN, can be associated with cardiovascular complications such as heart failure (Floras, 2009; Grassi *et al.*, 2003).

Presympathetic efferent projections from the PVN target other autonomic centres in the brain, such as the RVLM and the nucleus tractus solitarius (NTS). Neurones within this area also project to the IML of the spinal cord itself and a further population branches to both the RVLM and IML (Coote *et al.*, 1998; Hosoya *et al.*, 1991; Motawei *et al.*, 1999; Pyner and Coote, 1999; Pyner and Coote, 2000; Shafton *et al.*, 1998; Strack *et al.*, 1989a). These projections have been confirmed in rats using retrograde labelling and in viral tracing studies using the herpes simplex and pseudorabies viruses (Pyner *et al.*, 2001; Pyner and Coote, 2000). Evidence suggests these direct descending projections to the IML are involved in sympathetic influence as they terminate on or near the sympathetic preganglionic neurones in this area. In further viral tracing studies on rats performed by multiple groups these neurones themselves are shown to project to various end organs and ganglia (such as the heart, kidneys, liver, BAT and lumbar muscles), where many of these projections can affect these various systems via their autonomic influence (Jansen

et al., 1995a; Pyner *et al.*, 2001; Schramm *et al.*, 1993; Strack *et al.*, 1989a; Strack *et al.*, 1989b; Weiss *et al.*, 2001; Xiang *et al.*, 2014)

Tracing afferent projections to the PVN is also important for understanding the influence this nucleus has over the sympathetic nervous system. In particular, the NTS is an important region of the brain involved in the integration of autonomic and HPA stress responses. Cardiovascular vagal afferent projections terminate in the NTS; these neurones relay cardiovascular information such as blood pressure and volume from various cardiovascular receptors. This information is in turn received by presympathetic neurones within the PVN via their afferent projections from the NTS (Affleck *et al.*, 2012; Clement *et al.*, 1972; Karim *et al.*, 1972; Spyer, 1994).

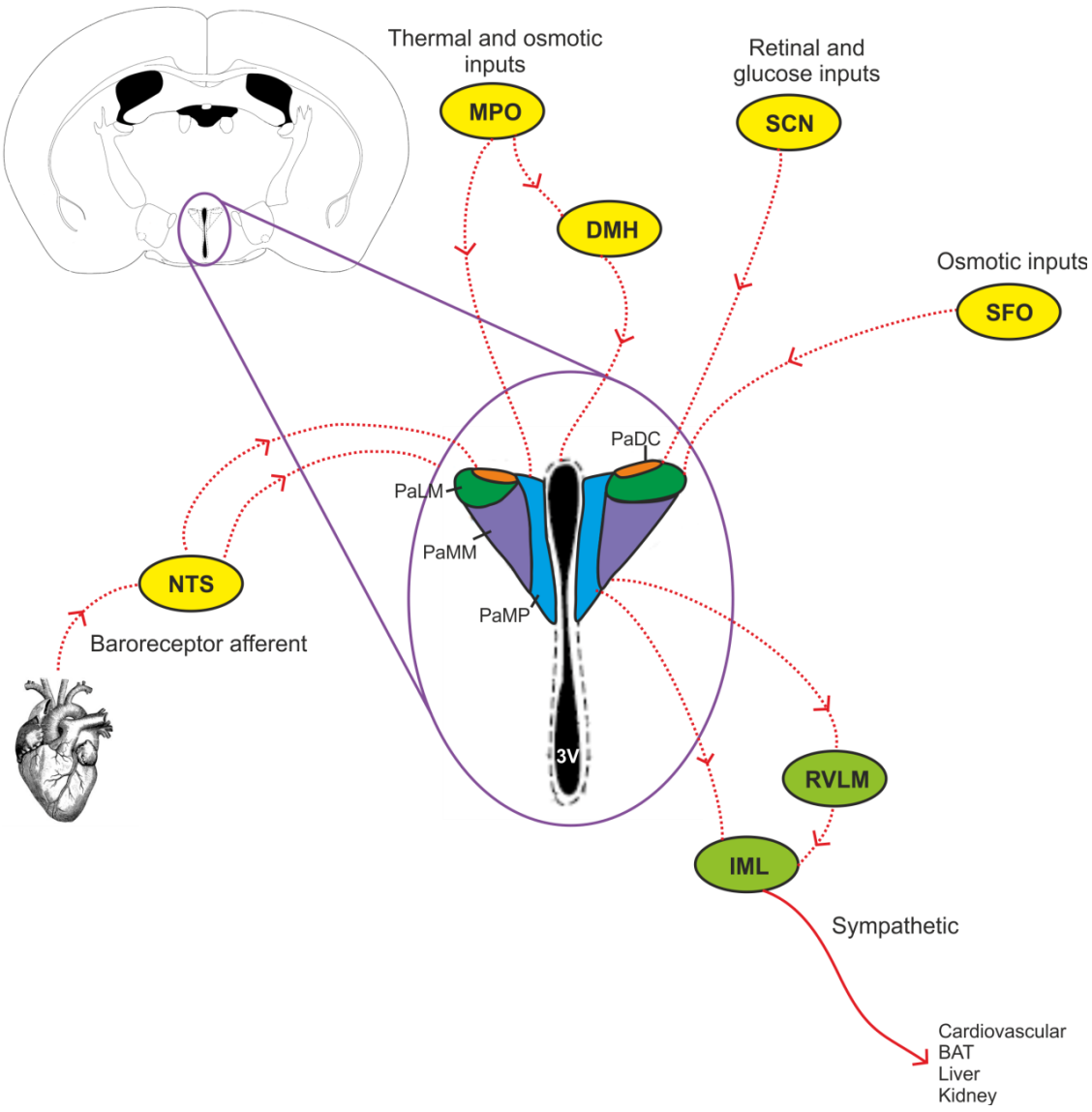

Figure 1.2 Efferent and afferent projections of the paraventricular nucleus affecting the autonomic nervous system.
A magnified schematic of the paraventricular nucleus of the hypothalamus showing some of the subregions and the chain of projections influencing the autonomic nervous system. PaLM – lateral magnocellular part, PaMM – medial magnocellular part, PaMP – medial parvocellular part and PaDC – dorsal cap.

Furthermore, the PVN is surrounded by both inhibitory GABAergic (γ-aminobutyric acid) and excitatory glutamatergic neurones innervating the area. In several tracing studies in rats and mice discrete sets of GABAergic neurones from the dorsomedial hypothalamus (DMH), medial preoptic area (MPo) and bed nucleus of the stria

terminalis (BST) have been found to directly innervate the PVN (Herman *et al.*, 2002b; Roland and Sawchenko, 1993). The MPO receives thermal and osmotic inputs, projecting to the PVN directly and via the DMH to influence thermogenesis and osmoregulation (Stocker and Toney, 2005). Furthermore, projections from the DMH are also found to be involved in metabolism and feeding (for more detail of these roles see Section 1.5 Functional role of the PVN (ter Horst and Luiten, 1986; Thompson *et al*., 1996)). In addition projections from these areas and the BST are involved in the HPA stress axis, with efferent projections continuing from the PVN to the pituitary (Myers *et al.*, 2013; Radley *et al.*, 2009). Transynaptic labelling using the herpes virus injected into the adrenal medulla of rats identified a population of GABAergic neurones projecting to the lateral and dorsal cap regions of the parvocellular PVN (Watkins *et al.*, 2009). These neurones themselves are also surrounded by neuronal nitric oxide synthase (nNOS)-containing neurones, as well as a population of these neurones present within the PVN itself (Watkins *et al.*, 2009). Affleck et al (2012) showed the afferent NTS-PVN projections terminate on or near (1) both the presympathetic and magnocellular neurones of the PVN, (2) the innervating GABAergic neurones surrounding the PVN and (3) the nNOS-containing neurones also found outside the PVN.

In combination these studies show that the PVN plays an important role in autonomic regulation, and its efferent and afferent projections have been incredibly well studied. The knowledge of the neural projections involved in maintaining normal sympathetic activity is vital.

1.3 Neurotransmitters and receptors

The regulation of PVN neurones is dependent upon both inhibitory and excitatory innervations from several sources, such afferent projections and the wide variety of neurotransmitters acting on them. Over 30 neurotransmitters have been identified within the PVN (Sawchenko and Swanson, 1982), these are a combination of those neurotransmitters released by the neurones within the PVN themselves and the neurotransmitters acting upon these neurones.

Of particular importance to the activity of neurones within the PVN is the complex interaction between glutamate, GABA and NO which has been identified in a variety of extensive immunohistochemical, *in vivo* and electrophysiological studies summarised in Table 1 (Figure 1.3). Briefly, GABA is responsible for the tonic inhibition of neuronal activity in the PVN; this action is enhanced by the release of nitric oxide (Watkins *et al*., 2009). Neuronal firing can be modulated by excitatory glutamate; however this action remains driven by tonic inhibition via GABA. This interaction has been beautifully demonstrated in a study by Martins-Pinge *et al*., (2012). In this study the heart rate and mean arterial pressure of rats were recorded whilst microinjections were performed directly in to the PVN. It was shown that blockade of ionotropic receptors produced small decreases in HR and MAP. In addition the $GABA_A$ receptor antagonist bicucullin and inhibition of NO-synthase led to increases in HR and MAP. Furthermore, an interaction between in GABA and NO was revealed when injection of the NO donor sodium nitroprusside produced depressor responses which were attenuated by bicucullin. Inhibition of NO synthase also potentiated increased in HR and MAP seen with activation of

ionotropic receptors. Those tonic excitatory effects of glutamate in the PVN were shown to be tonically attenuated by NO (Martins-Pinge *et al*., 2012).

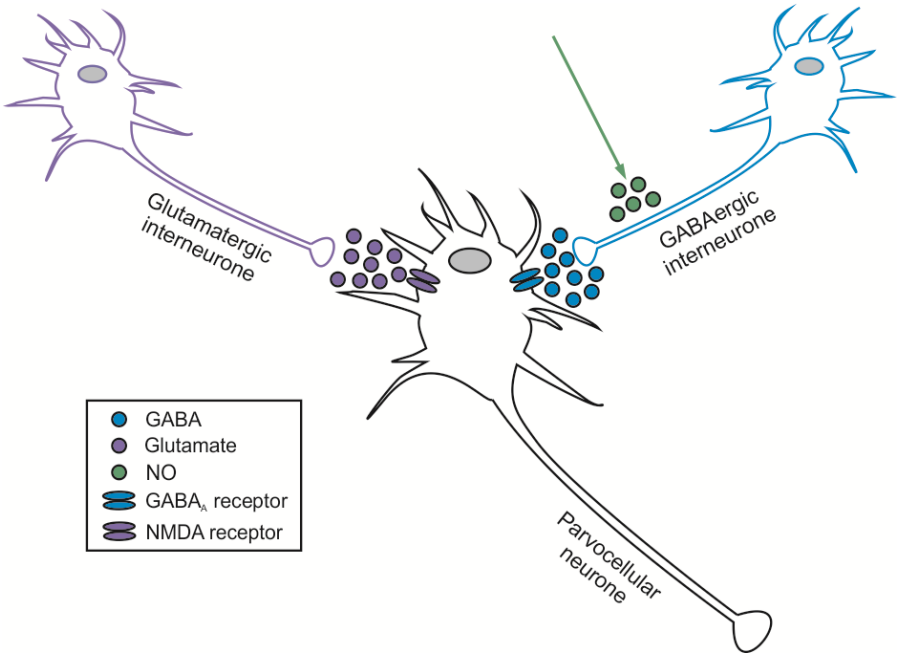

Figure 1.3 Interaction between glutamate, GABA and NO acting on parvocellular neurones of the PVN.

Several important reviews have been written in recent years summarising the combination of neurotransmitters found within the PVN (Kenney *et al.*, 2003; Nunn *et al.*, 2011; Pyner, 2009). Of particular interest in this work are the neurotransmitters released by and acting upon those preautonomic neurones of the PVN, which may have an important role in cardiovascular regulation due to their sympathetic innervation. The main neurotransmitters and their receptors present within the PVN have seen summarised in Table 1.

Although the interaction between glutamate, GABA and NO underlie the basic activity of the neurones of the PVN, this activity can be altered by various other neurotransmitters. Some of the main neurotransmitters found in the PVN area and the studies associated with them are described in Table 1.

Table 1 Summary of the main neurotransmitters and receptors found in the PVN and their known roles

Neurotransmitter	Receptor(s)	Function	Method	Relevance	Reference
GABA	$GABA_A$ $GABA_B$	Tonic inhibition Excitatory in immature Involved in development of PVN	Patch-clamp electrophysiology	50% synapses in the PVN GABAergic Tonic inhibition by $GABA_A$ Regulation of tonic inhibition by astroglial GABA transporters	(Affleck *et al.*, 2012; Li and Xu, 2008; Park *et al.*, 2009; Park *et al.*, 2007; Park and Stern, 2005)
			In vivo in healthy Targeted injections	Bicucullin ↑ HR, BP and modulates SNA Activation both receptors ↓RSNA, HR and BP Blockade of $GABA_B$ ↑ cardiac sympathetic afferent reflex	(Kenney *et al.*, 2001; Martin *et al.*, 1991; Zhong *et al.*, 2008b)
			In vivo in hypertensive/HF	Loss of GABA Function switch between $GABA_A$ and $GABA_B$ $GABA_A$ attenuated, $GABA_B$ enhanced in SHR; ↑HR and BP	(Carillo *et al.*, 2012; Chen and Pan, 2006; Davern *et al.*, 2014; Li and Pan, 2006; Li and Pan, 2007b; Li *et al.*, 2008a; Li *et al.*, 2008b; Wang *et al.*, 2009; Zhang *et al.*, 2002b)
Nitric oxide (NO) Synthesised by nNOS	-	Inhibitory modulator Enhances the action of GABA	Transynaptic labelling, immunohistochemisty	nNos projections from NTS to preautonomic cells nNos expressed in 6-10% PVN-IML, 12-25% PVN-RVLM Distinct from GABAergic neurones GABAergic neurones – target for NO, enhances release of GABA NO diffuses from magnocellular PVN	(Affleck *et al.*, 2012; Kantzides and Badoer, 2005; Li *et al.*, 2002; Li *et al.*, 2003b; Stern, 2004; Vincent and Kimura, 1992; Watkins *et al.*, 2009; Weiss *et al.*, 2001)
			Patch-clamp electrophysiology	↓ mIPSCs in PVN-IML with inhibition of nNOS, bicucullin or scavenging NO, ↑ mIPSCs in PVN-IML with NO donor	(Li *et al.*, 2004a; Li *et al.*, 2002)
			In vivo in healthy Targeted injections	NO donor ↓ RSNA, HR and BP, blockade of nNOS prevents effects	(Horn *et al.*, 1994; Zhang *et al.*, 1997; Zhang and Patel, 1998)
			In vivo in hypertensive/HF Targeted injections	↓ NO leads to ↑ SNA in HF, HF have blunted ↓RSNA in response to NO Exogenous NO ↓ cardiac SNA in HF	(Zhang *et al.*, 2001; Ramchandra *et al.*, 2014)
Glutamate	1. Ionotropic NMDA AMKP 2. Metabotropic 8 GPCRs in 3 groups	Excitatory Modulate neuronal activity	Patch-clamp electrophysiology	Ionotropic and group I metabotropic activation ↑ neuronal activity, group II ↓ neuronal activity and synaptic transmission	(Conn and Pin, 1997)
			In vivo healthy	Glutamate acts via NMDA ↑ neuronal activity, ↑ RSNA, HR and BP Stimulation of WAT induces adipose afferent reflex , ↑	(Busnardo *et al.*, 2009; Kawabe *et al.*, 2009; Li *et al.*, 2006) (Cui *et al.*, 2013; Shi *et al.*, 2012)

				RSNA, HR and BP	
			Hypertensive/HF	↑ glutamatergic inputs driven by ↑glutamate release ↑ NMDA function, ↑ group 1 metabotropic activity; supports ↑ SNA Group II metabotropic inhibit SNA by attenuation of ↑ glutamatergic input	(Li and Pan, 2007a; Li and Pan, 2006) (Li and Pan, 2010; Li *et al.*, 2014; Li *et al.*, 2003c; Li *et al.*, 2001) (Ye *et al.*, 2013)
Dopamine Acts on and produced by neurones in the PVN	D1 and D2	Influence SNA Influence penile erection and hyperphagia	Immunohistochemistry, tracing studies	TH staining identified large population Dopaminergic projections from medial, dorsal and periventricular PVN to RVLM and IML. Nerve terminals to sympathetic preganglionic neurons express receptors	(Dietl *et al.*, 1985; Gladwell and Coote, 1999; Jansen *et al.*, 1995b; Strack *et al.*, 1989b; Swanson *et al.*, 1981)
			Patch-clamp electrophysiology	2 subpopulations – inhibitory (D1) and indirect excitatory (D2) effects Mediates inhibitory effects on RSNA from stimulating PVN via D1	(Gladwell *et al.*, 1999) (Yang *et al.*, 2002)
Vasopressin and Oxytocin Co-expressed (neurtotransmission in sympathetic preganglionic neurones may be area specific)	OT-Rs VTa-Rs	Neuroendocrine Cardiovascular control	Immunohistochemistry, RT-PCR, in situ hybridisation, tracing studies	40% PVN-IML express oxytocin, up to 40% express vasopressin	(Hallbeck *et al.*, 2001; Hawthorn *et al.*, 1985; Jansen *et al.*, 1995b; Lee *et al.*, 2013; Sawchenko and Swanson, 1982; Swanson and McKellar, 1979)
			Patch-clamp electrophysiology	Oxytocin acts via both OT-Rs and VTa-Rs	(Sermasi and Coote, 1994)
			In vivo, immunoassay	PVN stimulation ↑vasopressin and oxytocin Mediate ↑RSNA and HR, effects ↓with V1a-R or OT-R antagonists OT-Rs involved in tonic neural control of baroreceptor reflex and cardiovascular variability	(Pittman *et al.*, 1984) (Malpas and Coote, 1994; Yang *et al.*, 2009; Yang *et al.*, 2004; Yang *et al.*, 2002) (Lozic *et al.*, 2014)
Angiotensin II (Ang II)	AT_1 and AT_2	Triggers adaptive homeostatic responses inc. SNA to modulate BP	Immunohistochemistry	Expressed by parvocellular PVN neurones, acting via AT_1 and AT_2.	(Alexander *et al.*, 2011; Allen *et al.*, 1999; de Gasparo *et al.*, 2000; Lenkei *et al.*, 1997; Lind *et al.*, 1985; Oldfield *et al.*, 2001)
			In vivo in healthy, patch clamp electrophysiology	Injection of Ang II leads to ↑ neuronal activity and BP, involving PVN-IML neurones Attenuated by AT_1 antagonist losartan	(Bains and Ferguson, 1995; Bains *et al.*, 1992; Huang *et al.*, 2014; Liu *et al.*, 2014; Osborn *et al.*, 2007; Zhang *et al.*, 2002b)

				Ang II directly modulates PVN-RVLM neurones, ↑ BP Action is indirect, AT_1 receptors co-localise with synaptophysin. ↑ neuronal activity, mediated by attenuation of GABAergic inputs.	(Cato and Toney, 2005) (Chen and Pan, 2007; Li *et al.*, 2003a; Li and Pan, 2005)
Tachykinins Substance P (SP) Neurokinin A Neurokinin B (See Chapter 7)	NK1, NK2 and NK3	Central cardiovascular control Stress response Pain	Immunohistochemistry	SP abundant in the PVN, NK receptors present in parvocellular PVN	(Ding *et al.*, 1996; Jessop *et al.*, 1991; Koutcherov *et al.*, 2000a; Nakayama *et al.*, 1992; Shults *et al.*, 1985)
			Patch-clamp electrophysiology	SP dependant pathway linking PVN to DMH and PVN-IML SP ↑ neuronal activity via disinhibition of $GABA_A$ currents	(Womack and Barrett-Jolley, 2007; Womack *et al.*, 2007)
			In vivo and *c-fos*	Central tachykinins ↑ SNA ↑ *c-fos* in response to noxious and psychological stress, blunted by NK antagonists and in NK KO mice Microinjection of SP ↑ RSNA, HR and BP	(Culman *et al.*, 2010; Ebner *et al.*, 2008; Santarelli *et al.*, 2002; Unger *et al.*, 1985; Womack *et al.*, 2007)
Corticotrophin releasing factor (CRF)	CRF_1 and CRF_2	Stress response	Immunohistochemistry, tracing studies	High expression of CRF_1 and CRF_2 in parvocellular PVN CRFergic neurones project from DMH to PVN	(Goncharuk *et al.*, 2002; Makino *et al.*, 2005; Yamada *et al.*, 2009) (Champagne *et al.*, 1998)
			In vivo, in situ hybridisation	↑ mRNA of CRF_1 with stress CRF release ↑ CRF_1 receptors, enhancing ACTH release	(Luo *et al.*, 1994; Makino *et al.*, 2005) (Ono *et al.*, 1985)

1.3.1 Others

Numerous other neurotransmitters and receptors are expressed in the PVN. Steroid hormones may play a role in altering excitability of preautonomic neurones within this nucleus as, for example, immunohistochemical studies in rats have shown oestrogen-β receptors are expressed on ~50% of the RVLM projecting neurones of the PVN, and is expressed weakly within the magnocellular region of the PVN. In this study the authors allude to these neurones influencing the autonomic and cardiovascular control (Stern and Zhang, 2003). In addition, electrophysiological studies in rats have shown that the steroid hormone tetrahyrdeoxycorticosterone can modulate neuronal activity in preautonomic cells o of the PVN (Womack *et al.*, 2006). High levels of cortisol also activate these neurones via inhibition of potassium channels (Zaki and Barrett-Jolley, 2002).

Purinergic receptors, classed as either P1 (adenosine receptors) or P2 receptors (ligand-gated ion channels) have also been identified in the brain using immunohistochemistry and electrophysiological studies in rodents (Collo *et al*., 1996; Vulcanova *et al*., 1996; Kanjhan *et al*., 1999). Although both are found on parvocellular PVN neurones (Cham *et al.*, 2006b; Li *et al.*, 2010), only P1 have been confirmed in spinally-projecting neurones. Adenosine inhibits activity in rat PVN neurones via both adenosine (P1) receptors and the adenosine triphosphate (ATP)-sensitive potassium channel (K_{ATP}) in this study (Li *et al.*, 2010).

The G-protein coupled receptors melanocortin 3/4 can also be found in the PVN, shown to be involved in heart rate and blood pressure modulation, and mediating sympathetic outflow in rats (Kawabe *et al.*, 2012; Li *et al.*, 2012; Ward *et al.*, 2011).

Both neuropeptide FF and neuropeptide VF are expressed in the PVN and excite neurones within both parvocellular and magnocellular regions of the PVN via inhibition of GABAergic signals in electrophysiological studies in rats (Jhamandas and MacTavish, 2003; Jhamandas *et al.*, 2007). However, their actions on spinally-projecting neurones within the parvocellular area are unknown.

Although the presence of a variety of neurotransmitters and receptors on the PVN is known, many of these studies lack specific evidence of a direct action on the preautonomic neurones in this area.

1.4 Electrophysiological properties of PVN neurones

1.4.1 Electrophysiological characterisation of PVN neurones

Neurones within the paraventricular nucleus have not only been characterised by their anatomical positions and expression of neurotransmitters, but although through several electrophysiological studies. The first of these studies was performed by Tasker and Dudek (1991) with the development of patch-clamp electrophysiology techniques. In this study Tasker and Dudek (1991) identified three electrophysiologically distinct types of PVN neurones; type I, type II and type III (Tasker and Dudek, 1991). They showed that neurosecretory magnocellular neurones of the PVN, also termed “type I” neurones, express a rapidly inactivated (or “A-type”) potassium conductance (Sonner and Stern, 2005; Tasker and Dudek, 1991). These cells are larger than type II and type III neurones, similar to those

magnocellular neurones found in the supraoptic nucleus and exhibit phasic bursting patterns.

Parvocellular neurones on the other hand (termed “type II” neurones) were shown to express a slowly inactivating delayed rectifier potassium conductance. These cells are distinguishable not only by their electrophysiological characteristics, but are also morphologically different from their magnocellular counterparts; smaller and with more complex process. At the time of this study different populations of neurones based on morphology and firing patterns were observed within the parvocellular region itself (Tasker and Dudek, 1991). Later these were shown to be neurosecretory (exhibiting electrophysiological properties similar to those cells found in the magnocellular area) and preautonomic neurones. Luther and Tasker (2000) later showed that the differences observed between the ‘type II’ parvocellular and ‘type I’ magnocellular cells may be due to differential expression of voltage-gated potassium and calcium currents (Luther and Tasker, 2000). Further studies have since shown that medulla-projecting neurones from the parvocellular area show strong inward rectification and “A-type” potassium conductance (Sonner and Stern, 2005; Stern, 2001) and spinally-projecting neurones show a slowly inactivating potassium conductance (Barrett-Jolley *et al.*, 2000).

Interestingly, due to the constant tonic influence of GABAergic innervations, neurones within the PVN are quiescent *in vivo* (Badoer *et al.*, 2002; Martin and Haywood, 1993; Martin *et al.*, 1991; Park and Stern, 2005). During electrophysiological experiments in brain slice, however, this tonic inhibition is not seen, and spontaneous action potentials are regularly observed (Stern, 2001;

Womack *et al.*, 2007). This implies that tonic inhibition may be lost *in vitro* during the preparation of brain slices, potentially by cutting off GABAergic innervations responsible for inhibition. Importantly, evidence suggests this inhibitory control is absent in times of stress and cardiovascular disease (Park *et al.*, 2009).

1.4.2 Ion channels

Ion channels are membrane proteins found on the plasma membrane of cells, responsible for setting membrane potential and shaping action potentials. They do so by allowing the flow of ions through a pore which is formed in the middle of an assembly of protein subunits. Opening of ion channels can be triggered by a number of stimuli, i.e.; voltage changes across the membrane (voltage-gated ion channels), the binding of a ligand (ligand-gated ion channels) or by mechanical stress (mechanically gated ion channels). Furthermore, many neurotransmitters can modulate ion channels within neurones, and the activation of ion channels can trigger the release of neurotransmitters. Activating an ion channel typically leads to a conformational change, opening the channel and allowing the flow of ions (e.g. K^+, Na^+, Ca^{2+}, Mg^{2+}, Cl^-). Due to their ability to alter membrane potential and therefore cell excitability, it is important to know what ion channels are present and their role in the PVN. Furthermore, evidence suggests that disruption of ion channel regulation can lead to increased neuronal excitability of presympathetic neurones, potentially contributing to sympathetic over activity (Sonner *et al.*, 2011).

1.4.2.1 Potassium channels

Potassium channels are the most abundant type of ion channel, and are considered the regulators of excitability; controlling action potential characteristics, hormone and neurotransmitter release and membrane potential. Four major classes exist; voltage-activated potassium channels (K_V), calcium-activated potassium channels (K_{Ca}), inwardly rectifying potassium channels and two-pore potassium channels (Alexander *et al.*, 2011; Goldstein *et al.*, 2005; Gutman *et al.*, 2005; Kubo *et al.*, 2005; Wei *et al.*, 2005).

Evidence suggests the differing electrophysiological properties of PVN neurones discussed may be due to the differential expression of different K_v channels (Luther and Tasker, 2000). Around 40 K_V channels have been identified (Gutman *et al.*, 2005), with many known to modulate neuronal excitability in most neuronal populations (Rudy *et al.*, 1999; Serodio and Rudy, 1998). A variety of K_V channels have been shown to be present in the PVN. Patch-clamp recordings of retrogradely labelled PVN-RVLM neurones in rat brain slices identified an "A-type" potassium current, identified as an important mechanism for controlling neuronal excitability with these neurones. Further immunohistochemical evidence suggested that this current is mediated by K_V1.4 and/or K_V4.3 channel subunits (Sonner *et al.*, 2008; Sonner and Stern, 2007; Sonner and Stern, 2005). In identified spinally-projecting neurones K_V channel currents have been shown to be slowly inactivating (Barrett-Jolley *et al.*, 2000). Immunoreactivity for K_V1.2 has also been identified within rat PVN neurones (Chung *et al.*, 2001). Furthermore, K_V1.1/1.2 channels have been shown to be downstream effectors of nitric oxide on synaptic GABA release to

identified spinally-projecting neurones of the rat PVN (Yang *et al.*, 2007). In a study using a combination of patch-clamp electrophysiology to record the type of neurone from the PVN and single cell reverse-transcriptase polymerase chain reaction (RT-PCR) in rats, expression profiles of K_V channels were identified. This study showed the expression of $K_V1.2$, $K_V1.3$, $K_V1.4$, $K_V4.1$, $K_V4.2$ and $K_V4.3$ in both types of neurones, with some co-expression seen. $K_V4.2$ and $K_V4.3$ expression higher in type I neurones, identifying molecular mechanisms for the differences in cell types (Lee *et al.*, 2012).

K_{Ca} channels are also abundantly found in the brain and are important regulators of neuronal excitability (Faber and Sah, 2003). This family consists of 3 groups, large-conductance (BK), intermediate-conductance (IK) and small conductance channels (SK) (further information regarding nomenclature and mechanism is provided in Chapter 3). Both BK, which is voltage dependant as well as activated by Ca^{2+}, and SK have been identified in the PVN and are known to modulate firing within this area (Kohler *et al.*, 1996; Sausbier *et al.*, 2006). Patch-clamp electrophysiology recordings revealed that these channels modulate the firing frequency of PVN-RVLM neurones in rats; inhibition of these channels leads to increased excitability (Chen and Toney, 2009). Further *in vivo* investigation demonstrated a role for the SK channels in regulating sympathetic nerve activity (SSNA and RSNA) and blood pressure in rats. By using targeted injections into the PVN of pharmacological inhibitors of SK they were able to induce increases in SNA, heart rate and blood pressure (Gui *et al.*, 2012). Although this investigation compliments the *in vitro* findings of Chen et al (2009), it is not possible to establish the neuronal population responsible for the responses observed. Recent evidence does implicate a role for

spinally-projecting neurones however, as patch-clamp recordings show that SK channel activity is reduced in hypertension, modulated by casein kinase II upregulation. This decreased functionality of SK contributes to the hyperactivity of these neurones (Pachuau *et al.*, 2014). Furthermore, to add complexity to the role of SK, several investigations have suggested functional couplings to non-selective cation channels such as the transient receptor potential (TRP) channels (Earley, 2011; Gao and Wang, 2010). A role for SK in the parvocellular PVN will be further discussed in Chapter 3.

In a study by Li et al (2010) ATP-sensitive potassium (K_{ATP}) channels were identified in spinally-projecting neurones of the rat PVN. Using patch-clamp electrophysiology this group demonstrated that adenosine results in the inhibition of excitability of this population of neurones (Li *et al.*, 2010). Furthermore, they found effect is mediated through adenosine receptors (discussed above), resulting in the opening of K_{ATP} and altered excitability. These findings were supported by a computational model and patch-clamp recordings from my group (Lewis *et al.*, 2010),

Finally, the g-protein coupled inwardly rectifying potassium (GIRK) channels have also been shown to be widely distributed throughout the rodent brain. These channels are activated by several neurotransmitters and are important in synaptic inhibition (Hille, 1994). GIRK channels mediate regulation of neuronal excitability through activation of various g-protein coupled receptors. Three subunits of GIRK exist; GIRK1, GIRK2 and GIRK3; all of which have shown to be present in the PVN using immunohistochemistry and *in situ* hybridisation (Saenz del Burgo *et al.*, 2008). In fact, GIRK1 has been shown to be expressed presynaptically in the PVN,

potentially having a role in presynaptic inhibition of neurotransmitter release in these neurones (Morishige *et al.*, 1996).

1.4.2.2 Sodium channels

Sodium channels are generally much less diverse than potassium channels. There are a few types of channel selective for sodium, the most common being voltage-gated sodium channels (Na_V), there are also epithelial sodium channels (EnaC) and finally sodium-leak channels, which are structurally part of the Na_V family, however they are non-selective and voltage-insensitive.

Na_V channels are widely distributed in excitable cells such as neurones (Yu and Catterall, 2003). Their primary function is to generate and propagate an action potentials (Catterall *et al.*, 2005a). Nine subtypes of Na_V have been identified in mammals ($Na_V1.1$-1.9) with four α subunits found in the central nervous system; type I, II, III and IV (IV is expressed in humans).

Na_V channels are expressed in the brain (Gordon *et al.*, 1987), with several studies demonstrating expression patterns in the rodent CNS focussing on mRNA expression and immunohistochemical techniques (Black *et al.*, 1994; Westenbroek *et al.*, 1989; Whitaker *et al.*, 2001). mRNA expression of type I, II, III have been shown in the hypothalamus, including the PVN. The spatial distribution pattern for each type of Na_V were shown to be very different, with type I being very weak, and type II and type III much stronger (Black *et al.*, 1994; Furuyama *et al.*, 1993). These results were similar to immunohistochemical patterns shown (Westenbroek *et al.*, 1989; Whitaker *et al.*, 2001). In addition, $Na_V1.2$ was shown to be predominantly

expressed on unmyelinated fibres in the hypothalamus, preferentially localised to the cell bodies (Jarnot and Corbett, 2006).

Very few studies have been performed investigating the presence of ENaC in the PVN (Teruyama *et al.*, 2012; Wang *et al.*, 2010). In situ hybridisation shows incredibly weak immunoreactivity for ENaC subunits In the parvocellular region compared to the magnocellular region of the rat PVN (Wang *et al.*, 2010).

1.4.2.3 Calcium channels

Calcium channels found on the plasma membrane are voltage-gated ion channels (Ca_V) and are considered ubiquitous. There are 10 cloned α subunits (pore-forming), which are divided into three categories; 1. High-voltage activated dihydropyridine-sensitive L-type ($Ca_V1.x$) channels, 2. High-voltage activated dihydropyridine-insensitive ($Ca_V2.x$) channels and 3. Low-voltage activated T-type ($Ca_V3.x$) channels, all expressing a variety of subunits (Catterall *et al.*, 2005b).

Although L-type Ca_V channels have been identified in the PVN using immunohistochemical techniques in rats (Chin *et al.*, 1992; Hetzenauer *et al.*, 2006), the predominant Ca_V current identified in parvocellular cells is the T-type Ca^{2+} current (Luther and Tasker, 2000; Tasker and Dudek, 1991). T-type Ca^{2+} channels modulate neuronal function via regulating Ca^{2+} influx, this action then leads to depolarisation of the cell and a burst of action potentials. Due to this action these channels are important in regulating action potential generation, influencing pacemaker and bursting behaviour (Perez-Reyes, 2003; Perez-Reyes, 1999). In further studies patch-clamp recordings were made in retrogradely labelled neurosecretory and non-labelled non-secretory parvocellular cells of rat PVN,

confirming that the non-secretory parvocellular cells generate a low-threshold spike (LTS) via T-type Ca^{2+} channels (Luther *et al.*, 2002; Sonner and Stern, 2007; Stern, 2001). These studies confirmed these different groups of cells in the parvocellular area exhibit different membrane electrical properties. In addition, more recent studies involving a combination of RT-PCR, immunohistochemistry and patch-clamp recordings have indicated that $Ca_V3.1$ is the major subtype of channel expressed in preautonomic cells mediating the T-type Ca^{2+} dependant LTS (Lee *et al.*, 2008). Moreover, it has been suggested in preautonomic PVN neurones that balance between the "A-type" K^+ and T-type Ca^{2+} currents consistent with a shift in expression of $K_V4.3$ and $Ca_V3.1$ results in enhanced neuronal excitability in hypertensive rats (Sonner and Stern, 2007). These results provide clear evidence that modulation of these channels is vital for normal activity of preautonomic PVN neurones.

1.4.2.4 Transient receptor potential channels

The transient receptor potential (TRP) group of ion channels are a large superfamily, consisting of 28 homologs in mammals. These are grouped roughly by common structure into seven subfamilies; TRPC (canonical; seven members), TRPV (vanilloid; six members), TRPA (ankyrin; 1 member), TRPM (melastatin; eight members), TRPML (mucolipin; 1 member), TRPP (polycystin; two members) and TRPN (NOMPC; only seen so far in non-mammals) (Nilius and Owsianik, 2011). TRPs are generally non-selective cation ion channels, permeable to both monovalent and divalent cations in different ratios. In addition, some members of this superfamily can also be trafficked from internal membranes to the plasma membrane. TRPs usually

consist of six membrane spanning domains with intracellular N and C termini, and show a variety of gating properties, although non show particular voltage sensitivity. The TRPC group act mainly as store operated channels, opening with a decrease in intracellular Ca^{2+}. TRPM's are responsible for various sensor/homeostatic roles, including exhibiting temperature sensing properties. TRPVs are described as the mechanosensitive group, although they are activated by a number of physical and chemical stimuli (Clapham, 2003; Clapham *et al.*, 2001; Nilius and Owsianik, 2011).

Non-selective cation currents have been observed in the rodent PVN; implying that non-selection cation channels, such as one or more of the TRPs, may be present. For example, it is known that angiotensin II depolarizes parvocellular neurons in paraventricular nucleus through modulation of putative non-selective cationic and potassium conductances in rats (Latchford and Ferguson, 2005) and leptin has been shown to depolarise PVN neurones, also indicative of non-selective cation conductance (Powis *et al.*, 1998).

Using a variety of techniques several TRPs have been specifically identified in the PVN, although many of these studies do not include functional characterisation of the channels observed. RT-PCR has shown both TRPC4 and TRPC5 mRNA is expressed within the PVN (Fowler *et al.*, 2007). Using a radiolabelled vanilloid agonist the presence of TRPV1 receptor protein was identified, although very weakly, in the PVN of mice (Roberts *et al.*, 2004). Patch clamp studies in rat brain slices have revealed TRPV1 receptor activation in the PVN induces glutamate release and postsynaptic firing (Li *et al.*, 2004b). Furthermore,

immunohistochemical studies show that TRPV1 is co-localised with liver-related PVN neurones (Zsombok *et al.*, 2011). Immunohistochemical techniques in the rat brain have identified the TRPV2 receptor in the magnocellular region of the PVN with some staining also observed in the posterior parvocellular region and dorsal horn (Nedungadi *et al.*, 2012). This study suggests that TRPV2 may have a role in regulating body fluid homeostasis, autonomic function and metabolism; although no functional studies have been carried out. Both TRPM4 and TRPM5 have been identified in magnocellular but not parvocellular regions of the PVN by confocal immunofluorescence in the rat, with differential expression dependant on the area of the neurone (Teruyama *et al.*, 2011).

It is evident that TRPs are necessary for cell homeostasis; they are of particular importance due to their role in Ca^{2+} regulation (reviewed by (Clapham, 2003)). As the PVN is involved in maintaining homeostasis itself, these channels may be of importance in sensing environmental changes and altering excitability of preautonomic neurones accordingly. These channels with be discussed in further detail in Chapter 2 and 3).

1.4.2.5 Others

A variety of additional ion channels exist, which have varying functions in the cell and may be present within this area of the brain, each contributing to the resting membrane potential and with the ability to modulate firing activity.

Surprisingly, although dogma states that anion channels, such as chloride channels, would be present in the plasma membrane of all cells, no studies have been

reported on their presence in the PVN. Chloride channels are functionally and structurally diverse with a range of functions such as cell volume regulation, regulation of pH and cell membrane potential control. As one of the main functions of these channels is to regulate excitability of neurones it is likely that chloride channels would be present with the PVN (Hille, 1986).

Acid-sensing ion channels (ASICs) are proton-gated voltage-insensitive cation channels, responsible, as their names suggests, for sensing pH. Immunoreactivity has been shown to be high in the rat PVN for ASIC3, suggesting an acid sensing role for neurones within this area (Meng *et al.*, 2009).

Pacemaker activity of PVN hypothalamic neurones is modulated by a hyperpolarisation activated current (I*h*) (Shirasaka *et al.*, 2007). A family of channels, hyperpolarisation-activated, cyclic nucleotide-gated (HCN) channels, has been identified as responsible for this pacemaker activity in neuronal cells. A study by Monteggia et al (2000) identified four members of this family HCN1-4; verifying expression patterns throughout the rat brain. All members of this family were shown to be present within the PVN; with expression profiles for mRNA ranging from weak for HCN2 to extremely strong for HCN3.

Although some excellent reviews have been published discussing receptors and neurotransmitters within the PVN (Nunn *et al.*, 2011; Pyner, 2009; Pyner, 2014), nothing has been written summarising the ion channels and their functions in this area. I have therefore summarised the findings of the existing literature in Table 2 and will discuss some of these channels in more depth in this thesis.

Table 2 Summary of the ion channels identified in the PVN and their known roles

Ion channel family	General Role	Subtype Identified	Method	Relevance	Reference
Potassium channels					
K_V Voltage-activated	Controlling action potential characteristics, modulate neuronal excitability	K_V1.1 and K_V1.2	Immunohistochemistry, patch clamp electrophysiology	Downstream effectors of NO on synaptic GABA release	(Chung *et al.*, 2001; Yang *et al.*, 2007)
		K_V1.4 and K_V4.3	Immunohistochemistry	"A"-type K^+ current	(Sonner *et al.*, 2008; Sonner and Stern, 2007; Sonner and Stern, 2005)
		K_V1.2, K_V1.3, K_V1.4, K_V4.1, K_V 4.2 and K_V4.3	Patch clamp electrophysiology and RT-PCR	↑ expression of K_V4.2 and K_V4.3 in "type I" neurones	(Lee *et al.*, 2012)
K_{Ca} Calcium-activated	Regulate neuronal excitability. Contribute to after-hyperpolarisation	BK	Immunohistochemistry	Voltage-dependant	(Sausbier *et al.*, 2006)
		SK1, SK2 and SK3	Immunohistochemistry, patch-clamp electrophysiology, targeted *in vivo* injections	Inhibition leads to ↑ excitability, ↑RSNA, ↑SSNA ↑HR, ↑BP Decreased functionality ↑hyperexcitability	(Chen and Toney, 2009; Gui *et al.*, 2012; Kohler *et al.*, 1996; Pachuau *et al.*, 2014)
K_{ATP} ATP-sensitive	Modulate excitability	-	Patch-clamp electrophysiology, computational modelling	Adenosine ↓excitability via adenosine receptors	(Lewis *et al.*, 2010; Li *et al.*, 2010)
GIRK g-protein coupled inwardly rectifying	Synaptic inhibition through activation of GPCRs	GIRK1, GIRK2 and GIRK3	Immunohistochemistry, *in situ* hybridisation	Role in presynaptic inhibition of neurotransmitter release?	(Morishige *et al.*, 1996; Saenz del Burgo *et al.*, 2008; Shirasaka *et al.*, 2007)
Sodium channels					
Na_V Voltage-activated	Generate and propagate action potentials	Type I, type II and type III	Immunohistochemistry, RT-PCR	Expression profiles: Type I weak Type II and III strong	(Black *et al.*, 1994; Furuyama *et al.*, 1993; Jarnot and Corbett, 2006; Westenbroek *et al.*, 1989; Whitaker *et al.*, 2001)
ENaC Epithelial sodium channel	Sodium homeostasis	-	*In situ* hybridisation	Weak immunoreactivity	(Teruyama *et al.*, 2012; Wang *et al.*, 2010)
Calcium channels					
Ca_V Voltage-activated	Involved in muscle contraction and excitation	L-type (Ca_V1.x)	Immunohistochemistry	-	(Chin *et al.*, 1992; Hetzenauer *et al.*, 2006)

	of neurones	T-type ($Ca_V3.x$) ($Ca_V3.1$)	Patch clamp electrophysiology, RT-PCR, immunohistochemistry	Activation leads to depolarisation, regulates action potential generation, bursting behaviour and pacemaker activity Generate low-threshold spike.	(Lee *et al.*, 2008; Luther *et al.*, 2002; Luther and Tasker, 2000; Perez-Reyes, 2003; Perez-Reyes, 1999; Sonner and Stern, 2007; Stern, 2001; Tasker and Dudek, 1991)
Transient receptor potential channels					
TRPC Canonical Store-operated	Calcium homeostasis, open with ↓ Ca^{2+}	TRPC4 and TRPC5	RT-PCR	-	(Fowler *et al.*, 2007)
TRPV Vanilloid (see Chapters 3 and 4)	Mechanosensitive and homeostatic roles	TRPV1	Radiolabelling, patch clamp electrophysiology	Activation leads to glutamate release and postsynaptic firing Co-localised with liver-related neurones	(Li *et al.*, 2004b; Roberts *et al.*, 2004; Zsombok *et al.*, 2011)
		TRPV2	Immunohistochemistry	Regulates body fluid homeostasis, autonomic control and metabolism?	(Nedungadi *et al.*, 2012)
		TRPV4	Immunohistochemistry, Western blot	↑ expression contributes to inappropriate vasopressin release in cirrhosis	(Carreno *et al.*, 2009)
TRPM Melastatin (see Chapter 3)	Sensor/homeostatic roles, exhibit temperature sensing properties	TRPM4 and TRPM5	Confocal immunofluorescence	Differential expression dependent upon area of neurone	(Teruyama *et al.*, 2011)
Others					
ASICs Acid-sensing	pH sensing	ASIC3	RT-PCR, Western blot	-	(Meng *et al.*, 2009)
HCN Hyperpolarisation-activated, cyclic-nucleotide-gated	Modulating pacemaker activity	HCN1-4	RT-PCR	Hyperpolarisation activated current responsible for pacemaker activity	(Monteggia *et al.*, 2000; Shirasaka *et al.*, 2007)

1.5 Functional role of the PVN

Extensive information has been acquired on the projections and influences on the autonomic nervous system of the presympathetic neurones of the PVN, with clear evidence suggesting altered function during cardiovascular disease (Floras, 2009; Patel, 2000). Evidence also suggests that the PVN has multiple and diverse roles, including involvement in stress, circadian rhythm and thermoregulation (for review see (Nunn *et al.*, 2011)).

1.5.1 Role of the PVN in cardiovascular control

Due to their influence on the SNS the neurones of the PVN have been implicated in the control of the cardiovascular system in various ways, such as; regulating the cardiac sympathetic afferent reflex (Zhong *et al.*, 2008a), blood volume regulation (Lovick *et al.*, 1993), circadian regulation of blood pressure (Cui *et al.*, 2001) and the cardiovascular response to stress (Jansen *et al.*, 1995a). Stimulation of the PVN in rodents (via electrical or pharmacological means) in a number of studies has resulted in rapid rises in heart rate, blood pressure and RSNA (Duan *et al.*, 1997; Kannan *et al.*, 1989; Kawabe *et al.*, 2009; Martin *et al.*, 1993; Martin *et al.*, 1991; Schlenker *et al.*, 2001; Zhang *et al.*, 1997). These parameters appear to be fundamentally regulated by a careful balance of the neurotransmitters GABA, glutamate and NO in the PVN as discussed above (Kawabe *et al.*, 2012; Martins-Pinge *et al.*, 2012).

Importantly studies in humans, sheep and rodents suggest that an increase in sympathetic drive, combined with a dysregulation of the baroreceptor reflex is

linked to an increased incidence in cardiovascular disease and heart failure (Floras, 2009; Grassi *et al.*, 2003; Patel, 2000; Ramchandra *et al.*, 2013;). In these cases elevated SNA has been linked to a combination of loss of nNOS expression, reduced GABA sensitivity of PVN neurones and an increase in glutamate/glutamate sensitivity (Carillo *et al.*, 2012; Li *et al.*, 2003c; Zhang *et al.*, 2002a; Zhang *et al.*, 1998). In support of this, inhibition of the PVN ameliorates the elevated SNA of spontaneously hypertensive rats (Allen, 2002; Itoi *et al.*, 1991). Furthermore, *in vivo* studies in rats suggest a reduction in the inhibitory actions of GABA leads to the increase in RSNA and BP seen in heart failure. Injections of the GABA agonist muscimol showed decreased effectiveness in reducing the RSNA and BP of rats with heart failure compared to control rats (Zhang *et al*., 2002a). In another study, cardiac SNA and baroreceptor control of cardiac SNA were restored in sheep given a intracerebroventricular infusion of the NO donor sodium nitroprusside. This study summised that a loss of inhibitory NO may be crucial to the increased sympathetic drive seen in heart failure (Ramchandra et al., 2014).

Due to the location, integration, and cardiovascular role of parvocellular neurones of the PVN they could be considered a prime target for potential therapeutics (Ferguson *et al.*, 2008). However, there is currently a distinct lack of integration of *in vitro* studies detailing the pathways and ionic mechanisms responsible for the cardiovascular control they demonstrate *in vivo*.

1.5.2 Role of the PVN in regulation of metabolism and thermogenesis

Body temperature is tightly controlled, with small changes in core body temperature resulting in several serious physiological issues (recently reviewed by

(Gomez, 2014)). In rats, body temperature is raised by the activation of interscapular brown adipose tissue (BAT) which increases thermogenesis, and tail artery vasoconstriction, which reduce heat loss, mediated by the SNS. Efferent projections from the dorsal and medial parvocellular PVN to BAT have been identified using pseudorabies viral tracing in Siberian hamsters (Bamshad *et al.,* 1999). The median and medial preoptic nuclei are known to receive thermal inputs, sending projections directly to the RPa and via the DMH-PVN projections to influence BAT sympathetic activity (ter Horst and Luiten, 1986; Thompson et al, 1996; Zaretskaia et al, 2008; Zhang et al 2011). A role for PVN neurones in regulation of metabolism and thermogenesis can be inferred from these projections, and further studies show increased sympathetic drive to BAT via microinjection of excitatory glutamate into the PVN of rats (Amir, 1990; Yoshimatsu *et al.*, 1993). However, Inenaga et al (1987) were the first to show the presence of thermosensitive neurones in the PVN itself. Using patch-clamp electrophysiology in rat brain slice both cold-sensitive and heat-sensitive neurones were identified in the PVN (Inenaga *et al.*, 1987). There have since been several studies demonstrating a role for the PVN in thermoregulation and thermogenesis (Cham and Badoer, 2008; Cham *et al.*, 2006a; Chen *et al.*, 2008; Leite *et al.*, 2012).

Poly-synaptic tracing using the pseudorabies virus in rats identified spinally-projecting neurones of the PVN specifically as being directly involved in thermoregulation (Smith *et al.*, 1998). The function of this pathway remains unknown, although sympathetic outflow via the PVN is hypothesised to affect the tails vascularisation, resulting in heat loss. Furthermore, exposure to heat has been shown to activate spinally-projecting neurones of the PVN, increasing c-fos

expression in these neurones (Bratincsak and Palkovits, 2004; Cham *et al.*, 2006a). RVLM projecting preautonomic neurones from the PVN have also been shown to be activated upon heat exposure (Cham and Badoer, 2008). In further studies, blockade of PVN neurones with lidocaine resulted in blunted RSNA, heart rate and blood pressure responses to heat stress, adding to evidence suggesting a thermosensing role within this region. In addition, this group also show heat loss through skin dilation depends on an NO mechanism within the PVN (Leite *et al.*, 2012). Furthermore, recent study showed a role for the PVN directly in thermogenesis (Cabral *et al*., 2012). Thyrotropin releasing hormone neurones (a neuropeptide necessary for cold-induced thermogenesis), located in the PVN, were were co-localised with c-fos under acute cold conditions, suggesting activation of these neurones (Cabral *et al.*, 2012). In addition, a study by Madden and Morrison (2009) showed an inhibitory role for preautonomic PVN neurones on BAT and slight decreases in SNA have been observed upon injection of the anoexigenic chlolecytokinin (Madden and Morrison, 2009; Yoshimatsu *et al.*, 1992).

Various studies using lesioning techniques and injections of various peptides into the nucleus results in either overeating and obesity, or reduced eating and anorexia (for review see (Leibowitz, 2007)). These studies provide direct evidence that neurones within the PVN have a role in the control of food intake and metabolism. One such peptide is the adipocyte-derived hormone leptin, which is known to reduce body weight through an inhibition of food intake and an increase in energy expenditure. ICV injection of leptin activates STAT3 phosphorylation in oxytocin neurones within the parvocellular PVN of rats. This study concluded that oxytocin neurones within the PVN mediate the effects of leptin on body weight in diet

induced obese rats and may be important for body weight control in both obese and control animals (Perello and Raingo, 2013). In a study by Jhanwar-Uniyal et al (1993), injections of neuropeptide-Y into the PVN stimulated feeding behaviour and specifically carbohydrate intake in rats (Jhanwar-Uniyal *et al.*, 1993). Furthermore, implants of steroid hormones such as corticosterone and aldosterone, into the PVN have stimulatory effects on carbohydrate and fat intake respectively (Tempel *et al.*, 1993).

Increases in blood pressure, heart rate and SNA to metabolic tissues have been observed by several groups when using glucagon-like peptide-1 in rodents (GLP-1: a neuropeptide that is known to control feeding and drinking behaviour) agonists (Baraboi *et al.*, 2011; Nunn *et al.*, 2013; Yamamoto *et al.*, 2002). Independent of the route of administration in these studies, injection of the GLP-1 agonist, exendin-4 produces increased c-fos response in the PVN and other brain regions in the rodent hypothalamus associated with sympathetic control, as well as in the medulla and spinal cord (Nunn *et al.*, 2013; Yamamoto *et al.*, 2002).

Although evidence suggests a clear role of the preautonomic neurones in metabolism and thermoregulation, even linking thermosensing to cardiovascular control, little is known about how these processes occur. The mechanisms responsible for thermosensation will therefore be explored in Chapter 3.

1.5.3 Role of the PVN in glucose control

Central glucose sensing is incredibly complex, involving different types of "glucose-sensing" neurones, with glucose-excited and glucose-inhibited cells identified in the

hypothalamus. In order to control glucose the brain receives input from various sensors such as the liver, carotid body and small intestine as well as glucose-sensing neurones within the brain itself (for review see (Levin, 2006)). To further complicate this, glucose levels in the brain are vastly lower than circulating plasma levels, as a protective measure for neuronal cells (glucose concentration in the VMH has been reported to be ~20% of levels recorded in the blood (de Vries *et al.*, 2003)). Due to these low levels found in the brain glucose-sensing neurones can be activated at low central glucose concentrations. PVN spinally-projecting neurones, initially receiving signals from GABAergic neurones from the SCN, are able to control plasma glucose concentrations in the rat via sympathetic innervation of the liver (Kalsbeek *et al.*, 2004). The role of the PVN in glucose sensing has been controversial, with lesioning studie by Sakaguchi et al (1988) showing no differences in SNA to autonomic neurones innervating the brown adipose tissue when rats received microinjections of excitatory kainic acid (Sakaguchi *et al.*, 1988). A reduction in SNA in this study was, however, observed in VMH lesioned animals. In a further study following microinjection of glucose or insulin into PVN there was a brief, yet small response to both challenges. Although the role of the PVN in glucose control was seemingly controversial at the time, later studies provide indirect evidence of this role by way of increased c-fos expression in the PVN in rats given intracarotid and peripheral injections of glucose (Carrasco *et al.*, 2001; Dunn-Meynell *et al.*, 1997). Further direct evidence by way of electrophysiology recording from brain slice show modulation of firing activity in preautonomic neurones of the PVN by hypoglycaemia, potentially in part driven by inhibition of K_{ATP} (Lewis *et al.*, 2010). In addition, a recent study in rats confirmed the presence of both glucose-

inhibited and glucose-excited neurones at low concentrations of glucose within the parvocellular PVN (Melnick *et al.*, 2011). Although, surprisingly, this study ruled out a role for K_{ATP} channels, the mechanisms for this glucose-sensing still remain a mystery.

1.5.4 Role of the PVN in blood volume

Changes in blood volume are regulated separately from blood pressure. Atrial stretch receptors sense changes in blood volume, expanding to accommodate any increase in volume with small changes in blood pressure. Small decreases in volume are dealt with by replenishing volume from splanchnic capacitance vessels (Greenway and Lister, 1974). A reflex (Bainbridge reflex) increase in heart rate leading to changes in the blood volume has been observed following activation of volume receptors, allowing the body to maintain fluid balance. Spinally-projecting PVN neurones in the rat have been suggested to be involved in the response to changes in blood volume in addition to their role in the regulation of blood pressure (Lovick *et al.*, 1993; Lovick and Coote, 1989; Lovick and Coote, 1988). Furthermore, in the rat, atrial stretch receptors were stimulated mechanically via insertion and inflation of a balloon placed at the junction of the superior vena cava and the right atrium. Inflation of the balloon resulted in inhibition of RSNA and repetitive inflation activated neurones located in the parvocellular area of the PVN, indicated by increased c-fos expression using immunohistochemistry (Pyner *et al.*, 2002). This has also been shown to result in a reflex increase in heart rate and leads to diuretic and natriuretic responses dependant on the afferent neural projections from cardiac receptors in conscious dogs, effects shown to be absent in cardiac

dennervated animals (see Figure 1.2) (Fater *et al.*, 1982). Further evidence shows activation of PVN neurones by targeted injections led to an increased pressor response, decreasing RSNA, and increasing splanchnic, adrenal and cardiac SNA. Interestingly, stimulation of neurones within the PVN using targeted injections at different sites, mainly located in the dorsal parvocellular region, led to an increase in RSNA in rabbits, which was reversed to a decrease by reducing the volume of injection (Deering and Coote, 2000). These differences observed in RSNA activity when stimulating the PVN is interesting, and could be as a result of species differences between rabbits and rodents. As many of these observations have been made by inducing stretch using implanted balloons in the branch of the vena cava and atrium, it is interesting to note the effects of removal of blood in rats has the same effects (Badoer *et al.*, 1993). Further studies by the same group, also showed increased expression of c-fos within the PVN in response to volume load, accompanied by a pressure change (Badoer *et al.*, 1997), a result which was not observed to the same extent in rabbits with heart failure (Akama *et al.*, 1998).

This body of evidence strongly suggests that neurones within the parvocellular PVN have a clear role in blood volume regulation, and it has been implicated that these are the same neuronal projections that affect blood pressure and heart rate during heart failure.

1.5.5 Role of the PVN in osmosensing

Body fluid osmolality is usually regulated within a narrow range (~290-300 mOsm). Although this is controlled largely through regulation of kidney function several areas within the central nervous system work to sense and maintain osmolality. In

particular, the area surrounding the third ventricle within the hypothalamus is particularly important for osmoregulation. Key areas identified to date include the SFO, OVLT, circumventricular organs, MPo and the PVN itself (Stocker and Toney, 2005; Stocker *et al.*, 2007; Toney *et al.*, 2003).

Previous studies in rodents show that application of hypertonic saline to the hypothalamus increases blood pressure (Bourque, 2008; Chen and Toney, 2001; Chu *et al.*, 2010) whereas hypotonic challenge decreases SNA, blood pressure and heart rate (Bourque and Oliet, 1997). This suggests that changes in osmolality affect the neurones projecting to the autonomic centers controlling the cardiovascular system (Nunn *et al.*, 2011; Toney *et al.*, 2003). As osmotically sensitive projections exist from both the SFO and MPo to the PVN, a role for the neurons within the PVN itself in osmosensing has been widely discussed. A clear role has been established for the neuroendocrine vasopressin neurones within the magnocellular region and a potential for this role in the parvocellular population has been discussed (Bourque, 2008; Bourque and Oliet, 1997). In a study by Yamashita et al (1988) altered excitability in mouse neurones throughout both regions of the PVN exposed to either NaCl or mannitol was observed (Yamashita *et al.*, 1988). This is a particularly important experimental design due to its use of mannitol to alter osmolality rather than solely NaCl, which will effect ionic concentrations. This study suggests both the magnocellular and parvocellular regions have osmosensing capabilities. Several investigations have shown that water deprivation increases expression of c-fos in pre-autonomic parvocellular neurones of the PVN (Arnhold *et al.*, 2007; Gottlieb *et al.*, 2006; Stocker *et al.*, 2004). Although an increase in osmolality could be responsible for the increase

seen in c-fos, it is equally as possible this is due to changes in blood volume (as discussed above) or the effects of altering ion concentrations (such as sodium). Further studies showing increases in action potential firing of spinally-projecting parvocellular neurones with hypertonic saline provide further evidence for a osmosensing role, although the authors suggest this is due to an NaCl sensitivity rather than the change in osmolality (Chu *et al.*, 2010). This is a recurring issue for some investigations into central osmosensing and as a result the mechanisms responsible for a potential role for osmosensing of parvocellular PVN neurones are not yet clear. Furthermore, it is important to identify whether these neurones themselves "sense" osmolality, or merely receive projections from the circumventricular organs in response to osmolality changes. Therefore the subject of osmosensing is investigated within this body of work, with particular focus on the parvocellular area of the PVN and specifically exploring changes in osmolality rather than ion concentrations (see Chapters 3, 4 and 6).

1.5.6 Role of the PVN in the stress response

"Stress" is a widely used term for when an animal responds to a challenge, whether this stressor is chemical or environmental in nature. As an initial response to stress the "fight-or-flight" response is activated via the SNS (Jansen *et al.*, 1995a). Cardiovascular responses have been recorded in a variety of "stressful" situations; in humans even the anticipation of exercise leads to increases in heart rate and blood pressure (Everson *et al.*, 1996) and performing mental arithmetic elicits similar responses (for review see (Herd, 1991)). In addition to this it has been clearly shown that simple laboratory routines, such as moving an animal's cage,

result in increases of hormonal markers of stress, including plasma corticosterone, as well as elevated heart rate and blood pressure (Balcombe *et al.*, 2004). Although these pressor responses are normal in reaction to stressful stimuli, if this response becomes excessive it has been shown to result in pathological increases in blood pressure and heart rate (Folkow, 2001; Rozanski *et al.*, 1999). It is therefore important to understand how this stress response occurs and how this mechanism can lead to pathogenesis.

The second, delayed response to stressful stimuli involves activation of the HPA axis, mediating glucocorticoid hormones (cortisol in humans and corticosterone in rodents). Circulation of these hormones determines the longer lasting behavioural, neural and hormonal response to stress; the PVN is central to the HPA component of stress (Flak *et al.*, 2014; Herman and Cullinan, 1997; Herman *et al.*, 2002a; Herman *et al.*, 2002b; Lucassen *et al.*, 2014; Maguire, 2014; Myers *et al.*, 2012; Tavares *et al.*, 2009). Chronic stress, however, leads to HPA axis dysregulation and an elevated sympathetic response (Cerqueira *et al.*, 2008). Research suggests that both neuroendocrine and preautonomic neurones in the PVN elicit physiological responses to stress and as the PVN has been shown to exert such a powerful influence on the cardiovascular system; it seems likely that preautonomic neurones would be involved. Several studies in rats support a role for the PVN in this function, with trans-synaptic viral labelling studies showing a direct coupling between the PVN and the stellate ganglion (supplying sympathetic innervation to the heart); a link for this nucleus in the stress response has been established (Jansen *et al.*, 1995a). Later, Duan et al (1997) showed that cardiovascular responses to stress in rabbits can be mimicked by electrical stimulation of the PVN

(Duan *et al.*, 1997). In addition, cardiovascular responses to restraint stress can be abolished by microinjection of a non-specific blocker of synaptic transmission directly into the rat PVN (Busnardo *et al.*, 2010). Furthermore, glutamatergic innervation of parvocellular PVN neurones expressing corticotropic-releasing hormone has been shown to be activated with chronic stress in rats (Flak *et al.*, 2009).

Although a role for the parvocellular preautonomic neurones of the PVN in this response is likely, the mechanisms which lead to this elevation in sympathetic drive are so far unknown. Neurotransmitters such as the tachykinins have been linked to the stress response in several studies (Culman and Unger, 1995; Herman and Cullinan, 1997; Jansen *et al.*, 1995a) (reviewed by (Aguilera, 1994)). The pathway and central areas responsible for this response are not yet known, but tachykinin receptors are present within the parvocellular PVN (Koutcherov *et al.*, 2000a; Nakayama *et al.*, 1992). Furthermore, *in vivo* studies have shown that tachykinins are important for sympathetic nervous activity, and therefore cardiovascular control as well as endocrine and behavioural responses to stress (Culman and Unger, 1995). Substance P, a tachykinin found at high levels in the PVN (Jessop *et al.*, 1991), has been shown to activate spinally–projecting neurones within the parvocellular PVN in electrophysiology rat brain slice experiments (Womack *et al.*, 2007).

However, controversy still remains in this field, with some groups arguing that it is the DMH which plays an integral part to the stress response (DiMicco *et al.*, 1995; Fontes *et al.*, 2001b; Stotz-Potter *et al.*, 1996). In a study performed by Stotz-Potter

et al (1996) cardiovascular response to air jet stress was alleviated by microinjection of the $GABA_A$ antagonist, bicuculline, into the DMH, but not the PVN (Stotz-Potter *et al.*, 1996). It has therefore been suggested that these observed differences may be due to the form of stress used, or the methodology used, as there is some discussion as to the role of GABA in this function (Womack *et al.*, 2007).

The topic of the function of the PVN in the stress response is obviously a complicated, yet interesting one. I will therefore discuss this further in Chapters 7 and 8.

1.5.7 Role of the PVN in circadian rhythm

Circadian rhythm is mainly controlled by the hypothalamus; of particular importance is the SCN. The SCN is known to be the primary circadian pacemaker in mammals, and has been shown to express several clock gene products (Reppert and Weaver, 2002; Tei *et al.*, 1997). Using electrophysiological studies it has been shown that neurones in this area have cyclically changing membrane potentials which allow general changes in activity on a 24 hour rhythm (Belle *et al.*, 2009; Brown and Piggins, 2007). As described previously, the SCN has excitatory and inhibitory projections to both neuroendocrine and autonomic regions of the PVN. (Cui *et al.*, 2001; Hermes *et al.*, 1996; Kalsbeek *et al.*, 2008).

Several studies have shown that secretion of the stress hormone corticosterone involves preautonomic neurones within the PVN projecting to the IML, as well as the HPA axis. These projections have been shown to determine daily changes in sensitivity of the adrenal gland to ACTH (Buijs *et al.*, 1999; Kalsbeek *et al.*, 1996;

Kaneko *et al.*, 1980). Furthermore, in a study performed by Kalsbeek et al (2000) bilateral injection of the GABA antagonist bicucullin into the rat PVN prevents light-induced inhibition of the hormone melatonin. In this study they concluded that the SCN regulated melatonin release via their GABAergic projections to the PVN (Kalsbeek *et al.*, 2000). It was also found that lesioning the PVN results in a lower night-time level of melatonin, whereas SCN lesion results in permanently high levels of melatonin. This study is supported by the work of Cui et al (2001), who showed subsequent to SCN stimulation identified spinally-projecting neurones of the PVN were inhibited by GABA in an electrophysiological study in rat brain slices. These results combined support a role for the PVN in setting circadian rhythm (reviewed by (Buijs *et al.*, 2003)). In addition, recent work by Kalsbeek et al (2008) showed activation of the PVN by glutamatergic agonists or GABAergic antagonists led to hyperglycaemia. In this work it was shown that GABAergic and glutamatergic innervations of the preautonomic neurones in the PVN from the SCN impact on the circadian control of plasma glucose via sympathetic projections to the liver (Kalsbeek *et al.*, 2008).

Studies have also shown that the 24 hour cyclic changes observed in membrane potential and hormonal levels are paralleled by changes in rodent heart rate (Nunn *et al.*, 2013). Human blood pressure follows a circadian rhythm being lower at night and rising again in the morning, just before waking (Kawano, 2011; Millar-Craig *et al.*, 1978). Interestingly, in some cases of hypertension, as well as an elevation in blood pressure, disturbed circadian patterns of blood pressure have also been observed (Head and Lukoshkova, 2008). In fact, in several studies blood pressure

has failed to decrease as is usual during night-time periods (Pickering, 1990; Pierdomenico *et al.*, 2014; Verdecchia *et al.*, 1995).

With this combined knowledge it has therefore been speculated that preautonomic neurones within the PVN may play a role in setting the circadian control of cardiovascular parameters such as blood pressure and heart rate. The role of the PVN in circadian rhythm is discussed further in Chapter 7.

1.6 Aims

There are several aims to this body of work studying the paraventricular nucleus. Firstly, to better understand the role of the parvocellular cells within this nucleus, it is important to characterise the ion channels present and their function using a combination of patch-clamp electrophysiology, calcium imaging, computer modelling and immunofluorescence techniques. Once this has been achieved, this knowledge can be used to see how this translates *in vivo* by recording cardiovascular parameters. Secondly, the role of the PVN in relation to stress is somewhat controversial, therefore this role will be further explored using lesioning and telemetry techniques *in vivo.*

2 Methods

2.1 Animals

CD1 mice and Wistar rats were purchased from Charles River (UK), and kept under standard 12hr/12hr light/dark conditions with unlimited access to water and normal chow diet. All animals were sacrificed by Schedule 1 methods, unless otherwise stated. All experiments were approved by the Home Office, UK.

2.2 Immunofluorescence

2.2.1 Immunofluorescence preparation

Animals were anaesthetised with an intraperitoneal (IP) injection of pentobarbitone sodium 20% (Pentoject, AnimalCare, UK). Hind limb withdrawal reflex was then checked in order to determine if the animal was fully anaesthetised. An incision was made laterally down the body. Using blunt dissection and cutting through the ribcage the heart was exposed and the right atrium was cut. The animals were then perfused with PBS intracardially until the circulatory system was completely flushed through. This was followed by perfusion of 4% paraformaldehyde (PFA) to fix the tissues. Once fixed, the animals were decapitated and the brain was carefully removed. The brains were subsequently postfixed using 4% PFA and stored in the fridge overnight at 4^{o}C. They were then transferred to a 30% sucrose solution to dehydrate the tissue until being sliced on a cryostat.

2.2.2 Sectioning

Tissues were embedded in OCT mounting medium (Thermo Scientific, UK) and frozen on a chuck in a Leica cryostat at around -27^{o}C. Sections were cut to 14µm thickness and then placed on a Superfrost slide (Thermo Scientific, UK). Slides were kept at -80^{o}C until use.

2.2.3 Staining protocol

14µm cryostat sections were removed from storage at -80^{o}C left at room temperature for 10 minutes to air dry and warm up. Slides were then washed for 5 minutes with PBS and subsequently blocked for 1 hour at room temperature in blocking solution (PBS 0.25% Triton X-100 and 10% Donkey serum). Sections were then incubated overnight at 4^{o}C with the appropriate primary antibody diluted in blocking solution (details below). After incubation overnight the slides were then washed three times for 15 minutes in PBS. They were then incubated in the dark for 1 hour at room temperature with secondary antibody diluted in blocking solution (details below). Sections were then washed a further three times for 15 minutes in the dark and mounted with VECTASHIELD mounting medium with DAPI (Vector laboratories, UK), left to air dry, sealed and stored at 4^{o}C in the dark.

2.2.4 Antibodies

In order to show the presence of the TRPV4 channel within the PVN immunofluorescence was performed using the primary antibody for TRPV4 (1:300; Abcam, UK), and secondary antibody anti-rabbit CY3 raised in goat (1:300; Abcam,

UK) and blue DAPI nuclei staining using VECTASHIELD mounting medium with DAPI (Vector laboratories, UK). Negative controls involved primary antibody omission, with the addition of the secondary antibody anti-rabbit CY3 raised in goat (1:300; Ex 548 nm; Em 561 nm; Abcam, UK). Low magnification images were collected with x10 Nikon plan Fluor dic L/N1 and x20 Nikon plan Fluor objectives limited through a DAPI filter set (Ex 365 nm with 30 nm bandpass; Em 440 nm with 40 nm bandpass) and TRITC filter set (Ex 535 nm with 36nm bandpass; Em 590 with 34 nm bandpass) mounted on a Nikon TE2000 microscope (Nikon, UK).

For confirmation of loss of the neurokinin-1 (NK1) receptor within the PVN, immunofluorescence was performed using primary antibody anti-rabbit Neurokinin-1 receptor (1:500; Abcam, UK) combined with the secondary antibody donkey anti-rabbit Dylight 594 (1:2000; ; Ex 593 nm; Em 618 nm; Abcam, UK) and blue DAPI nuclei staining (as above). Negative controls involved primary antibody omission, with the addition of the secondary antibody donkey anti-rabbit Dylight 594 (1:200; Abcam, UK). Low magnification images were collected with x10 Nikon plan Fluor dic L/N1 and x20 Nikon plan Fluor objectives using a DAPI filter set (Ex 365 nm with 30 nm bandpass; Em 440 nm with 40 nm bandpass) and Texas Red filter set (Ex 560 nm with 20 nm bandpass; Em 610 nm with 60 nm bandpass) mounted on a Nikon TE2000 microscope (Nikon, UK).

2.3 Tissue Dissection

2.3.1 Brain slice preparation

CD1 mice were euthanized by cervical dislocation followed by decapitation. The brain was swiftly removed and briefly placed in ice-cold low-Na^+ high-sucrose artificial cerebrospinal fluid (Low Na^+ ACSF (50mM sucrose); Table 3). The hypothalamus was then blocked and glued to a slicing stage. Coronal slices 200-300 µm thick were sliced using a Campden Instruments Ltd 752 M Vibroslice/Leica VT1000S. Slices were stored in a multiwell dish containing physiological ACSF (Table 3) and maintained at 35-37^oC in a water bath. Physiological ACSF solution was continuously perfused with 95% O_2/5% CO_2 in order to oxygenate the slices and maintain pH 7.4. Slices were then left to recover for at least 1 hr before recording. When ready to record from slices were placed in a recording chamber superfused constantly with isotonic/physiological ACSF, gassed with 95% O_2/5% CO_2 and left for at least 5 minutes to equilibrate.

2.3.2 Cell culture isolated cells

Connective tissue and other cell types such as glial cells increase in number as animals become older and proliferation of neuronal cell types decreases with age (Kuhn *et al.*, 1996). For these reasons young animals are used for cell culture, as to gain a purer population of proliferative neurones and reduce the need for enzymatic digestion as much as possible. Wistar rats aged 2-6 days were euthanized by cervical dislocation followed by decapitation. The brain was swiftly removed and stored in sterile ice-cold phosphate-buffered saline (PBS) while the

hypothalamus was blocked and glued to a slicing stage (Barrett-Jolley *et al.*, 2000). Hypothalamic brain slices were cut to 600 µm on a Campden Instruments Ltd 752 M Vibroslice/Leica VT1000S and a bilateral punch of the PVN area was made using a fire polished glass pipette (Figure 2.1). The tissue was then transferred to Neurobasal™ medium supplemented with 0.5mM L-glutamine (Sigma-Aldrich, UK) to improve neuronal growth via cell signalling, 2% penicillin/streptomycin and 1% amphotericin (Sigma-Aldrich, UK) to prevent infection. The suspension was triturated using a fire polished pipette until the cells were fully dispersed, centrifuged at 1400 RPM and the supernatant removed and the pellet was re-suspended in fresh media. This was repeated twice more to wash the cells before finally re-suspending in 2 ml Neurobasal™ medium supplemented as above plus 10% Fetal calf serum (FCS) and 10% B27 supplement; specifically used for culturing neuronal cells and transferred to 6-well plates (typically 3 punches per well). Cells were then incubated at 37°C for cells to grow in a monolayer culture. Once cells reached sufficient confluence (70%-100%) they were used for electrophysiological or calcium ratiometic recording.

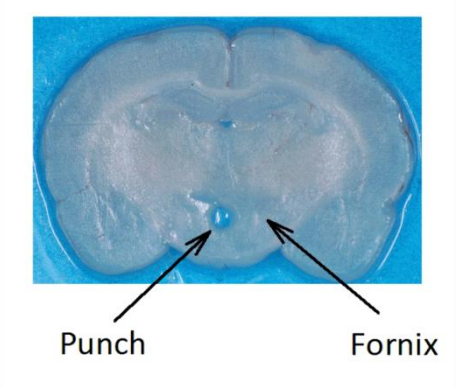

Figure 2.1 Example of a PVN tissue punched out of coronal section of a rat brain.

All cell culture reagents were from Invitrogen, UK, unless stated otherwise.

2.4 Electrophysiology

Electrophysiological recordings were performed either using brain slices whereby the PVN was located based on location and specific markers i.e fornix, or on isolated neuronal cells dissected and prepared as stated above.

All electrophysiological recordings were made using an Axopatch 200b amplifier (Molecular Devices Axon Instruments, USA). Low-pass filtering was set to 1 kHz and data digitised at 5 kHz with a Digidata 1200B interface. Neurons were visualised using a Hitachi KP-M3E/K CCD camera attached to a Nikon Eclipse microscope with an effective magnification of ~1000x.

Thick-walled patch-pipettes were fabricated using fire-polished 1.5 mm o.d. borosilicate glass capillary tubes (Sutter Instrument, Novato CA, USA supplied by Intracel, UK). They were pulled using a two-step electrode puller (Narishige, Japan) and filled with the appropriate pipette solution. When filled pipettes had resistances of approximately 3-8 MΩ depending on the patch clamp method used (explained below). All solutions used for electrophysiology experiments are shown in Table 3 and Table 4. Junction potentials were calculated using JpCalc (Barry and Lynch, 1991) and are stated in Table 4. Osmolality for all solutions was measured using a freezing point Advanced Instruments 3MO Micro-osmometer (Advanced Instruments, Norwood, USA).

All reagents used in the electrophysiology were from Sigma-Aldrich, UK, unless stated otherwise.

2.4.1 Action current recording

Hypothalamic brain slices from CD1 mice were used for action current recordings from putative parvocellular neurones, identified based on their location and morphology. Action currents were recorded using cell-attached patch clamp methods in voltage clamp using the equipment stated above. Analogue data was further amplified with a Tektronix FM122 (Beaverton, Oregon) AC coupled amplifier. To achieve cell-attached patch a small amount of positive pressure was applied to a glass pipette electrode before being lowered into the bath solution. Glass pipettes used for these experiments were higher in resistance to obtain lower noise recordings. Neurones patched were chosen based on their size and morphology. Once neurones were visualised the pipette was moved to the surface of the brain slice and positive pressure was released. A small amount of negative pressure could then be applied in order to form a gigaseal and record action currents. Analysis of action current frequency was performed using WinEDR and a custom program designed to detect action currents based on adaptive upper and lower boundary thresholds. All action current data was normalised by action current frequency/initial average action current frequency.

2.4.2 Single channel recording

Single channel recordings were made using the equipment stated above, without the use of the Tektronix FM122. In order to obtain single channel recordings cell-attached patch clamp was used, using the methods described above a gigaseal was formed and channel activity was recorded. Single-channel all-points amplitude

histograms were created in WinEDR. Amplitudes were taken at various holding potentials and used to create current-voltage (*IV*) curves. Reversal potential (V_{rev}) and slope conductance (*g*) were then calculated from the equation of the fitted line. Open probabilities were obtained using the QuB software (Qin et al, SUNY, Buffalo, NY) using a K-sequential means method (Qin, 2004; Qin *et al.*, 1996).

2.4.2.1 Equilibrium potentials

Using the Nernst equation it is possible to calculate the equilibrium potential (*E*) that occurs due to the separation of charged ions as a result of the selectively permeable membrane of a cell. Due to the differential distribution of ions in the intracellular and extracellular solutions it is known where the equilibrium potential for each ion lies. Using the Nernst equation (Equation 2.1) it is possible to calculate the E for each ion within a solution.

Equation 2.1 $$\boldsymbol{E = -58 * z * log\left(\frac{[I]_{in}}{[I]_{out}}\right)}$$

Where; E is the equilibrium potential of the ion, z is the valency of the ion and $[I]_{in}$ and $[I]_{out}$ are the intracellular and extracellular concentrations of the ion, respectively.

When an ion channel is selectively permeable to only one ion *E* equates to the reversal potential (V_{rev}) of the channel at which the channel current is zero. V_{rev} can then be compared to the experimentally measured value taken from the *IV* curve.

2.4.3 Whole-cell current clamp

Whole-cell current clamp recordings were made on isolated Wistar rat PVN cells, dissected and prepared as described above. Once cells had reached appropriate confluence (70%-100%), cells were released from the culture flask after washing with Neurobasal^{TM} media free from FCS using 1x trypsin. The enzymatic reaction was then quenched with Neurobasal^{TM} media containing FCS, centrifuged at 1400 RPM, the supernatant removed and the pellet re-suspended in media without FCS. The cells were plated out onto glass shards where they were incubated at 37^{o}C for 1 hour to lightly adhere ready for patch clamping. Cells were used when freshly isolated, after first expansion and up to their third passage to avoid de-differentation. Cells were chosen to patch based on their size and morphology and resting membrane potential (RMP). Cells with depolarised (>-45 mV) or hyperpolarised (>75 mV) membrane potentials were excluded.

RMP recordings were made in current clamp using the equipment stated above. The glass pipettes used had resistances of 3-5 MΩ, typically lower than those used in cell-attached patch clamp experiments as to break through the membrane of the cell. In order to do this the methods are the same as stated above for cell-attached patch clamp, although a larger amount of negative pressure after forming a gigaseal can be used to rupture the membrane creating “whole-cell seal mode”. Membrane potential was recorded to WinEDR as the cells environment is changed via perfusion of bath solutions.

2.5 Intracellular calcium recording

2.5.1 Preparation of cells

Isolated Wistar rat PVN neuronal cells were used for intracellular Ca^{2+} measurements; dissected and prepared as described above. Cells were plated out onto glass-bottomed dishes after releasing from culture flasks with trypsin and pre-incubated with Fura-2AM (5 μM) (Invitrogen, UK) for a minimum of 30 minutes at 37^{o}C. Fura-2AM is a cell-permeable ratiometric dye, which binds to free Ca^{2+} once it has moved inside the cell and the acetoxymethyl groups are removed by cellular esterases (Grynkiewicz *et al.*, 1985). After incubation with the dye the cells were then washed with HEPES ACSF for around 15 minutes to allow complete de-esterization of the dye.

2.5.2 Intracellular calcium measurements

Fura 2-AM fluorescence was excited by 365 and 385 nm Opto-Light-Emitting Diodes (OptoLED; Cairn Research, UK) limited through a 355 nm filter with 10 nm bandpass and a long pass 380nm filter respectively. Fluorescence images were captured and analysed using an image system consisting of an inverted phase contrast microscope (Nikon Diaphot 300) with a ×40 Fluor Nikon objective (Nikon, UK), a PC-controlled digital charge-coupled device camera (Exi Aqua; QImaging, Surrey, Canada), and Micro-Manager 1.4 software (University of California, San Francisco, USA). Regions of interest were highlighted and Fura-2AM was excited alternatively at 355 nm and 380 nm using a high-speed wavelength switcher (Dual OptoLED power supply; Cairn Research, UK). Fluorescence emission was limited through a

510 nm filter with 80 nm bandpass and was measured at intervals of 2 s and ratios are determined from the intensities emitted when the cells are excited at 355 nm/380 nm. Intracellular Ca^{2+} concentration was subsequently calculated using Equation 2.2 (below), after calibration using the calcium ionophore A23187 (1 µM) to release maximum Ca^{2+} (R_{max}) and EGTA (5 mM) to quench Ca^{2+} (R_{min}) (Sigma-Aldrich, UK):

Equation 2.2 $$[Ca^{2+}] = K_d \frac{(R - R_{min})}{(R_{max} - R)}$$

Where K_d is the dissociation constant (taken as 145nM at room temperature) for Fura-2AM calcium-binding; R is the ratio; and R_{max} and R_{min} are the ratio values measured under conditions of saturating calcium levels (A23187) and in the absence of calcium (EGTA) respectively.

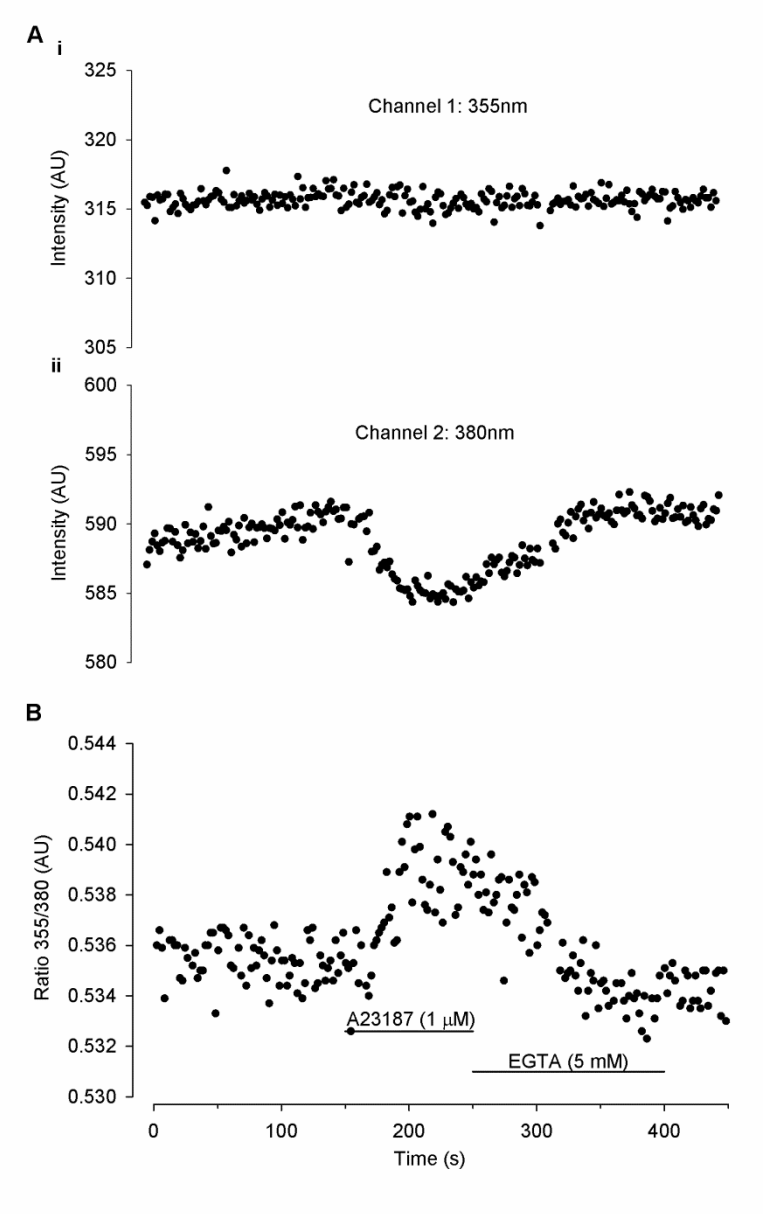

Figure 2.2 Calcium calibration using A23187 and EGTA.
(A) Raw trace of fluorescence intensities emitted upon excitation with **(i)** 355 nm and **(ii)** 380 nm with addition of the ionophore A23187 (1 μM) and Ca^{2+} chelator EGTA (5 mM). **(B)** Ratio of 355 nm/380 nm fluorescence intensities shown in (A). Ratios from the peak responses of A23187 and EGTA are used to obtain R_{max} and R_{min} respectively. These values are then used to calculate intracellular Ca^{2+} using Equation 2.2.

2.6 Drugs

Calcium ionophore A23187 (1 μM), 4-α-phorbol 12,13-didecanoate (4αPDD) (1 μM), GSK1016790A (100nM), RN1734 (5 μM), HC067047 (300nM), UCL-1684 (30 nM), TRAM-34 (30 nM) and iberiotoxin (IbTX) (1 nM, 10 nM, 30 nM and 100 nM), were all

dissolved in DMSO and diluted to a final working concentration of no more than 0.01% DMSO (0.01% DMSO had no effect alone). Calcium ionophore A23187, TRPV4 agonist 4αPDD (Vincent *et al.*, 2009), TRPV4 agonist GSK1016790A (Thorneloe *et al.*, 2008), and BK inhibitor IbTX (Candia *et al.*, 1992), were sourced from Sigma-Aldrich, UK and TRPV4 antagonist RN1734 (Vincent *et al.*, 2009), TRPV4 antagonist HC 067047 (Everaerts *et al.*, 2010), SK inhibitor UCL-1684 and IK inhibitor TRAM-34 (Nehme *et al.*, 2012), were sourced from Tocris, UK.

2.7 Blood pressure recording

2.7.1 Cannulation

Adult CD1 wild-type mice (30-40g; n=11) were anaesthetised with a combination of urethane (1.4-2.2 mg/kg, Sigma-Aldrich, UK) and α-chloralose (7-11 μg/kg, Sigma-Aldrich, UK), administered at an appropriate dose IP in saline. Urethane was used to minimise the effects on the cardiovascular system (Carruba *et al.*, 1987). Following injection of the anaesthetic, the mice were returned to their cage for several minutes until they lost consciousness. Body temperature was recorded immediately and continuously by rectal probe and maintained at 37±0.5°C by use of a heat lamp. Once loss of paw-withdrawal and eye-blink reflexes was achieved the trachea was exposed and intubated in order to maintain respiration. The left carotid artery was exposed and carefully dissected away from the surrounding tissue and vagus nerve. A permanent ligature was tied towards the cranial segment of the carotid artery and a temporary ligature fixed around the proximal segment to prevent the flow of blood. The artery was then cut and cannulated with stretched PE25 tubing filled

with heparinised saline and the cannula tied in place. Once the cannula was secure the temporary ligature was removed to direct blood flow to the pressure transducer attached. Blood pressure was recorded by the pressure transducer connected to a Neurolog (Digitimer Ltd, Herefordshire, UK) blood pressure amplifier. Raw BP signal was digitised to PC with a CED Micro1401 (Cambridge Electronic Design, Cambridge, UK) using WinEDR at 5 kHz.

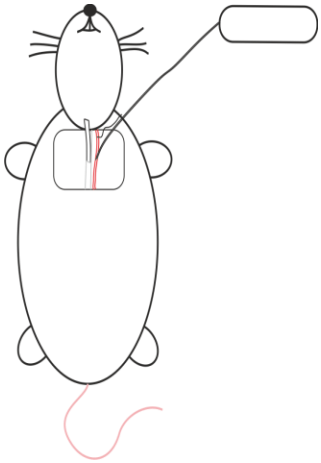

Figure 2.3 Cannulation of the carotid artery and blood pressure recording.
The trachea is intubated to aide breathing whilst under anaesthetic and then the carotid artery is cannulated. The cannula is attached to a pressure transducer which is then connected to an amplifier and blood pressure is recorded on a PC.

2.7.2 Heart rate measurement

Heartbeats were annotated to the amplified AC coupled blood pressure signal using Wabp from the PhysioNet suite of programs to give heart rate of the animals (Goldberger *et al.*, 2000). Briefly, the signal was analysed at 1/10th sampling frequency (ie. 500 Hz), and resampled to 125 Hz for optimal beat detection by Wabp. Annotated beats were then reverted to 10 times speed to give the actual heart rate.

2.7.3 Intracerebroventricular injections

For intracerebroventricular (ICV) injections the mouse was placed in a stereotaxic frame adapted for mice (Kopf instruments, California, USA). The head was clamped and held in a level position and the skull was exposed by making an incision down the midline of the head. Bregma was located at coordinates 3.8 ± 0.3 mm rostral and 5.8 ± 0.5mm dorsal to intraural line taken from the Paxinos and Franklin adult mouse stereotaxic atlas (Paxinos and Franklin, 2001); a hole was drilled 1 mm lateral and 0.2 mm caudal to Bregma.

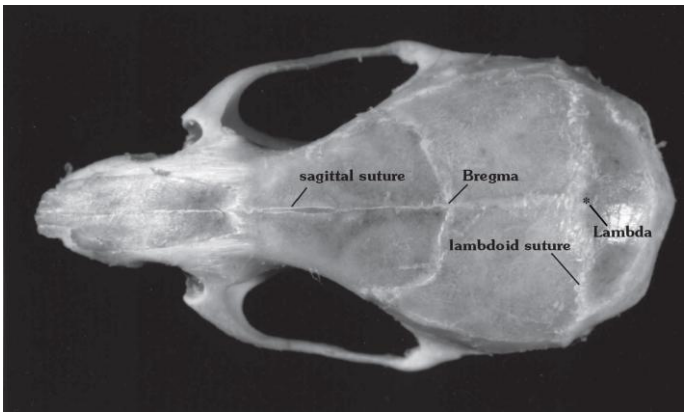

Figure 2.4 Mouse skull diagram
Dorsal view of the skull with the positions of bregma, lambda, the sagittal suture and the lambdoid suture.

All drugs were given in isotonic ACSF or hypotonic ACSF (Table 3) as the vehicle as stated below. Solutions were injected in a 1µl volume gradually over a 30 second period via a 10µL Hamilton syringe. All ICV injections were given into the lateral ventricle at the following coordinates through the previously drilled hole (0.2 mm caudal, 1 mm lateral, 3.2 mm vertical). The syringe was left at the injection site for 2 minutes and elevated to just above the injection site after this time, where it was kept in place for the duration of the recording. At the end of the procedure all

animals were injected with 1% pontamine blue dye (Sigma-Aldrich, UK) at the same injection site using the same volume over 30 seconds and left for 2 minutes before removing the syringe in order to confirm the correct location for the injection site. The mouse was then decapitated and the brain removed and sliced to 300 μm on a Campden Instruments Ltd 752 M Vibroslice to locate the injection site.

2.7.4 Drug injections

Drugs/vehicle controls used were; 1μL isotonic/isotonic+DMSO (0.01%) ACSF, hypotonic ACSF (~270 mosmol) and RN1734 (Tocris, UK) in vehicle (ACSF) (100nmol/kg).

2.8 Lesioning

Specific lesions of the PVN were performed by injection of the cytotoxic Substance P-saporin (SSP-SAP) (0.04 mg/ml; Advanced Targeting Systems, San Diego, USA); a conjugation of saporin and SSP, the Sar^{9}, $Met(O_2)^{11}$ analog of Substance P. This analog diffuses into the tissue it is injected into and is specifically cytotoxic to those cells expressing the Substance P receptor NK1.

2.8.1 Lesioning surgery

Prior to surgery adult male Wistar rats (n=8; 200-300g) were put under isoflurane gas anaesthesia (4% v/v induction; 2% v/v maintenance); surgery was performed under aseptic conditions. Once anaesthesia was confirmed by loss of toe-pinch reflex pre-operative subcutaneous injections of the analgesic buprenorphine

(Temgesic, 1.5 mg/kg; Reckitt Benckiser, Slough, UK), the antibiotic enrofloxacin (Baytril, 0.2 ml/kg; Bayer AG, Leverkusen, Germany) and the anti-inflammatory meloxicam (Metacam, 100 µg/kg; Boehringer Ingelheim, Germany) were given. Once anaesthetised the skin on top of the head was shaved and the rat was placed in a stereotaxic frame (Kopf Instruments, California, USA). The head was clamped in a stable and level position, an incision made down the midline of the head and the skull exposed. Bregma was located using the Paxinos and Watson adult rat brain atlas (Paxinos and Watson, 1986) and a hole was drilled at the approximate site of the PVN injection (1.8mm caudal, 1.8mm lateral). 50nl SSP-50 nl SSP-SAP (n=5) or 50 nl phosphate buffered saline (PBS) (control; n=3) were injected unilaterally in the right hand side gradually over 2 minutes via a 5µl Hamilton syringe at the defined PVN coordinates (1.8mm caudal, 1.8mm lateral, 9.2mm vertical at 10^{o}). These injections sites were based on the rat atlas and adjusted according to the size of the rat (Paxinos & Watson, 1986). The Hamilton syringe was left in the injection site for 5-10 minutes to avoid residual solution moving up the track from the syringe as much as possible. Once the Hamilton syringe was carefully removed the incision was sutured closed using Polysorb 4/0 and a small amount of surgical glue (Vetbond; 3M, Bracknell, UK). Post-operatively the rats were isolated and kept in a heated incubator unit to be monitored until they recovered from anaesthesia.

2.9 Telemetry

Telemetry devices were implanted in *Gnasxl* mice and their wildtype counterparts (aged ~4 months; n=18) and NK-1 lesioned rats (200-300g; n=6) in order to record electrocardiogram (ECG) using ETA-F20 transmitters (Data Sciences International,

MN, USA). These devices provide a huge benefit over other methods of cardiovascular recording such as cannulation as the mice are conscious and freely moving throughout the entire experimental procedure.

2.9.1 Telemetry surgery

During surgery animals were put under isoflurane gas anaesthesia (4% v/v induction; 2% v/v maintenance); surgery was performed under aseptic conditions Pre-operative subcutaneous injections of the analgesic buprenorphine (Temgesic, 1.5 mg/kg; Reckitt Benckiser, Slough, UK), the antibiotic enrofloxacin (Baytril, 0.2 ml/kg; Bayer AG, Leverkusen, Germany) and the anti-inflammatory meloxicam (Metacam, 100 µg/kg; Boehringer Ingelheim, Germany) were given. The skin was shaved to allow incisions to be made as shown in Figure 2.4 below. A section on the dorsal side was shaved in order to make an incision along the midline to accommodate a subcutaneous "pocket" for insertion of the transmitter. Once the initial incision was made the pocket was formed by blunt dissection. Two further smaller areas were shaved on the caudal side of the animal to allow incisions to be made for placement of the electrodes of the transmitters as shown below in Figure 2.4. Subcutaneous tunnels were then blunt dissected from the pocket to the small incisions on the front of the animal to allow the electrode leads to pass through. Once incisions were made the transmitter body was placed subcutaneously within the subcutaneous pocket and the two electrodes of the transmitter passed through the tunnels formed and stitched into position in the muscle in order to record ECG activity.

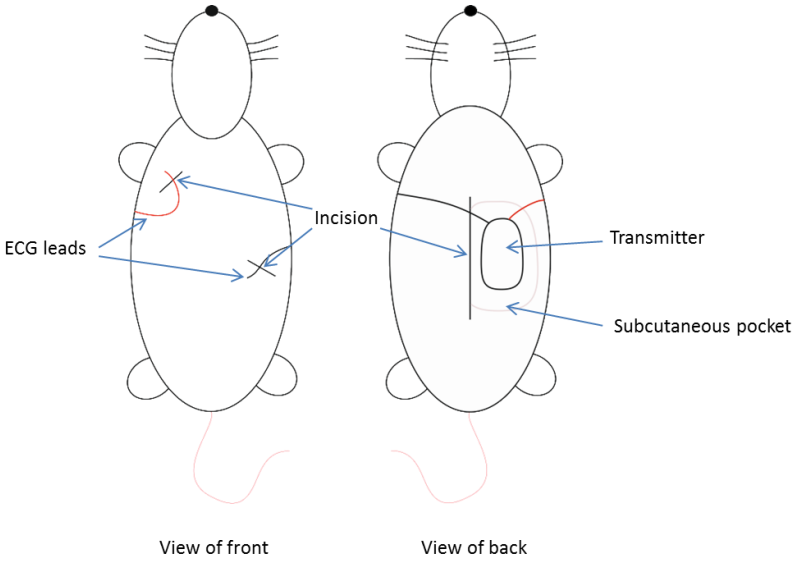

Figure 2.5 Implantation site of telemetric transmitters.
After incisions were made a subcutaneous pocket was made on the back of the animal. The main body of the transmitter was placed here and subcutaneous tunnels were made where the two leads were to be sutured to the muscle.

The incisions made during the surgery were then stitched closed using Polysorb 4/0 and then glued with surgical glue (Vetbond; 3M, Bracknell, UK). Post-operatively the animals were isolated and kept in a heated incubator unit to be monitored until they recovered from the anaesthesia.

2.9.2 ECG recording

After surgery was performed the animals were left to recover for a minimum of 5 days before 24-hour continuous recording began. Each animal was individually housed above a Data Sciences International (DSI) receiver pad (Data Sciences International, NL), kept at least one metre apart to prevent the cross-talk of signals. ECG signals were transmitted as a short range FM signal and received by the receiver pad where the signal was AC coupled. The receiver pad was connected to a DSI data exchange matrix (DEM) (Data Sciences International, NL) and a signal

output adapter, which was subsequently connected to a CED micro1401 interface (Cambridge Electronic Design, Cambridge, UK), where the signal was digitised. The data was recorded using Spike2 (Cambridge Electronic Design, Cambridge, UK) on a PC at 5 kHz. In the case of larger cages (i.e for telemetry on rats) two receiver pads were placed together and recorded from simultaneously.

2.9.3 Beat detection

Using a custom program developed in Java script (Netbeans IDE) heart beats from ECG were annotated. Raw ECG signal was cleaned up in Spike2 by DCremove using a time constant of 20 ms; this subtracts the average of 10 ms either side from each data point, having a similar effect as a high pass filter.

For analysis of daily variation in heart rate beats of more than 1000 bpm or less than 400 bpm, which are assumed to be ectopic or misread beats, were excluded. Heart rate responses to stress and heart rate variability were analysed directly from the raw heart beat annotation files, which contain heart beats annotated to a high degree of accuracy (ie. to within the sampling rate of 0.2 ms).

2.9.4 Heart rate variability

Heart rate variability (HRV) analysis was performed using Kubios HRV program (Niskanen *et al.*, 2004). Heart rate traces were visually inspected for 3-minute clean sections of stable heart rate. Heart rate was then resampled to 20 Hz and FFTs were produced using Welch's algorithm using 32-second windows with 50% overlap.

Much can be learnt in particular from frequency domain analysis, where power spectra, such as FFTs are produced. These spectra are a way of graphically

presenting the degree of heart rate variability across a range of frequencies. These frequencies can be banded and represent different aspects of the autonomic nervous system; these bands have been previously confirmed by my group (Nunn *et al.*, 2013). The high frequency (HF) domain has been reported to reflect only parasympathetic nervous activity (PNS); at a range of 1 Hz to 5 Hz. The low frequency (LF) domain has been confirmed to reflect both the SNS and PNS activity; this region extended from 0.15 Hz to 1 Hz. As there is no direct indication of SNS activity specifically, the LF/HF ratio is used a reflection of this activity, previously confirmed by (Nunn *et al.*, 2013).

Table 3 Bath solutions used during electrophysiological and Ca^{2+} measurements. All extracellular solutions were pH 7.4.

Bath (mM)	Na	K	Ca	Cl	Mg	SO_4	H_2PO_4	HCO_3	Glucose	HEPEs	pH adjustment
Physiological ACSF	127	3	2.4	133.6	1.3	1.3	1.2	26	5	0	95% O_2/5% CO_2
Isotonic ACSF (30 mM sucrose)	117	3	2.4	123.6	1.3	1.3	1.2	26	0	0	95% O_2/5% CO_2
Hypotonic ACSF	117	3	2.4	123.6	1.3	1.3	1.2	26	0	0	95% O_2/5% CO_2
Low Na^+ ACSF (50mM sucrose)	121	3	0.5	97.8	7	7	1.2	26	5	0	95% O_2/5% CO_2
RMP and Ca^{2+} – HEPES ACSF	142	3	2.4	143.8	1.3	1.3	0	0	5	10	NaOH

Table 4 Pipette solutions used during electrophysiological measurements. All pipette solutions were pH 7.4.

Pipette (mM)	Na	K	Ca	Cl	Mg	SO_4	$MeSO_4$	Gluconate	EGTA	HEPEs	pH adjustment
TRP – Single channel	100	40	0	5	0	0	100	35	0	10	KOH
TRP – Action current	100	40	0	105	0	0	0	35	5	10	KOH
RMP – Physiological saline	0	150	0	28	1	0	0	115	5	10	KOH

Table 5 Junction potentials (V_j) calculated for the combination of bath solutions and pipette solutions shown.
Calculations were performed using JpCalc (Barry and Lynch, 1991).

Bath solution	Pipette solution	V_j (mV)
Physiological ACSF	**TRP – Single channel**	+10.6
RMP and Ca^{2+} – HEPES ACSF	**RMP – Physiological saline**	-15.3

3 A Role for TRP Channels in Osmoregulation and Temperature Sensing

3.1 Introduction

Currently it is unknown exactly what the regulatory role of the parvocellular neurones within the paraventricular nucleus is and very little is known about the ion channels present or how they modulate activity. As the TRP channels are so abundant in the brain and it is known they play a huge role in regulating cell function, it follows these channels could be important players in the regulation of activity in the parvocellular neurones of the PVN.

The transient receptor potential (TRP) family of ion channels are a large superfamily, consisting of 28 homologs so far in mammals. They are grouped roughly by common structure into seven subfamilies. TRPC (canonical; seven members), TRPV (vanilloid; six members), TRPA (ankyrin; 1 member), TRPM (melastatin; eight members), TRPML (mucolipin; 1 member), TRPP (polycystin; two members) and TRPN (NOMPC; only seen so far in non-mammals) (Nilius and Owsianik, 2011). TRP channels are thought of as relatively non-selective cation ion channels, with differing permeablities to monovalent ions, Ca^{2+} and in some cases Mg^{2+}. TRP channels are usually found in the plasma membrane, capable of forming homo- or hetero-multimers. Although they have been much studied recently, little is known about their gating properties or functions. They are extremely important in cell regulation; in particular in Ca^{2+} regulation (reviewed by (Clapham, 2003)). As

the environment of neurones is so stringently regulated and expression of these ion channels is so widespread within the brain it follows that some TRP channels may have a role to play in regulation of neuronal activity in the paraventricular nucleus (PVN); a key area of the hypothalamus for maintaining homeostasis.

3.1.1 TRPV4 and osmosensing

The transient receptor potential vanilloid channel 4 (TRPV4) is an established mechanosensitive ion channel, known to be present in the PVN (Carreno *et al.*, 2009). This channel is activated by a number of factors such as; temperature (>27^{o}C), phorbal esters and increased osmolality (Guler *et al.*, 2002; Liedtke *et al.*, 2000; Strotmann *et al.*, 2000). It has been shown to be important for cell-volume regulation in a variety of cells (Becker *et al.*, 2005; Benfenati *et al.*, 2011; Guilak *et al.*, 2010; Phan *et al.*, 2009). Selective for Na^{+}, K^{+} and Ca^{2+} ions at a ratio of 1:1:6 respectively, cellular responses to changes in osmolality involve TRPV4 channel mediated elevation of intracellular Ca^{2+} (Liedtke *et al.*, 2003).

The PVN has an established role in osmotic homeostasis (Bourque, 2008). Furthermore, an investigation by (Stocker *et al.*, 2004) showed that water deprivation increases expression of the early response gene c-fos in parvocellular neurones of the PVN. However, previously there have been no reports of osmolality effects on parvocellular neurones of the PVN.

3.1.2 TRPM2 and temperature sensing

It has been shown in other neurones within the brain that changing temperature typically leads to altered neuronal activity (Sudbury and Bourque, 2013). As well as showing sensitivity to changes in osmolality, TRPV4 channels are also activated by temperatures above 27^{o}C (Guler *et al.*, 2002). However, various other TRP channels are also known to be affected by temperature, such as the transient receptor potential melastatin channel 2 (TRPM2) (also known at TRPC7). TRPM2 is found both on the plasma membrane and intracellularly. Recently reviewed by (Sumoza-Toledo and Penner, 2011), TRPM2 is widely expressed in the brain (Nagamine *et al.*, 1998). Activated by various endogenous agents such as nicotinamide adenine dinucleotide, ADP-ribose (Sano *et al.*, 2001) and H_2O_2 (Hara *et al.*, 2002), the TRPM2 channel also displays sensitivity to temperatures above 35^{o}C (Sumoza-Toledo and Penner, 2011).

Inegaga *et al* (Inenaga *et al.*, 1987) first showed thermosensitivity of the neurones in the PVN. These experiments showed both cold-sensitive and heat-sensitive neurones with no apparent preference for areas within the PVN. However, (Smith *et al.*, 1998) later showed that PVN spinally-projecting neurones are directly involved in thermoregulation using poly-synaptic viral tracing, There have since been several studies to demonstrate that the PVN is important in thermoregulation (Cham and Badoer, 2008; Chen *et al.*, 2008), and furthermore it has been shown that heat exposure activates spinally-projecting PVN neurones (Cham *et al.*, 2006a). However, throughout these studies the mechanisms responsible for this thermosensitivity have not been explored.

3.1.3 Aims

The aim of this chapter is to (i) identify potential TRP channels present within this area and (ii) investigate their function with respects to the effects of cellular environment on neuronal activity using a combination of cell-attached and whole-cell patch clamp electrophysiology and intracellular calcium recordings.

3.2 Methods

3.2.1 Investigating a potential role for TRPs in osmosensing in the PVN

3.2.1.1 Investigating the effects of osmolality on putative parvocellular PVN neurones

Action current frequency analysis using cell-attached patch clamp electrophysiology in brain slice was used to initially identify how osmolality affects the activity of putative parvocellular neurones of the PVN. Hypothalamic brain slices from CD1 mice were prepared as described in Chapter 2. The PVN area was located and cells were chosen based on location (Figure **Error! Reference source not found.**), size nd morphology.

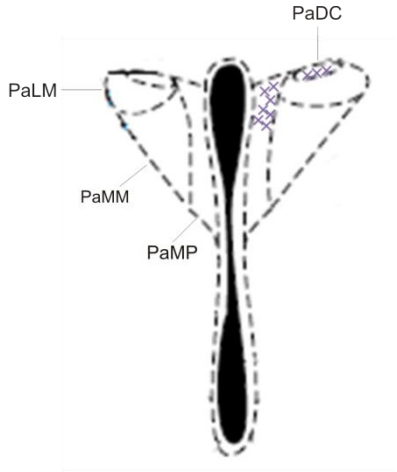

Figure 3.1 Diagram of the parvocellular area patched during osmolality patch clamp experiments.
Patched areas are indicated by the purple crosses, used in osmolality experiments. All further patches were obtained from the indicated areas. PaLM – lateral magnocellular part, PaMM – medial magnocellular part, PaMP – medial parvocellular part and PaDC – dorsal cap.

To obtain cell-attached patch, a glass pipette (of resistance ~8 MΩ) was lowered onto a visualised cell and a small amount of negative pressure was used to form a gigaseal. Action currents were then recorded in voltage clamp (for full methods see Chapter 2), and were used as an indication of action potentials. A seal was formed and the patched cell was left for a further 5 minutes before recording in order to establish equilibrium. Once recording began the slice was left in isotonic ACSF for 5 minutes to obtain a steady baseline and subsequently switched to the appropriate treatment. Hypotonic solutions were left to superfuse the slices for a minimum of 10 minutes to allow time for the solution to reach the recording chamber (timed at 2-3 minutes) and for complete changeover of solutions before wash off with isotonic ACSF. All cells were first checked for osmotic sensitivity by superfusing with hypotonic ACSF before addition of any drugs to the solutions. Only those which responded to the reduction in osmolality were then used for further analysis

(10/15) cells responded to osmolality). Drug treatments were left for 10 minutes before wash off with isotonic ACSF.

3.2.1.2 Single channel investigation

Single channel properties were investigated in cell-attached patch clamp mode (described fully in Chapter 2) in brain slices of CD1 mice. Once patched, cells were left for 5 minutes before recording began and held at -20 mV. Voltage steps were then ran in steps of 10 mV from -60 mV to +20 mV (holding potential). From this current-voltage curves were produced and mean slope unitary conductance (*g*) and reversal potential (V_{rev}) of the channel was be obtained. Once voltage steps were performed the cells were held at -20 mV and drugs were added. Single channel activity was analyzed using the Qub software (Qin et al, SUNY, Buffalo, NY) using a K-sequential means method (Qin, 2004; Qin *et al.*, 1996).

3.2.1.3 Intracellular response to osmotic challenge

Whole-cell current clamp recordings were made using isolated PVN neuronal cells (for full methods see Chapter 2). PVN cells were first released from well-plates using trypsin and plated on to glass shards and left in an incubator at 37^{o}C for 30 minutes to stick down sufficiently before placing in the recording chamber. Whole-cell mode was achieved by breaking through the plasma membrane with a glass pipette (~3 MΩ) using further negative pressure once a gigaseal was formed. Cells were left for a minimum of 5 minutes before recording began and a baseline resting membrane potential was recorded for at least 5 minutes before any treatment was added.

In order to obtain intracellular calcium measurements, isolated PVN neurones were plated out on glass-bottomed dishes (for full methods see Chapter 2) and left for 30 minutes in an incubator at 37^{o}C in order to stick down. Cells were incubated for a further 30 minutes with the ratiometric dye Fura-2AM (5 µM) and kept in the dark to avoid bleaching for the duration of the experiment. Once incubated the cells were superfused with HEPES ACSF for a minimum of 15 minutes to wash the remainder of the Fura-2AM off and equilibrate the cells to the solutions. Fluorescence was measured by highlighting regions of interest and Fura-2AM was excited alternatively at 355 nm and 380 nm, with fluorescence measured at intervals of 2 s. The ratios of these intensities were converted into total calcium levels using Equation 2.1 in Chapter 2. Once a steady baseline was achieved after a minimum of 5 minutes of recording the treatment was added.

3.2.2 Investigating a role for TRP channels in temperature sensing in the PVN

In cell-attached patch clamp mode temperature was regulated by use of a TC-10 npi temperature control system and a HPT-2A heated perfusion tube (Scientifica, East Sussex, UK). Temperature was kept stable at 22^{o}C for the first 10 minutes of recording and subsequently increased upwards in steps of 5^{o}C to 27^{o}C, 32^{o}C and finally to physiological temperatures of 37^{o}C, each for a minimum of 5 minutes. During this protocol action current firing was recorded (see Chapter 2 for methods) and drug treatment was introduced after the first 5 minutes of stable baseline recordings at 22^{o}C.

3.3 Results

3.3.1 Investigating a potential role for TRPs in osmosensing in the PVN

3.3.1.1 Confirmation of the presence of TRPV4 in the PVN

Immunofluorescence images of the parvocellular area of the PVN shows staining for the TRPV4 channel in this area.

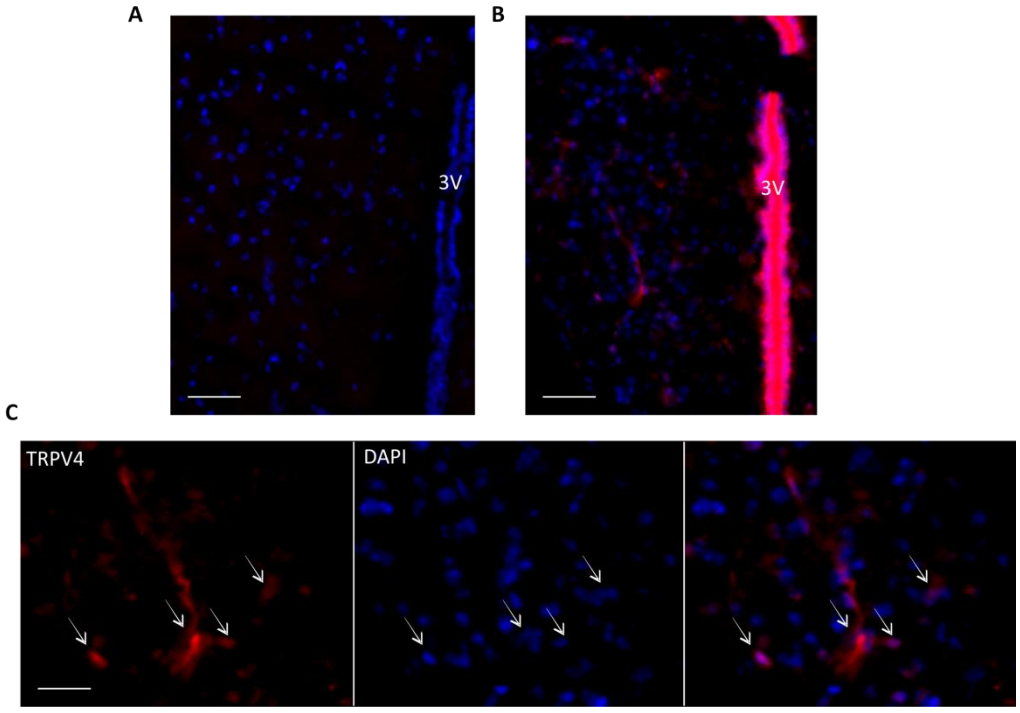

Figure 3.2 Immunofluorescent identification of TRPV4 in the paraventricular nucleus.
(A) Negative control showing DAPI blue, with the absence of red TRPV4 staining **(B)** Red staining is positive for the TRPV4 channel, blue is DAPI nuclei staining. Scale bar 100µm and 3V indicates the 3rd ventricle. **(C)** High magnification images of a section seen in (B). Red staining is TRPV4 and blue is DAPI nuclei staining; arrows indicate where overlap can be seen. Scale bar is 25 µm.

3.3.1.2 The effects of osmolality on putative parvocellular PVN neurones

Action current frequency was significantly decreased upon hypotonic challenge with a 79 ± 10 % reduction of action current frequency (Figure 3.3; *n*=10; *p*<0.001 by *t*-test), confirming that the PVN has a capacity to detect and respond to changes in osmolality.

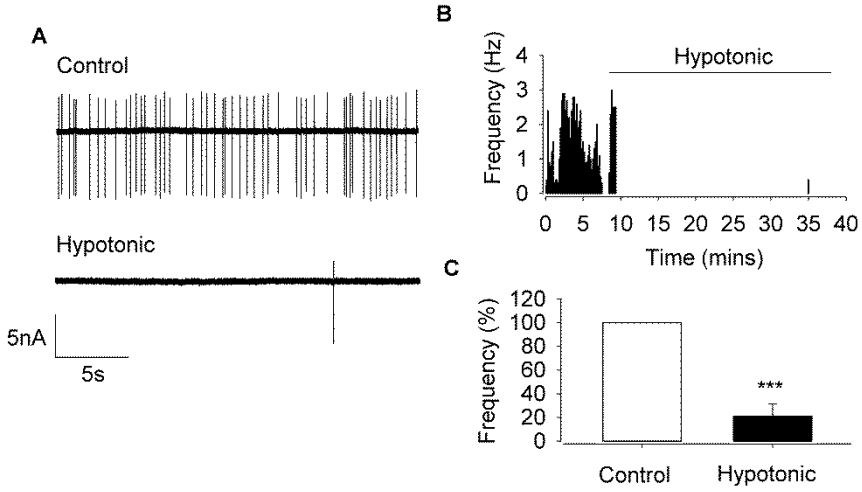

Figure 3.3 The effect of osmolality changes on action current frequency.
Cell-attached action current measurements in slice within the parvocellular area of the PVN (Figure 3.1). **(A)** Raw action current trace at 300 mosmol (control) and 270 mosmol (hypotonic challenge). **(B)** Representative frequency histogram showing action current response to hypotonic challenge of a single parvocellular neurone. **(C)** Mean percentage normalized action current frequency for 10 experiments similar to those illustrated in (A) and (B) (normalized to action current frequency during control conditions) is significantly reduced (*n*=10; ***p<0.001 by Student's *t*-test; see text for details). Data expressed as a % of control (isotonic is 100%).

3.3.1.3 Pharmacological identification of TRPV4

Superfusion of putative parvocellular neurones with the TRPV4 channel agonist 4αPDD (1 µM) reduced action current frequency by 36 ± 10 % (*n*=6; **p<0.01 by ANOVA with multiple comparison using Tukey's post hoc test). To provide further support the highly selective agonist GSK1016790A (100nM) was also used. The

more selective GSK1016790A reduced action current frequency by 72 ± 8 %. (Figure 3.4; *n*=6; *p*<0.05 by ANOVA with multiple comparison using Tukey's post hoc test); a significantly greater effect (Figure 3.4; *n*=8; *p*<0.01 by ANOVA with multiple comparison using Tukey's post hoc test).

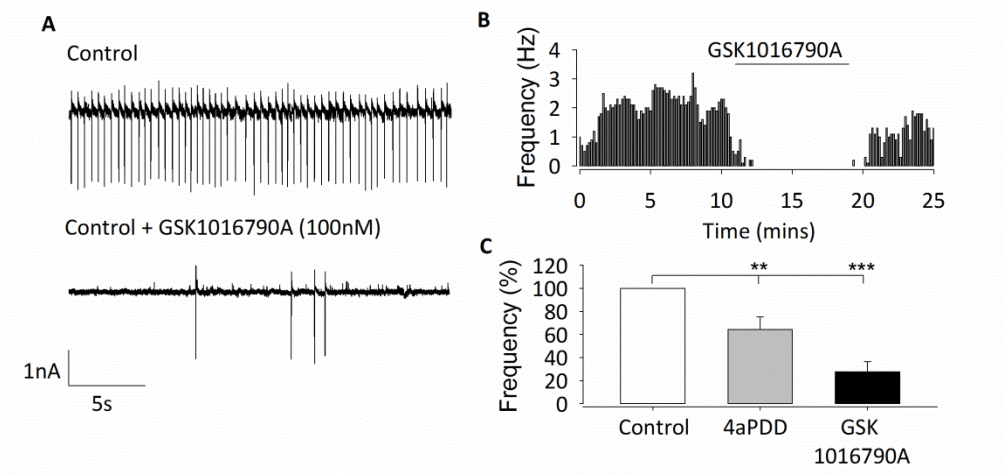

Figure 3.4 The effect of TRPV4 channel activators on action current frequency. Cell-attached action current measurements in slice within the medial and dorsal cap parvocellular area of the PVN (Figure 3.1).. **(A)** Raw action current trace at 300 mosmol (control) with and without the selective agonist GSK1016790A (100nM). **(B)** Representative frequency histogram showing action current responses to GSK1016790A. **(C)** Mean action current frequency from 6 experiments similar to those illustrated in (A) and (B) is significantly reduced upon addition of 4αPDD (*n*=6; ***p*<0.01) and GSK1016790A (*n*=8; ****p*<0.001).

The response to hypotonic solution was significantly reduced by the TRPV4 antagonists RN1734 (5 µM) and highly selective HC067047 (300 nM) (Figure 3.5) compared to hypotonic alone: 70 ± 14 % reduction *vs*. hypotonic with RN1734: 45 ± 15 % reduction (*n*=6; *p*<0.05 by ANOVA with multiple comparison using Tukey's post hoc test), and a 10 ± 13 % reduction with HC067047 in action current frequency (*n*=6; *p*<0.01 by ANOVA with multiple comparison using Tukey's post hoc test). Antagonists had no significant effect on action potential frequency when applied

alone (*n*=6). This data combined suggests a definite role for TRPV4 channels in osmosensing in the PVN.

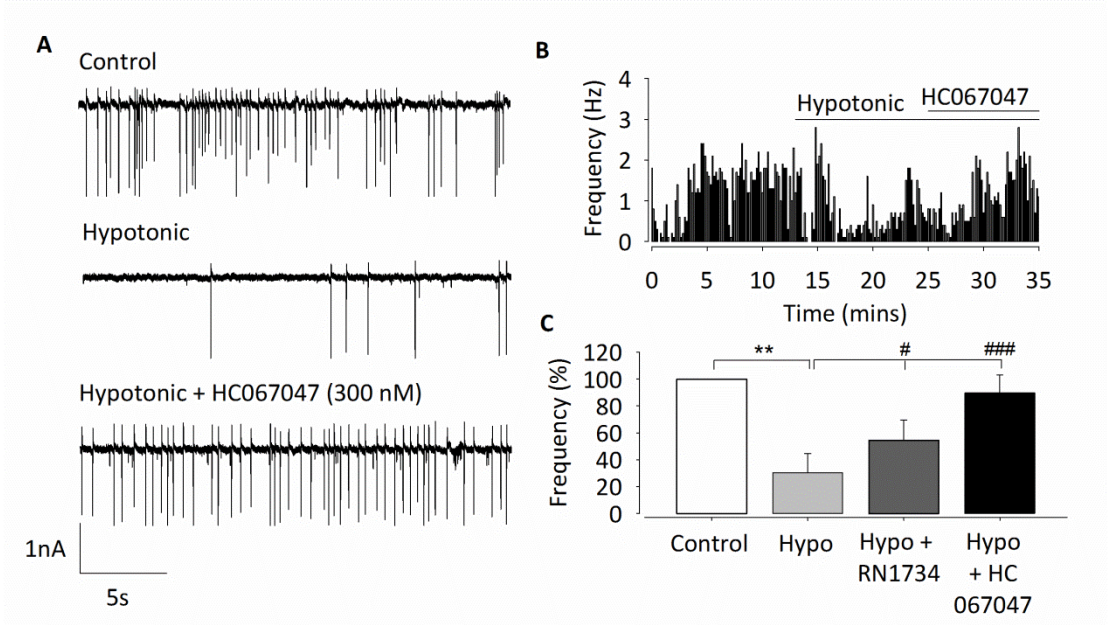

Figure 3.5 The effect of TRPV4 channel inhibitors on action current frequency. Cell-attached action current measurements in slice within the medial and dorsal cap parvocellular area of the PVN (Figure 3.1). **(A)** Raw action current trace at 300 mosmol (control), 270 mosmol (hypotonic) and with the addition of the TRPV4 antagonist HC067047 (300 nM) **(B)** Representative frequency histogram showing regain of action current frequency upon HC067047 addition after loss from hypotonic challenge. **(C)** Mean action current frequency from 6 experiments similar to those illustrated in (D) and (E) is significantly reduced upon hypotonic challenge (*n*=6; ***p*<0.01), but not in the presence of RN1734 or HC101679A, both of which showed a significant difference to hypotonic alone (*n*=6; #*p*<0.05 and *n*=6; ###*p*<0.001 respectively).

3.3.1.4 Single channel analysis of the TRPV4 channel

Using the TRPV4 channel activator, 4αPDD (1 µM), in cell-attached patch it was possible to record single channel activity. Figure 3.6 shows a representative raw trace of channel openings in real time. This particular channel is seen in 50% of recordings (8/16).

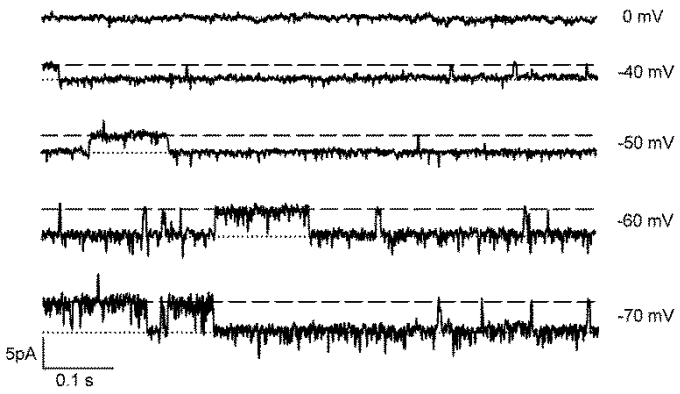

Figure 3.6 Single channel activity of a TRPV4-like channel in cell-attached patch. Representative raw single channel recordings in cell-attached patch clamp within the parvocellular area of the PVN (dashed line represents open state) (voltages shown at holding potential). Channel activity was seen in 50% of patches (8/16).

4αPDD caused a significant increase in P_o of 48 ± 9% (*n=4; p*<0.001 by *t*-test) upon addition of 4αPDD; showing TRPV4 channels are present in these neurones.

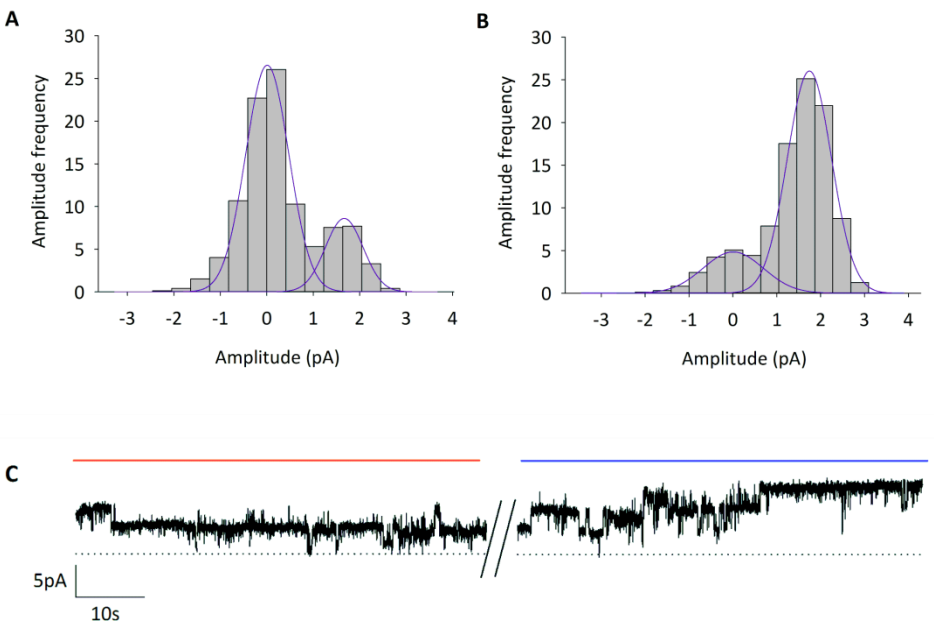

Figure 3.7 Representative amplitude histograms for TRPV4 channel activity. Cell-attached action current measurements in slice within the medial and dorsal cap parvocellular area of the PVN (Figure 3.1). **(A)** Representative amplitude histogram before and **(B)** after addition of 4αPDD at -40mV. P_o increased by 48±9% (*n*=4; *p*<0.001 by Student's *t*-test) upon addition of 4αPDD. **(C)** Representative trace of

channel activity increasing with the addition 4αPDD (red line indicates before addition of 4αPDD and blue line indicates after addition of 4αPDD).

From the IV curve (Figure 3.7) the channel seen in these experiments had a *g* of 57 ± 7 pS and V_{rev} of -5±3 mV (*n*=6; adjusted for junction potential); this indicates the presence of a non-selective cation channel, believed to be the TRPV4 channel.

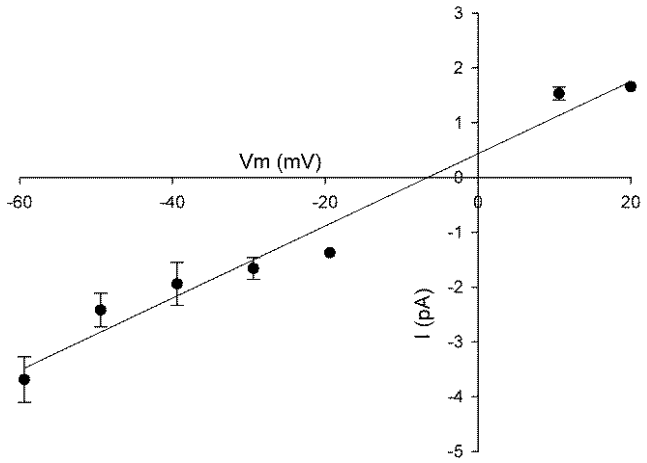

Figure 3.8 Current-voltage (IV) curve for single-channel voltage steps for TRPV4. IV curve shows mean slope unitary conductance of 57±7 pS and reversal potential of -5±3mV (*n=6*); indicative of a non-selective cation channel.

3.3.2 Intracellular response to osmotic challenge

Membrane potential response to TRPV4 channel activation was confirmed using whole-cell patch clamp. Neurones exhibited a resting membrane potential of -54 ± 5 mV (*n*=4) and 4αPDD superfusion resulted in a transient depolarisation of 11 ± 2 mV (Figure 3.9; *n*=4; *p*<0.05 by Students *t*-test).

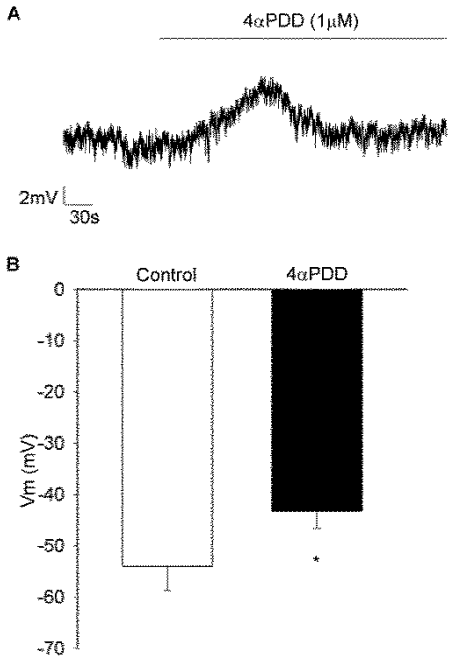

Figure 3.9 Whole-cell recordings in isolated PVN neurones during activation of TRPV4 channels with 4αPDD.
(A) Representative whole-cell current-clamp trace showing depolarization of the cell upon addition of 4αPDD. **(B)** Mean resting membrane potential of -54 ± 5 mV was recorded. A depolarisation of 11 ± 2 mV was observed with 4αPDD (*n*=4; *p*<0.05 by Student's *t*-test).

Again, the highly selective 4αPDD activator GSK1016790A (100nM) was also used. This caused a similar depolarisation of 12 ± 5 mV (Figure 3.10; *n*=5; *p*<0.05 by Student's *t*-test), although this effect was more sustained; membrane potential only returning to a baseline after the GSK1016790A was washed off.

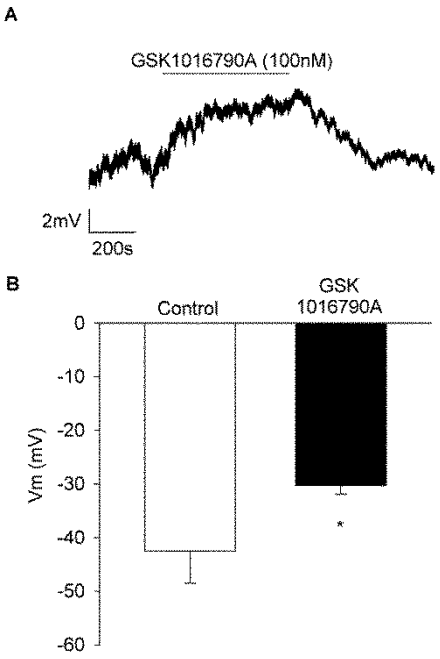

Figure 3.10: Whole-cell recordings in isolated PVN neurones during activation of TRPV4 with GSK1016790a.
(A) Representative whole-cell current-clamp trace showing depolarization of the cell upon addition of GSK1016790a. **(B)** A depolarisation of 12 ± 5 mV was observed with GSK1016790a (*n*=5; *p*<0.05 by Student's *t*-test).

Using the ratiometric dye Fura-2AM intracellular calcium $[Ca^{2+}]_I$ was measured; an average baseline $[Ca^{2+}]_I$ of 77 ± 3 nM was recorded (*n*=13). Addition of the TRPV4 channel activator, 4αPDD, significantly increased $[Ca^{2+}]_i$ (Figure 3.11; 75 ± 2 nM to 121 ± 14 nM, *n*=6*; p*<0.005 by Kruskal-Wallis ANOVA). Hypotonic challenge also caused a transient increase in $[Ca^{2+}]_i$ (Figure 3.11; 77 ± 3 nM to 19 8± 28 nM, *n*=8; *p*<0.001 by Kruskal-Wallis ANOVA); significantly higher than the increase seen with 4αPDD (p<0.001 by Kruskal-Wallis ANOVA).

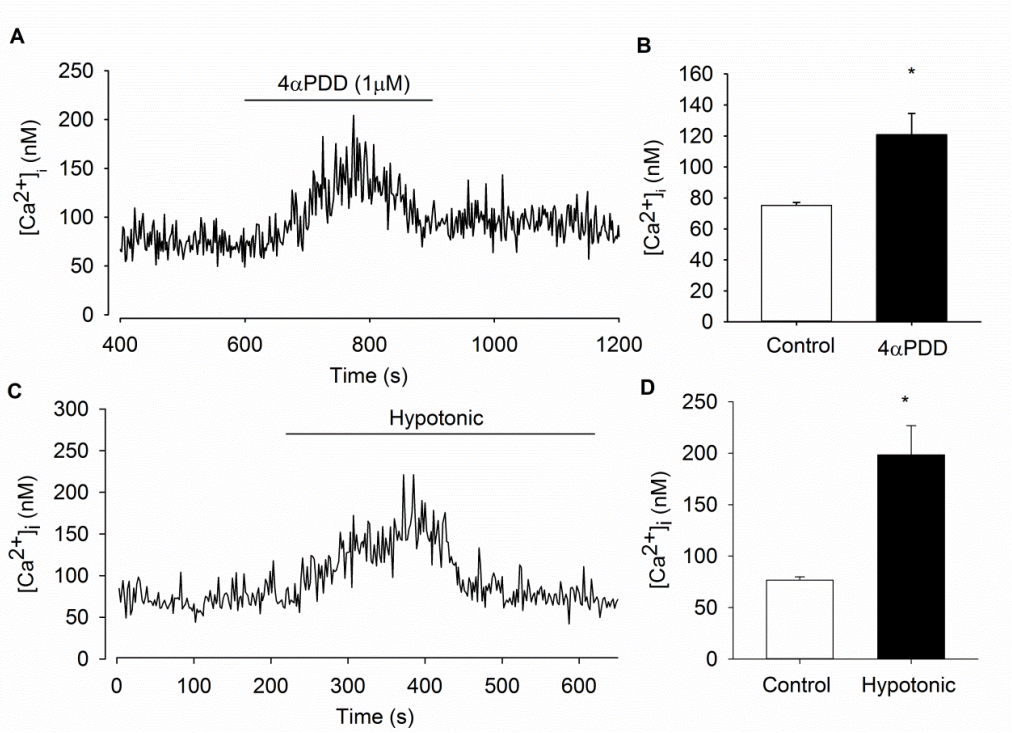

Figure 3.11 Effects of TRPV4 channel agonist and hypotonic challenge on intracellular Ca^{2+} in isolated PVN neurones.
(A) Representative Ca^{2+} trace showing a transient increase upon activation of TRPV4 channels with 4αPDD. **(B)** Mean intracellular Ca^{2+} shows a significant transient increase of 45 ± 12nM (*n*=6; *p*<0.005) with 4αPDD. **(C)** Representative Ca^{2+} trace showing a transient increase upon hypotonic challenge. **(D)** Mean intracellular Ca^{2+} shows a significant transient increase of 121 ± 28 nM (*n*=6; *p*<0.005) with hypotonic challenge.

3.3.3 Investigating a role for TRP channels in temperature sensing in the PVN

An increase in temperature resulted in a significant decrease in mean percentage normalized action current frequency. Reductions of 49 ± 11% at 27^{o}C, 88 ± 6% at 32^{o}C and 97 ± 2% at 37^{o}C were observed (Figure 3.12; *n*=6, *p*<0.001 by ANOVA with comparison against control using Dunnet's post hoc test).

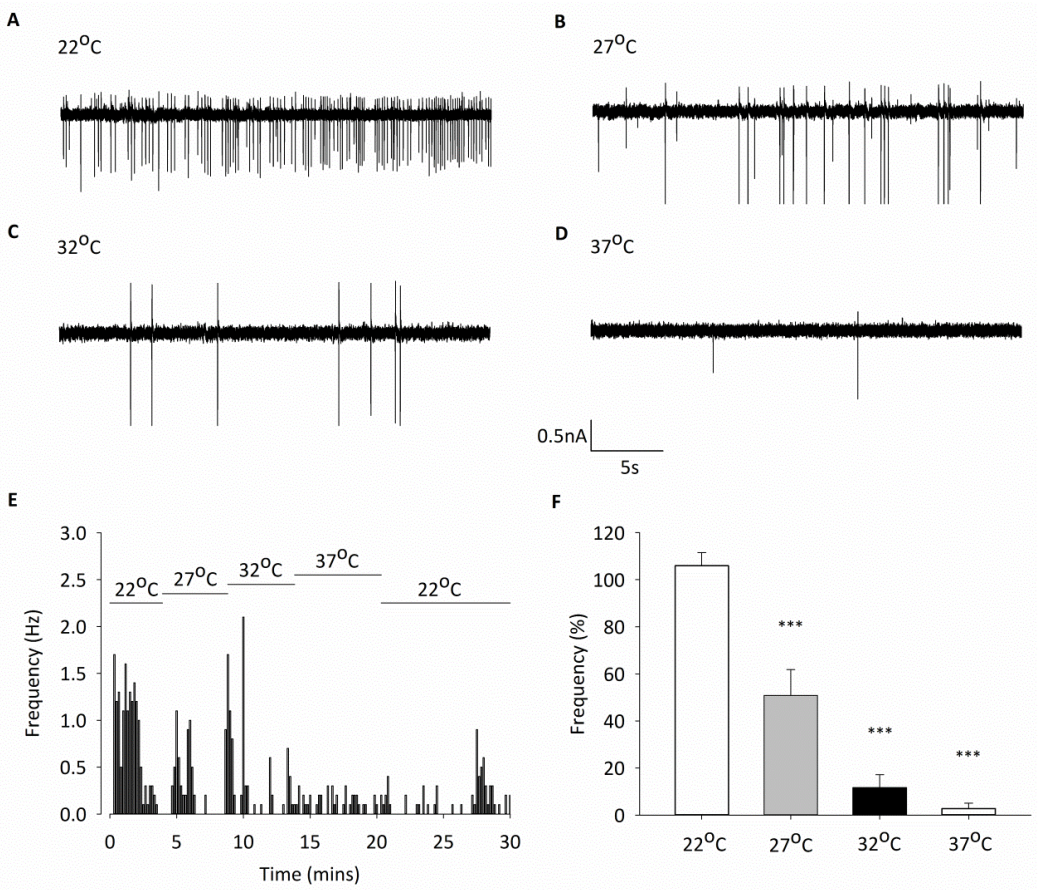

Figure 3.12 Temperature decreases action current frequency of parvocellular PVN neurones.
within the medial and dorsal cap parvocellular area of the PVN (Figure 3.1). **(A)** Raw trace of action currents at RT (22°C), increasing temperature to **(B)** 27°C, **(C)** 32°C and **(D)** physiological temperature (37°C) decreases action current frequency. **(E)** Representative frequency histogram showing action current response of a single parvocellular neurone to increasing temperature. **(F)** Mean percentage normalized action current frequency is significantly decreased with increasing temperature, showing reductions of 49 ± 11% at 27°C, 88 ± 6% at 32°C and 97 ± 2% at 37°C (*n*=6, *p*<0.001).

Increasing the bath temperature to 27°C and 32°C in the presence of the broad spectrum TRP channel antagonist, gadolinium (Gd^{3+} 100 µM) did not significantly affect action current frequency (Figure 3.13); showing there may be, in part, a temperature sensing role for a gadolinium-sensitive TRP channel. However, interestingly, at physiological temperatures the decrease in action current

frequency was *not* prevented by Gd^{3+} (100 µM). A significant decrease of action current frequency was still seen at 37°C (Figure 3.13; reduction of 94 ± 2% *n*=4; *p*<0.005; by ANOVA with comparison against control using Dunnet's post hoc test). This suggests that TRPV4 channels may not be involved at physiological temperatures, but another TRP channel; one which is insensitive to Gd^{3+} may be responsible.

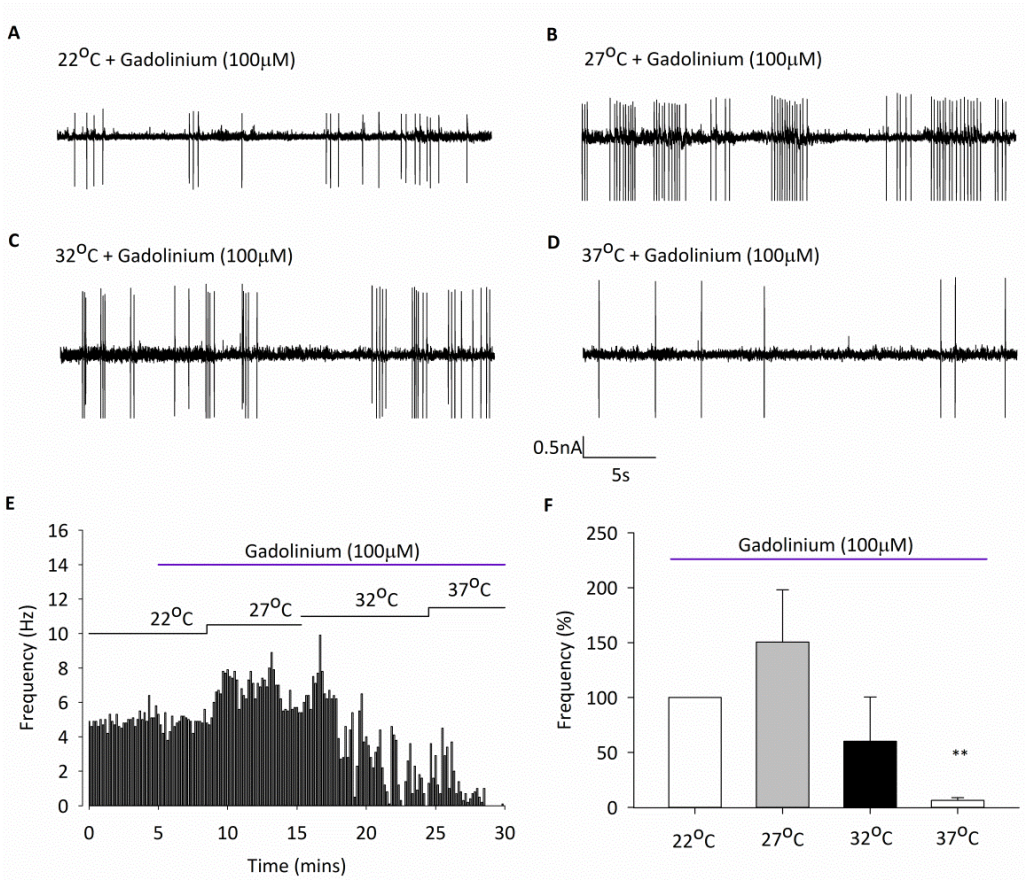

Figure 3.13 Temperature effect is largely insensitive to the broad spectrum TRP channel inhibitor gadolinium.
Cell-attached action current measurements in slice within the medial and dorsal cap parvocellular area of the PVN (Figure 3.1). **(A)** Raw trace of action currents at RT (22°C), increasing temperature to **(B)** 27°C, **(C)** 32°C and **(D)** 37°C in the presence of Gd^{3+}. **(E)** Representative frequency histogram showing AC response to increasing temperature of a single parvocellular neurone in the presence of Gd^{3+}. **(F)** Mean percentage normalized action current frequency shows a significant decrease at 37°C (reduction of 94 ± 2% *n*=4; *p*<0.005) in the presence of Gd^{3+}, despite this effect being prevented at 27°C and 32°C.

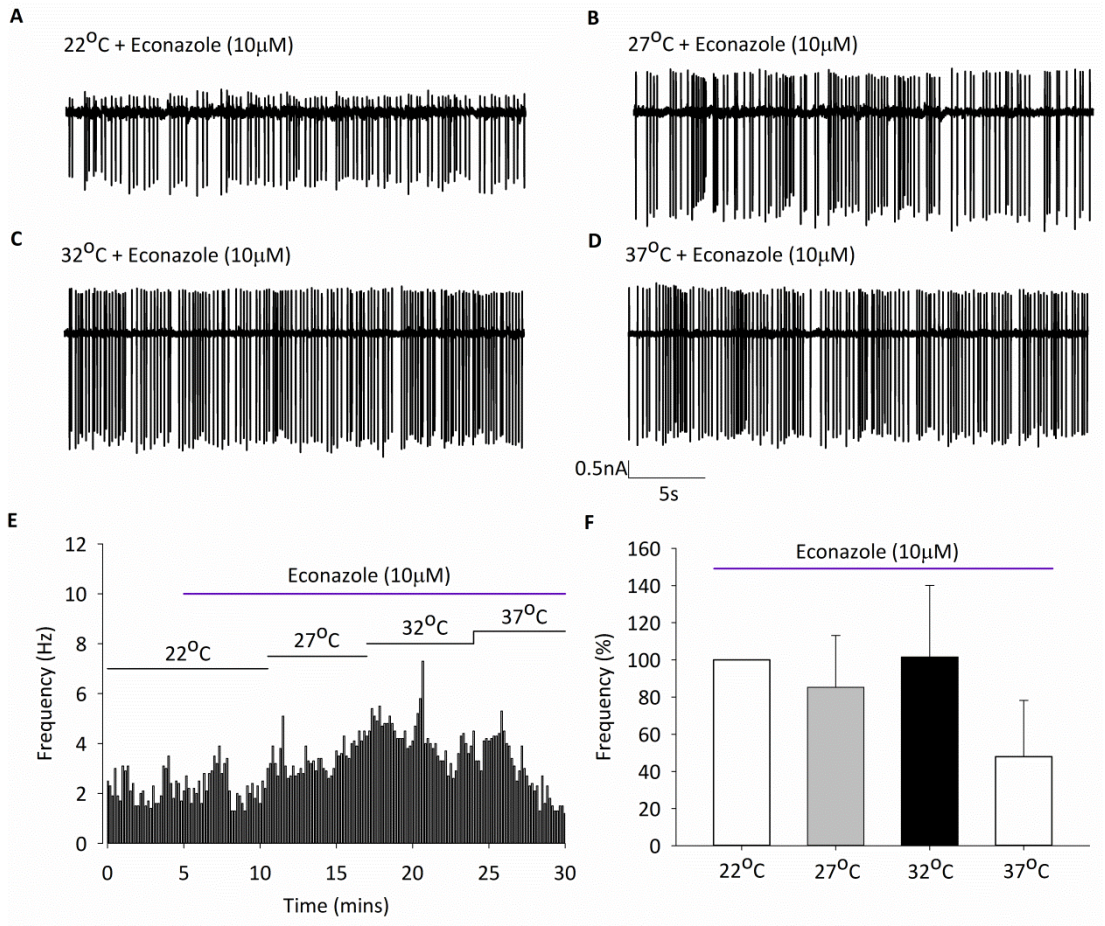

Figure 3.14 Temperature effect is blocked by the narrow spectrum TRP channel inhibitor econazole.

Cell-attached action current measurements in slice within the medial and dorsal cap parvocellular area of the PVN (Figure 3.1). **(A)** Raw trace of action currents at room temperature (22°C), increasing temperature to **(B)** 27°C, **(C)** 32°C and **(D)** 37°C in the presence of econazole. **(E)** Representative frequency histogram showing action current response to increasing temperature of a single parvocellular neurone in the presence of econazole. **(F)** Mean percentage normalized action current frequency shows the effect of temperature on action current frequency are prevented when in the presence of the TRPM2 inhibitor econazole (*n*=5; *p*>0.05).

Perfusion of the relatively selective TRPM2 inhibitor, econazole (10 μM), prevented the decrease in action current frequency throughout increasing temperatures up to 37°C (*n*=5; *p*>0.05 by ANOVA against control using Dunnet's post hoc test). This

shows a potential role for TRPM2 channels in temperature sensing within the paraventricular nucleus, however, the process appears complex.

3.4 Discussion

Under ordinary physiological circumstances, a number of nuclei in the hypothalamus contribute to both the maintenance of plasma osmolality within a narrow range (~290-300 mOsm) and maintaining body temperature at 37^{o}C. The paraventricular nucleus is one of these hypothalamic nuclei with established roles in both osmotic homeostasis (Bourque, 2008) and temperature regulation (Cham and Badoer, 2008; Cham *et al.*, 2006a; Chen *et al.*, 2008; Inenaga *et al.*, 1987; Smith *et al.*, 1998). Although these actions have been widely reported, little is known about the mechanisms responsible for this regulation.

The transient receptor potential channels are a group of non-selective cation channels highly involved in cell-regulation; particularly important for Ca^{2+} regulation (Clapham, 2003). As it is such an extensive group they are activated by a large variety of endogenous agents as well as some channels showing osmosensing and temperature sensing capabilities. TRP channels have been widely investigated recently, with knock-out animals becoming available, transcriptomics technology and pharmacological selectivity beginning to improve they have had much attention. Several TRP channels are widely expressed in the brain; therefore it follows that these would be ideal candidates as "sensors" within the PVN. With this is mind the aim of this chapter was therefore to explore what altering the osmolality and temperature did to neuronal activity *in vitro* and attempt to identify

the channels responsible for any sensing capabilities these neurons may express. This was carried out using a variety of methods.

3.4.1 Osmolality

Although the presence of TRPV4 channels has been shown in the PVN of the hypothalamus before (Carreno *et al.*, 2009), I confirmed this presence within the parvocellular area using immunofluorescence.

3.4.1.1 Action current recordings

The effects of osmolality on neuronal activity were explored using cell-attached patch clamp electrophysiology. By using this technique I was able to record action currents as an indication of action potentials and analyze the firing frequency of the neurone patched. It should be noted that this is not a direct recording of the action potentials themselves, which is usually done using whole-cell methods or sharp electrodes. These can result in disturbance of the cells intracellular milieu. Therefore I used cell-attached patch (which does not disturb the cell interior) since the purpose of these experiments was to alter the external environment (in this case osmolality) of the cell by changing the bath solution, without directly interfering with the intracellular cellular environment.

During osmolality experiments normal ACSF (300 mosmol) was perfused over the slice using a peristaltic pump system whilst recording action current frequency and the solution was then changed to one of a low osmolality (270 mosmol). This may seem a large difference, as levels are usually highly regulated from 300-290 mosmol (Bourque, 2008), however, levels as low as 250 mosmol have been reported in

people who have taken substances such as MDMA (Brvar *et al.*, 2004). These levels were therefore set to ensure any response was not too subtle to detect, yet staying within the bounds of normal physiology.

Whilst recording action currents it was observed that the majority of cells firing did so spontaneously and fairly rapidly. This is somewhat against the consensus these neurones remain quiescent *in vivo* (Park and Stern, 2005). However, the these low levels of activity are lost *in vitro*, where these neurones are spontaneously active (Stern, 2001; Womack *et al.*, 2007), perhaps due to a loss of tonic inhibition from GABAergic innervation during the slicing processes. From these action current recordings it was observed that frequency was massively decreased with reducing osmolality, showing an osmosensing role for this population of neurones. This was an observation which is supported by previous research showing altered neuronal activity as a result of changing osmolality in other areas of the brain (Bourque *et al.*, 2007). In order to then discover the potential mechanism behind this osmosensing capability several specific pharmacological agents were used. Both the TRPV4 channel agonists 4αPDD and the more selective GSK1016790A resulted in reduction of action current frequency. Interestingly the difference in reduction of action current frequency between GSK1016790A and 4αPDD was significantly different; this could be due to the action of these agonists or a difference in specificity. Upon this confirmation, the TRPV4 channel inhibitors RN1734 and HC067047 were used during perfusion of the hypotonic solution. Osmolality was reduced before these inhibitors were added to ensure osmosensitivity of the neuronal cell patched. The addition of both agonists resulted in a reversal of the effects of reduced osmolality

on action current frequency. These results show activation of TRPV4 channels using osmolality modulates neuronal activity within the parvocellular PVN.

3.4.1.2 Single channel recordings

As these experiments were performed in slice the neuronal network will still be somewhat intact. This means that any effects seen during the above set of experiments could potentially be indirect (i.e. effects imposed from further upstream in the network). This issue could potentially be resolved by using synaptic block by changing Ca^{2+} and Mg^{2+} levels of the solutions or using pharmacology However, as the nature of the recordings was to measure spontaneous action potentials, and these would be abolished in these circumstances, this was not done. Instead, cell-attached patch electrophysiology was used to record single channel events and the TRPV4 channel agonist 4αPDD was used to identify the channel in the neurones patched. TRP-like channels were identified in 50% of cells by measuring the conductance (57±7 pS) and reversal potential (-5±3mV) of the channel; both of which are indicative of a TRPV channel as described by Alexander *et al*. (2011). It possible to compare the reversal potential recorded in the single channel recordings to a calculated reversal potential based on the ionic concentrations used in these experiments. In a general TRPV channel case an adapted constant field equation can be used (Lewis, 1979):

Equation 3.1

$$Vrev = \frac{RT}{F}\, ln\left(\frac{[Na^+]_o + \left([K^+]_o\, \frac{PK}{PNa}\right) + 4\ PCa'.[Ca^{2+}]_o}{[Na^+]_i + \left([K^+]_i \frac{PK}{PNa}\right) + 4\ PCa'.[Ca^{2+}]_i .e^{F\,.Vrev\,/\,RT}}\right)$$

Where,

Equation 3.2 $$PCa' = \frac{PCa}{PNa}\left(\frac{1}{1+e^{F.Vrev/RT}}\right)$$

Lewis (Lewis, 1979) showed that with 2mM extracellular Ca^{2+} and zero assumed surface charge, this equation satisfactorily describes the V_{rev} of the K^+, Na^+ and Ca^{2+} permeant end-plate currents including those of TRPV4 (with permeability ratios of 6:1:1 for Ca^{2+}, Na^+, and K^+ respectively (Strotmann *et al*., 2010). Variants of this are widely used in calculations of non-specific cation permeabilities (Kamouchi *et al.*, 1999; Vennekens *et al.*, 2000; Owsianik *et al.*, 2006). Solving this equation gives a V_{rev} of +4.2 mV. Both the calculated and recorded reversal potentials are close to the 0 mV reversal potential expected to see from a non-selective cation channel such as TRPV4. Along with this evidence, the channel seen within these single channel recordings was ultimately identified by an increase in open probability upon addition of the TRPV4 selective activator, 4αPDD.

3.4.1.3 Whole cell and calcium investigations in isolated PVN cells

Furthermore, experiments investigating osmolality in this chapter were performed on isolated PVN neurones from the rat. The isolated neurone preparation eliminates issues of innervating neurones from the network as any calcium changes occur in individual cells. Rats were used instead of mice due to the size of the tissue; it is possible to punch out a PVN population from a rat, but this technique is inaccurate in the mouse.

Opening TRPV4 channels will result in an influx of Ca^{2+}, as this channel is more permeable to Ca^{2+} over other cations; this was verified using calcium recording with Fura-2AM. Ca^{2+} increases were seen with both hypotonic challenge and activation

with 4αPDD. In theory this increase in Ca^{2+} should result in a depolarization of the membrane potential as the cell becomes more positive. Whole-cell patch clamp electrophysiology in current clamp mode confirmed this showing depolarization with TRPV4 channel agonists, 4αPDD and GSK1016790a. The depolarisation of membrane potential due to activation of the TRPV4 channel is consistent with a model where TRPV4 channel activation results in an influx of Ca^{2+} into the neurone. Opening TRPV4 channels will move the membrane potential towards the equilibrium potential for Ca^{2+}, resulting in depolarisation. However, a depolarisation and increasing levels of Ca^{2+} would typically result in an increase in activity, not the decrease seen in these experiments. This is further discussed in Chapter 5.

This extensive set of experiments provides compelling evidence that neurones of the parvocellular PVN have osmosensing capabilities, and show for the first time the non-selective cation channel TRPV4 is at least in part responsible for this role in cell regulation. Other major areas for central osmosensing in the brain, particularly the circumventricular organs such as the subfornical organ, have been investigated extensively and changes in osmolality are known to alter sympathetic drive via their projections (Stocker and Toney, 2005). The current investigation has revealed that the putative parvocellular neurones of the PVN themselves directly "sense" osmolality, and therefore the afferent projections from the circumventricular organs that exist are not responsible for this process. As the PVN is located close to the third ventricle, and so can receive inputs from the cerebrospinal fluid circulating the brain; including osmolality. Questions remain, however, as to the function of this mechanism. It is likely that although the circumventricular organs may sense

immediate changes in osmolality and adjust sympathetic drive accordingly, the PVN may be responsible to long term sympathetic adjustments to osmolality. Further investigation is required to explore these possibilities.

3.4.2 Temperature

Having shown the presence of the TRPV4 channel within the parvocellular region of the PVN, it was thought that it may also have a temperature sensing role as it is activated at temperatures above 27^{o}C. Altering temperature of the bath solution in rising steps of 5^{o}C from 22^{o}C to 37^{o}C decreased action current frequency dramatically. This range was chosen as a lot of electrophysiological research is performed at room temperature, and anything over 37^{o}C in the brain can result in serious complications. The decrease seen was gradual throughout the temperatures used; either suggesting activation of a temperature sensitive channel such as a TRP channel or a more general effect of the temperature such as is seen with enzymatic reactions. The broad spectrum TRP channel blocker, gadolinium, was used to see if the effects of temperature were blocked. At lower temperatures of 27^{o}C and 32^{o}C action currents persisted, suggesting a temperature and gadolinium-sensitive channel (perhaps a TRPV4 channel) was activated. However, the effects of temperature remained when at physiological temperatures, suggesting another channel may be responsible for this reduction in action current frequency. A process of elimination led to the TRPM2 channel being a candidate, as it is not gadolinium sensitive, but is activated at temperatures above 35^{o}C. The only relatively selective pharmacological agent for this channel is econazole, which is also used as a TRPV5 channel inhibitor (however, this channel *is* gadolinium

sensitive). Treatment with econazole blocked the temperature effects altogether, providing some evidence that TRPM2 channels are responsible in part for temperature sensing in this area. Furthermore, the TRPM2 channel C-terminal region is almost entirely made up of an enzymatic domain, which is perhaps why action current frequency decreases in such a way with increasing temperature.

An interesting point to mention is that typically in neurones temperature elevation leads to an increase in activity (Sudbury and Bourque, 2013). I therefore speculate that decreasing activity is an indirect effect whereby TRPM2 channel activation excites inhibitory GABAergic neurones innervating the patched putative parvocellular neurones. This is a hypothesis that could be tested by further experiments or by mathematical model.

4 The Role of the TRPV4 Channel in Central Osmoregulation

4.1 Introduction

Body fluid osmolality is usually regulated within an extremely narrow range (~290-300 mosmol) (Bourque, 2008). Several areas surrounding the third ventricle, such as the subfornical organ and lamina terminalis have been implicated in central osmosensing and osmoregulation (Bourque, 2008). Both also project to the PVN (Sawchenko and Swanson, 1982), an area within close proximity that has been shown in Chapter 3 to have osmosensing capabilities itself *in vitro* via a mechanism involving the TRPV4 channel. This study implicated a role for TRPV4 channels in osmosensing, showing the ability of these channels combined to modulate firing frequency of putative parvocellular neurones depending on the osmolality of the environment. As the PVN is an area well known to modulate cardiovascular function and SNA (Coote *et al.*, 1998; Pyner, 2009; Yang and Coote, 1998; Yang *et al.*, 2009), reviewed by (Nunn *et al.*, 2011; Pyner, 2009), it seems likely that changes in osmolality would therefore influence cardiovascular parameters.

4.1.1 Physiological effects of osmolality

Both magnocellular and parvocellular subsections of the PVN have been suggested to play a role in osmoregulation (Arnhold *et al.*, 2007; Giovannelli *et al.*, 1992; Yamashita *et al.*, 1988). The majority of research has so far focussed on the

magnocellular area of the PVN; well known for its osmosensing capabilities. Haselton *et al* (1994) showed that the parvocellular PVN was involved in a reduction of RSNA during isotonic volume expansion. It has since been postulated that the parvocellular PVN may respond to changes not only in blood volume (Lovick *et al.*, 1993), but also in osmolality (Deering and Coote, 2000). Altering firing rates within the parvocellular PVN as a result of these environmental changes may therefore have an effect upon the cardiovascular system and SNA due to its projections to the IML and RVLM. Studies carried out by Stocker (2004) and Arnhold (2007) showing increased early c-fos expression following water deprivation induced hypertonicity in rats provide further evidence for a role of these spinally-projecting neurones of the parvocellular PVN in osmoregulation (Arnhold *et al.*, 2007; Stocker *et al.*, 2004). Furthermore, decreases in RSNA and arterial blood pressure have been noted with inhibition of spinally-projecting parvocellular neurones (Stocker *et al.*, 2004). In rats, hypertonic challenge by injection via the internal carotid artery with both NaCl and mannitol increased heart rate, mean arterial pressure and RSNA (Chen and Toney, 2001). Although the focus of these studies was the function of AT_1 receptors, they suggest that SNA is only in part modulated by activation of AT_1 receptors, leaving a gap in the knowledge of the potential mechanisms involved. Later studies by (Gao *et al.*, 2009) showed TRPV4 channel activation by the activator 4αPDD resulted in a decrease in mean arterial pressure, and although this study did not identify the mechanism by which this occurred the authors hypothesised several possibly routes; including central osmosensing within the PVN. Despite later studies implicating part of this mechanism was due to TRPV channels present on endothelium tissue of the mesenteric artery, no further investigation has been

made into a role for osmosensing within the PVN itself (Gao and Wang, 2010). This body of evidence, combined with the *in vitro* investigation presented in Chapter 3 les to the hypothesis that not only does the PVN have a role in central osmoregulation, and therefore an influence over cardiovascular parameters, but that the non-selective cation channel TRPV4 may be central to this mechanism.

4.1.2 Aims

This chapter will explore central osmosensation, with an aim to (1) investigate the effects of central osmolality on cardiovascular parameters *in vivo* by measuring blood pressure using arterial cannulation, and (2) pharmacologically identify whether the TRPV4 channel is involved in this mechanism of central osmosensation.

4.2 Methods

Blood pressure was recorded by a pressure transducer from adult CD1 wild-type mice (30-40g) as described fully in Chapter 2. Mice were placed in a stereotaxic frame and ICV injections of 1µL of isotonic/isotonic+DMSO ACSF, hypotonic ACSF (~270mOsm) and RN1734 (Tocris, UK) in vehicle (isotonic ACSF) (100 nM/kg) were performed slowly over a minimum of 1 minute using a 10µl Hamilton syringe and withdrawn carefully to prevent the solution travelling back up the needle track. Heartbeats were annotated using PhysioNet to give heart rate and R-R interval and all parameters were analysed by averaging a stable section of heart rate for 5 minutes before injection and during the peak response after the needle was removed. Once the recording was over the injection site was confirmed by lowering the Hamilton syringe into the same coordinates loaded with 1% pontamine blue

dye. 1µL of pontamine blue dye was injected in the same procedure as described above. Once sacrificed, the mouse was decapitated and the brain removed for slicing on the vibrotome to confirm the injection site (not shown).

4.3 Results

Average blood pressure and heart rate were not significantly changed in mice injected ICV with isotonic ACSF or isotonic ACSF plus DMSO 0.01% (~300 mosmol). A difference of -2 ± 1 mmHg in mean arterial pressure was observed after isotonic injection from 47 ± 4 mmHg to 44 ± 3 mmHg, and average heart rate remained statistically the same from 629 ± 19 bpm to 619 ± 21 bpm after isotonic injection (Figure 4.1 and Figure 4.4 n=6; p>0.05 by ANOVA using Tukey's post hoc comparison).

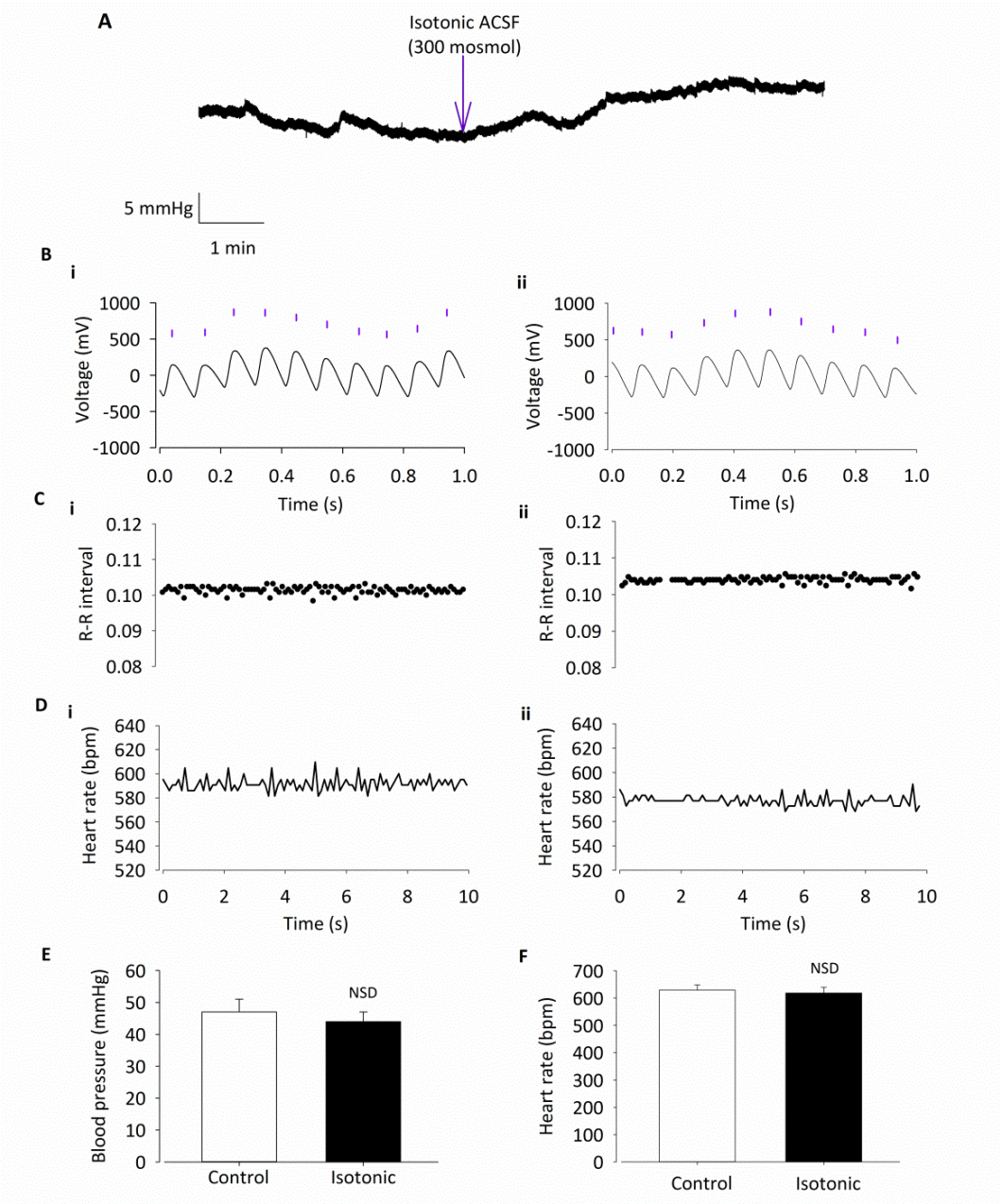

Figure 4.1 Intracerebroventricular injection of isotonic ASCF has no effect on cardiovascular parameters.

Adult male CD1 mice were anaesthetised with urethane-chloralose, and blood pressure was recorded by cannulation of the carotid artery. **(A)** Raw unamplified representative blood pressure trace. Arrow indicates ICV injection of isotonic (300 mosmol) ACSF. **(B)** Amplified blood pressure trace with annotated beats (purple lines), before (i) and after (ii) injection. Annotated beats are used to derive R-R interval and heart rate. **(C)** Example R-R interval trace shows no difference before (i) and after (ii) ICV injection of isotonic ACSF. **(D)** Example heart rate trace shows no difference before (i) and after (ii) injection of isotonic ACSF. **(E)** Average blood pressure and **(F)** heart rate do not change with injection of isotonic ACSF (n=6; p>0.05).

Hypotonic ACSF administered centrally resulted in a significant decrease in mean arterial pressure of -9 ± 2 mmHg from 45 ± 5 mmHg to 36 ± 4 mmHg (n=6; p<0.01 by ANOVA using Tukey's post hoc comparison). No change in heart rate was observed (Figure 4.1 and Figure 4.4; n=6; p>0.05 by ANOVA using Tukey's post hoc comparison; representative trace shown in Figure 4.2). Blood pressure change was significantly greater in mice injected ICV with hypotonic ACSF compared to those treated with the vehicle injection (isotonic/isotonic+ DMSO 0.01%) ACSF (Figure 4.4; -9 ± 2 mmHg vs -2 ± 1 mmHg; *n*=6; *p*<0.01 by ANOVA with Tukey's post hoc comparison). This suggests that central osmolality changes result in altered blood pressure.

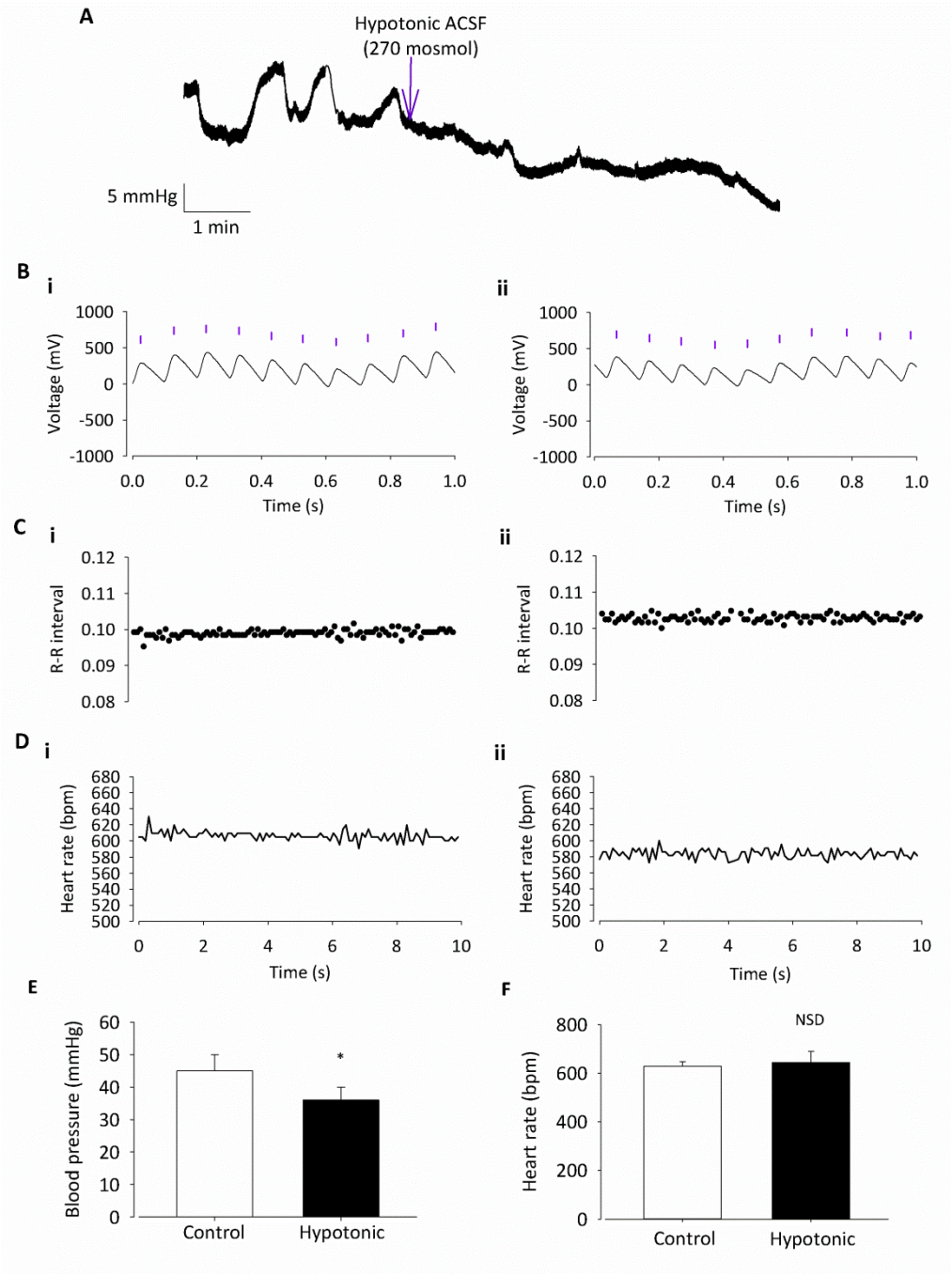

Figure 4.2 Intracerebroventricular injection of hypotonic ASCF decreases blood pressure but has no effect on heart rate.

(A) Raw unamplified representative blood pressure trace. Arrow indicates ICV injection of hypotonic (270 mosmol) ACSF. Blood pressure significantly decreases after injection of hypotonic ACSF. **(B)** Amplified blood pressure trace with annotated beats (purple lines), before (i) and after (ii) injection. Annotated beats are used to derive R-R interval and heart rate. **(C)** Example R-R interval trace shows no difference before (i) and after (ii) ICV injection of hypotonic ACSF. **(D)** Example heart rate trace shows no difference before (i) and after (ii) injection of hypotonic ACSF. **(E)** Average blood pressure is significantly reduced with injection of hypotonic ASCF (n=6; *p<0.01), but heart rate **(F)** remains unchanged (p>0.05).

Addition of the TRPV4 channel inhibitor RN1734 (100 nM/kg) prevented the reduction in mean arterial pressure observed with injection of hypotonic ACSF alone (see representative trace Figure 4.3). A non-significant change of -1 ± 1 mmHg was seen from 42 ± 4 mmHg to 41 ± 4 mmHg (Figure 4.3 and Figure 4.4; n=6; p>0.05 by ANOVA using Tukey's post hoc comparison). Again, no difference in heart rate was observed (Figure 4.3 and Figure 4.4; n=6; p>0.05 by ANOVA using Tukey's post hoc comparison).

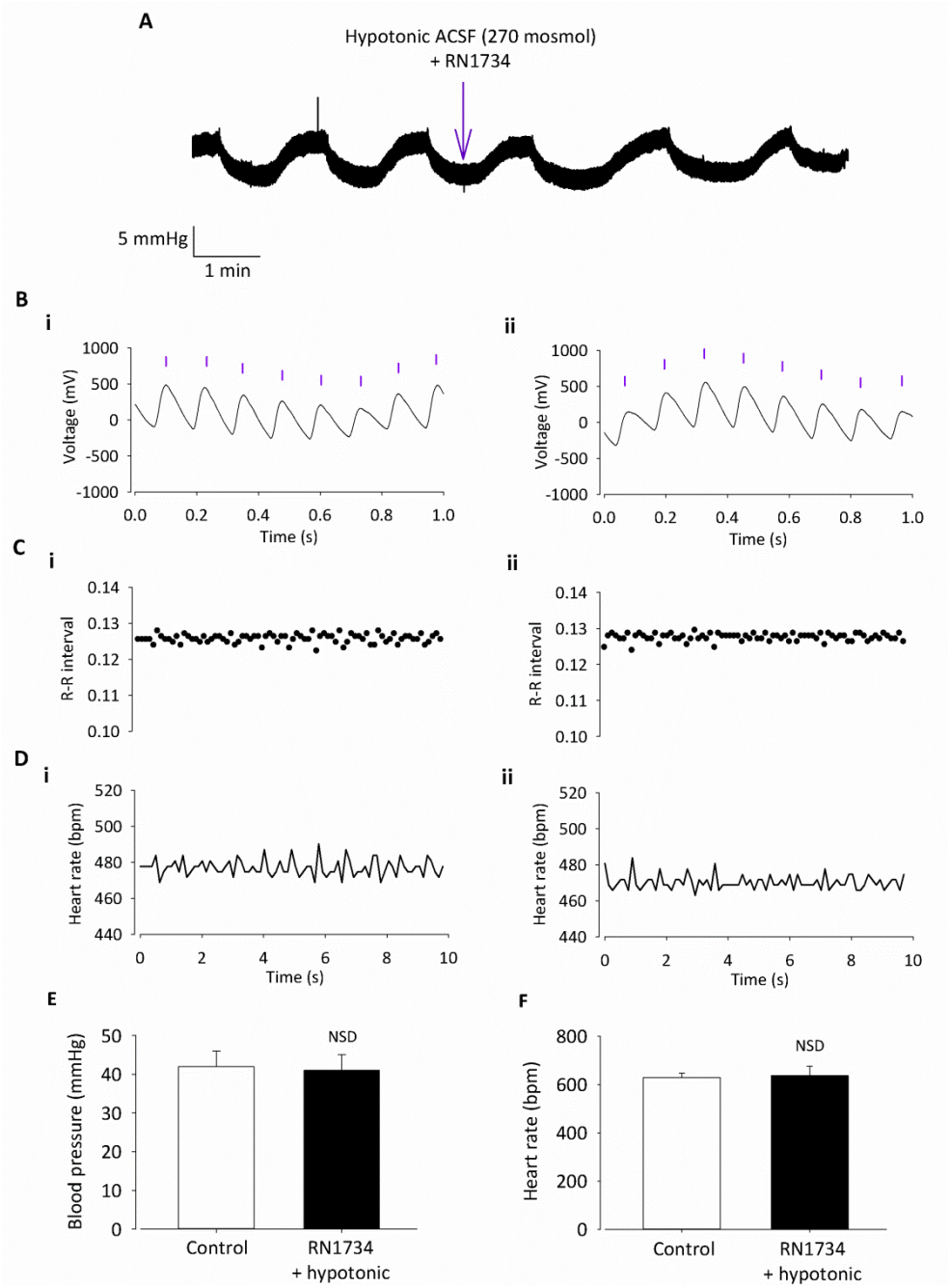

Figure 4.3 Intracerebroventricular injection of the TRPV4 channel inhibitor RN1734 prevents the effect of hypotonic ACSF on blood pressure.

(A) Raw unamplified representative blood pressure trace. Arrow indicates ICV injection of hypotonic (270 mosol) ACSF with the addition of RN1734 (100 nM/kg). Blood pressure does not change upon ICV injection of hypotonic ACSF in the presence of RN1734. **(B)** Amplified blood pressure trace with annotated beats (purple lines), before (i) and after (ii) injection. Annotated beats are used to derive R-R interval and heart rate. **(C)** Example R-R interval trace shows no difference before (i) and after (ii) ICV injection. **(D)** Example heart rate trace shows no difference before (i) and after (ii) ICV injection. **(E)** Average blood pressure response to hypotonic ASCF is prevented by injection of RN1734 (n=6; p>0.05). **(F)** Average heart rate remains unchanged (n=6; p>0.05).

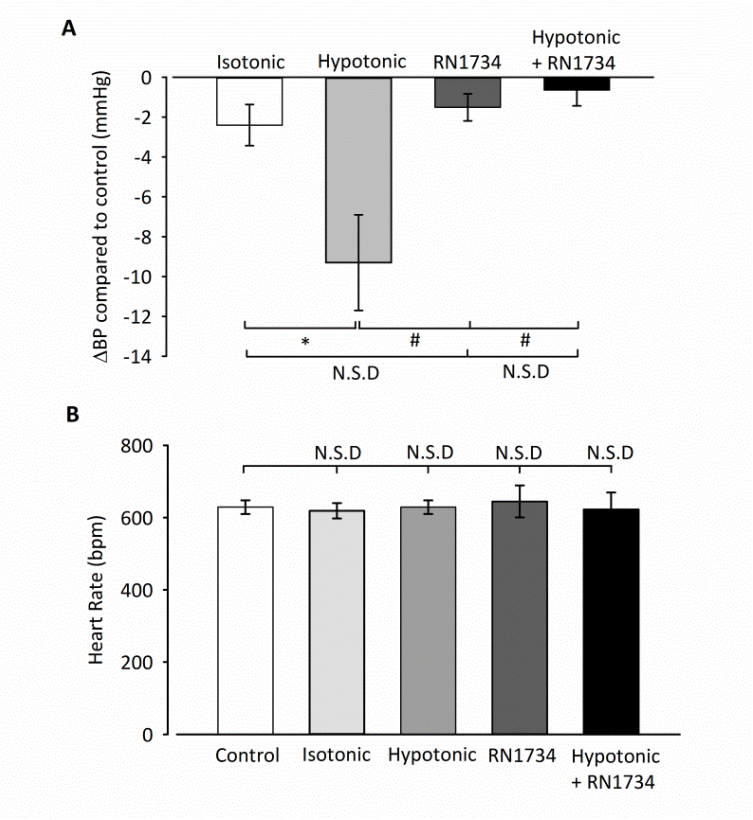

Figure 4.4 Summary average changes in cardiovascular parameters from ICV injections.
(A) Average change in blood pressure compared to control of several ICV injection treatments. No significant change was seen with vehicle (isotonic ACSF) or the TRPV4 channel inhibitor, RN1734 (100 nM/kg) alone *vs* control (n=6; p>0.05). Blood pressure is significantly reduced in animals injected with hypotonic ACSF compared to those injected with vehicle (n=6; *p<0.01). ICV injections with RN1743 + hypotonic ACSF did not produce a significant blood pressure change compared to vehicle injections (n=6; p>0.05), but blood pressure change was significantly reduced compared to hypotonic injections (n=6; #p<0.01). **(B)** Average heart rate did not change significantly between any of the conditions stated (n=6; p>0.05 by ANOVA).

4.4 Discussion

Previous studies have shown that changes in osmolality lead to changes in heart rate, RSNA and blood pressure (Chen and Toney, 2001; Stocker *et al.*, 2004), although most of these studies have not altered osmolality directly in the brain.

Chapter 3 showed that putative parvocellular neurones of the PVN are able to sense osmolality changes. Furthermore, these changes in osmolality resulted in modulated firing activity of these neurones via a TRPV4 channel-dependant mechanism. Preautonomic neurones within the PVN are known to modulate cardiovascular parameters via the autonomic nervous system; therefore it seems that central osmolality may in turn have an effect on the cardiovascular system via these same mechanisms. It has previously been shown that hypotonic infusion via the carotid artery resulted in a decrease In MAP, lumbar SNA and increased heart rate in water dehydrated rats, but not in water replete rats (Brooks *et al.*, 2005; Scrogin *et al.*, 1999); the authors hypothesise that one possible method of action is via the spinally-projecting neurones of the PVN. Furthermore, Holbein *et al* (2014), have recently shown PVN inhibition results in a decrease in blood pressure and splenic SNA in dehydrated rats, proposing that the PVN drives tonic splenic SNA. This evidence led me to investigate central osmolality in mice using ICV injections, and its effects on the cardiovascular system. In order to do this, mice were cannulated by the carotid artery whilst anaesthetised with a combination of urethane and α-chloralose. Although this combination is seen as less suitable in recent years due to carcinogenic effects, these anaesthetics are known for having little effects themselves on the cardiovascular system. It was felt it was most appropriate for this reason, and as cannulation is a terminal procedure any adverse effects to the welfare of the animal would not be an issue. Blood pressure was recorded from cannulated mice and heart rate and R-R interval could then be derived. Cannulation was chosen over tail cuff plethysmography for recording of blood pressure as it is a much more accurate method.

ICV injections of solutions were performed rather than direct PVN injections as the size of the PVN in adult mice is too small to accurately inject just the PVN area itself. As it has been hypothesised blood volume changes alone would have an effect on cardiovascular parameters it is important to check this first by injecting isotonic ACSF (~300 mosmol). No changes to blood pressure or heart rate were observed with this or the combination of isotonic and DMSO (used as a vehicle for the TRPV4 channel inhibitor RN1734).

Investigation continued in order to study the effects of central hypotonic ACSF (~270 mosmol) on cardiovascular parameters. The osmolality chosen for these experiments are the same values used in Chapter 3, however, compared to other *in vivo* studies such as those by Brooks et al (2005), where hypotonic solutions of 40 mosmol were used, this is a far more subtle change, within the bounds of physiology (Bourque, 2008; Brvar *et al.*, 2004). ICV injection of hypotonic ACSF resulted in a decrease of blood pressure, showing central osmosensation and suggesting the area responsible would (a) also have a role for modulating the cardiovascular system (such as the PVN) or (b) innervate such a nucleus. These data supports previous reports that changes in central osmolality results in the modulation of blood pressure (Brooks *et al.*, 2005; Scrogin *et al.*, 1999). In previous studies changes in heart rate have also been recorded upon osmotic change (Chen and Toney, 2001); however, our results show no statistical significant differences. This is not completely unexpected due to the baroreceptor reflex, which would be working to counteract the reduction in blood pressure (Spyer, 1994).

Lack of insight of the ionic mechanisms responsible for changes in blood pressure in this investigation led me to explore further. The mechanosensitive TRPV4 channel is known to be activated by osmolality changes (Liedtke *et al.*, 2000) and has a known role in volume control in other tissues (Becker *et al.*, 2005; Benfenati *et al.*, 2011; Guilak *et al.*, 2010); it has been suggested TRPV4 channels may be responsible for volume control centrally (Bourque, 2008). This theory was confirmed by performing ICV injection of RN1734, a selective TRPV4 channel inhibitor, with hypotonic challenge. RN1734 blocked the blood pressure response to hypotonic ACSF ICV injection. This strongly supports a role for central TRPV4 channels in sensing osmolality changes and initiating changes in blood pressure. Although the exact position of these channels centrally is unknown, this investigation complements the work previously shown in Chapter 3. In this study a putative parvocellular population of neurones has been shown to have a TRPV4 channel dependant osmosensing mechanism and it is well known that these neurones modulate the autonomic nervous system. It is therefore easy to infer these are the neurones responsible for the changes in blood pressure observed due to altering central osmolality; however, further investigation is necessary to confirm this.

Potentially, pharmacological modulation of blood pressure via TRPV4 channels could be useful in the treatment of cardiovascular disease; however, the widespread distribution of these ion channels could limit their practical usefulness. Therefore future studies will be aimed at identifying the receptor and neurotransmitter profile of PVN osmosensing neurones to determine if we can identify more specific therapeutic targets.

5 Small Conductance Calcium-Activated Potassium Channels Couple to TRPV4 to Sense Osmolality

5.1 Introduction

In Chapter 3 the process of osmosensation via the TRPV4 cation channel was investigated. This chapter clearly showed TRPV4 channels were present in the parvocellular area of the PVN and that they responded to osmolality changes and this in turn affected firing rate. Decreases in osmolality led to activation of TRPV4 channels resulting in an increase in Ca^{2+} within the cell and subsequently depolarisation of the cell was seen due to this Ca^{2+} influx. However, depolarisation of the cell would typically lead to an increase in firing rate, not the decrease shown, unless large amounts of Ca^{2+} flooded into the cell created a depolarising block. It was important to investigate this further to reveal the full mechanism responsible. There is a large body of evidence suggesting that there is coupling between the TRPV4 and calcium-activated potassium channels in other tissues; this therefore seemed a sensible set of channels to investigate.

5.1.1 Calcium-activated potassium channels

Calcium is a vital signalling molecule and a rise in intracellular Ca^{2+} has many consequences such as; a release of Ca^{2+} from intracellular stores (calcium-induced calcium release), activation of second messenger systems, regulation of gene expression and the activation of calcium dependent ion channels. Perhaps the best studied of these ion channels are the K_{Ca} channels. These channels consist of three

families identified based on their pharmacological and biophysical properties; notably the SK, IK and BK channels, with further subtypes identified within the SK channel family (SK1, SK2 and SK3)(Kohler *et al.*, 1996). The nomenclature of these channels is further complicated as they are often referred to as $K_{Ca}2.1$ (SK or SK1), $K_{Ca}2.2$ (SK or SK2), $K_{Ca}2.3$ (SK or SK3), $K_{Ca}3.1$ (SK4, or IK) and Slo (BK) (Alexander *et al.*, 2011). All are selectively permeable to potassium and are gated by a rise in intracellular calcium. Both BK and the SK channel subtypes can be found in the rodent brain and both are found within the PVN (Salzmann *et al.*, 2010; Sausbier *et al.*, 2006). These K_{Ca} channels play a vital physiological role in the modulation of neuronal firing (reviewed by (Faber and Sah, 2003)). This is thought to be due to their involvement in the after-hyperpolarisation (AHP) that occurs following an action potential. AHP happens in three phases, slow, medium and fast AHP; these phases are responsible for limiting firing frequency and generating spike frequency adaptation.

BK channels, with the largest single channel conductance ranging from 200-400 pS, are both dependent on calcium levels and membrane potential for activation (McManus, 1991). As a result they are activated on the upstroke of an action potential and responsible for fast AHP and therefore repolarization of the membrane (Adams *et al.*, 1982; Shao *et al.*, 1999). SK channels have a much smaller conductance of 2-20 pS and are activated by rises in intracellular Ca^{2+}, but are voltage insensitive. Ca^{2+} binds to calmodulin, leading to a conformational change and the opening of the channel to allow K^+ efflux. These channels mediate the medium AHP and can modulate firing frequency, as has been shown in the PVN (Chen and Toney, 2009; Gui *et al.*, 2012). They have also been suggested to be

involved in slow AHP and spike interval generation, although this is disputed (Faber and Sah, 2003).

5.1.2 K_{Ca} channel coupling to TRPV4 channels and feedback mechanisms

The K_{Ca} channels are both well placed and have the functional capabilities to exert the effects seen in Chapter 3. This action has been proposed in several other studies in a variety of cells (Earley, 2011; Jin *et al.*, 2012; Ma *et al.*, 2013; Sonkusare *et al.*, 2012). One study by (Gao and Wang, 2010) suggests a link with hypotension by activation of TRPV4 and BK channels in endothelial tissue, contributing to the evidence suggesting K_{Ca} channels are likely candidates for coupling with TRPV4 channels within the PVN.

As shown in Figure 5.1, the hypothesis is that Ca^{2+}entry upon activation of the TRPV4 channel would result in activation of one or more K_{Ca} channels. This in turn would lead to an efflux of K^+, hyperpolarization[1] of the cell and a decrease in action potential firing (Nilius and Droogmans, 2001). Furthermore, feedback mechanisms have been proposed within this system. Firstly, a negative feedback loop whereby TRPV4 channels become inactivated by increasing levels of Ca^{2+} above a threshold point (Chun *et al.*, 2012), presumably in order to prevent triggering cell-death signalling by elevated Ca^{2+}. Additionally, membrane hyperpolarisation may increase the driving force for Ca^{2+} entry, leading to an increase in intracellular Ca^{2+}, activating further K_{Ca} channels, in a positive feedback loop (Watanabe *et al.*, 2002). Such hyperpolarisation of autonomic neurones would be expected to have widespread

[1] In Chapter 3 we see depolarisation of the cell with activation of TRPV4 channels in whole cell recordings, however this is inconsistent with the decrease in activity observed in cell attached recordings. See *Discussion* for full explanation of these findings.

physiological consequences such as a decrease in blood pressure or sympathetic activity due to decreased firing rate.

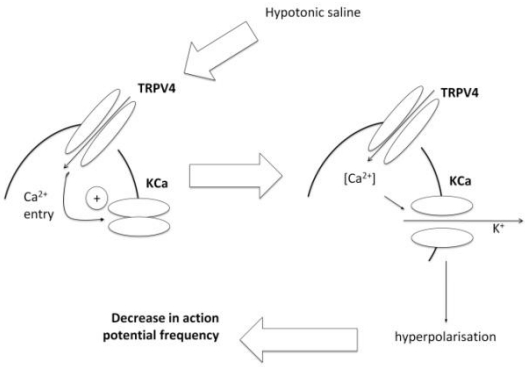

Figure 5.1 Positive feedback mechanism proposed by Nilius and Droogmans (Nilius and Droogmans, 2001).
Influx of Ca^{2+} from the opening of TRPV4 channels increases K_{Ca} channel activity which hyperpolarises the cell and increases the inward flux of Ca^{2+} by increasing the driving force (G [Vm– E_{Ca}]) for Ca^{2+} entry. (Vm= membrane potential, E_{Ca} is the equilibrium potential for Ca^{2+} ions and G is the conductance of the Ca^{2+} entry pathway).

5.1.3 Aims

Chapter 3 showed that hypotonic challenge results in a decrease in action current frequency in the putative parvocellular population of the PVN via activation of the TRPV4 channel. From the evidence presented it is possible that the calcium-activated potassium channels may have a part to play in this complex process. Therefore the aim of this chapter is to (1) explore any potential coupling role with TRPV4 channels in osmosensation for one or more of these channels and (2) uncover any evidence for feedback systems within this increasingly complex process using patch clamp electrophysiology and calcium recordings.

5.2 Methods

Hypothalamic brain slices from CD1 mice were used for action current recordings using cell-attached patch clamp as described fully in Chapters 2 and 3.

Isolated PVN neurones were plated out on glass-bottomed dishes (for full methods see Chapter 2 and Chapter 3) for intracellular Ca^{2+} recording. Cells were incubated for at least 30 minutes with the ratiometric dye Fura-2AM (5 µM) and kept in the dark to avoid bleaching. Regions of interest were highlighted and measurements were made at intervals of 2 s by exciting Fura-2AM alternately at 355 nm and 380 nm. The ratios of these intensities were converted into total calcium levels using Equation 2.1 in Chapter 2.

5.3 Results

5.3.1.1 Small-conductance calcium activated potassium channels

The effects of hypotonic challenge on action current frequency were significantly reduced by the SK inhibitor UCL-1684 (30 nM) (Figure 5.2), with a 79 ± 10% reduction in action current frequency with hypotonic alone, compared to a 37 ± 7 % reduction with hypotonic and UCL-1684 (n=5; p<0.01 by General linear model with multiple comparison using Tukey's post hoc test). No significant changes in action current frequency were seen with UCL-1684 alone (Figure 5.2C; n=6; p>0.05).

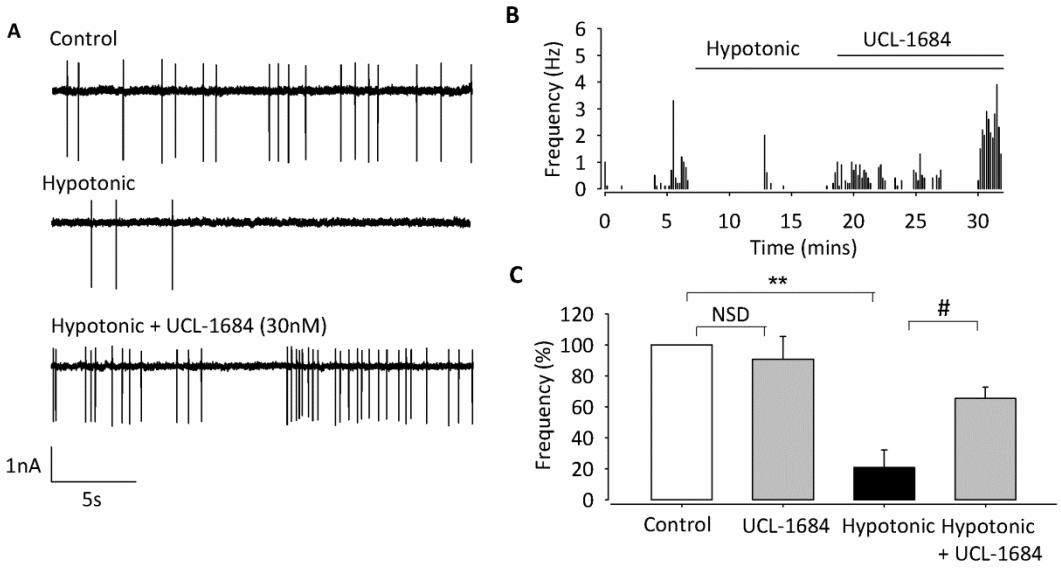

Figure 5.2 Inhibition of the small-conductance K_{Ca} channel reverses the effect of osmotic sensitivity on putative parvocellular PVN neurones.
Cell-attached action current measurements in slice within the medial and dorsal cap parvocellular area of the PVN (Figure 3.1). **(A)** Raw action current trace at 300 mosol (control), 270 mosmol (hypotonic), and with the addition of the SK inhibitor UCL-1684 (30 nm) in hypotonic conditions. **(B)** Representative frequency histogram showing the regain of action current frequency upon addition of UCL-1684, after loss from hypotonic challenge. **(C)** Mean action current frequency is significantly reduced at 270 mosmol (*n*=5; ***p*<0.01 by General linear model with multiple comparison using Tukey's post hoc test), but not in the presence of the SK inhibitor. Data expressed as a % of control (isotonic is 100%). Taken from 5 experiments similar to those illustrated in (A) and (B).

5.3.1.2 Intermediate-conductance calcium activated potassium channels

Again, hypotonic challenge resulted in a decrease in action current frequency, however, this was not significantly affected by the IK channel inhibitor TRAM-34 (30 nM) (Figure 5.3; *n*=5; *p*>0.05 by General linear model with multiple comparison using Tukey's post hoc test).

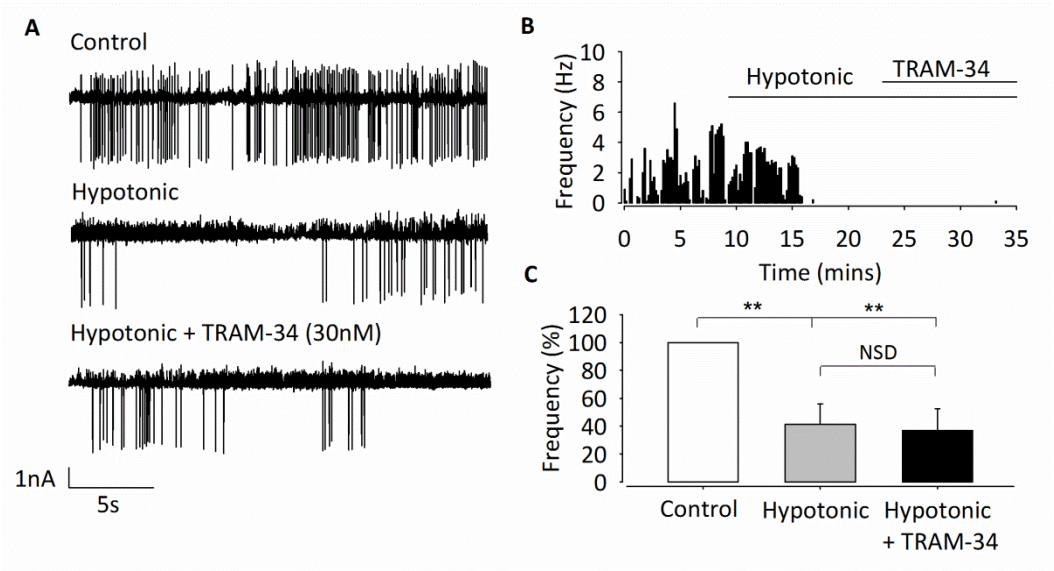

Figure 5.3 Inhibition of the intermediate-conductance K_{Ca} channel has no effect on osmotic sensitivity of putative parvocellular PVN neurones.
Cell-attached action current measurements in slice within the medial and dorsal cap parvocellular area of the PVN (Figure 3.1). **(A)** Raw action current trace at 300 mosmol, 270 mosmol and with the addition of the IK inhibitor TRAM-34 (30 nm). **(B)** Representative frequency histogram showing TRAM-34 has no effect on action current frequency. **(C)** Mean action current frequency from 5 experiments similar to those illustrated in (A) and (B) is significantly reduced upon hypotonic challenge (*n*=5; ***p*<0.01 by General linear model with multiple comparison using Tukey's post hoc test); osmotic sensitivity is unchanged upon addition of TRAM-34.

5.3.1.3 Large-conductance calcium activated potassium channels

No effects on osmosensitivity were observed at concentrations of 1nM, 10nM, 30nM or 100nM of the BK inhibitor iberiotoxin (Figure 5.4; *n*=6; *p*>0.05 by General linear model with multiple comparison using Tukey's post hoc test).

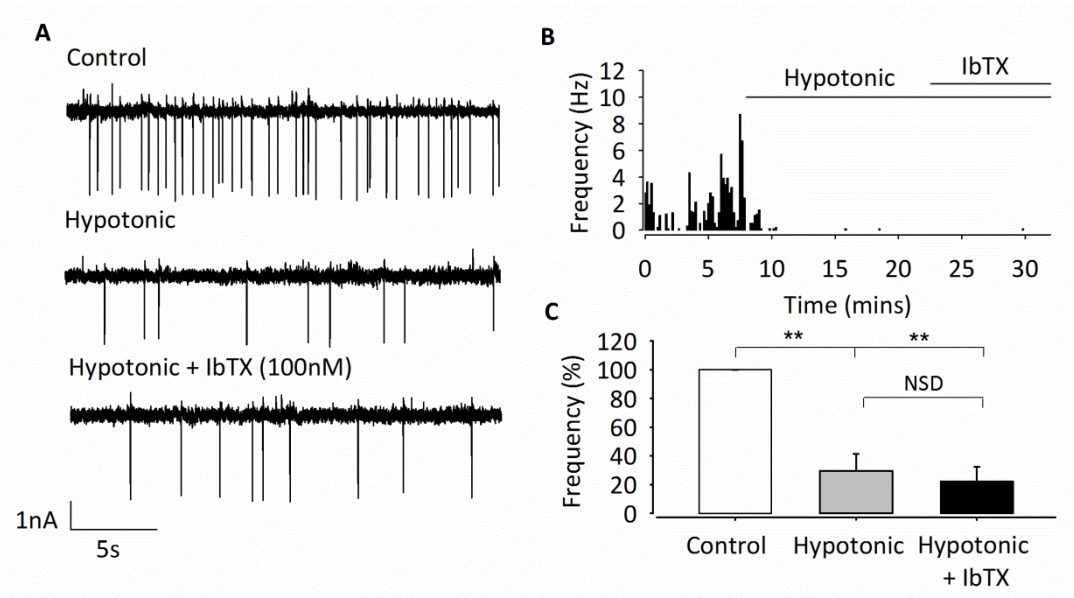

Figure 5.4 Inhibition of the large-conductance K_{Ca} channel has no effect on osmotic sensitivity of PVN neurones.
Cell-attached action current measurements in slice within the medial and dorsal cap parvocellular area of the PVN (Figure 3.1). **(A)** Raw action current trace at 300 mosmol, 270 mosmol, and with the addition of the BK inhibitor iberiotoxin (IbTX) (10 nm). **(B)** Representative frequency histogram showing IbTX has no effect on action current frequency. **(C)** Mean action current frequency from 6 experiments similar to those illustrated in (A) and (B) is significantly reduced upon hypotonic challenge (n=6; **p<0.01 by General linear model with multiple comparison using Tukey's post hoc test); osmotic sensitivity is unchanged upon addition of IbTX.

5.3.1.4 Functional coupling of TRPV4 and K_{Ca} channels

The selective TRPV4 activator, GSK1016790A (100 nM) was shown to reduce action current activity in Chapter 3. By using this activator in combination with the SK inhibitor, UCL-1684 (30nM), it is possible to explore if there is a coupling between these channels. The combination of GSK1016790A and UCL-1684 led to no change in action current frequency (n=7; p>0.05 by Students paired t-test).

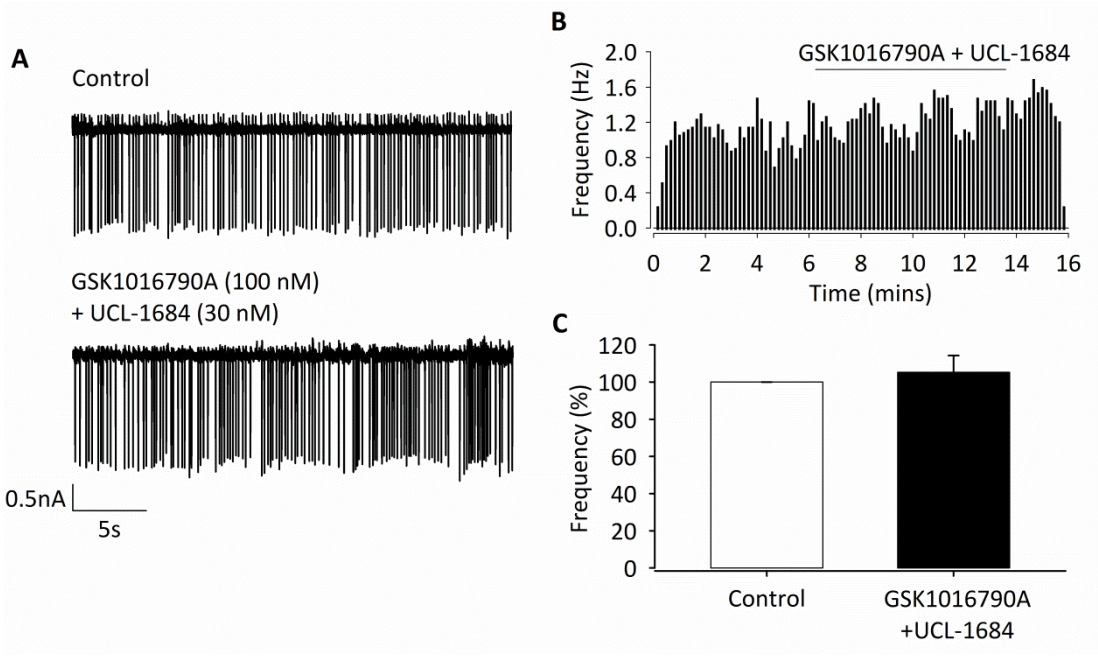

Figure 5.5 Activation of TRPV4 and inhibition of SK combined results in no change of action potential.
Cell-attached action current measurements in slice within the medial and dorsal cap parvocellular area of the PVN (Figure 3.1). **(A)** Raw action current frequency at 300 msomol and with the addition of both GSK1016790A (100 nM) and UCL-1684 (30 nM). **(B)** Representative histogram showing GSK1016790A and UCL-1684 together have no effect on action current frequency. **(C)** Mean action current frequency from 7 experiments similar to those illustrated in (A) and (B) is not significantly changed with addition of GSK1016790A and UCL-1684 (*n*=7; *p*>0.05 by Students paired *t*-test).

5.3.2 Calcium recording

Upon hypotonic challenge with hypotonic ACSF (270 mosmol) a transient increase in $[Ca^{2+}]_i$ was observed from the basal level of 77 ± 3 nM to 198 ± 28 nM (Figure 5.6; *n*=8; *p*<0.001). When subjected to hypotonic challenge in the presence of the SK inhibitor, UCL-1684 (30 nM), an increase in $[Ca^{2+}]_I$ was still observed (from 79 ± 3 nM to 144 ± 8 nM). This increase however was significantly reduced compared to with hypotonic alone and in this case it was sustained until the treatment was washed off with isotonic ACSF. An increase of 121 ± 28 nM with hypotonic alone *vs* 65 ± 8 nM with hypotonic plus UCL-1684 was observed (Figure 5.6; *n*=13; *p*<0.05 by

General linear model with multiple comparison using Tukey's post hoc test). UCL-1684 alone did not affect Ca^{2+} levels (*n*=13; *p*>0.05).

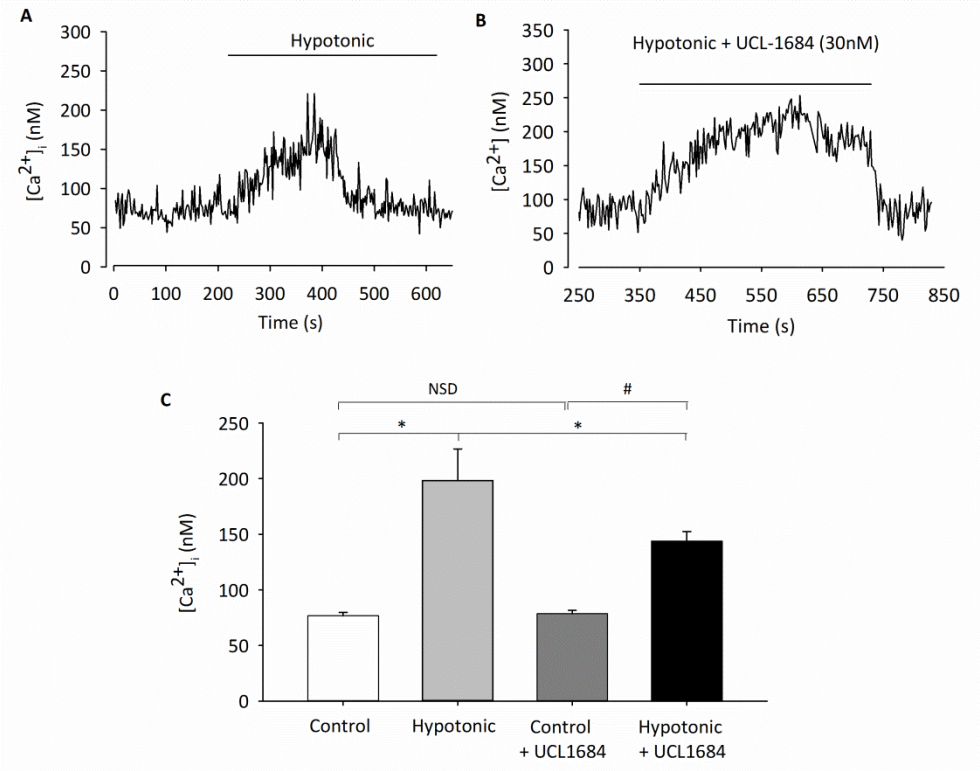

Figure 5.6 Hypotonic challenge results in an increase in intracellular calcium which is dependent on feedback systems driven by K_{Ca} channels.
(A) Representative Ca^{2+}trace showing a transient increase at 270 mosmol (hypotonic challenge). **(B)** Representative Ca^{2+}trace showing a sustained increase in the presence of the SK channel inhibitor UCL-1684 at 270 mosmol. **(C)** Mean intracellular Ca^{2+} from several experiments show Ca^{2+} levels are significantly increased at 270 mosmol with and without the presence of UCL-1684 compared to at 300 mosmol (*n*=10; **p*<0.001 and *n*=13*;*# p*<0.001 respectively by General linear model with comparison against control using Dunnet's post hoc test). Ca^{2+} rise with hypotonic challenge was significantly reduced and sustained when cells are superfused with UCL-1684 (*p*<0.05).

5.4 Discussion

Chapter 3 showed a role for the TRPV4 channel in osmosensation in putative parvocellular cells of the paraventricular nucleus. Upon activation by either low

levels of osmolality, or an activator of the channel, such as 4αPDD, (shown in Chapter 3) there is a decrease in cell excitability and an influx of Ca^{2+} into the cell. It would then follow that this increase in intracellular Ca^{2+}may then activate a Ca^{2+}-activated ion channel; a theory which has been investigated by many groups. Although several Ca^{2+}-activated ion channels exist, the K_{Ca} channels have been extensively researched. The BK and SK channels are known to be widely expressed in the brain, including in the PVN and as discussed have a role in modulating firing activity in neurones (Salzmann *et al.*, 2010; Sausbier *et al.*, 2006). There has been particular focus recently on their co-localisation with TRP channels and several studies in a variety of tissues have shown that K_{Ca} channels are activated by local increases in intracellular Ca^{2+} due to TRPV4 channel opening (Earley, 2011; Jin *et al.*, 2012; Ma *et al.*, 2013; Sonkusare *et al.*, 2012). Activation of K_{Ca} channels will result in a K^+ efflux and therefore hyperpolarisation of the cell and a decrease in excitability (see Figure 5.1); a hypothesis proposed by (Nilius and Droogmans, 2001). For these combined reasons the aim of this chapter was therefore to investigate a possible role for one or more of this family of K_{Ca} ion channels in the osmosensing process.

Primarily it was important to explore which, if any, of the K_{Ca} channels may have been responsible for modulating firing frequency during hypotonic challenge. To do this cell-attached patch clamp was used to record action current firing in brain slice. The appropriate K_{Ca} channel inhibitors were perfused in ACSF and the cells were then subjected to hypotonic challenge. Firing frequency decreased with a reduction in tonicity as expected. The IK channel inhibitor, TRAM-34, did not have an effect on the osmotic sensitivity of these cells. Iberiotoxin, the BK channel inhibitor, also

showed no effect on osmotic sensitivity of PVN cells, or in fact a change in firing frequency on its own. This remained true for increasing concentrations of the inhibitor. This effect is somewhat surprising, as BK channels are present in the PVN, and their inhibition is known to effect action potential duration and frequency (Salzmann *et al.*, 2010). There are at least two possibilities as to why there is no effect on firing frequency in this incidence: 1. Simply, BK channels in these cells are not in close enough proximity to TRPV4 channels to be affected by localized Ca^{2+} entry and therefore it is not involved in this process, or 2. as BK channel activation is highly dependent upon voltage the membrane potential of the neurone this may either mean BK channels remain active regardless of the introduction of iberiotoxin or is continuously inactive during this process (Contreras *et al.*, 2012).

Inhibition of the SK channel with the specific blocker, UCL-1684, did affect osmotic sensitivity of putative parvocellular PVN cells. Use of this blocker prevented the reduction in firing rate caused by hypotonic challenge. The effect seen in these experiments is backed up by studies performed by (Chen and Toney, 2009), where they have shown the presence of SK channels in neurones within the PVN projecting to the RVLM. They use whole-cell patch clamp experiments to show that firing rate in these neurones is regulated by SK channel activity, concluding that SK channel activation results in a medium after-hyperpolarisation resulting in a decrease in excitability of these cells (Chen and Toney, 2009). In Chapter 3, however, I recorded a depolarisation within the cells upon addition of both of the TRPV4 channel activators, 4αPDD and GSK1016790A. If the hypothesis described is correct, one would also have expected to see a hyperpolarisation in these experiments. However, during these whole cell experiments described in Chapter 3 EGTA, a

Ca^{2+}chelator, is used in the patch pipette. During these experiments EGTA would effectively "mop-up" any Ca^{2+} within the cell and therefore prevent the subsequent activation of SK channels via the Ca^{2+}-calmodulin complex, resulting in a depolarisation. This hypothesis would need to be further investigated by investigating membrane potential changes in cells which were Ca^{2+} is only weakly buffered.

It is worth noting here that there are 3 SK channels; SK1, 2 and 3. Although it is not possible to distinguish these using pharmacology, due to a lack of specificity of compounds available, some more specific antibodies are available for immunohistochemical studies. It would therefore be interesting to explore this point further, potentially by investigating co-localisation of these SK channels with TRPV4 channels in the parvocellular area of the PVN.

In addition, a functional coupling of TRPV4 and SK channels is supported by use of more complex pharmacology in cell-attached patch recordings of action currents. Using a combination of the TRPV4 channel activator GSK1016790A and SK channel inhibitor UCL-1684 no change in action current was seen. This suggests that although the influx of Ca^{2+} entry through TRPV4 channels remains, the block of SK channels prevents K^{+} efflux and subsequent hyperpolarisation of the cell and therefore no change of action potential frequency occurs.

In order further to understand the role of SK channels in the osmosensing process, and explore and feedback systems that occur Ca^{2+} recordings were made using the ratiometric dye Fura-2AM in isolated PVN cells. Hypotonic challenge, as expected, resulted in a similar rise in Ca^{2+} to what was seen in Chapter 3 with the activator of

the TRPV4 channel, 4αPDD. A transient increase was seen with both, suggesting negative feedback is occurring. Raising intracellular Ca^{2+} levels above a certain threshold will close the TRPV4 channel to prevent toxic levels occurring and subsequent cell death. Interestingly, when the SK channel inhibitor UCL-1684 is perfused, the increase in Ca^{2+} observed is sustained until isotonic solution is run through and was significantly lower than with hypotonic alone. Levels may be lower as a result of inhibition of SK channel-mediated K^+ efflux. This would mean no subsequent hyperpolarisation and no increase in the driving force for Ca^{2+} entry into the cell (see positive feedback mechanism Figure 5.1). This in turn may prevent Ca^{2+} levels reaching threshold amounts to then trigger the negative feedback block of TRPV4 channels observed with hypotonic alone.

Combined, these results suggest a functional coupling for the TRPV4 and SK ion channels in the complex process of osmosensing in the parvocellular PVN. Hypotonic challenge activates the mechanosensitive TRPV4 channel, increasing intracellular Ca^{2+}. An accumulation of Ca^{2+} within the cell then appears to activate SK channels, hyperpolarising the neurones and therefore decreasing action potential firing frequency. Since these neurones are established to have an effect on the autonomic nervous system reduced firing could potentially lead to a decrease in blood pressure, a role which is discussed in Chapter 4.

6 Modelling TRPV4 and K_{Ca} Channel Coupling

6.1 Introduction

Bernstein (1902) originally proposed that potentials occurred across selectively permeable membranes, which separate ionic concentrations. Furthermore, in order to achieve excitation it was suggested that there was an increase in permeability across the membrane. It was much later that these theories were confirmed with experimental evidence. Resting membrane potential was shown to occur due to local currents (Hodgkin, 1937a; Hodgkin, 1937b), and membrane permeability was shown to increase with excitability (Cole and Curtis, 1939). However, at that time, the theory of ion channels had not yet been discussed and it was believed that a linear electrical gradient existed across the whole membrane; the constant field theory (Goldman, 1943). The concept of selective permeability to particular ions was discovered later, when Hodgkin and Katz showed that the resting membrane is permeable to K^+, Cl^- and Na^+, but to a lesser extent (Hodgkin and Katz, 1949). They hypothesised that as the membrane became depolarised, it became more permeable to Na^+ and therefore suggested that instead of crossing the membrane in an ionic form, Na^+ was able to bind to a lipid soluble molecule in the membrane and cross when the membrane became depolarised. With this the concept of the ion channel came into existence. What followed this discovery was a series of pioneering voltage clamp experiments studying the kinetics of two individual permeability's responsible for the generation of action potentials; Na^+ and K^+, and the propagation of this signal along a nerve fibre (Hodgkin and Huxley,

1952a; Hodgkin and Huxley, 1952b; Hodgkin and Huxley, 1952c; Hodgkin and Huxley, 1952d; Hodgkin and Huxley, 1952e; Hodgkin *et al.*, 1952). Combined with the theory presented by Goldman it was suggested that in order to maintain a steady state resting potential these cells contain ion channels, selective pores in the membrane which are able to control the flow of ions in and out of the cell. The GHK equation was developed as a result of these findings:

Equation 6.1 $$E_{rev} = \frac{RT}{F} ln \left(\frac{P_{Na^+}[Na^+]out + P_{K^+}[K^+]out + P_{Cl^-}[Cl^-]in}{P_{Na^+}[Na^+]in + P_{K^+}[K^+]in + P_{Cl^-}[Cl^-]out} \right)$$

Where E_{rev} is the reversal potential, $[X]_{out}$ and $[X]_{in}$ are the extracellular and intracellular concentrations of the relevant ions, P_x are the permeability coefficients of the ions and *R*, *T* and *F* have their standard definitions. This equation can also be modified to include ions such as Ca^{2+}.

Combined with those observations of Hodgkin and Huxley in 1952, it was shown that the current moving across the membrane could be separated according to the currents carried by Na^+, K^+ and Cl^- (deemed a leakage current). These currents were defined by the equation below:

Equation 6.2 $$I_X = g_X[Vm - E_X]$$

Where I_X is the current of a particular ion, determined by (g_X) the conductance of that ion channel, and the difference between the membrane potential (*Vm*) and the equilibrium potential (E_X) of that ion.

Using this knowledge it is possible to explore the electrophysiological properties of individual cells as well as networks of cells using computational modelling. This is of

particular important as it does not require experimentation, and therefore adheres to the 3R's (replacement, reduction and refinement). Computational modelling is advantageous as it can be used as both a predictor of possible results as well as for verification of mechanisms which may otherwise prove difficult to show experimentally. Within models it is possible to alter a multitude of properties including neuronal conduction, environmental conditions and ion channel populations. One such system which has proven useful in developing a model of a neuronal network is the NEURON simulation environment (Hines and Carnevale, 1997). Using the NEURON simulation environment I have been able to develop a computational model of parvocellular neurones. The development and outputs of the model I have constructed will be discussed in this chapter.

6.1.1 NEURON model of spinally-projecting neurone

This model is based on a previous model of spinally-projecting parvocellular autonomic neurones developed by my group (Feetham and Barrett-Jolley, 2012; Lewis *et al.*, 2010). Inputs to the spinally-projecting neurone arise from both excitatory ''Netstim'' neurones and inhibitory interneurons. The interneurons are also driven by excitatory ''Netstim'' neurons (see Figure 6.1). As described previously excitatory neurones are glutamatergic in nature, and those inhibitory innervations are GABAergic. These innervations of the PVN have been described in depth within this thesis and in the literature (Badoer *et al.*, 2002).

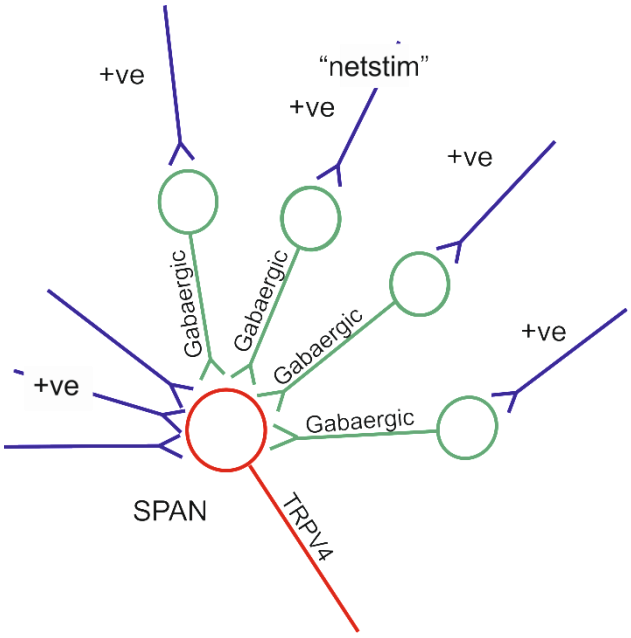

Figure 6.1 Schematic of NEURON model.

Showing a spinally-projecting neurone (SPAN) (in red) innervated by excitatory glutamatergic (in purple) and inhibitory GABAergic neurones (in green). GABAergic inputs are themselves innervated by excitatory "netstim" inputs.

The model also includes the presence of Hodgkin and Huxley channels, which would account for the K^+ and Na^+ currents in the neurone responsible for action potential firing (Hodgkin and Huxley, 1952e). K_{ATP} channels have also been added to the model (originally developed from (Courtemanche *et al.*, 1998)). These channels are known to be present within the PVN and can modulate neuronal firing of spinally-projecting neurones (Lewis *et al.*, 2010; Li *et al.*, 2010).

6.1.2 Addition of TRPV4 and K_{Ca} channels

This model was further developed to include channels based on the experimental evidence taken from Chapter 3 and 5 (parameters added are shown in Table 6). TRPV4 and K_{Ca} channels are present within the parvocellular area of the PVN and

functionally couple to modulate neuronal excitability in response to changes in osmolality. The K_{Ca} channel added has been modified from Benedetti et al (2008) and TRPV4 channel conductance taken from Deng et al (2010). TRPV4 is a non-selective ion channel and has a permeability ratio of 1:1:6 for Na^+, K^+, and Ca^{2+} respectively. These ratios and a whole-cell conductance for the TRPV4 channel were also added using the algorithm of Strotmann et al (2010) as described in the equations below:

Equation 6.3 $$I_{Ca} = g\left(Vm - \left(\frac{RT}{zF}\right)\left(\frac{Cao}{Cai}\right)\right)$$

Equation 6.4 $$I_K = \left(\frac{g}{6}\right)(Vm - E_K)$$

Equation 6.5 $$I_{Na} = \left(\frac{g}{6}\right)(Vm - E_{Na})$$

Equation 6.6 $$I_{TRP} = I_{Ca} + I_K + I_{Na}$$

Where I_X is the current provided by the relevant ion, *g* is the conductance of the channel, *Cao* is extracellular Ca^{2+} concentration, *Cai* is intracellular Ca^{2+} concentration, *Vm* is membrane potential and E_x is reversal potential.

The model contains a subroutine to alter osmolality within the environment; these parameters were taken from results obtained in Chapter 3. Hypo-osmolality is assumed to activate TRPV4 channels in a sigmoidal manner, resulting in an influx in Ca^{2+}.

Equation 6.7 $$g = Gmax_{TRP}\left(1 - \frac{\Delta osmol^h}{\Delta osmol^h + k_{osmol}^h}\right)$$

Equation 6.8 $$\Delta osmol = osmol - basos$$

Where *(Δosmol)* is the simulated change of osmolality, *osmol* is the current osmolality, *basos* is the base osmolality (the lowest used in experiments being 270 mosmol) and *h* is the slope of activation by osmolality. For model parameters see Table 6.

The model simulates intracellular Ca^{2+} accumulation according to Carnevale et al (2006). Ca^{2+} equilibrium is maintained by the incorporation of a simple Ca^{2+} pump (Carnevale and Hines, 2006) and by incorporating both positive and negative feedback for the TRPV4 channels, inclusive of forward and reverse rates. These rates of activation and inactivation were taken from fitting influx and efflux of Ca^{2+} seen in calcium recordings upon activation of the TRPV4 channel with 4αPDD (Chapter 5) (see Table 6). Elevated intracellular Ca^{2+} levels are known to increase open probability of TRPV4 channels via a Ca^{2+}/calmodulin activation complex in a positive feedback system, and further increasing levels inhibit the channel in an negative feedback system, by a so far unknown mechanism (Watanabe *et al.*, 2002).

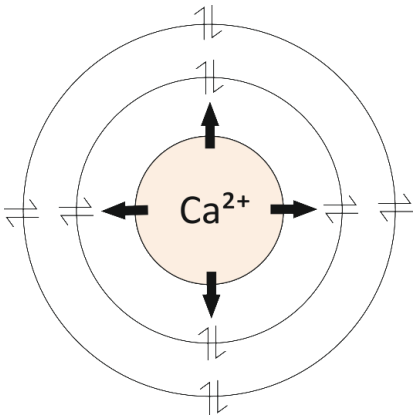

Figure 6.2 Representative figure of Ca^{2+} diffusion around a neuronal cell body within the NEURON model.
Ca^{2+} pumps (solid black arrows) are present in the cell membrane in order to pump Ca^{2+} out when intracellular concentrations become too high within the cell (beige circle) as to avoid toxic concentrations. Rings of diffusion (bidirectional arrows) are also included in the model to demonstrate what would occur in the extracellular environment as Ca^{2+} is pumped out.

Table 6 Parameters included in the NEURON model.

Parameter		Unit	Meaning	Source
$Gmax_{TRP}$	$0.35x10^{-5}$	S/cm^2	Maximum conductance for TRP channel	(Deng *et al.*, 2010)
k	1.5	mosmol	Dissociation constant	
osmol	320	mosmol	Current osmolality of solution	(Dunn *et al.*, 1973)
basos	280	mosmol	Base osmolality	Value used in our experiments.
k1	9.4	nM/s	Forward rate	Estimated from fit of Ca^{2+} data (Chapter 5).
k2	0.05	nM/s	Reverse rate	

The model also includes a subroutine to simulate block of TRPV4 and/or K_{Ca} channels via altering the permeability of the selected channel.

6.2 Results

6.2.1 Altering osmolality

The model simulates the activation of TRPV4 channels upon hypo-osmolality and closely matches experimental data. Output from the model led to action potential frequency decreasing with decreases in osmolality (Figure 6.3A, B, C and D). The osmolality at which action potential frequency was half maximum was 297 ± 0.4 mosmol (Figure 6.3). Furthermore, simulated block of either TRPV4 or K_{Ca} channels prevented this effect.

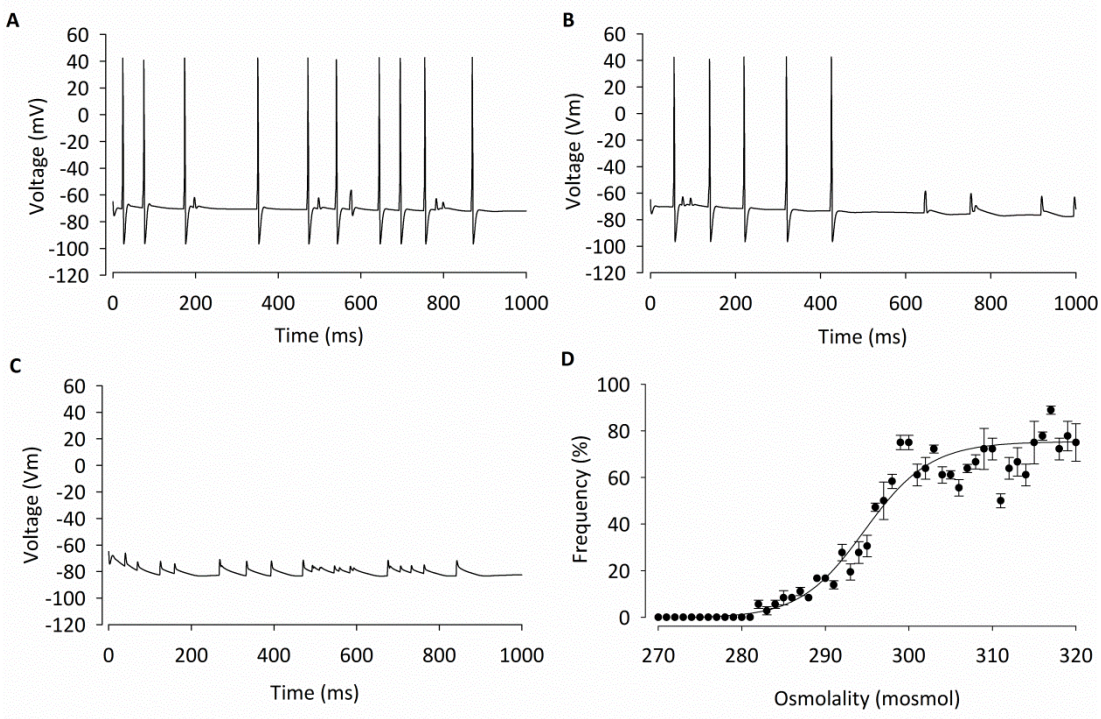

Figure 6.3 Simulated action potential firing is modulated by altering osmolality. **(A)** Action potentials during hypertonic conditions (320 mosmol). **(B)** Decrease in action potential frequency when osmolality is reduced to 300 mosmol, and **(C)** further decreased action potential frequency at 270 mosmol. **(D)** Dose response curve during changes in osmolality within the model.

6.2.2 Block of K_{Ca} channels

I went on to test the positive feedback suggested, whereby K_{Ca} channel-induced hyperpolarisation leads to an increase in Ca^{+2} driving force and draws in further Ca^{2+}. TRPV4 channel activity was simulated by reducing osmolality to 270 mosmol and intracellular Ca^{2+} was calculated. Intracellular Ca^{2+} concentrations with K_{Ca} channel conductance and with a reduced K_{Ca} channel conductance were then compared. Breakage of this positive feedback loop resulted in significantly reduced TRPV4 channel Ca^{2+} current and intracellular decrease of Ca^{2+} (Figure 6.4; 12 nA cm^2/s *vs*. 8 nA cm^2/s; n=7; p<0.001).

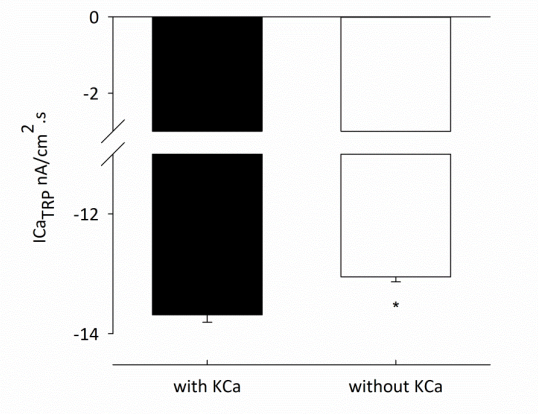

Figure 6.4 NEURON analysis of positive feedback between TRPV4 and K_{Ca} channels in PVN neurones.
Running a number of simulations reveals a reduced mean Ca^{2+} current through the TRP channel (n=7; p<0.001) when K_{Ca} is effectively "blocked", as predicted.

These results support the hypothesis suggested in Chapter 3 and 5 for a functional coupling of the TRPV4 and K_{Ca} channels with the inclusion of both positive and negative feedback systems.

6.3 Discussion

In this chapter I have described the development of a computational model using the NEURON simulation environment and demonstrated some of the abilities of this model. It is evident that computational simulations such as this one are both effective and useful not only as tools for verification of experimental theory but also for predictive measures. I have been able to show that by inputting those parameters from the existing literature and my own experimentally derived data (see Chapters 3 and 5) the model works as those parvocellular cells do in response to osmolality when patched in slice. Upon hypotonic challenge, action potential frequency decreases in a sigmoidal fashion due to the activation of the TRPV4 channel, creating an influx of Ca^{2+} into the cell. This in turn activated K_{Ca} channels, leading to efflux of K^{+} out of the cell and hyperpolarisation occurs. This functional coupling suggested, however, is difficult to fully explore *in vitro*, and so this is where the model becomes particularly useful. Using NEURON it is possible to change any number of parameters, be it the channels added themselves, or the surrounding environment. It is also possible to perform these simulations with the innervations still intact, something which cannot happen during in slice recordings as these connections may have been severed. Furthermore, by blocking the TRPV4 channel by reducing its conductance to zero (which cannot necessarily be done using pharmacological inhibitors *in vitro*), the effects of osmolality are prevented and action potential firing continues. To demonstrate the positive feedback mechanism suggested by (Nilius and Droogmans, 2001), it is possible to block the K_{Ca} channel in the same way, by reducing the conductance of the channel to zero. Upon block of

this channel, combined with activation of the TRPV4 channel by hypotonic challenge, the TRPV4 channel Ca^{2+} current reduced significantly. Ca^{2+} influx was also reduced. These results are consistent with the Ca^{2+} recordings observed in Chapter 5, where a reduced but sustained increase in Ca^{2+} was observed with hypotonic solution and UCL-1684 combined.

Despite its obvious benefits the NEURON simulation environment has some faults, which can be altered to perfect the model. For example, it is important to highlight that by default, the Hodgkin-Huxley channels that NEURON uses to convey the kinetics of the potassium and sodium channels responsible for generation and propagation of action potentials are based on those observations of the giant squid axon (Hodgkin and Huxley, 1952b). Within these channels NEURON uses a temperature coefficient (*k*) to adapt the kinetics of channel opening and closing rates of the channels (Equation 6.9):

Equation 6.9 $$\boldsymbol{k = Q_{10}^{(T-T_0)/10}}$$

Where Q_{10} is a measure of the increase in the opening and closing rates of the ion channels when the temperature (*T*) rises 10°C above the laboratory temperature (Carnevale and Hines, 2006).

Although this system has been adapted for mammalian neurons within NEURON itself, K_V channels were added which use experimentally derived parameters from my groups' previous work in spinally-projecting PVN neurones (Lewis *et al.*, 2010). With ion channel additions derived from experimental parameters such as these, the model becomes much more robust.

In addition, it would be good practice to include any further channels which have been found within the parvocellular PVN and their particular parameters to fully encapsulate this area of the hypothalamus. Much could be done to develop this model, such as the inclusion of the temperature dependant TRPM2 channel, discussed in Chapter 3, onto the GABAergic innervations of the spinally-projecting neurone. As this is a theory only suggested, addition to the model will be a good verification measure to support this theory before further experiments are planned.

Although limitations to this model do exist, its development appears boundless, which adds to its appeal as both a tool for verifying and predicting *in vitro* experimental results.

7 The Role of the Neurokinin 1 Receptor in the Cardiovascular Response to Stress

7.1 Introduction

As discussed in Chapter 1, there are a number of neurotransmitters and modulators that are known to act on PVN neurones. These include GABA, glutamate, nitric oxide, adenosine and the tachykinin family of neuropeptides (Nunn *et al.*, 2011; Pyner, 2009). Tachykinins are particularly interesting to focus on as they have been shown to be important for the central control of the cardiovascular system (Culman and Unger, 1995) and the tachykinin receptors are present within the parvocellular PVN (Koutcherov *et al.*, 2000a; Nakayama *et al.*, 1992). They have also been linked to the stress response in several studies (Herman and Cullinan, 1997; Jansen *et al.*, 1995a) (reviewed by (Aguilera, 1994), however an exact pathway has not yet been shown.

7.1.1 Substance P in the PVN

Substance P (SP) is an important endogenous neuropeptide which acts as a neurotransmitter and neuromodulator via the neurokinin 1 receptor (NK1). SP has been shown to be widely expressed in the brain and is particularly abundant within the PVN (Jessop *et al.*, 1991). In work carried out by Womack and Barrett-Jolley (2007), an SP dependant pathway was characterised, linking the PVN to the dorsalmedial hypothalamus (DMH); another important cardiovascular control centre in the hypothalamus. In a further study they also identified an SP activated

pathway projecting from the PVN to the IML (Womack *et al.*, 2007). These projections are known to influence the sympathetic nervous system.

Traditionally associated with pain perception (De Felipe *et al.*, 1998), SP has also more recently been linked with the regulation of mood disorders, anxiety and stress (Ebner *et al.*, 2008), with levels within the PVN increasing during inflammatory stress (Chowdrey *et al.*, 1995). Studies have also demonstrated that *in vivo* central tachyknins increase efferent sympathetic activity (Unger *et al.*, 1985). Furthermore, it has been shown *in vitro* that SP results in the disinhibition (i.e., activation) of spinally-projecting cardiovascular control neurones of the PVN via NK1 receptor inhibition of $GABA_A$ currents (Womack *et al.*, 2007).

7.1.2 Cardiovascular role for neurokinin 1 receptor in the stress response

A number of studies have shown neurokinin receptors in the CNS to be important for the cardiovascular response to stress (Culman *et al.*, 2010; Culman and Unger, 1995). In these studies it was shown that the noxious stress response (subcutaneous formalin) was sensitive to CSF application of selective NK1 and NK2 receptor antagonists (Culman *et al.*, 2010), despite the relative sparseness of NK1 receptors in the PVN (Shults *et al.*, 1985). Additionally, ICV injection of these antagonists blunted the early gene c-fos expression by corticotrophin expressing PVN neurones in response to stress. Complementary data to this was more recently published by Culman *et al* (Culman *et al.*, 2010). Culman *et al* used a psychological stress test (elevated plus maze test); the authors discovered that behavioural markers of stress and anxiety are reduced by ICV injection of a selective NK1 receptor antagonist. In the Culman study stress-induced c-fos expression within the

PVN was also lower in rats receiving pharmacological block of the NK1 receptor (Ebner *et al.*, 2008). Consistent with this data, it has also been observed that knock-out of the NK1 receptor (NK1R-/-) reduces PVN c-fos expression and levels of stress hormone (cortisol) in response to the elevated plus maze test (Santarelli *et al.*, 2002; Santarelli *et al.*, 2001).

This combined evidence suggests that the pathway identified within the PVN by (Womack *et al.*, 2007) may be important for increases in heart rate and blood pressure in response to stress. However, despite the evidence presented, the theory the PVN is important for the cardiovascular response to stress remains controversial, with several studies disputing this role (DiMicco *et al.*, 2002; Fontes *et al.*, 2001a; Stotz-Potter *et al.*, 1996). There could be a few reasons for this conflicting view. As "stress" is a term which describes a wide range of physiological and psychological stimuli, certain forms of stress (such as subcutaneous formalin, a form of noxious stress (Culman *et al.*, 2010)) may activate a tachykinin-mediated PVN response, whereas perhaps psychological stress does not. Another possibility is that this pathway may mediate other facets of cardiovascular control, such as circadian control of the blood pressure as has been implicated by (Cui *et al.*, 2001). Blood pressure acts on a diurnal rhythm, and neurones within the hypothalamus (in particular the PVN) play a role in setting this circadian rhythm (Belle *et al.*, 2009; Cui *et al.*, 2001).

7.1.3 Aims

Although the above studies strongly suggest that the NK1 receptors located within the PVN are involved in the cardiovascular response to stress, these investigations

have not been able to verify the pathways involved and are somewhat disputed. These studies also do not answer fundamental questions such as; (1) is there a role for NK1 receptor-expressing PVN neurones in the cardiovascular response to psychological stress, and (2) is there any further cardiovascular role for these NK1 receptor-expressing neurones? This chapter aims to address these caveats by performing specific NK1 receptor lesions. By doing this it is possible to investigate the role of these NK1 receptor-expressing neurones in the cardiovascular response to mild psychological stress by investigating heart rate and heart rate variability (HRV) in both lesioned and control Wistar rats. Due to the continuous nature of ECG recording by radiotelemetry, investigation into any other possible cardiovascular role of this population of neurones is possible; such as their involvement in circadian rhythm.

7.2 Methods

7.2.1 Verification of selective lesion of NK1 receptor neurones in the rat PVN

Primarily, it was necessary to verify the loss of NK1 receptor expressing neurones and ensure survival of the animals after surgery. Therefore male Wistar rats (*n*=2) were given specific injections of 50nl of the highly selective SSP-SAP into the PVN under gaseous isoflurane anaesthesia as described in Chapter 2. Coordinates for the PVN injection were calculated using the Paxinos and Watson (Paxinos and Watson, 1986) stereotaxic atlas according to the following distances from Bregma at a 10^{o} angle; 1.8mm caudal, 1.8mm lateral, 9.2mm vertical. The efficacy of the SSP-SAP lesion and the position of the injection site was confirmed with

immunofluorescence using the primary antibody anti-rabbit NK1 receptor (1:500; Abcam, UK) combined with the secondary antibody donkey anti-rabbit Dylight 594 (1:2000; Abcam, UK) and blue DAPI nuclei staining using VECTASHIELD mounting medium with DAPI (Vector laboratories, UK).

7.2.2 Lesioning

Once the original pilot study had taken place and efficacy and coordinates had been confirmed a full cohort of male Wistar rats were injected in the PVN with either 50nl of SSP-SAP (*n*=3) or ACSF as a control (*n*=3) and implanted with radiotelemeters (for full methods see Chapter 2). Animals were individually housed and left to fully recover for a period of 7 days; allowing the lesion to fully develop.

7.2.3 ECG recording

Once recovered rats were placed on the receivers to record ECG continuously; a method which is preferred as the animals remain conscious and are freely moving. ECG was recorded using Spike2 (Cambridge Electronic Design, Cambridge, UK) on a PC at 5 kHz.

7.2.4 Heart rate and heart rate variability

Heart rate was analysed using a custom beat annotation program, and heart rate variability data was analysed using Kubios (Niskanen *et al.*, 2004), as described fully in Chapter 2.

Heart rate was averaged per 4 hours over a period of 68 hours in order to analyse daily variation in heart rate. After 2 days of baseline recording rats were subjected to 1 minute of mild handling stress where the rats were picked up by the tails and restrained (Balcombe *et al.*, 2004). Up until this point the animals were handled only when necessary in order to prevent habituation to handling. Once handled the rats were returned to their home cages to recover. To analyse the heart rate and HRV response to stress these parameters were looked at 15-20 minutes before and an hour after handling stress at the same time each day (around 12pm in order for the animals to be adjusted fully to daytime).

7.3 Results

7.3.1 Verification of selective lesion of NK1 receptor neurones in the rat PVN

Using immunofluorescence it was possible to show clear loss of NK1 receptor antibody staining in the lesioned side of the PVN (efficacy of lesion was confirmed to be 100%; Figure 7.1). As unilateral injections were performed the intact side was used as a positive control for comparison, showing that the NK1 receptor is still present on this side.

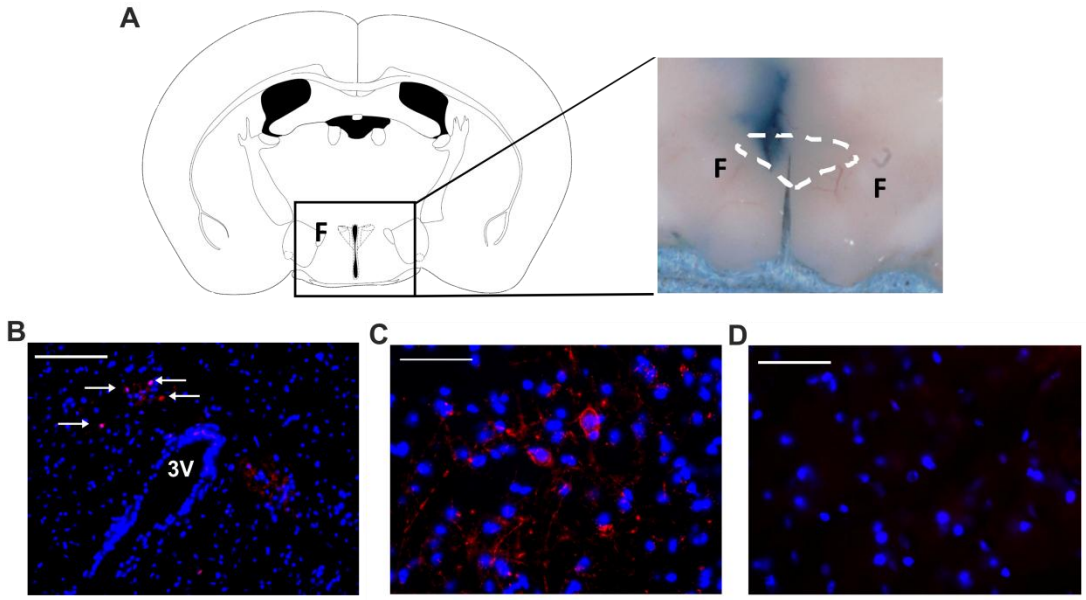

Figure 7.1 Selective lesion of NK1 expressing neurones in rat PVN.
(A) Unilateral injection with pontamine blue (1%). F=fornix. The dotted line indicates the approximate position of the PVN. Note that no dye crosses to the contralateral side. **(B)** Low magnification image of coronal section of PVN showing orientation using the 3rd ventricle. Intact side (left of the 3rd ventricle) and lesioned side (right of the 3rd ventricle), showing clear red staining for the NK1 receptor using the primary antibody anti-rabbit Neurokinin-1 receptor (1:500; Abcam, UK) combined with the secondary antibody donkey anti-rabbit Dylight 594 (1:2000; Abcam, UK) and blue DAPI nuclei staining (white arrows indicate staining). Scale bar is 100µm. **(C)** Intact side of the PVN used as a positive control. Scale bar is 50µm. **(D)** Lesioned side of the PVN from the same Wistar rat shows an absence of red NK1 receptor staining; blue DAPI nuclei staining remains. Scale bar is 50µm.

7.3.2 ECG recording

From continuous ECG recording it was possible to obtain heart rate intervals (R-R interval), and subsequently heart rate and heart rate variability parameters (see Figure 7.2 for typical representative traces for control rats and Figure 7.3 for lesioned rats)

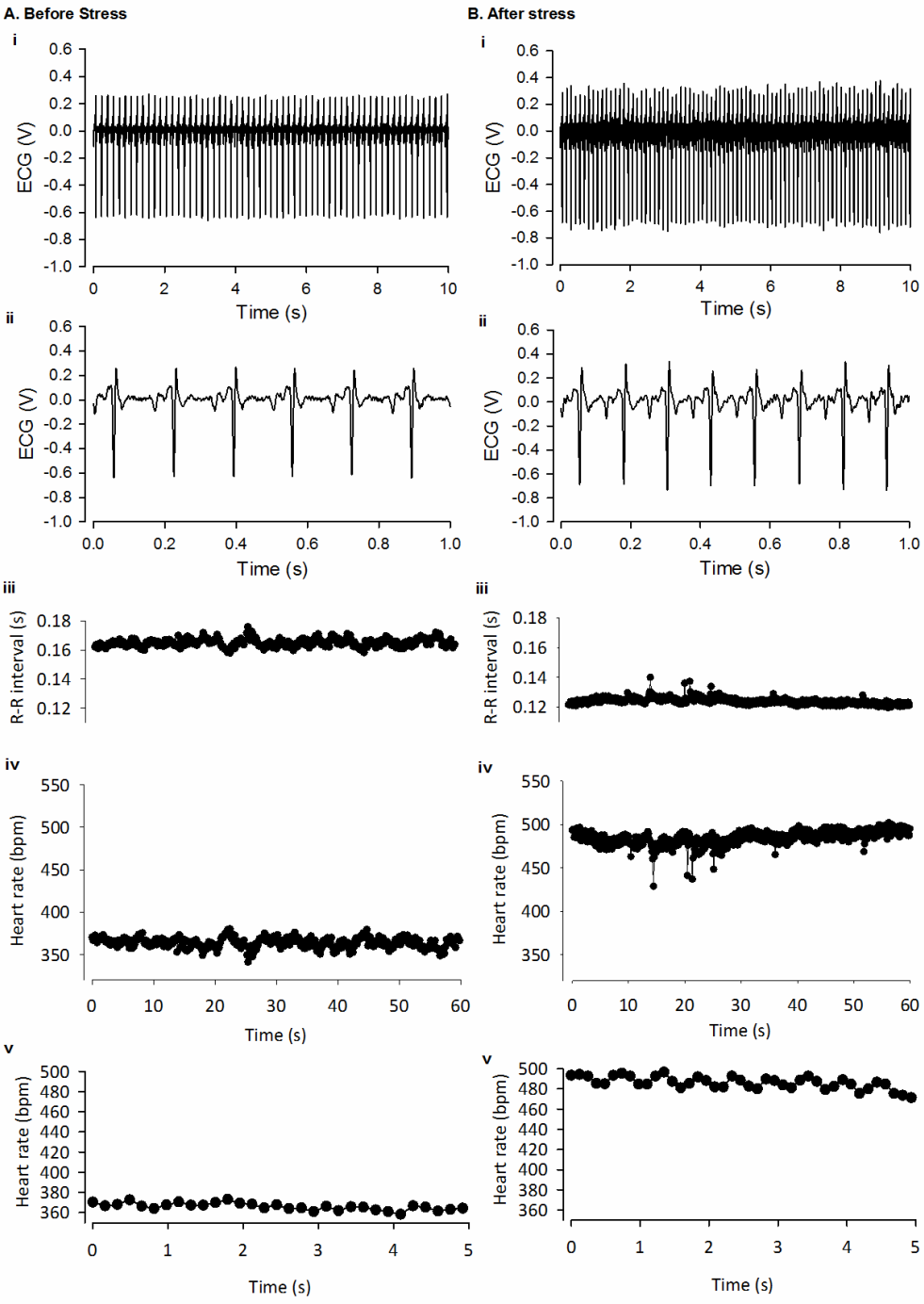

Figure 7.2 ECG responses to mild handling stress of control rats.

Continuous recordings were made from conscious freely moving rats implanted with radiotelemeters. Representative raw traces show differences **(A)** before stress and **(B)** after mild handling stress of control Wistar rats. These show (i) ECG trace over a period of 10 seconds at an appropriate time, (ii) a zoomed in region of the same time point as (i), each beat was annotated using a custom annotation program, (iii) typical heart beat (R-R) intervals, (iv) the raw heart rate trace to match the R-R intervals and finally a zoomed in trace (v) of heart rate to demonstrate heart rate variability changes over time.

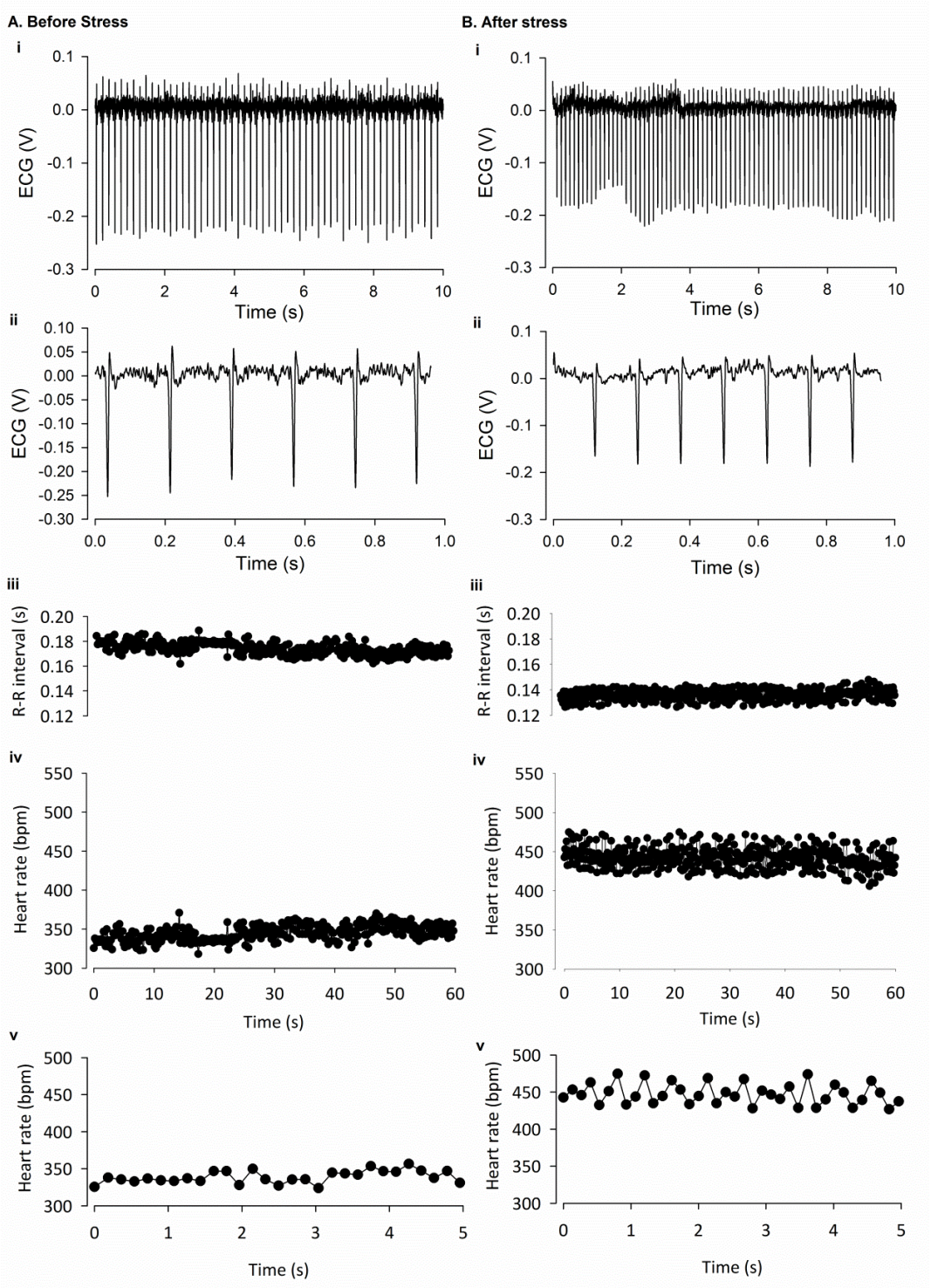

Figure 7.3 ECG responses to mild handling stress of SSP-SAP lesioned rats.
Continuous recordings were made from conscious freely moving rats implanted with radiotelemeters. Representative raw traces show differences **(A)** before stress and **(B)** after mild handling stress of control Wistar rats. These show (i) ECG trace over a period of 10 seconds at an appropriate time, (ii) a zoomed in region of the same time point as (i), each beat was annotated using a custom annotation program, (iii) typical heart beat (R-R) intervals, (iv) the raw heart rate trace to match the R-R intervals and finally a zoomed in trace (v) of heart rate to demonstrate heart rate variability changes over time.

7.3.2.1 Daily variation of heart rate

A significant increase in heart rate was observed during the night compared to day in both groups of rats (Figure 7.4). In control rats heart rate increased from 387 ± 6 bpm to 423 ± 5 bpm (*n*=3 control; *p*<0.001 by one way ANOVA) and 399 ± 6 bpm to 436 ± 5 bpm in lesioned rats (*n*=3 lesioned; *p*<0.001 by one way ANOVA). However, no differences between these two groups, either in average daytime or night time heart rates was seen (*n*=6; *p*<0.05 by one way ANOVA). Despite this, a distinct shift in the daily variation of heart rate in the SSP-SAP lesioned animals was observed, and average heart rate was significantly different over two time points (Figure 7.4**;** at 17:00 on day 3; SSP-SAP rats 420 ± 26 bpm *vs* control rats 372 ±4 bpm, at 21:00 on day 3; SSP-SAP rats 446 ± 35 bpm *vs* control rats 402 ± 9 bpm; *n*=6; **p*<0.05 by repeated measures), suggesting NK1 receptor expressing neurones may have an influence over setting the daily variation of heart rate.

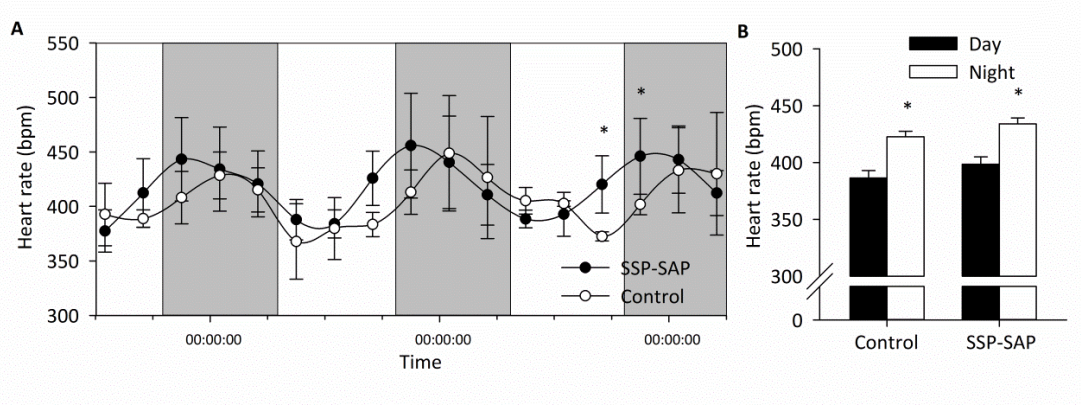

Figure 7.4 Daily variation in 24 hour heart rate in SAP-SSP lesioned rats.
(A) Daily variation in heart rate was plotted as average heart rate per 4 hours in both control and SSP-SAP lesioned rats. Mean heart rate was significantly different over two time points (*n*=6; *p*<0.05). **(B)** Control and lesioned rats both show increased heart rate at night compared to during the day; from 387 ± 6 to 423 ± 5 beats min^{-1} in control (*n*=3; *p*<0.001 by one way ANOVA) and 399 ± 6 to 436 ± 5 beats min^{-1} in lesioned rats (*n*=3; *p*<0.001 by one way ANOVA). No differences between the two groups were observed.

7.3.2.2 Heart rate response to mild handling stress

Mild handling stress increased heart rate significantly (Figure 7.5), as expected in the control animals from 345 ± 2 to 414 ± 5 bpm (*n*=3; *p*<0.001 by one way ANOVA). This same increase could also be seen in the lesioned rats from 354 ± 3 to 396 ± 11 bpm (*n*=3; *p*<0.05 by one way ANOVA). No differences in heart rate response to stress between these two groups was observed.

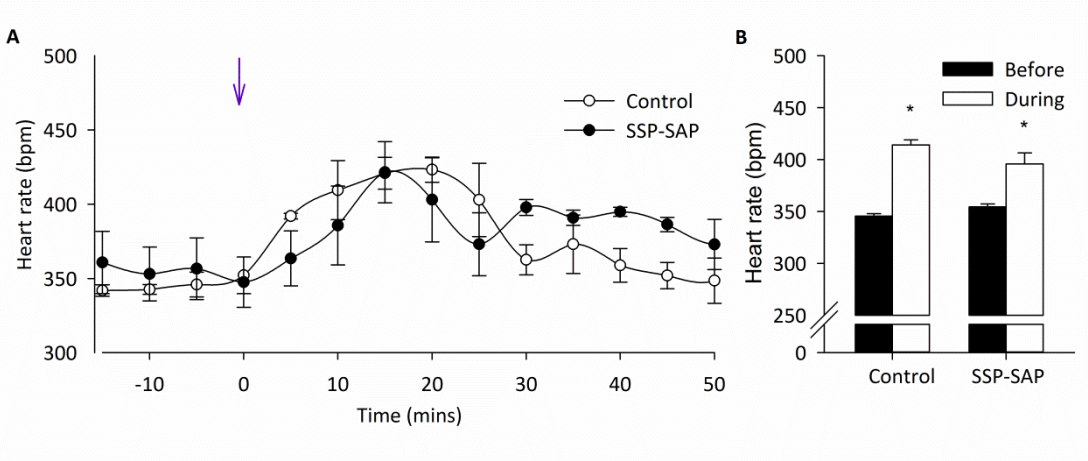

Figure 7.5 Mild stress increases average heart rate of SSP-SAP lesioned and control rats.
(A) Average heart rate per 5 minutes in both groups of rats. Arrow indicates time of mild handling stress. **(B)** Heart rate significantly increases both in control rats from 345 ± 2 to 414 ± 5 bpm (n=3 control; p<0.001 by one way ANOVA) and in lesioned rats from 354 ± 3 to 396 ± 11 bpm (p<0.05 by one way ANOVA; n=3 lesioned). No difference in heart rate response to stress between the two groups was observed.

7.3.2.3 Heart rate variability response to mild handling stress

Examples of FFTs produced by the Kubios program (Niskanen *et al.*, 2004) with the bandings included can be seen in Figure 7.6. These show representative traces produced from both control and lesioned rats before and after stress. It can be seen in stressed control rats it is clear there is an increase in LF and a reduction in

HF activities. This is reflected in a significant increase in average LF/HF ratio of these animals from 0.84 ± 0.14 to 2.02 ± 0.15 a.u (n=3 control; p<0.05 by one way ANOVA), indicating an increase in sympathetic activity. In the representative traces from the lesioned rats, a decrease in both LF and HF activity can be seen, also reflected by LF/HF ratio not changing (n=3 lesioned; p>0.05 by one way ANOVA). These results indicate that lesion of the NK1 receptors abolishes the sympathetic response to mild psychological stress.

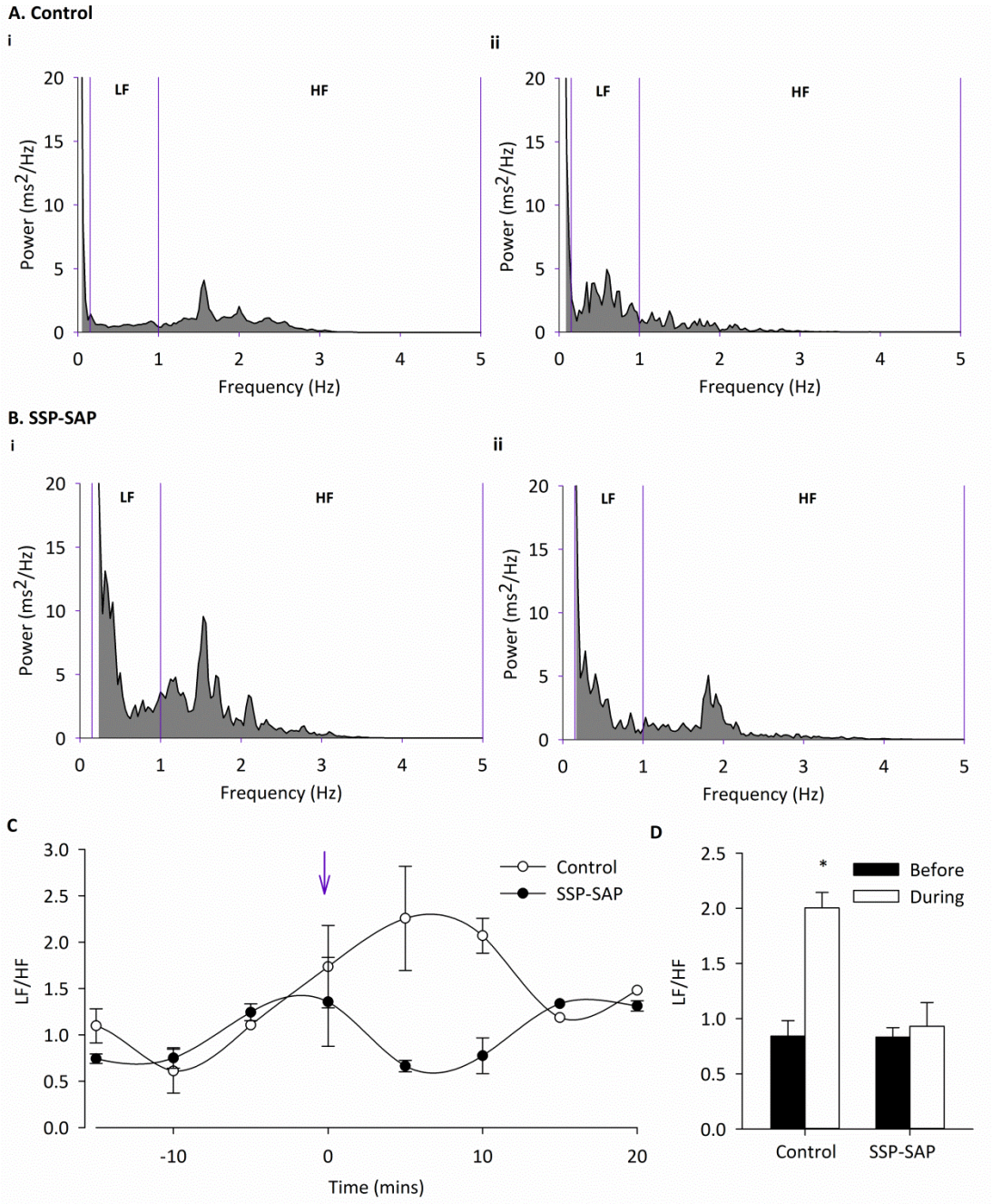

Figure 7.6 LF/HF response to stress in control and SAP-SSP lesioned rats.
(A) Representative fast fourier transfor in control rats (i) before and (ii) after stress. **(B)** Representative fast fourier transform of SAP-SSP lesioned rats (i) before and (ii) after stress. In control animals an increase in LF and decrease of HF power is seen as a result of stress. Both LF and HF are reduced in lesioned rats after stress. **(C)** Average LF/HF ratio per 5 minutes in both groups of rats. Arrow indicates time of mild handling stress. **(D)** LF/HF ratio significantly increases in control animals subjected to stress from 0.84 ± 0.14 to 2.02 ± 0.15 a.u (*n*=3 control; $p<0.05$ by one way ANOVA). This response was abolished in SSP-SAP lesioned rats (*n*=3 lesioned; $p>0.05$).

7.4 Discussion

Koutcherov *et al* (Koutcherov *et al.*, 2000a) showed the presence neurokinin 1 receptor within the paraventricular nucleus and it has been shown by (Culman and Unger, 1995) that tachykinins are important for cardiovascular control. Furthermore, Culman *et al* (2010) have shown substance P is involved in the cardiovascular response to noxious stress. However, there has only been circumstantial evidence so far to support the theory that PVN neurones expressing NK1 receptors are involved in this process. The aim of this study was to explore the pathway involved in the cardiovascular response to stress and marry up those *in vivo* and *in vitro* investigations which support this hypothesis, showing if this response is stressor dependant. It was also important to explore any other possible cardiovascular role for these NK1 receptor expressing neurones, such as any involvement they may have in setting circadian rhythm of the cardiovascular system. In order to do this NK1 receptor expressing neurones in the PVN were lesioned with SSP-SAP and continuous ECG was recorded from conscious, freely moving Wistar rats. The rats were then subjected to mild handling stress and heart rate and heart rate variability were investigated throughout.

SSP-SAP injections were given unilaterally into the PVN. The cytotoxic SSP-SAP has been shown to be selective in many studies (Khasabov and Simone, 2013; Talman and Lin, 2013). Despite this, it was important to confirm the efficacy of the specific lesion of NK1 expressing receptors within the PVN and the location of the injection. It was decided to perform unilateral injections as it was unknown how the lesion would affect the animals; it also meant that the rats injected could be used as their

own positive controls in immunofluorescence imaging of the expression of the NK1 receptor. No behavioural or physiological changes were observed within two weeks of the lesion. Subsequently, immunofluorescence confirmed complete loss of the NK1 receptor in the lesioned side of the PVN; the intact side still showed expression of the receptor (Figure 7.4). It is important to note that the injections of SSP-SAP were given slowly, over at least 1 minute and the Hamilton syringe was only removed after a few minutes, to prevent the solution travelling back up the needle track. The localisation of the injection was also confirmed using the immunofluorescence images.

Once efficacy and location had been confirmed 2 cohorts of Wistar rats were given direct unilateral injections into the right side of the PVN of either the SSP-SAP or PBS as a control, as to ensure there were no effects of performing the injection itself. These rats were also implanted with radiotelemeters designed to record continuous ECG from conscious, freely moving rats. From this data it is possible to derive heart rate and heart rate variability.

As these recordings are continuous, it is possible to observe daily variation of the rats' heart rate over the first few days of baseline recording. The circadian involvement of PVN spinally projecting neurones was initially suggested by (Cui *et al.*, 2001) who showed that spinally projecting neurones received input from the suprachiasmatic nucleus; a key centre of the hypothalamus involved with circadian rhythm. Cyclically changing membrane potentials of neurones within this area have also been reported, allowing general changes in activity on a 24 hour rhythm (Belle *et al.*, 2009). A previous study performed by my group in mice shows this is

paralleled by changes in heart rate (Nunn *et al.*, 2013). I have been able to confirm in this study that changes in the daily variation of the heart rate can also be seen in rats and involves PVN NK1 neurones (Figure 7.4). In both lesioned and control rats nighttime heart rate was significantly increased compared to daytime. This is unsurprising, as rodents are nocturnal and so are awake and more active during the night. No difference in day or nighttime heart rate could be observed between the two groups. However, it is interesting to note that at several time points the heart rate of the SSP-SAP lesioned rats is significantly different from its control counterparts. Furthermore, a distinct shift of the lesioned rats' daily heart rate variation can be seen, whereby the increasing night time heart rate increases earlier in these animals, suggesting these neurones play a role in setting circadian rhythm of heart rate (Figure 7.4A). Although many of these time points are not significant, it is an interesting trend, and it is important to note *n*=3 for each cohort of this study. With increasing numbers of animals used, and a longer duration of baseline recording it would be interesting to see if there was more of a significant shift in rhythm, or if it became more pronounced further on in a longer study. Interestingly, substance P levels have been shown to oscillate throughout the day in other areas of the brain and spinal cord (Weber *et al.*, 2004; Zhang *et al.*, 2012), therefore this could be a potential explanation for the shift observed in the lesioned animals. In future studies it would be of interest to investigate if the loss of the NK1 receptors within the PVN affects circadian rhythm by altering the light cycles the animals are exposed to. This role of the NK1 expressing neurones is potentially of huge relevance, since in humans, circadian variation in cardiovascular control is

strongly linked to a spate of heart attacks that occurs in first thing the morning (Muller *et al.*, 1989; Spielberg *et al.*, 1996).

A number of studies have shown the PVN is important to cardiovascular control (Badoer *et al.*, 2002; Coote, 2005; Ramchandra *et al.*, 2013) and although others show the PVN to be central to the HPA component of the stress response (Herman and Cullinan, 1997; Herman *et al.*, 2002a; Tavares *et al.*, 2009) there are few studies showing direct involvement of the PVN in the sympathetic and cardiovascular stress response. Spinally-projecting sympathetic PVN neurones have been shown to express neurokinin receptors and modulate the CVS (Womack *et al.*, 2007). Although (Ebner *et al.*, 2008) showed decreases in behavioural response, and a decrease in c-fos expression as a result psychological stress with ICV injection of NK1 receptor antagonist, no cardiovascular studies were undertaken. Studies by (Culman *et al.*, 2010) showed ICV injection of specific neurokinin receptor antagonists reduces the cardiovascular (and hormonal) response to noxious stress and decreased CRF c-fos expression. These studies do show an obvious role for NK1 receptors in the cardiovascular and behavioural responses to severe (noxious) and psychological stress respectively, however they both have caveats. In this chapter we address these caveats, such as; does mild psychological stress affect the cardiovascular response, and specifically is it these NK1 receptor expressing neurones involved. It was found that mild psychological stress by handling increased heart rate significantly in both sets of rats; there were no differences between the two groups (Figure 7.5). This is perhaps surprising as these neurones are known to have a role in cardiovascular response to stress; therefore you may expect them to have a significant impact on this response if removed. However,

this lack of difference could be explained in a number of ways; (i) perhaps this could mean that the type of stressor involved *is* important in the cardiovascular response, (ii) it could be that although heart rate remained unchanged, blood pressure may be altered (a parameter we were unable to measure using this equipment), and some sort of feedback mechanism (i.e the baroreceptor reflex) may be responsible for keeping the heart rate stable, (iii) as only unilateral injections were performed, the intact side "took over" the role for maintaining the heart rate response to stress or simply (iv) NK1 receptor expressing neurones are not directly responsible in this cardiovascular control.

In future studies it would be interesting to do this set of investigations with various stressors and by altering the side of the unilateral injections or by using bilateral injections if the survival of animals could be ensured.

As it is known that the cardiovascular control neurones project to the sympathetic pregangilonic neurones it follows that any alteration in their activity/loss of these neurones may in turn affect the sympathetic activity. To investigate this further I used heart rate varability to look at the effects of stress on the sympathetic nervous system. Heart rate variability analysis is used as a method for quantifying the autonomic influence on the cardiovascular system based on heart rate variation over time. These natural rhythms occur at different frequencies associated with the sympathetic and parasympathetic nervous system influences. Heart rate variability is therefore widely used as an accurate indicator of autonomic balance (Baudrie *et al.*, 2007; Malpas, 2002; Thireau *et al.*, 2008) and autonomic response to stress (Farah *et al.*, 2006). Although there is no direct indicator of sympathetic activity, a

number of studies, including our own, have shown the LF/HR ratio is a valid measure of autonomic balance and therefore it is possible to determine changes in sympathetic activity using this parameter (Katoh *et al.*, 2002; Nunn *et al.*, 2013). Heart rate variability analysis of the ECG data obtained from control rats showed a significant increase in the LF/HF ratio (an indicator of sympathetic activity), resulting from a simultaneous decrease in HF and increase in LF. Interestingly, this increase in LF/HF ratio is seen *before* the increase in heart rate itself. This is an indication that it is in fact the sympathetic nervous system that is driving the change in heart rate. This sympathetic response to psychological stress was abolished in SSP-SAP lesioned rats, where both LF and HF frequencies decreased simultaneously, leading to no significant change in LF/HF ratio (Figure 7.6). This result confirms a role for the NK1 receptor expressing neurones in modulation of the sympathetic response to psychological stress.

Together the results obtained in this chapter show, for the first time, that PVN NK1 expressing neurones are involved with setting heart rate circadian rhythm and also the sympathetic component of the response to mild psychological stress.

8 Cardiovascular stress response in mice lacking XLαs

8.1 Introduction

The sympathetic nervous system plays a major role in the cardiovascular system and the control of energy balance (Hall *et al.*, 2010). An elevation of sympathetic activity influences the cardiovascular system, resulting in increases in blood pressure and heart rate; chronic elevations being identified as a characteristic of cardiovascular disease (for review see (Fisher *et al.*, 2009)). This is believed to be due to combined effects of a decrease in inhibitory GABA and an increase in excitatory glutamate in certain brain regions controlling the autonomic nervous system, such as the PVN. Although there is evidence suggesting this occurs, the mechanisms behind this altered regulation are unknown. One such method for exploring these possibilities is to use model animals such as the spontaneously hypertensive rat (SHR) or more commonly used mouse models (Doggrell and Brown

, 1998). The Schlager hypertensive mouse, for example, is hypertensive due to an increase in sympathetic activity and is reported to have an elevated stress response (Davern *et al.*, 2009). This could/may involve the PVN as well as other brain regions associated with cardiovascular control and stress. One such mouse model has been used by my group previously, which I will look at in this chapter; the *Gnasxl* knockout mouse.

8.1.1 The Gnasxl knockout mouse

Gnasxl knockout mice are deficient for XLαs, a stimulatory G-protein α-subunit found richly within the PVN (Krechowec *et al.*, 2012). Activation of adenylyl cyclases occurs via ligand binding to G protein-coupled receptors, leading to production of the second messenger cAMP (Plagge *et al.*, 2008). However, the specific receptors that signal through XLαs remain unknown.

Adult mice lacking XLαs have elevated sympathetic stimulation of the brown and white adipose tissues, which results in increased metabolism (Xie *et al.*, 2006). My group has also recently confirmed a global increase in sympathetic activity in these mice, resulting in the hypermetabolism and hypertension observed (Nunn *et al.*, 2013). Normal levels of parasympathetic tone were also confirmed in this investigation. Knockout mice showed elevated blood pressure, heart rate and temperature; alterations which are not associated with increased levels of locomotion. These effects are further supported by the strong levels of expression of XLαs in areas influencing the sympathetic nervous system and cardiovascular system (Plagge *et al.*, 2008); most notably for this project, the PVN (Coote, 2007; Loewy, 1991; Nunn *et al.*, 2011). In addition to this evidence, heart rate and blood pressure are reduced in the specific PVN knockout for a shorter splice variant of the *Gnasxl* mouse (mPVNGsKO), which exhibits the opposite phenotype to the longer splice variant. This suggests that the cardiovascular effects of loss of Gsα in the brain are caused specifically by loss of expression in the PVN (Chen *et al.*, 2012). As shown in Chapter 7 the PVN exerts an influence to the autonomic system response to stress. Importantly for this work the *Gnasxl* KO phenotype is also consistent with

a permanently activated stress reaction (Farah *et al.*, 2006; Grippo *et al.*, 2003). It was therefore interesting to investigate the stress response in these knockout mice compared to their wild type counterparts as it stands to reason this may be altered, as demonstrated in the Schlager mice (Davern *et al.*, 2009).

8.1.2 Aims

The XLαs protein is abundant in the PVN, known to influence cardiovascular parameters and the stress response. In fact, as discussed, the *Gnasxl* knockout is hypothesised to be in a permanent state of stress, with constantly elevated sympathetic activity. The aim of this chapter, therefore, is to assess the effects of handling stress on heart rate and heart rate variability of *Gnasxl* knockout mice in comparison to their wild type counterparts using continuous ECG recording with radiotelemeter implants. It will then be possible to confirm if XLαs is associated with the stress response and provide further insight into the role of the neurones associated with this protein.

8.2 Methods

To examine the effects of stress on the cardiovascular system young adult male (~4 months) *Gnasxl* knockout mice and their wildtype siblings were implanted with radiotelemeters under isoflurane anaesthesia. The placing of transmitters was done with the assistance of Dr. Nunn. Mice were then individually housed and once recovered were placed on receiver pads and ECG was continuously recorded using Spike2 (Cambridge Electronic Design, Cambridge, UK) (for full details see Chapter 2).

Custom beat detection software was used to analyse heart rate and heart rate variability data was analysed using Kubios (Niskanen *et al.*, 2004).

After 2 days of baseline recording mice were subjected to 1 minute of mild handling stress whereby they were picked up by the tails and scruffed (Balcombe *et al.*, 2004). Up until this point the animals were handled only when necessary in order to prevent habituation to handling. Once handled mice were returned to their home cages to recover. To analyse the heart rate and HRV response to stress these parameters were looked at 15-20 minutes before and an hour after handling stress at the same time each day (around 2 pm in order for the animals to be adjusted fully to daytime).

To examine the degree of sympathetic stimulation on the cardiovascular system during stress, mice were injected IP with the sympatholytic reserpine (Sigma-Aldrich, UK) dissolved in 1% acetic acid solution and injected at 1 mg/kg at least 3 hours before subjected to handling stress. Reserpine inhibits catecholamine uptake into secretory vesicles and thereby release at sympathetic nerve terminals (Iversen*et al.* 1965), selectively diminishing sympathetic stimulation of peripheral tissues.

8.3 Results

Wildtype and knockout mice were shown to have comparable increases in heart rate upon mild stress, showing no significant difference between the two groups (67 ± 37 bpm in WT *vs* 58 ± 22 bpm in KO (Figure 8.1; n=18; p>0.05 by Student's unpaired t-test). WT heart rate significantly increased from 568 ± 13 bpm to 634 ±

17 bpm (Figure 8.1**Error! Reference source not found.**; *n*=9; *p*<0.05 by Student's aired *t*-test) and a significant increase from 615 ± 12 bpm to 674 ± 19 bpm was observed in the KO mice (Figure 8.1; *n*=9; *p*<0.05 by Student's paired *t*-test). Although baseline average heart rate was significantly elevated in KO mice, after stress there was no longer a difference observed in heart rate between the 2 cohorts (*n*=18; *p*>0.05 by Student's unpaired *t*-test).

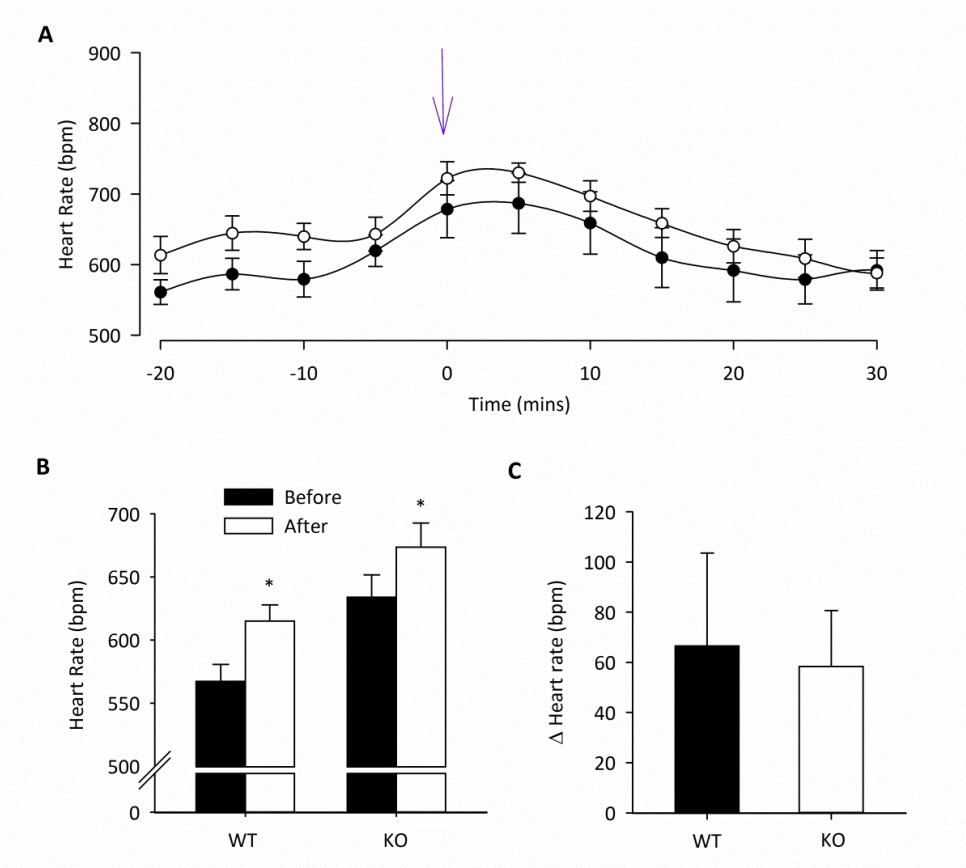

Figure 8.1 Heart rate increases in both *Gnasxl* knockout and wildtype mice upon mild psychological stress.
(A) Average heart rate per 5 minutes before and after handling stress (open circles represents KO mice and black circles represent WT mice; arrow indicates time of handling). **(B)** KO mice have a significantly increased heart rate before stress. Heart rate significantly increases in both cohorts when subjected to handling stress from 568 ± 13 bpm to 634 ± 17 bpm in WT (*n*=9; *p*<0.05) and 615 ± 12 bpm to 674 ± 19 in KO mice (n=9; p<0.05). **(C)** Stress induced comparative increases in the two cohorts; increases of 67 ± 37 bpm in WT *vs* 58 ± 22 bpm in KO were observed, and were not significantly different (*n*=18; *p*>0.05). There was however, no longer a significant difference between the KO and WT heart rates after handling stress (*n*=18; *p*>0.05).

Subsequent to handling stress LF/HF ratio was significantly increased in wildtype mice from 1.24 ± 0.09 to 1.74 ± 0.11 (Figure 8.2; *n*=9; *p*<0.01 by Student's paired *t*-test). No difference, however, was seen in KO mice (from 2.16 ± 0.09 to 1.81 ± 0.11; *n*=9; *p*>0.05 by Student's *t*-test). After handling stress there was no significant difference between LF/HF ratio in wildtype and knockout mice (*n*=18; *p*>0.05 by Student's unpaired *t*-test).

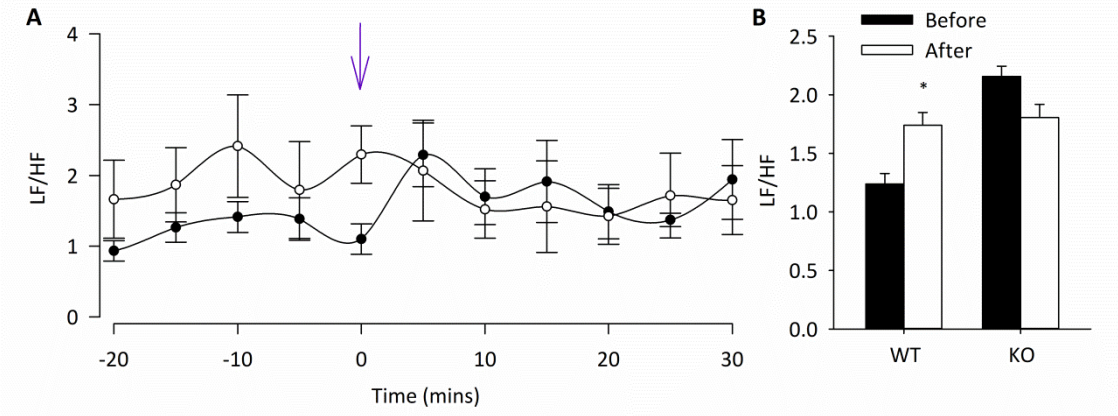

Figure 8.2 LF/HF ratio is increased in wildtype but not *Gnasxl* mice from heart rate variability analysis.
(A) Average LF/HF ratio per five minutes before and after handling stress (open circles represents KO mice and black circles represent WT mice; arrow indicates time of handling). **(B)** LF/HF ratio is significantly increased in WT mice (from 1.24 ± 0.09 to 1.74 ± 0.11; *n*=9; *p*<0.01) but not in the already elevated KO mice (*n*=9; *p*>0.05).

To investigate the effects of suppressing the sympathetic response on autonomic stress response heart rate was again measured before and after handling stress in mice which had been injected IP with reserpine (1mg/kg). Stress induced a significant increase of average heart rate from 454 ± 4 bpm to 499 ± 1 bpm in WT mice (Figure 8.3; n=5; p<0.01 by Student's paired *t*-test). In the KO cohort, however, no significant change in heart rate was observed (525 ± 6 bpm to 545 ± 2 bpm; Figure 8.3; *n*=4; *p*>0.05 by Student's paired *t*-test). The difference in heart

rate change upon handling stress between these two cohorts, however, was not significant (46 ± 14 bpm in WT *vs* 20 ± 20 bpm in WT; Figure 8.3; *n*=9; *p*>0.05 by Student's unpaired *t*-test).

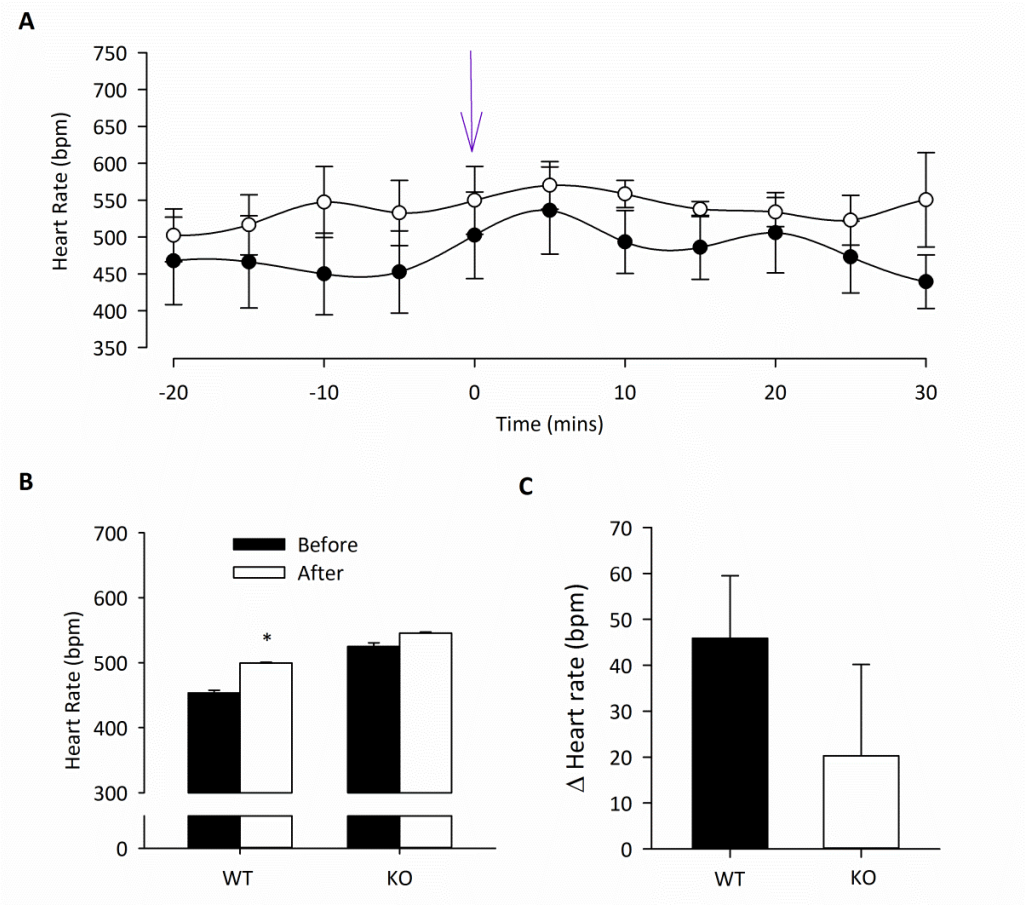

Figure 8.3 Heart rate response to stress in *Gnasxl* and wildtype mice after reserpine injection.
(A) Average heart rate per 5 minutes before and after handling stress (open circles represents KO mice and black circles represent WT mice; arrow indicates time of handling). **(B)** Heart rate in WT significantly increases from 454 ± 35 bpm to 499 ± 30 bpm (*n*=5; *p*<0.01) but not in KO mice (from 525 ± 28 bpm to 545 ± 12 bpm; *n*=4; *p*>0.05). **(C)** A difference of 46 ± 14 bpm in WT compared to 20 ± 20 bpm was observed. There were no significant differences between these (*n*=10; *p*>0.05).

Furthermore, upon handling stress after injection of reserpine no significant change was observed in either the WT or KO mice, suggesting a blunted sympathetic response to stress. In WT mice LF/HF ratio before stress was 0.79 ± 0.08 *vs* 0.87 ±

0.21 after (Figure 8.4; *n*=5; *p*>0.05 by Student's *t*-test). In KO LF/HF ratio was still significantly reduced by stress; from 0.49 ± 0.07 before stress to 0.43 ± 0.05 after stress (Figure 8.4; *n*=5; *p*>0.05 by Student's *t*-test).

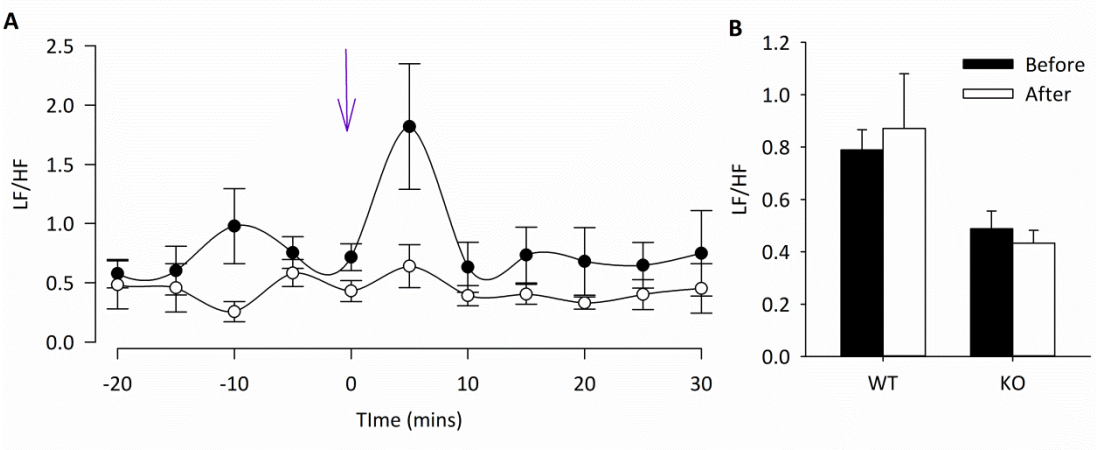

Figure 8.4 LF/HF response to stress in *Gnasxl* and wildtype mice after reserpine injection.
(A) Average LF/HF ratio per five minutes before and after handling stress. Open circles represents KO mice and black circles represent WT mice; arrow indicates time of handling. **(B)** LF/HF ratio is not significantly changed in either WT (*n*=5; *p*>0.05) or KO mice (*n*=4; *p*>0.05).

8.4 Discussion

The *Gnasxl* knockout phenotype is known to be consistent with a permanently activated stress response (Farah *et al.*, 2006; Grippo *et al.*, 2003). Xie *et al* first postulated that these mice had elevated sympathetic nervous activity (Xie *et al.*, 2006). This was recently confirmed by my group, who have shown that this knockout mouse has elevated sympathetic nervous activity, increased heart rate, blood pressure and basal temperature (Nunn *et al.*, 2009; Nunn *et al.*, 2013). Although the mechanisms are unknown it has been postulated an seems likely that XLαs might, for example, mediate signal transduction from a G-protein-coupled

receptor(s) in a population of neurons that inhibit neighbouring sympathetic control neurons (i.e. spinally-projecting neurones of the PVN). As the PVN is also hypothesised to be involved in the cardiovascular stress response it was therefore of interest to investigate the stress response in the knockout mouse in comparison to its wildtype counterpart. Furthermore, an overactivity of the sympathetic nervous system is known to be linked to cardiovascular disease, with a particular prevalence of heart failure and ischemic attacks in those people who also suffer from chronic stress (Floras, 2009). As the *Gnasxl* knockout mouse is considered to be in a permanently stressed state it is therefore interesting to look at this mouse as a possible model for the overactive sympathetic activity seen in individuals who are prone to cardiovascular disease (Drenjancevic *et al.*, 2014).

In order to investigate the effects of stress on the cardiovascular parameters of the *Gnasxl* knockout and wildtype mice, conscious, freely moving mice were implanted with radiotelemeters to record continuous ECG. Mice were then subjected to mild psychological handling stress and heart rate and its variability were investigated. Using this method comparable heart rate increases were seen in both the wildtype and knockout mice in response to stress (Figure 8.1). This is to be expected in animals with their sympathetic control mechanisms and baroreceptor reflex intact. An increase in the LF/HF ratio of heart rate variability was observed in wildtype mice but was absent in the knockout mice. This would be consistent with a model whereby the classic reduction in parasympathetic cardiac inhibition by stress still occurs (Farah *et al.* 2006), but the sympathetic excitation does not increase further in the *Gnasxl* knockout mice due to an already elevated basal cardiovascular sympathetic tone.

Further investigation into the sympathetic component to the stress response observed required the use of the sympatholytic reserpine. Reserpine was injected IP into both cohorts of mice and heart rate and heart rate variability was recorded in a study by my group (Nunn *et al.*, 2013). The study by Nunn et al (2013) shows reserpine treatment results in significantly reduced LF/HF ratios in both knockout and wildtype mice. No significant decrease in heart rate was detected in knockouts, but since variability was high this could represent a type II error (an effect may have been present, but missed). Thus our previous study (Nunn et al 2013) showed reserpine to be useful tool to detect autonomic changes dependent upon modulation of sympathetic activity. In the present study I therefore investigated the cardiovascular stress response of these mice after injection of reserpine. Although heart rate still significantly increased in the wildtype mice, the average LF/HF ratio increase was ablated, suggesting that the sympathetic response was blunted.

Both heart rate increase and LF/HF increases in response to stress were abolished in the *Gnasxl* knockout mice by injection of reserpine. This finding verifies the hypothesis that the stress response in these animals is driven by the sympathetic nervous system. Interestingly, the heart rate changes in response to stress when compared between the knockout and wildtype mice are not significant, although the variation in these changes are so large it makes this may be due to a type II error.

Whatever the mechanisms responsible for the overactive sympathetic nervous system of these knockout mice, these results are partly consistent with the

hypothesis that they are indeed in a permanently “stressed” state. However, in this instance, although stress results in an increase in heart rate, it does not lead to any detectable effects on the resting LF/HF ratio (sympathetic activity) in the KO mouse. This result seems illogical, as you would expect increased sympathetic activity to drive an increase in heart rate; again, this could be due to a type II error, as the data obtained was variable in this instance.

Further investigation would need to be done to ascertain whether this knockout mouse is an ideal model for those patients who have cardiovascular complications associated with chronic stress. Also, further steps need to be taken to identify the receptor(s) and indeed the areas of the brain which are associated with the XLαs protein driving this sympathetic overactivity. Of particular importance to follow of from this work would be to ascertain if the XLαs protein is present on those spinally-projecting neurones responsible for cardiovascular control.

9 General Discussion

This study has used a combination of techniques from mathematical modelling to whole-animal physiology to investigate the normal functional role of parvocellular PVN neurones and the mechanisms responsible. The main novel findings are as follows:

(1) Putative parvocellular PVN neurones play a role in osmosensing and temperature sensing.
(2) Osmosensing and temperature sensing both involve the modulation of transient receptor potential (TRP) non-selective ion channels.
(3) In the case of osmosensing, this involves coupling between small calcium-activated potassium (SK) and TRPV4 channels.
(4) A mathematical model in NEURON can be adapted to predict and validate a number of fine points of parvocellular neurone regulation.
(5) Tachykinergic PVN neurones are important for controlling the daily of heart rate and are involved in the autonomic response to stress.

9.1 Roles of the PVN

The paraventricular nucleus of the hypothalamus is known to play a role in central cardiovascular control. Extensive studies provide support for this role due to the location, cytoarchitecture and projections of this nucleus (Pyner, 2009; Pyner and Coote, 2000; Sawchenko and Swanson, 1982; Swanson and Kuypers, 1980). Despite this wealth of information so far little is known about the influence the PVN has

over the autonomic system, how this fits with other levels of control and why it is important. Furthermore, the mechanisms involved in this control are not fully understood. This thesis has addressed some of these questions and has revealed several roles for the neurones within the parvocellular region of the PVN and, importantly, has identified some of the mechanisms behind them. These findings point to the parvocellular region of the PVN as being a multifunctional nucleus of the hypothalamus and are summarised below (Figure 9.1).

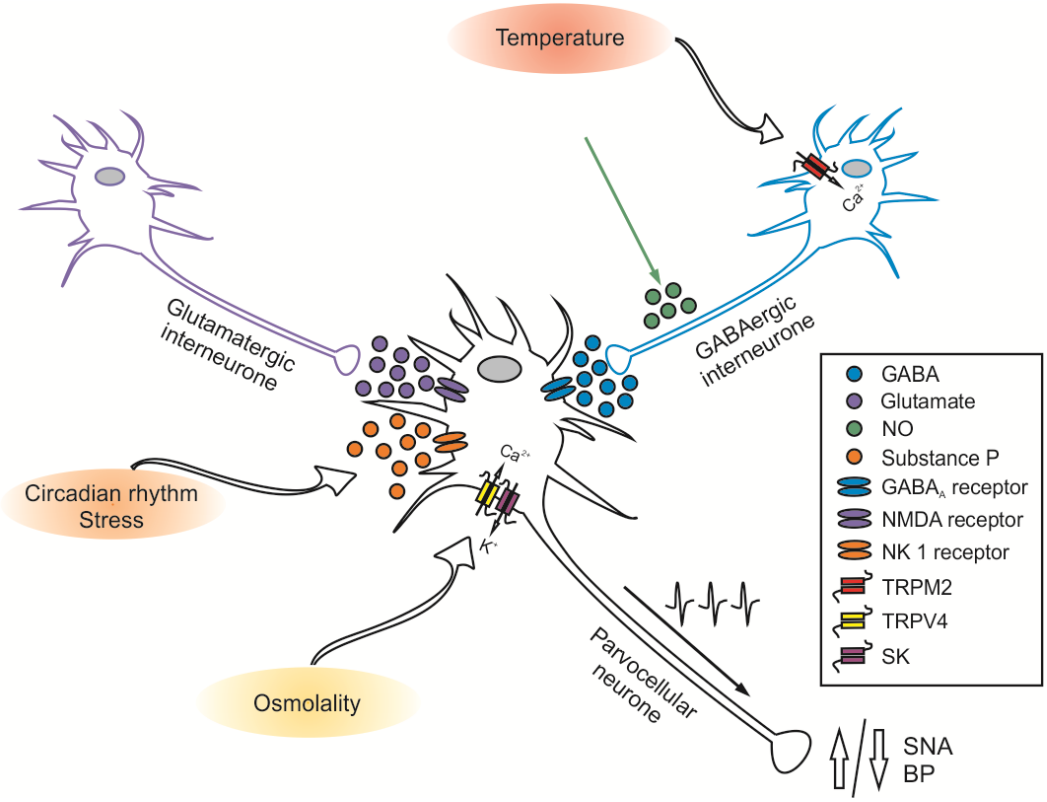

Figure 9.1 Summary of the main findings of this thesis.
Parvocellular neurones of the PVN can modulate sympathetic nervous activity by altering neuronal activity in response to environmental stimuli. They are innervated by both excitatory glutamatergic neurones and inhibitory GABAergic neurones. This thesis has identified a potential pathway for temperature sensing on these GABAergic innervations in the form of the temperature sensitive TRPM2 channel. In addition, a coupling between the TRPV4 and SK channels was revealed to be responsible for osmosensing in the parvocellular neurones themselves. A role for NK1 receptor expressing neurones was also identified in the autonomic response to stress, a system also shown to be involved in the setting of the daily variation of heart rate.

9.1.1 Osmosensing in the PVN

Blood osmolality is strictly regulated within a narrow range (290-300 mosmol) and is sensed centrally by osmosensitive neurones (Bourque, 2008; Bourque and Oliet, 1997). However, a role for those neurones within the parvocellular PVN has up until now been somewhat disputed (Yamashita *et al.*, 1988). In this thesis I have shown that neurones within the parvocellular PVN are sensitive to changes in osmolality and uncovered the mechanisms for this osmosensing role in a series of extensive experiments using a combination of *in vitro* and *in silico* methods (Chapters 3, 4, 5 and 6; for summary see Table 7).

The osmosensitive TRPV4 channel has previously been identified using immunohistochemistry in the PVN (Carreno *et al.*, 2009), which I have been able to confirm within putative parvocellular neurones using a variety of techniques (Chapter 3). Although action current frequency recordings indicated that putative parvocellular cells of the PVN were involved in osmosensing via the TRPV4 channel, it is not possible to say for certain that this is a direct effect. I was able to confirm this using a combination of single channel recordings in slice and whole-cell patch clamp and calcium recordings in isolated PVN cells. It became clear that the mechanism responsible for osmosensing in these neurones was more complex than previously anticipated. Activation of TRPV4 using either hypotonic challenge or a pharmacological activator, such as 4αPDD, resulted in a decrease in neuronal activity, an effect you would not expect to see with a depolarisation of the cells membrane potential (as seen in Chapter 3). I went on to investigate an alternative explanation for this reduction in activity in Chapter 5 of a potential functional

coupling of the TRPV4 channel with a calcium activated channel, as has been shown in other cell types (Gao and Wang, 2010). Upon further investigation, the K_{Ca} channels were considered for this coupling, as both BK and SK can be found in the parvocellular PVN and can alter neuronal activity (Salzmann *et al.*, 2010; Sausbier *et al.*, 2006). The theory that developed is explained in Chapter 5. Briefly, upon influx of Ca^{2+}, a K_{Ca} channel is activated, resulting in hyperpolarisation of the cell and subsequent decrease in neuronal activity. This hypothesis would answer the question of why a decrease in activity is seen in these cells with activation of TRPV4.

Findings from Chapter 5 go on to support the hypothesis of a functional coupling of the TRPV4 and SK channels. Using more complex pharmacology involving both a TRPV4 channel activator and an SK channel inhibitor, action current recordings show that despite the activation of TRPV4, no change in neuronal activity occurs as hyperpolarisation of the cell by efflux of K^+ through SK was prevented. This hypothesis is reinforced by further calcium recordings, as are positive and negative feedback mechanisms suggested by Watanabe et al (2002). The reduced, yet sustained increase in intracellular Ca^{2+} observed in these experiments was an important finding for two reasons: 1. It provides further support for a coupling of TRPV4 and SK, and 2. it suggests that both negative feedback is not achieved as Ca^{2+} levels do not obtain a high enough level, and positive feedback is in play, maintaining the increased levels of Ca^{2+}. Furthermore, this entire mechanism has been able to be recreated *in silico* in Chapter 6 using the NEURON simulation environment, verifying that my proposed mechanism is plausible.

Although revealing an osmosensing role for these neurones and identifying the mechanism behind this is of great interest, it is imperative to see how this translates in the whole animal. This is important, both as there are some concerns as to the effects of over-hydration post MDMA usage or during exercise, but also because it presents a potential pharmacological target for reducing blood pressure (Brvar *et al.*, 2004; Haselton *et al.*, 1994). The question of whether central osmosensing has an impact on cardiovascular control is central to these findings and is addressed in Chapter 4 using blood pressure recordings from cannulated mice. My results suggest that there is a central mechanism for osmosensing which affects the cardiovascular system involving TRPV4. However, it is not clear which specific areas are involved as these injections are not specifically targeted, for example injected substances could have reached other areas such as the DMH or the VMH. Although a clear mechanism for osmosensing in the parvocellular PVN has been identified *in vitro* there are other areas within the hypothalamus which have known osmosensing roles, such as the vasopressinergic neurones within the magnocellular area, and it would be interesting to explore how these systems interact (Bourque, 2008).

There are some further issues which would be interesting to address when considering the central osmosensing role revealed in this thesis. Firstly, recording cardiovascular parameters whilst the baroreceptor reflex has been abolished through either denervation or pharmacologically to see if heart rate was changed as well as blood pressure could be beneficial. Secondly, as the hypothesis for this mechanism includes a role for the SK channel, this should also be investigated i*n vivo*, using similar cannulation and targeted injection techniques as described.

Table 7 Summary of experimental evidence for the osmosensing role of the parvocellular PVN and the mechanisms responsible

Treatment	Method	Parameter	Result	Figure
Osmolality				
Hypotonic	Cell-attached patch	Action current	↓ frequency	3.2
	Calcium imaging	$[Ca^{2+}]$	↑$[Ca^{2+}]_i$ transient	5.5
	Cannulation/ICV	Blood pressure Heart rate	↓blood pressure No change in heart rate	4.2, 4.4
TRPV4				
4αPDD	Cell-attached patch	Action current	↓ frequency	3.3
		Single channel activity	↑ P_o	3.5, 3.6
		Current amplitude	G and V_{rev} indicative of TRP	3.7
	Whole-cell patch	*Vm*	Depolarised cell	3.8
	Calcium imaging	$[Ca^{2+}]$	↑$[Ca^{2+}]_i$	3.10
GSK1016790A	Cell-attached patch	Action current	↓ frequency	3.3
	Whole-cell patch	*Vm*	Depolarised cell	3.9
RN1734 + Hypotonic	Cell-attached patch	Action current	Restore frequency	3.4
	Cannulation/ICV	Blood pressure Heart rate	No change in blood pressure No change in heart rate	4.3, 4.4
HC067047 + Hypotonic	Cell-attached patch	Action current	Restore frequency	3.4
K_{Ca} and TRPV4 coupling				
UCL-1684 + Hypotonic	Cell-attached patch	Action current	Restore frequency	5.2
	Calcium imaging	$[Ca^{2+}]$	↑$[Ca^{2+}]_i$ sustained	5.6
TRAM-34 + Hypotonic	Cell-attached patch	Action current	No change	5.3
IbTX + Hypotonic	Cell-attached patch	Action current	No change	5.4
UCL-1684 + GSK1016790A	Cell-attached patch	Action current	No change	5.7

9.1.2 Temperature sensing in the PVN

In Chapter 3 a mechanism for temperature sensing within the parvocellular PVN was explored as TRPV4 is known to be activated at temperatures above 27^{o}C (Guler *et al.*, 2002). An increase in bath temperature led to a decrease in activity of the parvocellular neurones patched, in keeping with the hypothesis of coupling between the TRPV4 and SK channels. It was therefore important to identify the channel responsible for this change in activity. There are 28 TRP channels, several of which show temperature sensitivity, however, experiments revealed a role for the TRPM2 channel in this mechanism in the PVN. Interestingly, increasing temperature in other areas of the brain has typically been shown to result in increased neuronal activity (Sudbury and Bourque, 2013). As there is no evidence to suggest TRPM2 will be coupled to a calcium-activated channel, activation of this channel should result in a depolarisation and increased activity, as seen in other areas. I therefore hypothesised that the TRPM2 channel is not present in the neurone being patched, but in an upstream target such as an inhibitory GABAergic innervation (Myers *et al.*, 2013; Roland and Sawchenko, 1993). As this reduction in activity is seen at physiological temperatures, it is possible that there is some involvement in the tonic inhibition of the parvocellular PVN (Badoer *et al.*, 2002; Martin and Haywood, 1993; Martin *et al.*, 1991; Park and Stern, 2005).

Interestingly, many groups patch at room temperature (~25^{o}C). In light of the evidence shown in this thesis this may potentially be one of the reasons that the quiescent nature of the parvocellular neurones is lost in slice recordings, combined with a loss of some of the GABAergic innervations in the slicing procedure (Stern,

2001; Womack *et al.*, 2007). Further whole-cell patch clamp investigation may be particularly beneficial in order to uncover the mechanism behind the changes seen in neuronal activity. In addition, the NEURON model could be further developed to incorporate the TRPM2 channel into the GABAergic innervations of the SPAN to see if this is feasible before any further *in vitro* work is carried out.

Furthermore, it is important to note that stress can increase core body temperature and increased heart rate and blood pressure has been shown in humans and other animals subjected to different forms of stress (Balcombe *et al.*, 2004; Everson *et al.*, 1996; Herd, 1991). It would be interesting to study these effects combined *in vivo*.

9.1.3 Cardiovascular responses to stress – an involvement for the NK-1 receptor

Substance P (SP) is abundant in the PVN and its receptor NK1 is expressed with the parvocellular PVN (Jessop *et al.*, 1991; Shults *et al.*, 1985). My group has previously shown that SP increases neuronal activity potentially by disinhibition of spinally-projecting neurones of the PVN (Womack and Barrett-Jolley, 2007; Womack *et al.*, 2007). Furthermore, studies have shown that NK receptors within the CNS are involved in the cardiovascular response to noxious stress, implicating the PVN in this response (Culman *et al.*, 2010). Although evidence suggests that NK receptors in the PVN may be important for physiological responses to psychological stressors (Santarelli *et al.*, 2002; Santarelli *et al.*, 2001), no direct evidence has been previously shown. In Chapter 7 I provide evidence which suggests that the NK1 receptor is involved in cardiovascular response to mild psychological stress. HRV analysis revealed that increased LF/HF (an indicator of sympathetic activity) in response to stress was ablated in NK1 receptor lesioned rats. Furthermore, a

distinct shift in the circadian pattern of heart rate was also observed in the NK1 lesioned animals, suggesting a role for these receptors in setting circadian variation of heart rate.

Further work on NK1 expressing neurones within the PVN would also help shed light on the role this receptor plays on setting circadian rhythm and in the cardiovascular response to stress. A simple addition to this study would be to lesion NK1 receptors bilaterally, as only unilateral lesions were performed. It would be interesting to see if this would produce more severe changes in the cardiovascular response to stress. One can't help but think that the pathways involved in this process are complex, as it is known the PVN has many afferent and efferent projections (Affleck *et al.*, 2012; Coote *et al.*, 1998; Pyner and Coote, 1999; Pyner and Coote, 2000). The SCN, for example, is known to play a part in circadian rhythm and projects to the PVN (Reppert and Weaver, 2002; Tei *et al.*, 1997). The use of conditional knockouts would be an interesting step in this research, as there would be the potential to knock out the NK1 receptors on those neuronal populations of interest. It would also be interesting to record additional parameters, such as blood pressure and temperature, as it is known that both of these parameters are altered during stress and the PVN has a role in modulating both. As seen in this thesis, blood pressure changes occur when heart rate remains unaffected (Chapter 4). It may therefore be that although heart rate remains increased in the lesioned rats with stress, blood pressure may be affected as well as SNA.

The effects of stress on the cardiovascular system were also considered in Chapter 8 when looking at the Gnasxl KO mouse. My group has shown that these mice have

elevated sympathetic nervous activity, increased heart rate and blood pressure as well as basal temperature (Nunn *et al.*, 2009; Nunn *et al.*, 2013). Interestingly, my group hypothesise that the effects of XLαs are indirect, whereby it provides tonic inhibitory input to downstream SNS control neurones, for example via GABA (Nunn *et al.*, 2013). If this hypothesis is correct it means the Gnasxl KO mouse would be a good tool to investigate the elevated SNA seen in cardiovascular disease due to this loss of tonic inhibitory input. In my study I showed that the increase in LF/HF ratio (an indicator of sympathetic activity) seen in the wildtype mice subjected to stress was not present in the KO mice, indicating sympathetic activity is elevated with stress in the wildtype, but not in KO mice. This is potentially due to its already elevated sympathetic activity at rest. Although these results are interesting, the mechanisms responsible are still unknown and should be explored further.

9.2 Conclusions

This work has revealed the multifunctional nature of the parvocellular neurones of the PVN and the mechanisms responsible for these roles. As dysregulation of neuronal activity in the PVN projecting to sites of autonomic influence has been linked to cardiovascular disease, understanding its normal functional role in the cardiovascular system is vital. Investigation of the mechanisms involved may provide ion channel and receptor targets for pharmacological intervention of elevated sympathetic nervous activity.

One of the main findings of this thesis is an osmosensing role for the parvocellular PVN, via a TRPV4 and SK channel coupling, which has the ability to affect the

cardiovascular system. Central changes in osmolality can modulate blood pressure, an affect which would presumably be engaged as a homeostatic function to return plasma osmolality back to a normal level to prevent any damage which may occur from cell swelling or Ca^{2+} toxicity.

I also demonstrated that there is an indirect role for the PVN in sensing temperature changes. Again, this seems to be a homeostatic function, which would in turn lead to downstream effects on the autonomic nervous system via the PVN.

Although these homeostatic roles are important and require further investigation, how the PVN influences the cardiovascular response to stress is of particular importance. This is a role which may also affect those normal homeostatic functions if an individual was in a highly stressed state over an extended period of time. This level of stress has been shown to lead to elevated sympathetic nervous activity, such as is seen in the *Gnasxl* KO mouse, via a loss of tonic inhibition by GABA and has been linked to increased risk of cardiovascular disease (Floras, 2009; Grassi *et al.*, 2003; Nunn *et al.*, 2013). The findings of this thesis suggest that substance P and the NK1 receptor are involved in the cardiovascular response to stress and the circadian setting of heart rate. This finding may be the key to beginning to understanding the elevated sympathetic nervous activity observed and also means that potentially, selective inhibition of preautonomic PVN neurones could be therapeutically useful for modulation of stress related heart disease.

Appendix

Publications from this work:

1. Nunn, N., Feetham, C.H., Martin, J., Barrett-Jolley, R. and Plagge, A. (2013) Elevated blood pressure, heart rate and body temperature in mice lacking the XLαs protein of the *Gnas* locus is due to increased sympathetic tone. *Exp Physiol*. 98:1432-1445.
2. Feetham C.H., Nunn N., Lewis R. and Barrett-Jolley R. (2014) TRPV4 and K_{Ca} functionally couple as osmosensors in the PVN. *Currently submitted to Br J Pharmacol 2014 under revision*
3. Feetham C.H. and Barrett-Jolley R. (2014) NK1-receptor expressing paraventricular nucleus neurones modulate circadian rhythm and stress induced changes in heart rate variability. S*ubmitted to Physiol. Reports 2014 under revision.*

Conference proceedings from this work:

1. Nunn N., Feetham C., Plagge A. and Barrett-Jolley R. (2011) Investigation of cardiovascular parameters as indicators of sympathetic activity in lean and hypermetabolic Gnasxl knock-out mice*. J. Physiol. Proc. Physiol. Soc. 23: PC27*
2. Feetham C.H. and Barrett-Jolley, R. (2012) Osmosensing in the PVN: A role for TRPV4*. J. Physiol. Proc. Physiol. Soc. 27: PC76.*

3. Nunn, N., Feetham C., Plagge, A. and Barrett-Jolley R. (2012) Hypermetabolic Gnasxl knock-out mice have increased sympathetic control of heart rate variability. *J. Physiol. Proc. Physiol. Soc. 27: PC226.*
4. *Feetham C.H. and Barrett-Jolley R.* (2012) Volume Control within the PVN: A role for TRPV4. *Biophysical Society Meeting Abstracts. Biophysical Journal*, Supplement, 546a, Abstract, 2780-Pos.
5. *Feetham C.H., Lewis, R. and Barrett-Jolley R.* (2013) TRPV4 and KCa: Modelling the perfect couple? *Biophysical Society Meeting Abstracts. Biophysical Journal*, Supplement, 163a, Abstract.
6. Feetham C.H. and Barrett-Jolley R. (2013) TRPV4 and KCa: The model couple? *J Physiol. Proc 37th IUPS, PCD132.*
7. Feetham C.H and Barrett-Jolley R. (2014) Mechanistic insights into osmosensing in the PVN. *FASEB J 28:1182.2.*
8. Feetham C.H and Barrett-Jolley R. (2014) Exploring thermosensitivity in the PVN. *Proc. Physiol. Soc: PCB57.*

References

Adams PR, Constanti A, Brown DA, Clark RB (1982). Intracellular Ca2+ activates a fast voltage-sensitive K+ current in vertebrate sympathetic neurones. *Nature* **296**(5859)**:** 746-749.

Affleck VS, Coote JH, Pyner S (2012). The projection and synaptic organisation of NTS afferent connections with presympathetic neurons, GABA and nNOS neurons in the paraventricular nucleus of the hypothalamus. *Neuroscience* **219:** 48-61.

Aguilera G (1994). Regulation of Pituitary Acth-Secretion During Chronic Stress. *Frontiers in Neuroendocrinology* **15**(4)**:** 321-350.

Akama H, McGrath BP, Badoer E (1998). Volume expansion fails to normally activate neural pathways in the brain of conscious rabbits with heart failure. *Journal of the autonomic nervous system* **73**(1)**:** 54-62.

Alexander SP, Mathie A, Peters JA (2011). Guide to Receptors and Channels (GRAC), 5th edition. *British Journal of Pharmacology* **164 Suppl 1:** S1-324.

Allen AM (2002). Inhibition of the Hypothalamic Paraventricular Nucleus in Spontaneously Hypertensive Rats Dramatically Reduces Sympathetic Vasomotor Tone. *Hypertension* **39**(2)**:** 275-280.

Allen AM, MacGregor DP, McKinley MJ, Mendelsohn FA (1999). Angiotensin II receptors in the human brain. *Regulatory peptides* **79**(1)**:** 1-7.

Amir S (1990). Stimulation of the paraventricular nucleus with glutamate activates interscapular brown adipose tissue thermogenesis in rats. *Brain Research* **508**(1)**:** 152-155.

Armstrong WE, Warach S, Hatton GI, McNeill TH. (1980). Subnuclei in the rat hypothalamic paraventricular nucleus: a cytoarchitectural, horseradish peroxidase and immunocytochemical analysis. *Neuroscience* **5**(11): 1931-1958.

Arnhold MM, Wotus C, Engeland WC (2007). Differential regulation of parvocellular neuronal activity in the paraventricular nucleus of the hypothalamus following single vs. repeated episodes of water restriction-induced drinking. *Experimental Neurology* **206**(1)**:** 126-136.

Badoer E, McKinlay D, Trigg L, McGrath BP (1997). Distribution of activated neurons in the rabbit brain following a volume load. *Neuroscience* **81**(4)**:** 1065-1077.

Badoer E, McKinley MJ, Oldfield BJ, McAllen RM (1993). A comparison of hypotensive and non-hypotensive hemorrhage on Fos expression in spinally

projecting neurons of the paraventricular nucleus and rostral ventrolateral medulla. *Brain Research* **610**(2)**:** 216-223.

Badoer E, Ng CW, De Matteo R (2002). Tonic sympathoinhibition arising from the hypothalamic PVN in the conscious rabbit. *Brain Research* **947**(1)**:** 17-24.

Bains JS, Ferguson AV (1995). Paraventricular nucleus neurons projecting to the spinal-cord receive excitatory input from the subfornical organ. *American Journal of Physiology-Regulatory Integrative and Comparative Physiology* **268**(3)**:** R625-R633.

Bains JS, Potyok A, Ferguson AV (1992). Angiotensin-ii actions in paraventricular nucleus - functional evidence for neurotransmitter role in efferents originating in subfornical organ. *Brain Research* **599**(2)**:** 223-229.

Balcombe JP, Barnard ND, Sandusky C (2004). Laboratory routines cause animal stress. *Contemporary topics in laboratory animal science / American Association for Laboratory Animal Science* **43**(6)**:** 42-51.

Bamshad M, Song CK, Bartness TJ (1999). CNS origins of the sympathetic nervous system outflow to brown adipose tissue. *American Journal of Physiology* **276**(6 Pt 2): R1569-1578.

Baraboi ED, St-Pierre DH, Shooner J, Timofeeva E, Richard D (2011). Brain activation following peripheral administration of the GLP-1 receptor agonist exendin-4. *American journal of physiology. Regulatory, integrative and comparative physiology* **301**(4)**:** R1011-1024.

Barrett-Jolley R, Pyner S, Coote JH (2000). Measurement of voltage-gated potassium currents in identified spinally-projecting sympathetic neurones of the paraventricular nucleus. *Journal of Neuroscience Methods* **102**(1)**:** 25-33.

Barry PH, Lynch JW (1991). Liquid junction potentials and small cell effects in patch-clamp analysis. *Journal of Membrane Biology* **121**(2)**:** 101-117.

Baudrie V, Laude D, Elghozi JL (2007). Optimal frequency ranges for extracting information on cardiovascular autonomic control from the blood pressure and pulse interval spectrograms in mice. *American journal of physiology. Regulatory, integrative and comparative physiology* **292**(2)**:** R904-912.

Becker D, Blase C, Bereiter-Hahn J, Jendrach M (2005). TRPV4 exhibits a functional role in cell-volume regulation. *Journal of Cell Science* **118**(11)**:** 2435-2440.

Belle MD, Diekman CO, Forger DB, Piggins HD (2009). Daily electrical silencing in the mammalian circadian clock. *Science (New York, N.Y.)* **326**(5950)**:** 281-284.

Benedetti M, Rorato R, Castro M, Machado BH, Antunes-Rodrigues J, Elias LLK (2008). Water deprivation increases Fos expression in hypothalamic corticotropin-

releasing factor neurons induced by right atrial distension in awake rats. *American Journal of Physiology-Regulatory Integrative and Comparative Physiology* **295**(5)**:** R1706-R1712.

Benfenati V, Caprini M, Dovizio M, Mylonakou MN, Ferroni S, Ottersen OP*, et al.* (2011). An aquaporin-4/transient receptor potential vanilloid 4 (AQP4/TRPV4) complex is essential for cell-volume control in astrocytes. *Proceedings of the National Academy of Sciences of the United States of America* **108**(6)**:** 2563-2568.

Bernstein J (1902). Untersuchungen zur Thermodynamik der bioelektrischen Ströme. *Pflügers Archives* **92**(10-12)**:** 521-562.

Black JA, Yokoyama S, Higashida H, Ransom BR, Waxman SG (1994). Sodium channel mRNAs I, II and III in the CNS: cell-specific expression. *Brain Research Molelecular Brain Research* **22**(1-4)**:** 275-289.

Bourque CW (2008). Central mechanisms of osmosensation and systemic osmoregulation. *Nature Reviews Neuroscience* **9**(7)**:** 519-531.

Bourque CW, Ciura S, Trudel E, Stachniak TJ, Sharif-Naeini R (2007). Neurophysiological characterization of mammalian osmosensitive neurones. *Experimental physiology* **92**(3)**:** 499-505.

Bourque CW, Oliet SH (1997). Osmoreceptors in the central nervous system. *Annual review of physiology* **59:** 601-619.

Bratincsak A, Palkovits M (2004). Activation of brain areas in rat following warm and cold ambient exposure. *Neuroscience* **127**(2)**:** 385-397.

Brooks VL, Qi Y, O'Donaughy TL (2005). Increased osmolality of conscious water-deprived rats supports arterial pressure and sympathetic activity via a brain action. *American journal of physiology. Regulatory, integrative and comparative physiology* **288**(5)**:** R1248-1255.

Brown TM, Piggins HD (2007). Electrophysiology of the suprachiasmatic circadian clock. *Progress in Neurobiology* **82**(5)**:** 229-255.

Brvar M, Kozelj G, Osredkar J, Mozina M, Gricar M, Bunc M (2004). Polydipsia as another mechanism of hyponatremia after 'ecstasy' (3,4 methyldioxymethamphetamine) ingestion. *European Journal of Emergency Medicine* **11**(5)**:** 302-304.

Buijs RM, van Eden CG, Goncharuk VD, Kalsbeek A (2003). The biological clock tunes the organs of the body: timing by hormones and the autonomic nervous system. *The Journal of Endocrinology* **177**(1)**:** 17-26.

Buijs RM, Wortel J, Van Heerikhuize JJ, Feenstra MG, Ter Horst GJ, Romijn HJ, Kalsbeek A (1999). Anatomical and functional demonstration of a multisynaptic suprachiasmatic nucleus adrenal (cortex) pathway. *European Journal of Neuroscience* **11**(5)**:** 1535-1544.

Busnardo C, Tavares RF, Correa FMA (2009). Role of N-Methyl-D-Aspartate and non-N-Methyl-D-Aspartate receptors in the cardiovascular effects of L-Glutamate microinjection Into the hypothalamic paraventricular nucleus of unanesthetized rats. *Journal of Neuroscience Research* **87**(9)**:** 2066-2077.

Busnardo C, Tavares RF, Resstel LB, Elias LL, Correa FM (2010). Paraventricular nucleus modulates autonomic and neuroendocrine responses to acute restraint stress in rats. *Autonomic neuroscience : basic & clinical* **158**(1-2)**:** 51-57.

Cabral A, Valdivia S, Reynaldo M, Cyr NE, Nillni EA, Perello M (2012). Short-term cold exposure activates TRH neurons exclusively in the hypothalamic paraventricular nucleus and raphe pallidus. *Neuroscience Letters* **518**(2)**:** 86-91.

Candia S, Garcia ML, Latorre R (1992). Mode of action of iberiotoxin, a potent blocker of the large conductance Ca2+-activated K+ channel. *Biophysical Journal* **63**(2)**:** 583-590.

Carillo BA, Oliveira-Sales EB, Andersen M, Tufik S, Hipolide D, Santos AA*, et al.* (2012). Changes in GABAergic inputs in the paraventricular nucleus maintain sympathetic vasomotor tone in chronic heart failure. *Autonomic neuroscience : basic & clinical* **171**(1-2)**:** 41-48.

Carnevale NT, Hines ML (2006). *The NEURON book*. edn. Cambridge University Press: Cambridge, UK.

Carrasco M, Portillo F, Larsen PJ, Vallo JJ (2001). Insulin and glucose administration stimulates Fos expression in neurones of the paraventricular nucleus that project to autonomic preganglionic structures. *Journal of Neuroendocrinology* **13**(4)**:** 339-346.

Carreno FR, Ji LL, Cunningham JT (2009). Altered central TRPV4 expression and lipid raft association related to inappropriate vasopressin secretion in cirrhotic rats. *American Journal of Physiology. Regulatory, integrative and comparative physiology* **296**(2)**:** R454-466.

Carruba MO, Bondiolotti G, Picotti GB, Catteruccia N, Da Prada M (1987). Effects of diethyl ether, halothane, ketamine and urethane on sympathetic activity in the rat. *European Journal of Pharmacololgy* **134**(1)**:** 15-24.

Cato MJ, Toney GM (2005). Angiotensin II excites paraventricular nucleus neurons that innervate the rostral ventrolateral medulla: An in vitro patch-clamp study in brain slices. *Journal of Neurophysiololgy* **93**(1)**:** 403-413.

Catterall WA, Goldin AL, Waxman SG (2005a). International Union of Pharmacology. XLVII. Nomenclature and structure-function relationships of voltage-gated sodium channels. *Pharmacological reviews* **57**(4)**:** 397-409.

Catterall WA, Perez-Reyes E, Snutch TP, Striessnig J (2005b). International Union of Pharmacology. XLVIII. Nomenclature and structure-function relationships of voltage-gated calcium channels. *Pharmacological Reviews* **57**(4): 411-425.

Cerqueira JJ, Almeida OF, Sousa N (2008). The stressed prefrontal cortex. Left? Right! *Brain, Behaviour and Immunity* **22**(5)**:** 630-638.

Cham JL, Badoer E (2008). Exposure to a hot environment can activate rostral ventrolateral medulla-projecting neurones in the hypothalamic paraventricular nucleus in conscious rats. *Experimental physiology* **93**(1)**:** 64-74.

Cham JL, Klein R, Owens NC, Mathai M, McKinley M, Badoer E (2006a). Activation of spinally projecting and nitrergic neurons in the PVN following heat exposure. *American Journal of Physiology. Regulatory, integrative and comparative physiology* **291**(1)**:** R91-101.

Cham JL, Owens NC, Barden JA, Lawrence AJ, Badoer E (2006b). P2X purinoceptor subtypes on paraventricular nucleus neurones projecting to the rostral ventrolateral medulla in the rat. *Experimental Physiology* **91**(2)**:** 403-411.

Champagne D, Beaulieu J, Drolet G (1998). CRFergic innervation of the paraventricular nucleus of the rat hypothalamus: a tract-tracing study. *Journal of Neuroendocrinology* **10**(2)**:** 119-131.

Chen F, Dworak M, Wang Y, Cham JL, Badoer E (2008). Role of the hypothalamic PVN in the reflex reduction in mesenteric blood flow elicited by hyperthermia. *American Journal of Physiology. Regulatory, integrative and comparative Physiology* **295**(6)**:** R1874-R1881.

Chen M, Berger A, Kablan A, Zhang J, Gavrilova O, Weinstein LS (2012). Gsα deficiency in the paraventricular nucleus of the hypothalamus partially contributes to obesity associated with Gsα mutations. *Endocrinology* **153**(9):4256-65.

Chen Q, Pan HL (2006). Regulation of synaptic input to hypothalamic presympathetic neurons by GABA(B) receptors. *Neuroscience* **142**(2)**:** 595-606.

Chen Q, Pan HL (2007). Signaling mechanisms of angiotensin II-induced attenuation of GABAergic input to hypothalamic presympathetic neurons. *Journal of Neurophysiology* **97**(5)**:** 3279-3287.

Chen QH, Toney GM (2001). AT(1)-receptor blockade in the hypothalamic PVN reduces central hyperosmolality-induced renal sympathoexcitation. *American*

Journal of Physiology. Regulatory, integrative and comparative physiology **281**(6)**:** R1844-1853.

Chen QH, Toney GM (2009). Excitability of paraventricular nucleus neurones that project to the rostral ventrolateral medulla is regulated by small-conductance Ca2+-activated K+ channels. *Journal of Physiology* **587**(17)**:** 4235-4247.

Chin H, Smith MA, Kim HL, Kim H (1992). Expression of dihydropyridine-sensitive brain calcium channels in the rat central nervous system. *FEBS Letters* **299**(1): 69-74.

Chowdrey HS, Larsen PJ, Harbuz MS, Lightman SL, Jessop DS (1995). Endogenous substance P inhibits the expression of corticotropin-releasing hormone during a chronic inflammatory stress. *Life Sciences* **57**(22)**:** 2021-2029.

Chu CP, Kannan H, Qiu DL (2010). Effect of hypertonic saline on rat hypothalamic paraventricular nucleus parvocellular neurons in vitro. *Neuroscience Letters* **482**(2)**:** 142-145.

Chun J, Shin SH, Kang SS (2012). The negative feedback regulation of TRPV4 Ca2+ ion channel function by its C-terminal cytoplasmic domain. *Cellular signalling* **24**(10)**:** 1918-1922.

Chung YH, Kim HS, Shin CM, Kim MJ, Cha CI (2001). Immunohistochemical study on the distribution of voltage-gated K(+) channels in rat brain following transient focal ischemia. *Neuroscience Letters* **308**(3)**:** 157-160.

Clapham DE (2003). TRP channels as cellular sensors. *Nature* **426**(6966)**:** 517-524.

Clapham DE, Runnels LW, Strubing C. The TRP ion channel family. *Nature Reviews Neuroscience* **2**(6): 387-396.

Clement DL, Pelletier CL, Shepherd JT (1972). Role of vagal afferents in the control of renal sympathetic nerve activity in the rabbit. *Circulation Research* **31**(6)**:** 824-830.

Cole KS, Curtis HJ (1939). Electric impedance of the squid giant axon during activity. *The Journal of General Physiology* **22**(5)**:** 649-670.

Collo G, North RA, Kawashima E, Merlo-Pich E, Neidhart D, Surprenant A, Buell G (1996). Cloning of P2X5 and P2X6 receptors and the distribution and properties of an extended family of ATP-gated ion channels. *Journal of Neuroscience* **16**(8): 2495-2507.

Conn PJ, Pin JP (1997). Pharmacology and functions of metabotropic glutamate receptors. *Annual Review of Pharmacology and Toxicology* **37:** 205-237.

Contreras GF, Neely A, Alvarez O, Gonzalez C, Latorre R (2012). Modulation of BK channel voltage gating by different auxiliary beta subunits. *Proceedings of the National Academy of Sciences of the United States of America* **109**(46)**:** 18991-18996.

Coote JH (2007). Landmarks in understanding the central nervous control of the cardiovascular system. *Experimental Physiology* **92**(1)**:** 3-18.

Coote JH (2005). A role for the paraventricular nucleus of the hypothalamus in the autonomic control of heart and kidney. *Experimental Physiology* **90**(2)**:** 169-173.

Coote JH, Yang Z, Pyner S, Deering J (1998). Control of sympathetic outflows by the hypothalamic paraventricular nucleus. *Clinical and Experimental Pharmacology and Physiology* **25**(6)**:** 461-463.

Courtemanche M, Ramirez RJ, Nattel S (1998). Ionic mechanisms underlying human atrial action potential properties: insights from a mathematical model. *American Journal of Physiology* **275**(2)**:** H301-321.

Cui BP, Li P, Sun HJ, Ding L, Zhou YB, Wang JJ*, et al.* (2013). Ionotropic glutamate receptors in paraventricular nucleus mediate adipose afferent reflex and regulate sympathetic outflow in rats. *Acta Physiologica (Oxford)* **209**(1): 45-54.

Cui LN, Coderre E, Renaud LP (2001). Glutamate and GABA mediate suprachiasmatic nucleus inputs to spinal-projecting paraventricular neurons. *American Journal of Physiology. Regulatory, integrative and comparative physiology* **281**(4)**:** R1283-1289.

Culman J, Das G, Ohlendorf C, Haass M, Maser-Gluth C, Zuhayra M, Zhao Y, Itoi K (2010). Blockade of tachykinin NK1/NK2 receptors in the brain attenuates the activation of corticotrophin-releasing hormone neurones in the hypothalamic paraventricular nucleus and the sympathoadrenal and pituitary-adrenal responses to formalin-induced pain in the rat. *Journal of Neuroendocrinology* **22**(5)**:** 467-476.

Culman J, Unger T (1995). Central tachykinins: mediators of defence reaction and stress reactions. *Canadian Journal of Physiology and Pharmacology* **73**(7)**:** 885-891.

Dampney RA, Horiuchi J, Killinger S, Sheriff MJ, Tan PS, McDowall LM (2005). Long-term regulation of arterial blood pressure by hypothalamic nuclei: some critical questions. *Clinical and Experimental Pharmocology and Physiology* **32**(5-6): 419-425.

Davern PJ, Chowdhury S, Jackson KL, Nguyen-Huu TP, Head GA (2014). GABAA receptor dysfunction contributes to high blood pressure and exaggerated response to stress in Schlager genetically hypertensive mice. *Journal of Hypertension* **32**(2)**:** 352-362.

Davern PJ, Nguyen-Huu TP, La Greca L, Abdelkader A, Head GA (2009). Role of the sympathetic nervous system in Schlager genetically hypertensive mice. *Hypertension* **54**(4)**:** 852-859.

De Felipe C, Herrero JF, O'Brien JA, Palmer JA, Doyle CA, Smith AJ*, et al.* (1998). Altered nociception, analgesia and aggression in mice lacking the receptor for substance P. *Nature* **392**(6674)**:** 394-397.

de Gasparo M, Catt KJ, Inagami T, Wright JW, Unger T (2000). International union of pharmacology. XXIII. The angiotensin II receptors. *Pharmacological Reviews* **52**(3)**:** 415-472.

de Vries MG, Arseneau LM, Lawson ME, Beverly JL (2003). Extracellular glucose in rat ventromedial hypothalamus during acute and recurrent hypoglycemia. *Diabetes* **52**(11)**:** 2767-2773.

Deering J, Coote JH (2000). Paraventricular neurones elicit a volume expansion-like change of activity in sympathetic nerves to the heart and kidney in the rabbit. *Experimental Physiology* **85**(2)**:** 177-186.

Deng HX, Klein CJ, Yan J, Shi Y, Wu Y, Fecto F*, et al.* (2010). Scapuloperoneal spinal muscular atrophy and CMT2C are allelic disorders caused by alterations in TRPV4. *Nature Genetics* **42**(2)**:** 165-169.

Dietl M, Arluison M, Mouchet P, Feuerstein C, Manier M, Thibault J (1985). Immunohistochemical demonstration of catecholaminergic cell bodies in the spinal cord of the rat. Preliminary note. *Histochemistry* **82**(4)**:** 385-389.

DiMicco JA, Samuels BC, Zaretskaia MV, Zaretsky DV (2002). The dorsomedial hypothalamus and the response to stress: Part renaissance, part revolution. *Pharmacology Biochemistry and Behavior* **71**(3)**:** 469-480.

DiMicco JA, Stotz-Potter EH, Monroe AJ, Morin SM (1996). Role of the dorsomedial hypothalamus in the cardiovascular response to stress. *Clinical and Experimental Pharmocology and Physiology* **23**(2): 171-176.

Ding YQ, Shigemoto R, Takada M, Ohishi H, Nakanishi S, Mizuno N (1996). Localization of the neuromedin K receptor (NK3) in the central nervous system of the rat. *Journal of Comparative Neurololgy* **364**(2)**:** 290-310.

Doggrell SA, Brown L (1998). Rat models of hypertension, cardiac hypertrophy and failure. *Cardiovascular Research* **39**(1)**:** 89-105.

Drenjancevic I, Grizelj I, Harsanji-Drenfjancevic I, Cavka A, Selthofer-Relatic K (2014). The interplay between sympathetic overactivity, hypertension and heart rate variability (review, invited). *Acta Physiologica Hungarica* **101**(2)**:** 129-142.

Duan YF, Winters R, McCabe PM, Green EJ, Huang Y, Schneiderman N (1997). Cardiorespiratory components of defense reaction elicited from paraventricular nucleus. *Physiology and Behaviour* **61**(2)**:** 325-330.

Dunn-Meynell AA, Govek E, Levin BE (1997). Intracarotid glucose selectively increases Fos-like immunoreactivity in paraventricular, ventromedial and dorsomedial nuclei neurons. *Brain Research* **748**(1-2)**:** 100-106.

Dunn FL, Brennan TJ, Nelson AE, Robertson GL (1973). The role of blood osmolality and volume in regulating vasopressin secretion in the rat. *The Journal of Clinical Investigation* **52**(12)**:** 3212-3219.

Earley S (2011). Endothelium-dependent cerebral artery dilation mediated by transient receptor potential and Ca2+-activated K+ channels. *Journal of Cardiovascular Pharmacology* **57**(2)**:** 148-153.

Ebner K, Muigg P, Singewald G, Singewald N (2008). Substance P in stress and anxiety: NK-1 receptor antagonism interacts with key brain areas of the stress circuitry. *Annals of the New York Academy of Sciences* **1144:** 61-73.

Everaerts W, Zhen X, Ghosh D, Vriens J, Gevaert T, Gilbert JP*, et al.* (2010). Inhibition of the cation channel TRPV4 improves bladder function in mice and rats with cyclophosphamide-induced cystitis. *Proceedings of the National Academy of Sciences of the United States of America* **107**(44)**:** 19084-19089.

Everson SA, Kaplan GA, Goldberg DE, Salonen JT (1996). Anticipatory blood pressure response to exercise predicts future high blood pressure in middle-aged men. *Hypertension* **27**(5)**:** 1059-1064.

Faber ES, Sah P (2003). Calcium-activated potassium channels: multiple contributions to neuronal function. *The Neuroscientist: a review journal bringing neurobiology, neurology and psychiatry* **9**(3)**:** 181-194.

Farah VM, Joaquim LF, Morris M (2006). Stress cardiovascular/autonomic interactions in mice. *Physiology and Behaviour* **89**(4)**:** 569-575.

Fater DC, Schultz HD, Sundet WD, Mapes JS, Goetz KL (1982). Effects of left atrial stretch in cardiac-denervated and intact conscious dogs. *American Journal of Physiology* **242**(6)**:** H1056-1064.

Feetham CH, Barrett-Jolley R (2012). Volume control in the PVN: a role for TRPV4. *Biophysical Journal* **102**(3)**:** 546a.

Ferguson AV, Latchford KJ, Samson WK (2008). The paraventricular nucleus of the hypothalamus - a potential target for integrative treatment of autonomic dysfunction. *Expert Opinion on Therapeutic Targets* **12**(6)**:** 717-727.

Fisher JP, Young CN, Fadel PJ (2009). Central sympathetic overactivity: maladies and mechanisms. *Autonomic Neuroscience: basic & clinical* **148**(1-2)**:** 5-15.

Flak JN, Myers B, Solomon MB, McKlveen JM, Krause EG, Herman JP (2014). Role of paraventricular nucleus-projecting norepinephrine/epinephrine neurons in acute and chronic stress. *European Journal of Neuroscience* **39**(11)**:** 1903-1911.

Flak JN, Ostrander MM, Tasker JG, Herman JP (2009). Chronic stress-induced neurotransmitter plasticity in the PVN. *The Journal of Comparative Neurology* **517**(2)**:** 156-165.

Floras JS (2009). Sympathetic nervous system activation in human heart failure: clinical implications of an updated model. *Journal of the American College of Cardiology* **54**(5)**:** 375-385.

Folkow B (2001). Mental stress and its importance for cardiovascular disorders; physiological aspects, "from-mice-to-man". *Scandinavian Cardiovascular Journal* **35**(3)**:** 163-172.

Fontes MAP, Tagawa T, Polson JW, Cavanagh SJ, Dampney RAL (2001a). Descending pathways mediating cardiovascular response from dorsomedial hypothalamic nucleus. *American Journal of Physiology. Heart and Circulatory Physiology* **280**(6)**:** H2891-H2901.

Fowler MA, Sidiropoulou K, Ozkan ED, Phillips CW, Cooper DC (2007). Corticolimbic expression of TRPC4 and TRPC5 channels in the rodent brain. *PLoS One* **2**(6)**:** e573.

Furuyama T, Morita Y, Inagaki S, Takagi H (1993). Distribution of I, II and III subtypes of voltage-sensitive Na+ channel mRNA in the rat brain. *Brain Research Molecular Brain Research* **17**(1-2)**:** 169-173.

Gao F, Sui D, Garavito RM, Worden RM, Wang DH (2009). Salt intake augments hypotensive effects of transient receptor potential vanilloid 4: functional significance and implication. *Hypertension* **53**(2)**:** 228-235.

Gao F, Wang DH (2010). Hypotension induced by activation of the transient receptor potential vanilloid 4 channels: role of Ca2+-activated K+ channels and sensory nerves. *Journal of Hypertension* **28**(1)**:** 102-110.

Giovannelli L, Shiromani PJ, Jirikowski GF, Bloom FE (1992). Expression of c-fos protein by immunohistochemically identified oxytocin neurons in the rat hypothalamus upon osmotic stimulation. *Brain Research* **588**(1)**:** 41-48.

Gladwell SJ, Coote JH (1999). Inhibitory and indirect excitatory effects of dopamine on sympathetic preganglionic neurones in the neonatal rat spinal cord in vitro. *Brain Research* **818**(2)**:** 397-407.

Gladwell SJ, Pyner S, Barnes NM, Coote JH (1999). D-1-like dopamine receptors on retrogradely labelled sympathoadrenal neurones in the thoracic spinal cord of the rat. *Experimental Brain Research* **128**(3)**:** 377-382.

Goldberger AL, Amaral LAN, Glass L, Hausdorff JM, Ivanov PC, Mark RG, Mietus JM, Moody GB, Peng CK, Stanley HE (2000). PhysioBank, PhysioToolkit, and PhysioNet: Components of a New Research Resource for Complex Physiologic Signals. *Circulation* **101**(23)**:** e215-220.

Goldman DE (1943). Potential, impedance, and rectification in membranes. *The Journal of General Physiology* **27**(1)**:** 37-60.
Gomez CR (2014). Disorders of body temperature. *Handbook of Clinical Neurology* **120:** 947-957.

Goldstein SA, Bayliss DA, Kim D, Lesage F, Plant LD, Rajan S (2005). International Union of Pharmacology. LV. Nomenclature and molecular relationships of two-P potassium channels. *Pharmacological reviews* **57**(4)**:** 527-540.

Goncharuk VD, van Heerikhuize J, Swaab DF, Buijs RM (2002). Paraventricular nucleus of the human hypothalamus in primary hypertension: Activation of corticotropin-releasing hormone neurons. *Journal of Comparative Neurology* **443**(4)**:** 321-331.

Gottlieb HB, Ji LL, Jones H, Penny ML, Fleming T, Cunningham JT (2006). Differential effects of water and saline intake on water deprivation-induced c-Fos staining in the rat. *American Journal of Physiology. Regulatory, integrative and comparative physiology* **290**(5)**:** R1251-1261.

Grassi G, Seravalle G, Quarti-Trevano F, Dell'Oro R, Bolla G, Mancia G (2003). Effects of hypertension and obesity on the sympathetic activation of heart failure patients. *Hypertension* **42**(5)**:** 873-877.

Greenway CV, Lister GE (1974). Capacitance effects and blood reservoir function in the splanchnic vascular bed during non-hypotensive haemorrhage and blood volume expansion in anaesthetized cats. *Journal of Physiology* **237**(2)**:** 279-294.

Grippo AJ, Beltz TG, Johnson AK (2003). Behavioral and cardiovascular changes in the chronic mild stress model of depression. *Physiology and Behaviour* **78**(4-5)**:** 703-710.

Grynkiewicz G, Poenie M, Tsien RY (1985). A new generation of Ca2+ indicators with greatly improved fluorescence properties. *Journal of Biological Chemistry* **260**(6)**:** 3440-3450.

Gui L, LaGrange LP, Larson RA, Gu M, Zhu J, Chen QH (2012). Role of small conductance calcium-activated potassium channels expressed in PVN in regulating

sympathetic nerve activity and arterial blood pressure in rats. *American Journal of Physiology. Regulatory, integrative and comparative physiology* **303**(3)**:** R301-310.

Guilak F, Leddy HA, Liedtke W (2010). Transient receptor potential vanilloid 4: The sixth sense of the musculoskeletal system? *Annals of the New York Academy of Sciences* **1192:** 404-409.

Guler AD, Lee H, Iida T, Shimizu I, Tominaga M, Caterina M (2002). Heat-evoked activation of the ion channel, TRPV4. *Journal of Neuroscience* **22**(15)**:** 6408-6414.

Gutman GA, Chandy KG, Grissmer S, Lazdunski M, McKinnon D, Pardo LA*, et al.* (2005). International Union of Pharmacology. LIII. Nomenclature and molecular relationships of voltage-gated potassium channels. *Pharmacological reviews* **57**(4)**:** 473-508.

Hallbeck M, Larhammar D, Blomqvist A (2001). Neuropeptide expression in rat paraventricular hypothalamic neurons that project to the spinal cord. *Journal of Compartive Neurology* **433**(2)**:** 222-238.

Hara Y, Wakamori M, Ishii M, Maeno E, Nishida M, Yoshida T, Yamada H, Shimizu S, Mori E, Kudoh J, Shimizu N, Kurose H, Okada Y, Imoto K, Mori Y (2002). LTRPC2 Ca2+-permeable channel activated by changes in redox status confers susceptibility to cell death. *Molecular cell* **9**(1)**:** 163-173.

Haselton JR, Goering J, Patel KP (1994). Parvocellular neurons of the paraventricular nucleus are involved in the reduction in renal nerve discharge during isotonic volume expansion. *Journal of the Autonomic Nervous System* **50**(1)**:** 1-11.

Hawthorn J, Ang VT, Jenkins JS (1985). Effects of lesions in the hypothalamic paraventricular, supraoptic and suprachiasmatic nuclei on vasopressin and oxytocin in rat brain and spinal cord. *Brain Research* **346**(1)**:** 51-57.

Head GA, Lukoshkova EV (2008). Understanding the morning rise in blood pressure. *Clinical and Experimental Pharmacology and Physiology* **35**(4)**:** 516-521.

Herd JA (1991). Cardiovascular response to stress. *Physiological Reviews* **71**(1)**:** 305-330.

Herman JP, Cullinan WE (1997). Neurocircuitry of stress: Central control of the hypothalamo-pituitary-adrenocortical axis. *Trends in Neurosciences* **20**(2)**:** 78-84.

Herman JP, Cullinan WE, Ziegler DR, Tasker JG (2002a). Role of the paraventricular nucleus microenvironment in stress integration. *European Journal of Neuroscience* **16**(3)**:** 381-385.

Herman JP, Tasker JG, Ziegler DR, Cullinan WE (2002b). Local circuit regulation of paraventricular nucleus stress integration: glutamate-GABA connections. *Pharmacology, Biochemistry and Behaviour* **71**(3)**:** 457-468.

Hermes ML, Coderre EM, Buijs RM, Renaud LP (1996). GABA and glutamate mediate rapid neurotransmission from suprachiasmatic nucleus to hypothalamic paraventricular nucleus in rat. *Journal of Physiology* **496**(3): 749-757.

Hetzenauer A, Sinnegger-Brauns MJ, Striessnig J, Singewald N (2006). Brain activation pattern induced by stimulation of L-type Ca2+-channels: contribution of Ca(V)1.3 and Ca(V)1.2 isoforms. *Neuroscience* **139**(3): 1005-1015.

Hille B (1986). Ionic channels: molecular pores of excitable membranes. *Harvey Lectures* **82:** 47-69.

Hille B (1994). Modulation of ion-channel function by G-protein-coupled receptors. *Trends in Neurosciences* **17**(12)**:** 531-536.

Hines ML, Carnevale NT (1997). The NEURON simulation environment. *Neural Computation* **9**(6)**:** 1179-1209.

Hodgkin AL (1937a). Evidence for electrical transmission in nerve: Part I. *Journal of Physiology* **90**(2)**:** 183-210.

Hodgkin AL (1937b). Evidence for electrical transmission in nerve: Part II. *Journal of Physiology* **90**(2)**:** 211-232.

Hodgkin AL, Huxley AF (1952a). The components of membrane conductance in the giant axon of Loligo. *Journal of Physiology* **116**(4)**:** 473-496.
Hodgkin AL, Huxley AF (1952b). Currents carried by sodium and potassium ions through the membrane of the giant axon of Loligo. *Journal of Physiology* **116**(4)**:** 449-472.

Hodgkin AL, Huxley AF (1952c). The dual effect of membrane potential on sodium conductance in the giant axon of Loligo. *Journal of Physiology* **116**(4)**:** 497-506.

Hodgkin AL, Huxley AF (1952d). Propagation of electrical signals along giant nerve fibers. *Proceedings of the Royal Society of London. Series B, Containing papers of a Biological character. Royal Society (Great Britain)* **140**(899)**:** 177-183.

Hodgkin AL, Huxley AF (1952e). A quantitative description of membrane current and its application to conduction and excitation in nerve. *Journal of Physiology* **117**(4)**:** 500-544.

Hodgkin AL, Huxley AF, Katz B (1952). Measurement of current-voltage relations in the membrane of the giant axon of Loligo. *Journal of Physiology* **116**(4)**:** 424-448.

Hodgkin AL, Katz B (1949). The effect of sodium ions on the electrical activity of the giant axon of the squid. *Journal of Physiology* **108**(1)**:** 37-77.

Holbein WW, Bardgett ME, Toney GM (2014). Blood pressure is maintained during dehydration by hypothalamic PVN driven tonic sympathetic nerve activity. *Journal of Physiology* **592**(Pt 17): 3783-3799.

Horn T, Smith PM, McLaughlin BE, Bauce L, Marks GS, Pittman QJ*, et al.* (1994). Nitric oxide actions in paraventricular nucleus: cardiovascular and neurochemical implications. *American Journal of Physiology* **266**(1 Pt 2)**:** R306-313.

Hosoya Y, Sugiura Y, Okado N, Loewy A, Kohno K (1991). Descending input from the hypothalamic paraventricular nucleus to sympathetic preganglionic neurons in the rat. *Experimental Brain Research* **85**(1)**:** 10-20.

Huang BS, Chen A, Ahmad M, Wang HW, Leenen FH (2014). Mineralocorticoid and AT1 receptors in the paraventricular nucleus contribute to sympathetic hyperactivity and cardiac dysfunction in rats post myocardial infarct. *Journal of Physiology* **592**(Pt 15)**:** 3273-3286.

Inenaga K, Osaka T, Yamashita H (1987). Thermosensitivity of neurons in the paraventricular nucleus of the rat slice preparation. *Brain Research* **424**(1)**:** 126-132.

Itoi K, Jost N, Badoer E, Tschope C, Culman J, Unger T (1991). Localization of the substance P-induced cardiovascular responses in the rat hypothalamus. *Brain Research.* **558**(1)**:** 123-126.

Jansen AS, Nguyen XV, Karpitskiy V, Mettenleiter TC, Loewy AD (1995a). Central command neurons of the sympathetic nervous system: basis of the fight-or-flight response. *Science* **270**(5236)**:** 644-646.

Jansen ASP, Wessendorf MW, Loewy AD (1995b). Transneuronal Labeling of Cns Neuropeptide and Monoamine Neurons after Pseudorabies Virus Injections into the Stellate Ganglion. *Brain Research* **683**(1)**:** 1-24.

Jarnot M, Corbett AM (2006). Immunolocalization of NaV1.2 channel subtypes in rat and cat brain and spinal cord with high affinity antibodies. *Brain Research* **1107**(1)**:** 1-12.

Jessop DS, Chowdrey HS, Biswas S, Lightman SL (1991). Substance-P and Substance-K in the Rat Hypothalamus Following Monosodium Glutamate Lesions of the Arcuate Nucleus. *Neuropeptides* **18**(3)**:** 165-170.

Jhamandas JH, MacTavish D (2003). Central administration of neuropeptide FF causes activation of oxytocin paraventricular hypothalamic neurones that project to the brainstem. *Journal of Neuroendocrinology* **15**(1)**:** 24-32.

Jhamandas JH, Simonin F, Bourguignon JJ, Harris KH (2007). Neuropeptide FF and neuropeptide VF inhibit GABAergic neurotransmission in parvocellular neurons of the rat hypothalamic paraventricular nucleus. *American Journal of Physiology. Regulatory Integrative and Comparative Physiology* **292**(5)**:** R1872-R1880.

Jhanwar-Uniyal M, Beck B, Jhanwar YS, Burlet C, Leibowitz SF (1993). Neuropeptide Y projection from arcuate nucleus to parvocellular division of paraventricular nucleus: specific relation to the ingestion of carbohydrate. *Brain Research* **631**(1)**:** 97-106.

Jin M, Berrout J, Chen L, O'Neil RG (2012). Hypotonicity-induced TRPV4 function in renal collecting duct cells: modulation by progressive cross-talk with Ca2+-activated K+ channels. *Cell Calcium* **51**(2)**:** 131-139.

Kalsbeek A, Foppen E, Schalij I, Van Heijningen C, van der Vliet J, Fliers E*, et al.* (2008). Circadian control of the daily plasma glucose rhythm: an interplay of GABA and glutamate. *PLoS One* **3**(9)**:** e3194.

Kalsbeek A, Garidou ML, Palm IF, Van Der Vliet J, Simonneaux V, Pevet P*, et al.* (2000). Melatonin sees the light: blocking GABA-ergic transmission in the paraventricular nucleus induces daytime secretion of melatonin. *European Journal of Neuroscience* **12**(9)**:** 3146-3154.

Kalsbeek A, La Fleur S, Van Heijningen C, Buijs RM (2004). Suprachiasmatic GABAergic inputs to the paraventricular nucleus control plasma glucose concentrations in the rat via sympathetic innervation of the liver. *Journal of Neuroscience* **24**(35)**:** 7604-7613.

Kalsbeek A, van Heerikhuize JJ, Wortel J, Buijs RM (1996). A diurnal rhythm of stimulatory input to the hypothalamo-pituitary-adrenal system as revealed by timed intrahypothalamic administration of the vasopressin V1 antagonist. *Journal of Neuroscience* **16**(17)**:** 5555-5565.

Kamouchi M, Mamin A, Droogmans G, Nilius B (1999). Nonselective cation channels in endothelial cells derived from human umbilical vein. *The Journal of Membrane Biology* **169**(1): 29-38.

Kanjhan R, Housley GD, Burton LD, Christie DL, Kippenberger A, Thorne PR, Luo L, Ryan AF (1999). Distribution of the P2X2 receptor subunit of the ATP-gated ion channels in the rat central nervous system. *Journal of Comparative Neurology* **407**(1): 11-32.

Kaneko M, Hiroshige T, Shinsako J, Dallman MF (1980). Diurnal changes in amplification of hormone rhythms in the adrenocortical system. *American Journal of Physiolology* **239**(3)**:** R309-316.

Kannan H, Hayashida Y, Yamashita H (1989). Increase in Sympathetic Outflow by Paraventricular Nucleus Stimulation in Awake Rats 1. *American Journal of Physiology* **256**(6)**:** R1325-R1330.

Kantzides A, Badoer E (2005). nNOS-containing neurons in the hypothalamus and medulla project to the RVLM. *Brain Research* **1037**(1-2)**:** 25-34.

Karim F, Kidd C, Malpus CM, Penna PE (1972). The effects of stimulation of the left atrial receptors on sympathetic efferent nerve activity. *Journal of Physiology* **227**(1)**:** 243-260.

Katoh K, Nomura M, Nakaya Y, Iga A, Nada T, Hiasa A*, et al.* (2002). Autonomic nervous activity before and after eradication of Helicobacter pylori in patients with chronic duodenal ulcer. *Alimentary Pharmacology & Therapeutics* **16 Suppl 2:** 180-186.

Kawabe T, Chitrauanshi VC, Nakamura T, Kawabe K, Sapru HN (2009). Mechanism of heart rate responses elicited by chemical stimulation of the hypothalamic paraventricular nucleus in the rat. *Brain Research* **1248:** 115-126.

Kawabe T, Kawabe K, Sapru HN (2012). Cardiovascular responses to chemical stimulation of the hypothalamic arcuate nucleus in the rat: role of the hypothalamic paraventricular nucleus. *PLoS One* **7**(9)**:** e45180.

Kawano Y (2011). Diurnal blood pressure variation and related behavioral factors. *Hypertension Research* **34**(3)**:** 281-285.

Kenney MJ, Weiss ML, Haywood JR (2003). The paraventricular nucleus: an important component of the central neurocircuitry regulating sympathetic nerve outflow. *Acta Physiologica Scandanavia* **177**(1)**:** 7-15.

Kenney MJ, Weiss ML, Patel KP, Wang Y, Fels RJ (2001). Paraventricular nucleus bicuculline alters frequency components of sympathetic nerve discharge bursts. *American Journal of Physiology. Heart and Circulatory Physiology* **281**(3)**:** H1233-1241.

Khasabov SG, Simone DA (2013). Loss of neurons in rostral ventromedial medulla that express neurokinin-1 receptors decreases the development of hyperalgesia. *Neuroscience* **250:** 151-165.

Kiss J, Martos J, Palkovits M (1991). Hypothalamic paraventricular nucleus: a quantitative analysis of cytoarchitectonic subdivisions in the rat. *The Journal of Comparative Neurology* **313**(4)**:** 563-573.

Kohler M, Hirschberg B, Bond CT, Kinzie JM, Marrion NV, Maylie J*, et al.* (1996). Small-conductance, calcium-activated potassium channels from mammalian brain. *Science (New York, N.Y.)* **273**(5282)**:** 1709-1714.

Koutcherov Y, Ashwell KWS, Paxinos G (2000a). The distribution of the neurokinin B receptor in the human and rat hypothalamus. *Neuroreport* **11**(3)**:** 3127-3131.

Koutcherov Y, Mai J, Ashwell K, Paxinos G (2000b). Organization of the human paraventricular hypothalamic nucleus. *The Journal of Comparative Neurology* **423**(2)**:** 299-318.

Krechowec SO, Burton KL, Newlaczyl AU, Nunn N, Vlatkovic N, Plagge A (2012). Postnatal changes in the expression pattern of the imprinted signalling protein XLalphas underlie the changing phenotype of deficient mice. *PLoS One* **7**(1)**:** e29753.

Kubo Y, Adelman JP, Clapham DE, Jan LY, Karschin A, Kurachi Y*, et al.* (2005). International Union of Pharmacology. LIV. Nomenclature and molecular relationships of inwardly rectifying potassium channels. *Pharmacological reviews* **57**(4)**:** 509-526.

Kuhn HG, Dickinson-Anson H, Gage FH (1996). Neurogenesis in the dentate gyrus of the adult rat: age-related decrease of neuronal progenitor proliferation. *Journal of Neuroscience* **16**(6)**:** 2027-2033.

Latchford KJ, Ferguson AV (2005). Angiotensin depolarizes parvocellular neurons in paraventricular nucleus through modulation of putative nonselective cationic and potassium conductances. *American Journal of Physiology-Regulatory Integrative and Comparative Physiology* **289**(1)**:** R52-R58.

Lee S, Han TH, Sonner PM, Stern JE, Ryu PD, Lee SY (2008). Molecular characterization of T-type Ca(2+) channels responsible for low threshold spikes in hypothalamic paraventricular nucleus neurons. *Neuroscience* **155**(4): 1195-1203..

Lee SK, Lee S, Shin SY, Ryu PD, Lee SY (2012). Single cell analysis of voltage-gated potassium channels that determines neuronal types of rat hypothalamic paraventricular nucleus neurons. *Neuroscience* **205:** 49-62.

Lee SK, Ryu PD, Lee SY (2013). Differential distributions of neuropeptides in hypothalamic paraventricular nucleus neurons projecting to the rostral ventrolateral medulla in the rat. *Neuroscience Letters* **556:** 160-165.

Leibowitz SF (2007). Overconsumption of dietary fat and alcohol: mechanisms involving lipids and hypothalamic peptides. *Physiology and Behaviour* **91**(5)**:** 513-521.

Leite LH, Zheng H, Coimbra CC, Patel KP (2012). Contribution of the paraventricular nucleus in autonomic adjustments to heat stress. *Experimental Biology and Medicine* **237**(5)**:** 570-577.

Lenkei Z, Palkovits M, Corvol P, LlorensCortes C (1997). Expression of angiotensin type-1 (AT1) and type-2 (AT2) receptor mRNAs in the adult rat brain: A functional neuroanatomical review. *Frontiers in Neuroendocrinology* **18**(4)**:** 383-439.

Levin BE (2006). Metabolic sensing neurons and the control of energy homeostasis. *Physiology and Behaviour* **89**(4)**:** 486-489.

Lewis CA (1979). Ion-concentration dependence of the reversal potential and the single channel conductance of ion channels at the frog neuromuscular junction. *Journal of Physiology* **286**: 417-445.

Lewis R, Mills AF, Barrett-Jolley R (2010). Models Of Paraventricular Nucleus (PVN) Sympathetic Neurone Modulation by Glucose and Hypoglycaemia. *Biophysical Journal* **98**(3, Suppl 1)**:** 140a-140a.

Li DP, Chen SR, Finnegan TF, Pan HL (2004a). Signalling pathway of nitric oxide in synaptic GABA release in the rat paraventricular nucleus. *Journal of Physiology* **554**(1)**:** 100-110.

Li DP, Chen SR, Pan HL (2010). Adenosine inhibits paraventricular pre-sympathetic neurons through ATP-dependent potassium channels. *Journal of Neurochemistry* **113**(2)**:** 530-542.

Li DP, Chen SR, Pan HL (2003a). Angiotensin II stimulates spinally projecting paraventricular neurons through presynaptic disinhibition. *Journal of Neuroscience* **23**(12)**:** 5041-5049.

Li DP, Chen SR, Pan HL (2002). Nitric oxide inhibits spinally projecting paraventricular neurons through potentiation of presynaptic GABA release. *Journal of Neurophysiology* **88**(5)**:** 2664-2674.

Li DP, Chen SR, Pan HL (2004b). VR1 receptor activation induces glutamate release and postsynaptic firing in the paraventricular nucleus. *Journal of Neurophysiology* **92**(3)**:** 1807-1816.

Li DP, Pan HL (2005). Angiotensin II attenuates synaptic GABA release and excites paraventricular-rostral ventrolateral medulla output neurons. *Journal of Pharmacology and Experimental Therapeutics* **313**(3)**:** 1035-1045.

Li DP, Pan HL (2007a). Glutamatergic inputs in the hypothalamic paraventricular nucleus maintain sympathetic vasomotor tone in hypertension. *Hypertension* **49**(4)**:** 916-925.

Li DP, Pan HL (2010). Increased group I metabotropic glutamate receptor activity in paraventricular nucleus supports elevated sympathetic vasomotor tone in hypertension. *American Journal of Physiology. Regulatory, integrative and comparative physiology* **299**(2)**:** R552-561.

Li DP, Pan HL (2006). Plasticity of GABAergic control of hypothalamic presympathetic neurons in hypertension. *American Journal of Physiology. Heart and Circulatory Physiology* **290**(3)**:** H1110-1119.

Li DP, Pan HL (2007b). Role of gamma-aminobutyric acid (GABA)(A) and GABA(B) receptors in Paraventricular nucleus in control of sympathetic vasomotor tone in hypertension. *Journal of Pharmacology and Experimental Therapeutics* **320**(2)**:** 615-626.

Li DP, Yang Q, Pan HM, Pan HL (2008a). Plasticity of pre- and postsynaptic GABA(B) receptor function in the paraventricular nucleus in spontaneously hypertensive rats. *American Journal of Physiology. Heart and Circulatory Physiology* **295**(2)**:** H807-H815.

Li DP, Yang Q, Pan HM, Pan HL (2008b). Pre- and postsynaptic plasticity underlying augmented glutamatergic inputs to hypothalamic presympathetic neurons in spontaneously hypertensive rats. *Journal of Physiology* **586**(6)**:** 1637-1647.

Li DP, Zhu LH, Pachuau J, Lee HA, Pan HL (2014). mGluR5 Upregulation Increases Excitability of Hypothalamic Presympathetic Neurons through NMDA Receptor Trafficking in Spontaneously Hypertensive Rats. *Journal of Neuroscience* **34**(12)**:** 4309-4317.

Li K, Xu E (2008). The role and the mechanism of gamma-aminobutyric acid during central nervous system development. *Neuroscience bulletin* **24**(3)**:** 195-200.

Li P, Cui BP, Zhang LL, Sun HJ, Liu TY, Zhu GQ (2012). Melanocortin 3/4 Receptors in Paraventricular Nucleus Modulates Sympathetic Outflow and Blood Pressure. *Experimental Physiology* **98**(2): 435-443.

Li Y, Zhang W, Stern JE (2003b). Nitric oxide inhibits the firing activity of hypothalamic paraventricular neurons that innervate the medulla oblongata: Role of GABA. *Neuroscience* **118**(3)**:** 585-601.

Li YF, Cornish KG, Patel KP (2003c). Alteration of NMDA NR1 receptors within the paraventricular nucleus of hypothalamus in rats with heart failure. *Circulation Research* **93**(10)**:** 990-997.

Li YF, Jackson KL, Stern JE, Rabeler B, Patel KP (2006). Interaction between glutamate and GABA systems in the integration of sympathetic outflow by the paraventricular nucleus of the hypothalamus. *American Journal of Physiology. Heart and Circulatory Physiology* **291**(6)**:** H2847-H2856.

Li YF, Mayhan WG, Patel KP (2001). NMDA-mediated increase in renal sympathetic nerve discharge within the PVN: role of nitric oxide. *American Journal of Physiology. Heart and Circulatory Physiology* **281**(6)**:** H2328-H2336.

Liedtke W, Choe Y, Marti-Renom MA, Bell AM, Denis CS, Sali A, Hudspeth AJ, Friedman JM, Heller S (2000). Vanilloid receptor-related osmotically activated channel (VR-OAC), a candidate vertebrate osmoreceptor. *Cell* **103**(3)**:** 525-535.

Liedtke W, Tobin DM, Bargmann CI, Friedman JM (2003). Mammalian TRPV4 (VR-OAC) directs behavioral responses to osmotic and mechanical stimuli in Caenorhabditis elegans. *Proceedings of the National Academy of Sciences of the United States of America* **100**(Suppl 2): 14531-14536.

Lind RW, Swanson LW, Bruhn TO, Ganten D (1985). The distribution of angiotensin-II-immunoreactive cells and fibers in the paraventriculo-hypophysial system of the rat. *Brain Research* **338**(1)**:** 81-89.

Liposits Z, Phelix C, Paull WK (1986). Electron microscopic analysis of tyrosine hydroxylase, dopamine-beta-hydroxylase and phenylethanolamine-N-methyltransferase immunoreactive innervation of the hypothalamic paraventricular nucleus in the rat. *Histochemistry* **84**(2)**:** 105-120.

Liu Q, Wang T, Yu H, Liu B, Jia R (2014). Interaction between interleukin-1 beta and angiotensin II receptor 1 in hypothalamic paraventricular nucleus contributes to progression of heart failure. *Journal of Interferon and Cytokine Research* **34**(11): 870-875.

Loewy A (1991). Forebrain nuclei involved in autonomic control. *Progress in Brain Research* **87:** 253.

Lovick T, Malpas S, Mahony M (1993). Renal vasodilatation in response to acute volume load is attenuated following lesions of parvocellular neurones in the paraventricular nucleus in rats. *Journal of the Autonomic Nervous System* **43**(3)**:** 247-255.

Lovick TA, Coote JH (1989). Circulating atrial natriuretic factor activates vagal afferent inputs to paraventriculo-spinal neurones in the rat. *Journal of the Autonomic Nervous System* **26**(2)**:** 129-134.

Lovick TA, Coote JH (1988). Effects of volume loading on paraventriculo-spinal neurones in the rat. *Journal of the Autonomic Nervous System* **25**(2-3)**:** 135-140.

Lozic M, Greenwood M, Sarenac O, Martin A, Hindmarch C, Tasic T, Paton J, Murphy D, Japundzic-Zigon N (2014). Over-expression of oxytocin receptors 1 in the hypothalamic PVN increases BRS and buffers BP variability in conscious rats. *British Journal of Pharmacology* **171**(19): 4385-4398.

Lucassen PJ, Pruessner J, Sousa N, Almeida OF, Van Dam AM, Rajkowska G, Swaab DF, Czeh B (2014). Neuropathology of stress. *Acta Neuropathologica* **127**(1)**:** 109-135.

Luo X, Kiss A, Makara G, Lolait SJ, Aguilera G (1994). Stress-specific regulation of corticotropin releasing hormone receptor expression in the paraventricular and supraoptic nuclei of the hypothalamus in the rat. *Journal of Neuroendocrinology* **6**(6)**:** 689-696.

Luther JA, Daftary SS, Boudaba C, Gould GC, Halmos KC, Tasker JG (2002). Neurosecretory and non-neurosecretory parvocellular neurones of the hypothalamic paraventricular nucleus express distinct electrophysiological properties. *Journal of Endocrinology* **14**(12): 929-932.
Luther JA, Tasker JG (2000). Voltage-gated currents distinguish parvocellular from magnocellular neurones in the rat hypothalamic paraventricular nucleus. *Journal of Physiology* **523**(1)**:** 193-209.

Ma X, Du J, Zhang P, Deng J, Liu J, Lam FF, Li RA, Huang Y, Jin J, Yao X (2013). Functional role of TRPV4-KCa2.3 signaling in vascular endothelial cells in normal and streptozotocin-induced diabetic rats. *Hypertension* **62**(1)**:** 134-139.

Madden CJ, Morrison SF (2009). Neurons in the paraventricular nucleus of the hypothalamus inhibit sympathetic outflow to brown adipose tissue. *American Journal of Physiology. Regulatory Integrative and Comparative Physiology* **296**(3)**:** R831-R843.

Maguire J (2014). Stress-induced plasticity of GABAergic inhibition. *Frontiers in Cellular Neuroscience* **8:** 157.

Makino S, Tanaka Y, Nazarloo HP, Noguchi T, Nishimura K, Hashimoto K (2005). Expression of type 1 corticotropin-releasing hormone (CRH) receptor mRNA in the hypothalamic paraventricular nucleus following restraint stress in CRH-deficient mice. *Brain Research* **1048**(1-2)**:** 131-137.

Malpas SC (2002). Neural influences on cardiovascular variability: possibilities and pitfalls. *American Journal of Physiology. Heart and Circulatory Physiology* **282**(1)**:** H6-20.

Malpas SC, Coote JH (1994). Role of vasopressin in sympathetic response to paraventricular nucleus stimulation in anesthetized rats. *American Journal of Physiology* **266**(1)**:** R228-R236.

Martin DS, Haywood JR (1993). Hemodynamic responses to paraventricular nucleus disinhibition with bicuculline in conscious rats. *American Journal of Physiology* **265**(5 Pt 2)**:** H1727-H1733.

Martin DS, Haywood JR, Thornhill JA (1993). Stimulation of the hypothalamic paraventricular nucleus causes systemic venoconstriction. *Brain Research* **604**(1-2)**:** 318-324.

Martin DS, Segura T, Haywood JR (1991). Cardiovascular responses to bicuculline in the paraventricular nucleus of the rat. *Hypertension* **18**(1)**:** 48-55.

Martins-Pinge MC, Mueller PJ, Foley CM, Heesch CM, Hasser EM (2012). Regulation of arterial pressure by the paraventricular nucleus in conscious rats: interactions among glutamate, GABA, and nitric oxide. *Frontiers in Physiology* **3:** 490.

McManus OB (1991). Calcium-activated potassium channels: regulation by calcium. *Journal of Bioenergetics and Biomembranes* **23**(4)**:** 537-560.

Melnick IV, Price CJ, Colmers WF (2011). Glucosensing in parvocellular neurons of the rat hypothalamic paraventricular nucleus. *European Journal of Neuroscience* **34**(2)**:** 272-282.

Meng QY, Wang W, Chen XN, Xu TL, Zhou JN (2009). Distribution of acid-sensing ion channel 3 in the rat hypothalamus. *Neuroscience* **159**(3)**:** 1126-1134.

Millar-Craig MW, Bishop CN, Raftery EB (1978). Circadian variation of blood-pressure. *The Lancet* **1**(8068)**:** 795-797.

Mizuno A, Matsumoto N, Imai M, Suzuki M (2003). Impaired osmotic sensation in mice lacking TRPV4. *American Journal of Physiology. Cell physiology* **285**(1)**:** C96-101.

Monteggia LM, Eisch AJ, Tang MD, Kaczmarek LK, Nestler EJ (2000). Cloning and localization of the hyperpolarization-activated cyclic nucleotide-gated channel family in rat brain. *Molecular Brain Research* **81**(1–2)**:** 129-139.

Morishige KI, Inanobe A, Takahashi N, Yoshimoto Y, Kurachi H, Miyake A, Tokunaga Y, Maeda T, Kurachi Y (1996). G protein-gated K+ channel (GIRK1) protein is expressed presynaptically in the paraventricular nucleus of the hypothalamus. *Biochemical and Biophysical Research Communications* **220**(2)**:** 300-305.

Motawei K, Pyner S, Ranson RN, Kamel M, Coote JH (1999). Terminals of paraventricular spinal neurones are closely associated with adrenal medullary sympathetic preganglionic neurones: immunocytochemical evidence for vasopressin as a possible neurotransmitter in this pathway. *Experimental Brain Research* **126**(1)**:** 68-76.

Muller JE, Tofler GH, Stone PH (1989). Circadian variation and triggers of onset of acute cardiovascular disease. *Circulation* **79**(4)**:** 733-743.

Myers B, Mark Dolgas C, Kasckow J, Cullinan WE, Herman JP (2013). Central stress-integrative circuits: forebrain glutamatergic and GABAergic projections to the dorsomedial hypothalamus, medial preoptic area, and bed nucleus of the stria terminalis. *Brain Structure and Function* **219**(4): 1287-1303.

Myers B, McKlveen JM, Herman JP (2012). Neural regulation of the stress response: the many faces of feedback. *Cellular and Molecular Neurobiology* **32**(5): 683-694.

Nagamine K, Kudoh J, Minoshima S, Kawasaki K, Asakawa S, Ito F, Shimizu N (1998). Molecular cloning of a novel putative Ca2+ channel protein (TRPC7) highly expressed in brain. *Genomics* **54**(1)**:** 124-131.

Nakayama Y, Takano Y, Saito R, Kamiya H (1992). Central pressor actions of tachykinin NK-3 receptor in the paraventricular nucleus of the rat hypothalamus. *Brain Research.* **595**(2)**:** 339-342.
Nedungadi TP, Dutta M, Bathina CS, Caterina MJ, Cunningham JT (2012). Expression and distribution of TRPV2 in rat brain. *Experimental Neurology* **237**(1)**:** 223-237.

Nehme B, Henry M, Mouginot D, Drolet G (2012). The expression pattern of the Na(+) sensor, Na(X) in the hydromineral homeostatic network: a comparative study between the rat and rouse. *Frontiers in Neuroanatomy* **6:** 26.

Nilius B, Droogmans G (2001). Ion channels and their functional role in vascular endothelium. *Physiological Reviews* **81**(4)**:** 1415-1459.

Nilius B, Owsianik G (2011). The transient receptor potential family of ion channels. *Genome biology* **12**(3)**:** 218.

Niskanen JP, Tarvainen MP, Ranta-Aho PO, Karjalainen PA (2004). Software for advanced HRV analysis. *Computer Methods and Programs in Biomedicine* **76**(1)**:** 73-81.

Nunn N, Barrett-Jolley R, Plagge A (2009). Brown adipose tissue development and cardiovascular parameters in Gnasxl knock-out mice. *PA2 online* **James Black Conference**.

Nunn N, Feetham CH, Martin J, Barrett-Jolley R, Plagge A (2013). Elevated blood pressure, heart rate and body temperature in mice lacking the XLalphas protein of the Gnas locus is due to increased sympathetic tone. *Experimental physiology* **98**(10)**:** 1432-1445.

Nunn N, Womack M, Dart C, Barrett-Jolley R (2011). Function and pharmacology of spinally-projecting sympathetic pre-autonomic neurones in the paraventricular nucleus of the hypothalamus. *Current Neuropharmacology* **9**(2)**:** 262-277.

Oldfield BJ, Davern PJ, Giles ME, Allen AM, Badoer E, McKinley MJ (2001). Efferent neural projections of angiotensin receptor (AT1) expressing neurones in the hypothalamic paraventricular nucleus of the rat. *Journal of Neuroendocrinology* **13**(2)**:** 139-146.

Ono N, Bedran de Castro JC, McCann SM (1985). Ultrashort-loop positive feedback of corticotropin (ACTH)-releasing factor to enhance ACTH release in stress.

Proceedings of the National Academy of Sciences of the United States of America **82**(10)**:** 3528-3531.

Osborn JW, Fink GD, Sved AF, Toney GM, Raizada MK (2007). Circulating angiotensin II and dietary salt: converging signals for neurogenic hypertension. *Current Hypertension Reports* **9**(3)**:** 228-235.

Owsianik G, Talavera K, Voets T, Nilius B (2006). Permeation and selectivity of TRP channels. *Annual Review of Physiology* **68**: 685-717.

Pachuau J, Li DP, Chen SR, Lee HA, Pan HL (2014). Protein kinase CK2 contributes to diminished small conductance Ca -activated K channel activity of hypothalamic pre-sympathetic neurons in hypertension. *Journal of Neurochemistry* **130**(5): 657-667.

Park JB, Jo JY, Zheng H, Patel KP, Stern JE (2009). Regulation of tonic GABA inhibitory function, presympathetic neuronal activity and sympathetic outflow from the paraventricular nucleus by astroglial GABA transporters. *Journal of Physiology* **587**(19)**:** 4645-4660.

Park JB, Skalska S, Son S, Stern JE (2007). Dual GABAA receptor-mediated inhibition in rat presympathetic paraventricular nucleus neurons. *Journal of Physiology* **582**(Pt 2)**:** 539-551.

Park JB, Stern JE (2005). A tonic, GABAA receptor-mediated inhibitory postsynaptic current restrains firing activity in preautonomic and magnocellular neuroendocrine neurons of the paraventricular nucleus of the hypothalamus (PVN). *Faseb Journal* **19**(4)**:** A599-A599.

Patel KP (2000). Role of paraventricular nucleus in mediating sympathetic outflow in heart failure. *Heart Failure Reviews* **5**(1)**:** 73-86.

Paxinos G, Franklin K (2001). *The Mouse Brain in Stereotaxic Coordinates.* edn. Academic Press.

Paxinos G, Watson C (1986). *The Rat Brain in Stereotaxic Coordinates*. edn. Academic Press Inc: London.

Perello M, Raingo J (2013). Leptin activates oxytocin neurones of the paraventricular nucleus in both control and diet-induced obses rodents. *PLoS One* **8**(3): e59625. doi:10.1371/journal.pone.0059625.

Perez-Reyes E (2003). Molecular physiology of low-voltage-activated T-type calcium channels. *Physiological Reviews* **83**(1)**:** 117-161.

Perez-Reyes E (1999). Three for T: Molecular analysis of the low voltage-activated calcium channel family. *Cellular and Molecular Life Sciences* **56**(7-8)**:** 660-669.

Phan MN, Leddy HA, Votta BJ, Kumar S, Levy DS, Lipshutz DB*, et al.* (2009). Functional characterization of TRPV4 as an osmotically sensitive ion channel in porcine articular chondrocytes. *Arthritis and Rheumatology* **60**(10)**:** 3028-3037.

Pickering TG (1990). The clinical significance of diurnal blood pressure variations. Dippers and nondippers. *Circulation* **81**(2)**:** 700-702.

Pierdomenico SD, Pierdomenico AM, Cuccurullo F (2014). Morning blood pressure surge, dipping, and risk of ischemic stroke in elderly patients treated for hypertension. *American Journal of Hypertension* **27**(4)**:** 564-570.

Pittman Q, Riphagen C, Lederis K (1984). Release of immunoassayable neurohypophyseal peptides from rat spinal cord, in vivo. *Brain Research* **300**(2)**:** 321-326.

Plagge A, Kelsey G, Germain-Lee EL (2008). Physiological functions of the imprinted Gnas locus and its protein variants Galpha(s) and XLalpha(s) in human and mouse. *The Journal of Endocrinology* **196**(2)**:** 193-214.

Powis JE, Bains JS, Ferguson AV (1998). Leptin depolarizes rat hypothalamic paraventricular nucleus neurons. *American Journal of Physiology-Regulatory Integrative and Comparative Physiology* **274**(5)**:** R1468-R1472.

Pyner S (2009). Neurochemistry of the paraventricular nucleus of the hypothalamus: implications for cardiovascular regulation. *J Chem Neuroanat* **38**(3)**:** 197-208.

Pyner S (2014). The paraventricular nucleus and heart failure. *Experimental Physiology* **99**(2)**:** 332-339.

Pyner S, Cleary J, Buchan PM, Coote JH (2001). Tracing functionally identified neurones in a multisynaptic pathway in the hamster and rat using herpes simplex virus expressing green fluorescent protein. *Experimental physiology* **86**(6)**:** 695-702.

Pyner S, Coote JH (1999). Identification of an efferent projection from the paraventricular nucleus of the hypothalamus terminating close to spinally projecting rostral ventrolateral medullary neurons. *Neuroscience* **88**(3)**:** 949-957.

Pyner S, Coote JH (2000). Identification of branching paraventricular neurons of the hypothalamus that project to the rostroventrolateral medulla and spinal cord. *Neuroscience* **100**(3)**:** 549-556.

Pyner S, Deering J, Coote JH (2002). Right atrial stretch induces renal nerve inhibition and c-fos expression in parvocellular neurones of the paraventricular nucleus in rats. *Experimental Physiology* **87**(1)**:** 25-32.

Qin F (2004). Restoration of single-channel currents using the segmental k-means method based on hidden Markov modeling. *Biophysical Journal* **86**(3)**:** 1488-1501.

Qin F, Auerbach A, Sachs F (2000). A direct optimization approach to hidden Markov modeling for single channel kinetics. *Biophysical Journal* **79**(4)**:** 1915-1927.

Qin F, Auerbach A, Sachs F (1996). Estimating single-channel kinetic parameters from idealized patch-clamp data containing missed events. *Biophysical Journal* **70**(1)**:** 264-280.

Radley JJ, Gosselink KL, Sawchenko PE (2009). A discrete GABAergic relay mediates medial prefrontal cortical inhibition of the neuroendocrine stress response. *Journal of Neuroscience* **29**(22)**:** 7330-7340.

Ramchandra R, Hood SG, Frithiof R, McKinley MJ, May CN (2013). The role of the paraventricular nucleus of the hypothalamus in the regulation of cardiac and renal sympathetic nerve activity in conscious normal and heart failure sheep. *Journal of Physiology* **591**(Pt 1)**:** 93-107.

Ramchandra R, Hood SG, May CN (2014). Central exogenous nitric oxide decreases cardiac sympathetic drive and improves baroreflex control of heart rate in ovine heart failure. *American Journal of Physiology. Regulatory, integrative and comparative physiology* **307**(3)**:** R271-280.

Reppert SM, Weaver DR (2002). Coordination of circadian timing in mammals. *Nature* **418**(6901)**:** 935-941.

Roberts JC, Davis JB, Benham CD (2004). [3H]Resiniferatoxin autoradiography in the CNS of wild-type and TRPV1 null mice defines TRPV1 (VR-1) protein distribution. *Brain Research* **995**(2)**:** 176-183.

Roland BL, Sawchenko PE (1993). Local origins of some GABAergic projections to the paraventricular and supraoptic nuclei of the hypothalamus in the rat. *The Journal of Comparative Neurology* **332**(1)**:** 123-143.

Rozanski A, Blumenthal JA, Kaplan J (1999). Impact of psychological factors on the pathogenesis of cardiovascular disease and implications for therapy. *Circulation* **99**(16)**:** 2192-2217.

Rudy B, Chow A, Lau D, Amarillo Y, Ozaita A, Saganich M*, et al.* (1999). Contributions of Kv3 channels to neuronal excitability. *Annals of the New York Academy of Sciences* **868:** 304-343.

Saenz del Burgo L, Cortes R, Mengod G, Zarate J, Echevarria E, Salles J (2008). Distribution and neurochemical characterization of neurons expressing GIRK channels in the rat brain. *The Journal of Comparative Neurology* **510**(6)**:** 581-606.

Sakaguchi T, Bray GA, Eddlestone G (1988). Sympathetic activity following paraventricular or ventromedial hypothalamic lesions in rats. *Brain Research Bulletin* **20**(4)**:** 461-465.

Salzmann M, Seidel KN, Bernard R, Pruss H, Veh RW, Derst C (2010). BKbeta1 subunits contribute to BK channel diversity in rat hypothalamic neurons. *Cellular and Molecular Neurobiology* **30**(6)**:** 967-976.

Sano Y, Inamura K, Miyake A, Mochizuki S, Yokoi H, Matsushime H*,* Furuichi K (2001). Immunocyte Ca2+ influx system mediated by LTRPC2. *Science (New York, N.Y.)* **293**(5533)**:** 1327-1330.

Santarelli L, Gobbi G, Blier P, Hen R (2002). Behavioral and physiologic effects of genetic or pharmacologic inactivation of the substance P receptor (NK1). *Journal of Clinical Psychiatry* **63**(Suppl 11)**:** 11-17.

Santarelli L, Gobbi G, Debs PC, Sibille ET, Blier P, Hen R, Heath MJ (2001). Genetic and pharmacological disruption of neurokinin 1 receptor function decreases anxiety-related behaviors and increases serotonergic function. *Proceedings of the National Academy of Sciences of the United States of America* **98**(4)**:** 1912-1917.

Sausbier U, Sausbier M, Sailer CA, Arntz C, Knaus HG, Neuhuber W*, et al.* (2006). Ca2+ -activated K+ channels of the BK-type in the mouse brain. *Histochemistry and Cell Biology* **125**(6)**:** 725-741.

Sawchenko PE, Swanson LW (1982). Immunohistochemical Identification of Neurons in the Paraventricular Nucleus of the Hypothalamus That Project to the Medulla or to the Spinal-Cord in the Rat. *Journal of Comparative Neurology* **205**(3)**:** 260-272.

Serodio P, Rudy B (1998). Differential expression of Kv4 K+ channel subunits mediating subthreshold transient K+ (A-type) currents in rat brain. *J Neurophysiol* **79**(2)**:** 1081-1091.

Schlenker E, Barnes L, Hansen S, Martin D (2001). Cardiorespiratory and metabolic responses to injection of bicuculline into the hypothalamic paraventricular nucleus (PVN) of conscious rats. *Brain Research* **895**(1-2)**:** 33-40.

Schramm LP, Strack AM, Platt KB, Loewy AD (1993). Peripheral and central pathways regulating the kidney: a study using pseudorabies virus. *Brain Research* **616**(1-2)**:** 251-262.

Scrogin KE, Grygielko ET, Brooks VL (1999). Osmolality: a physiological long-term regulator of lumbar sympathetic nerve activity and arterial pressure. *American Journal of Physiology* **276**(6 Pt 2)**:** R1579-1586.

Sermasi E, Coote JH (1994). Oxytocin acts at V-1 receptors to excite sympathetic preganglionic neurones in neonatal rat spinal-cord in-vitro. *Brain Research* **647**(2)**:** 323-332.

Shafton AD, Ryan A, Badoer E (1998). Neurons in the hypothalamic paraventricular nucleus send collaterals to the spinal cord and to the rostral ventrolateral medulla in the rat. *Brain Research* **801**(1-2)**:** 239-243.

Shao LR, Halvorsrud R, Borg-Graham L, Storm JF (1999). The role of BK-type Ca2+-dependent K+ channels in spike broadening during repetitive firing in rat hippocampal pyramidal cells. *Journal of Physiology* **521**(Pt 1): 135-146.

Shi Z, Chen WW, Xiong XQ, Han Y, Zhou YB, Zhang F, Gao XY, Zhu GQ (2012). Sympathetic activation by chemical stimulation of white adipose tissues in rats. *Journal of Applied Physiology(1985)* **112**(6)**:** 1008-1014.

Shirasaka T, Kannan H, Takasaki M (2007). Activation of a G protein-coupled inwardly rectifying K+ current and suppression of Ih contribute to dexmedetomidine-induced inhibition of rat hypothalamic paraventricular nucleus neurons. *Anesthesiology* **107**(4)**:** 605-615.

Shults CW, Buck SH, Burcher E, Chase TN, O'Donohue TL (1985). Distinct binding sites for substance P and neurokinin A (substance K): co-transmitters in rat brain. *Peptides* **6**(2)**:** 343-345.

Smith JE, Jansen AS, Gilbey MP, Loewy AD (1998). CNS cell groups projecting to sympathetic outflow of tail artery: neural circuits involved in heat loss in the rat. *Brain Research* **786**(1-2)**:** 153-164.

Sonkusare SK, Bonev AD, Ledoux J, Liedtke W, Kotlikoff MI, Heppner TJ, Hill-Eubanks DC, Nelson MT (2012). Elementary Ca2+ signals through endothelial TRPV4 channels regulate vascular function. *Science* **336**(6081)**:** 597-601.

Sonner PM, Filosa JA, Stern JE (2008). Diminished A-type potassium current and altered firing properties in presympathetic PVN neurones in renovascular hypertensive rats. *Journal of Physiology* **586**(6)**:** 1605-1622.

Sonner PM, Lee S, Ryu PD, Lee SY, Stern JE (2011). Imbalanced K+ and Ca2+ subthreshold interactions contribute to increased hypothalamic presympathetic neuronal excitability in hypertensive rats. *Journal of Physiology* **589**(Pt 3)**:** 667-683.

Sonner PM, Stern JE (2007). Functional role of A-type potassium currents in rat presympathetic PVN neurones. *Journal of Physiology* **582**(Pt 3)**:** 1219-1238.

Sonner PM, Stern JE (2005). Role of A-type potassium currents on the excitability and firing activity of RVLM-projecting PVN neurons. *Faseb Journal* **19**(4)**:** A599-A599.

Spielberg C, Falkenhahn D, Willich SN, Wegscheider K, Voller H (1996). Circadian, day-of-week, and seasonal variability in myocardial infarction: comparison between working and retired patients. *American Heart Journal* **132**(3)**:** 579-585.

Spyer KM (1994). Annual-Review Prize Lecture - Central Nervous Mechanisms Contributing to Cardiovascular Control. *Journal of Physiology* **474**(1)**:** 1-19.

Stern JE (2001). Electrophysiological and morphological properties of pre-autonomic neurones in the rat hypothalamic paraventricular nucleus. *Journal of Physiology* **537**(1)**:** 161-177.

Stern JE (2004). Nitric oxide and homeostatic control: an intercellular signalling molecule contributing to autonomic and neuroendocrine integration? *Progress in Biophysics and Molecular Biology* **84**(2-3)**:** 197-215.

Stern JE, Zhang W (2003). Preautonomic neurons in the paraventricular nucleus of the hypothalamus contain estrogen receptor beta. *Brain Research* **975**(1-2): 99-109.

Stocker SD, Cunningham JT, Toney GM (2004). Water deprivation increases Fos immunoreactivity in PVN autonomic neurons with projections to the spinal cord and rostral ventrolateral medulla. *American Journal of Physiology-Regulatory Integrative and Comparative Physiology* **287**(5)**:** R1172-R1183.
strottmann
Stocker SD, Osborn JL, Carmichael SP (2007). Forebrain osmotic regulation of the sympathetic nervous system. *Clin Exp Pharmacol Physiol* **35**(5-6)**:** 695-700.

Stocker SD, Toney GA (2005). Median preoptic neurones projecting to the hypothalamic paraventricular nucleus respond to osmotic, circulating Ang II and baroreceptor input in the rat. *J Physiol* **568**(2)**:** 599-615.

Stotz-Potter EH, Morin SM, DiMicco JA (1996). Effect of microinjection of muscimol into the dorsomedial or paraventricular hypothalamic nucleus on air stress-induced neuroendocrine and cardiovascular changes in rats. *Brain Research* **742**(1-2)**:** 219-224.

Strack AM, Sawyer WB, Hughes JH, Platt KB, Loewy AD (1989a). A general pattern of CNS innervation of the sympathetic outflow demonstrated by trans-neuronal pseudorabies viral-infections. *Brain Research* **491**(1)**:** 156-162.

Strack AM, Sawyer WB, Platt KB, Loewy AD (1989b). CNS cell groups regulating the sympathetic outflow to adrenal-gland as revealed by trans-neuronal cell body labeling with pseudorabies virus. *Brain Research* **491**(2)**:** 274-296.

Strotmann R, Harteneck C, Nunnenmacher K, Schultz G, Plant TD (2000). OTRPC4, a nonselective cation channel that confers sensitivity to extracellular osmolarity. *Nature Cell Biology* **2**(10)**:** 695-702.

Sudbury JR, Bourque CW (2013). Dynamic and permissive roles of TRPV1 and TRPV4 channels for thermosensation in mouse supraoptic magnocellular neurosecretory neurons. *Journal of Neuroscience* **33**(43)**:** 17160-17165.

Sumoza-Toledo A, Penner R (2011). TRPM2: a multifunctional ion channel for calcium signalling. *Journal of Physiology* **589**(Pt 7)**:** 1515-1525.

Swanson L, Kuypers H (1980). The paraventricular nucleus of the hypothalamus: cytoarchitectonic subdivisions and organization of projections to the pituitary, dorsal vagal complex, and spinal cord as demonstrated by retrograde fluorescence double-labeling methods. *The Journal of Comparative Neurology* **194**(3)**:** 555-570.

Swanson LW, McKellar S (1979). The distribution of oxytocin- and neurophysin-stained fibers in the spinal cord of the rat and monkey. *The Journal of Comparative Neurology* **188**(1)**:** 87-106.

Swanson LW, Sawchenko PE (1983). Hypothalamic Integration - Organization of the Paraventricular and Supraoptic Nuclei. *Annual Reviews in Neuroscience* **6:** 269-324.

Swanson LW, Sawchenko PE, Berod A, Hartman BK, Helle KB, Vanorden DE (1981). An immunohistochemical study of the organization of catecholaminergic cells and terminal fields in the paraventricular and supraoptic nuclei of the hypothalamus. *The Journal of Comparative Neurology* **196**(2)**:** 271-285.

Talman WT, Lin LH (2013). Sudden death following selective neuronal lesions in the rat nucleus tractus solitarii. *Autonomic Neuroscience: basic & clinical* **175**(1-2)**:** 9-16.

Tasker JG, Dudek FE (1991). Electrophysiological properties of neurones in the region of the paraventricular nucleus in slices of rat hypothalamus. *Journal of Physiology* **434:** 271-293.

Tavares RF, Pelosi GG, Correa FM (2009). The paraventricular nucleus of the hypothalamus is involved in cardiovascular responses to acute restraint stress in rats. *Stress* **12**(2)**:** 178-185.

Tei H, Okamura H, Shigeyoshi Y, Fukuhara C, Ozawa R, Hirose M*,* Sakaki Y (1997). Circadian oscillation of a mammalian homologue of the Drosophila period gene. *Nature* **389**(6650)**:** 512-516.

Tempel DL, Kim T, Leibowitz SF (1993). The paraventricular nucleus is uniquely responsive to the feeding stimulatory effects of steroid hormones. *Brain Research* **614**(1-2)**:** 197-204.

Ter Horst GJ, Luiten PG (1986). The projections of the dorsomedial hypothalamic nucleus in the rat. *Brain Research Bulletins* **16**(2): 231-148).

Teruyama R, Sakuraba M, Kurotaki H, Armstrong WE (2011). Transient receptor potential channel m4 and m5 in magnocellular cells in rat supraoptic and paraventricular nuclei. *Journal of Neuroendocrinology* **23**(12)**:** 1204-1213.

Teruyama R, Sakuraba M, Wilson LL, Wandrey NE, Armstrong WE (2012). Epithelial Na(+) sodium channels in magnocellular cells of the rat supraoptic and paraventricular nuclei. *American Journal of Physiology. Endocrinology and metabolism* **302**(3)**:** E273-285.

Thireau J, Poisson D, Zhang BL, Gillet L, Le Pecheur M, Andres C, London J, Babuty D (2008). Increased heart rate variability in mice overexpressing the Cu/Zn superoxide dismutase. *Free Radical Biology and Medicine* **45**(4)**:** 396-403.

Thompson RH, Canteras NS, Swanson LW (1996). Organization of projections from the foromedial nucleus of the hypothalamis: a PHA-L study in the rat. *The Journal of Comparative Neurology* **376**(1): 142-173.

Thorneloe KS, Sulpizio AC, Lin Z, Figueroa DJ, Clouse AK, McCafferty GP, Chendrimada TP, Lashinger ES, Gordon E, Evans L, Misajet BA, Demarini DJ,Nation JH, Casillas LN, Marquis RW, Votta BJ, Sheardown SA, Xu X, Brooks DP, Laping NJ, Westfall TD (2008). N-((1S)-1-{[4-((2S)-2-{[(2,4-dichlorophenyl)sulfonyl]amino}-3-hydroxypropanoyl)-1 -piperazinyl]carbonyl}-3-methylbutyl)-1-benzothiophene-2-carboxamide (GSK1016790A), a novel and potent transient receptor potential vanilloid 4 channel agonist induces urinary bladder contraction and hyperactivity: Part I. *Journal of Pharmacology and Experimental Therapeutics* **326**(2)**:** 432-442.

Toney GM, Chen QH, Cato MJ, Stocker SD (2003). Central osmotic regulation of sympathetic nerve activity. *Acta Physiologia Scandanavia* **177**(1)**:** 43-55.

Unger T, Becker H, Petty M, Demmert G, Schneider B, Ganten D, Lang RE (1985). Differential effects of central angiotensin II and substance P on sympathetic nerve activity in conscious rats. Implications for cardiovascular adaptation to behavioral responses. *Circulation Research* **56**(4)**:** 563-575.

Vennekens R, Hoenderop JG, Prenen J, Stuiver M, Willems PH, Droogmans G, Nilius B, Bindels RJ (2000). Permeation and gating properties of the novel epithelial Ca(2+) channel. *The Journal of Biological Chemistry* **275**(6): 3963-3969.

Verdecchia P, Schillaci G, Borgioni C, Ciucci A, Sacchi N, Battistelli M, Guerreri M, Comparato E, Porcellati C (1995). Gender, day-night blood pressure changes, and left ventricular mass in essential hypertension. Dippers and peakers. *American Journal of Hypertension* **8**(2)**:** 193-196.

Vincent F, Acevedo A, Nguyen MT, Dourado M, DeFalco J, Gustafson A, Spiro P, Emerling DE, Kelly MG, Duncton MA (2009). Identification and characterization of novel TRPV4 modulators. *Biochemical and Biophysical Research Communications* **389**(3)**:** 490-494.

Vincent SR, Kimura H (1992). Histochemical mapping of nitric oxide synthase in the rat brain. *Neuroscience* **46**(4)**:** 755-784.

Vulchanova L, Arvidsson U, Riedl M, Wang J, Buell G, Surprenant A, North RA, Elde R (1996). Differential distribution of two ATP-gated channels (P2X receptors) determined by immunocytochemistry. *Proceedings of the National Academy of Sciences in the United States of America* **93**(15): 8063-8067.

Wang HW, Amin MS, El Shahat E, Huang BS, Tuana BS, Leenen FH (2010). Effects of central sodium on epithelial sodium channels in rat brain. *American Journal of Physiology. Regulatory, Integrative and Comparative Physiology* **299**(1): R222-233.

Wang RJ, Zeng QH, Wang WZ, Wang W (2009). GABA(A) and GABA(B) receptor-mediated inhibition of sympathetic outflow in the paraventricular nucleus is blunted in chronic heart failure. *Clinical and Experimental Pharmacology and Physiology* **36**(5-6)**:** 516-522.

Ward KR, Bardgett JF, Wolfgang L, Stocker SD (2011). Sympathetic response to insulin is mediated by melanocortin 3/4 receptors in the hypothalamic paraventricular nucleus. *Hypertension* **57**(3)**:** 435-441.

Watanabe H, Davis JB, Smart D, Jerman JC, Smith GD, Hayes P*,* Vriens J, Cairns W, Wissenbach U, Prenen J, Flockerzi V, Droogmans G, Benham CD, Nilius B (2002). Activation of TRPV4 channels (hVRL-2/mTRP12) by phorbol derivatives. *Journal of Biological Chemistry* **277**(16)**:** 13569-13577.

Watkins ND, Cork SC, Pyner S (2009). An immunohistochemical investigation of the relationship between neuronal nitric oxide synthase, GABA and presympathetic paraventricular neurons in the hypothalamus. *Neuroscience* **159**(3)**:** 1079-1088.

Weber M, Lauterburg T, Tobler I, Burgunder JM (2004). Circadian patterns of neurotransmitter related gene expression in motor regions of the rat brain. *Neuroscience Letters* **358**(1)**:** 17-20.

Wei AD, Gutman GA, Aldrich R, Chandy KG, Grissmer S, Wulff H (2005). International Union of Pharmacology. LII. Nomenclature and molecular relationships of calcium-activated potassium channels. *Pharmacological reviews* **57**(4)**:** 463-472.

Weiss ML, Chowdhury SI, Patel KP, Kenney MJ, Huang J (2001). Neural circuitry of the kidney: NO-containing neurons. *Brain Research* **919**(2)**:** 269-282.

Westenbroek RE, Merrick DK, Catterall WA (1989). Differential subcellular localization of the RI and RII Na+ channel subtypes in central neurons. *Neuron* **3**(6)**:** 695-704.

Whitaker WR, Faull RL, Waldvogel HJ, Plumpton CJ, Emson PC, Clare JJ (2001). Comparative distribution of voltage-gated sodium channel proteins in human brain. *Brain Research Molecular Brain Research* **88**(1-2)**:** 37-53.

Womack MD, Barrett-Jolley R (2007). Activation of paraventricular nucleus neurones by the dorsomedial hypothalamus via a tachykinin pathway in rats. *Experimental Physiology* **92**(4)**:** 671-676.

Womack MD, Morris R, Gent TC, Barrett-Jolley R (2007). Substance P targets sympathetic control neurons in the paraventricular nucleus. *Circulation research* **100**(11)**:** 1650-1658.

Womack MD, Pyner S, Barrett-Jolley R (2006). Inhibition by alpha-tetrahydrodeoxycorticosterone (THDOC) of pre-sympathetic parvocellular neurones in the paraventricular nucleus of rat hypothalamus. *British Journal of Pharmacology* **149**(5)**:** 600-607.

Xiang HB, Liu C, Liu TT, Xiong J (2014). Central circuits regulating the sympathetic outflow to lumbar muscles in spinally transected mice by retrograde transsynaptic transport. *International Journal of Clinical and Experimental Pathology* **7**(6)**:** 2987-2997.

Xie T, Plagge A, Gavrilova O, Pack S, Jou W, Lai EW*,* Frontera M, Kelsey G, Weinstein LS (2006). The alternative stimulatory G protein alpha-subunit XLalphas is a critical regulator of energy and glucose metabolism and sympathetic nerve activity in adult mice. *Journal of Biological Chemistry* **281**(28)**:** 18989-18999.

Yamada T, Mochiduki A, Sugimoto Y, Suzuki Y, Itoi K, Inoue K (2009). Prolactin-Releasing Peptide Regulates the Cardiovascular System Via Corticotrophin-Releasing Hormone. *Journal of Neuroendocrinology* **21**(6)**:** 586-593.

Yamamoto H, Lee CE, Marcus JN, Williams TD, Overton JM, Lopez ME, Hollenberg AN,Baggio L, Saper CB, Drucker DJ, Elmquist JK (2002). Glucagon-like peptide-1 receptor stimulation increases blood pressure and heart rate and activates autonomic regulatory neurons. *The Journal of Clinical Investigation* **110**(1)**:** 43-52.

Yamashita H, Inenaga K, Dyball RE (1988). Thermal, osmotic and chemical modulation of neural activity in the paraventricular nucleus: in vitro studies. *Brain Research Bulletin* **20**(6)**:** 825-829.

Yamashita H, Inenaga K, Koizumi K (1984). Possible projections from regions of paraventricular and supraoptic nuclei to the spinal-cord - Electrophysiological studies. *Brain Research* **296**(2)**:** 373-378.

Yang Q, Chen SR, Li DP, Pan HL (2007). Kv1.1/1.2 channels are downstream effectors of nitric oxide on synaptic GABA release to preautonomic neurons in the paraventricular nucleus. *Neuroscience* **149**(2)**:** 315-327.

Yang Z, Coote JH (1998). Influence of the hypothalamic paraventricular nucleus on cardiovascular neurones in the rostral ventrolateral medulla of the rat. *Journal of Physiology* **513**(2)**:** 521-530.

Yang Z, Han D, Coote JH (2009). Cardiac sympatho-excitatory action of PVN-spinal oxytocin neurones. *Autonomic Neuroscience. Basic & Clinical* **147**(1-2)**:** 80-85.

Yang Z, Smith L, Coote JH (2004). Paraventricular nucleus activation of renal sympathetic neurones is synaptically depressed by nitric oxide and glycine acting at a spinal level. *Neuroscience* **124**(2)**:** 421-428.

Yang Z, Wheatley M, Coote JH (2002). Neuropeptides, amines and amino acids as mediators of the sympathetic effects of paraventricular nucleus activation in the rat. *Experimental Physiology* **87**(6)**:** 663-674.

Ye ZY, Li DP, Pan HL (2013). Regulation of hypothalamic presympathetic neurons and sympathetic outflow by group II metabotropic glutamate receptors in spontaneously hypertensive rats. *Hypertension* **62**(2)**:** 255-262.

Yoshimatsu H, Egawa M, Bray GA (1992). Effects of Cholecystokinin on Sympathetic Activity to Interscapular Brown Adipose-Tissue. *Brain Res* **597**(2)**:** 298-303.

Yoshimatsu H, Egawa M, Bray GA (1993). Sympathetic nerve activity after discrete hypothalamic injections of L-glutamate. *Brain Research* **601**(1-2)**:** 121-128.

Yu FH, Catterall WA (2003). Overview of the voltage-gated sodium channel family. *Genome Biology* **4**(3)**:** 207.

Zaki A, Barrett-Jolley R (2002). Rapid neuromodulation by cortisol in the rat paraventricular nucleus: an in vitro study. *British Journal of Pharmacology* **137**(1)**:** 87-97.

Zhang J, Li H, Teng H, Zhang T, Luo Y, Zhao M, Li YQ, Sun ZS (2012). Regulation of peripheral clock to oscillation of substance P contributes to circadian inflammatory pain. *Anesthesiology* **117**(1)**:** 149-160.

Zhang K, Li YF, Patel KP (2001). Blunted nitric oxide-mediated inhibition of renal nerve discharge within PVN of rats with heart failure. *American Journal of Physiology. Heart and Circulatory Physiology* **281**(3)**:** H995-H1004.

Zhang K, Li YF, Patel KP (2002). Reduced endogenous GABA-mediated inhibition in the PVN on renal nerve discharge in rats with heart failure. *American Journal of Physiology. Regulatory Integrative and Comparative Physiology* **282**(4)**:** R1006-R1015.

Zhang K, Mayhan WG, Patel KP (1997). Nitric oxide within the paraventricular nucleus mediates changes in renal sympathetic nerve activity. *American Journal of Physiology. Regulatory Integrative and Comparative Physiology* **273**(3)**:** R864-R872.

Zhang K, Patel KP (1998). Effect of nitric oxide within the paraventricular nucleus on renal sympathetic nerve discharge: role of GABA. *American Journal of Physiology. Regulatory Integrative and Comparative Physiology* **275**(3)**:** R728-R734.

Zhang K, Zucker IH, Patel KP (1998). Altered number of diaphorase (NOS) positive neurons in the hypothalamus of rats with heart failure. *Brain Research* **786**(1-2)**:** 219-225.

Zhang WF, Stern JE (2002). Preautonomic neurons in the paraventricular nucleus (PVN) of the hypothalamus express estrogen receptor-B immunoreactivity. *Faseb Journal* **16**(4)**:** A501-A501.

Zhang ZH, Francis J, Weiss RM, Felder RB (2002b). The renin-angiotensin-aldosterone system excites hypothalamic paraventricular nucleus neurons in heart failure. *American Journal of Physiology. Heart and Circulatory Physiology* **283**(1)**:** H423-H433.

Zhong MK, Duan YC, Chen AD, Xu B, Gao XY, De W*,* Zhu GQ (2008a). Paraventricular nucleus is involved in the central pathway of cardiac sympathetic afferent reflex in rats. *Experimental Physiology* **93**(6)**:** 746-753.

Zhong MK, Shi Z, Zhou LM, Gao J, Liao ZH, Wang W*,* Gao XY, Zhu GQ (2008b). Regulation of cardiac sympathetic afferent reflex by GABA(A) and GABA(B) receptors in paraventricular nucleus in rats. *European Journal of Neuroscience* **27**(12)**:** 3226-3232.

Zsombok A, Gao H, Miyata K, Issa A, Derbenev AV (2011). Immunohistochemical localization of transient receptor potential vanilloid type 1 and insulin receptor substrate 2 and their co-localization with liver-related neurons in the hypothalamus and brainstem. *Brain Research* **1398:** 30-39.